Physiological response of *Rhizobium leguminosarum* during bacteroid development

Graham A. Hood

This thesis is submitted in fulfilment of the requirements of the degree of
Doctor of Philosophy at the University of East Anglia

Department of Molecular Microbiology

John Innes Centre

Norwich

September 2013

Date

24/09/2013

I declare that the work contained in this thesis, submitted by me for the degree of Doctor of Philosophy, is to the best of my knowledge my own original work, except where due reference is made.

Signed

Graham A. Hood

Acknowledgements

My first words of gratitude go to Philip Poole for his time, advice and encouragement. I am wholeheartedly thankful for Phil giving me the opportunity to work in his lab. The wisdom, motivation and ideas of Allan Downie were also invaluable to this thesis, particularly during the write-up stage. It was a tremendous pleasure working with them both.

Everyone in the Poole group was a joy to know. Starting his PhD at the same time as me, Tom Turner got me through all the project's rough patches by making me laugh or feeding me flapjacks. Despite a few harmless squabbles as a consequence of his love to complain, I would also like to thank Andrzej Tkacz for his friendship and entertainment. Like he has done with so many scientists that have joined and left the Poole group, Karunakaran Ramakrishnan (KK) trained me in PCR, cloning and mutagenesis for which I am enormously appreciative. I would like to thank Jason Terpolilli for giving me the opportunity to help write a literature review. I would also like to mention Adrian Tett for his discussions on efflux systems and Alison East for her support.

There are many people outside of the Poole group that need to be thanked, starting with Sue Bunnewell and Kim Findlay for their assistance with microscopy. Dave Hart (Institute of Food Research) was extremely helpful when using atomic absorption spectroscopy for the quantification of Mg. I would also like to give a huge thanks to the media kitchen staff as they often went beyond their duties in order to help. I am grateful to Jon Seaman (University of Reading), Koichi Ito (The University of Tokyo) and Andy Johnston (University of East Anglia) for contributing some of the strains used in this project.

Among the friends I've made in Norwich, I would like to thank Mark Woodcock for being a memorable housemate and Matthew Donaldson for making all those long days in the library bearable. Finally, I would like to thank Lily and my parents for being so understanding when it came to my absence on many occasions due to work commitments.

Abstract

In legume-rhizobia symbioses, free-living rhizobia colonise root nodules and develop into N_2 fixing specialists known as bacteroids. During bacteroid development, rhizobia must adapt to the nodule environment, consisting of reactive oxygen species, low oxygen, antimicrobial secondary metabolites, low pH and in some nodules, antimicrobial peptides. This study offers a holistic insight into the processes required by *R. leguminosarum* during bacteroid development in nodules formed on four legumes: *Pisum sativum*, *Vicia faba*, *Vicia hirsuta* and *Phaseolus vulgaris*.

Initially, a high-throughput mutagenesis strategy was used to target genes upregulated during bacteroid development. Screening forty-two mutants on *P. sativum* identified some moderate phenotypes but more importantly, highlighted functional redundancy between certain gene products. A clear example of functional redundancy was seen between the Mn^{2+} transporters SitABCD and MntH. Single mutations in *sitA* or *mntH* did not cause a symbiotic phenotype whereas the double mutant could not form bacteroids on *P. sativum*, *V. faba* or *V. hirsuta*. Intriguingly, no symbiotic phenotype for the double mutant was observed on *P. vulgaris*. In addition to Mn^{2+} transporters, a Mg^{2+} channel, MgtE, that is essential for growth in Mg^{2+}-limited medium at low pH was identified. As with the Mn^{2+} transporters, the requirement of MgtE during symbiosis depended upon the species of the host-legume. Reasons for host-dependent requirement of SitABCD, MntH and MgtE are discussed.

The requirement of three O_2-responsive regulators that govern regulatory pathways essential to N_2 fixation was also investigated. FnrN appears to be the major O_2-responsive regulator required for symbiosis but in addition to *fnrN*, two genes, *fixL* and *fixL*c, need to be mutated to prohibit N_2 fixation. Other findings include a putative toxin-antitoxin system that hinders N_2 fixation when disturbed.

Abbreviations

:pK19mob	Mutagenesis by integration of pK19mob
:pRU877	Mutagenesis by integration of pRU877
::mTn5	Mutagenesis by mTn5-insertion
ΩKm	Mutagenesis by insertion of Ω intersposon carrying kanamycin resistance
ΩSpc	Mutagenesis by insertion of Ω intersposon carrying spectinomycin resistance
ΩTc	Mutagenesis by insertion of Ω intersposon carrying tetracycline resistance
Δ	Deletion of genetic region
aa	Amino acid
AAA+	ATPase associated with diverse cellular activities
AAS	Atomic Absorption Spectroscopy
ABC	ATP-binding cassette
AU	Absorbance units
Amp	Ampicillin
Amp^r	Ampicillin resistance
AMS	Acid minimal salts
ATP	Adenosine triphosphate
BLAST	Basic local alignment search tool
bv.	Biovar
CBS	Cystathionine β-synthase
CFU	Colony forming units
CuOOH	Cumene hydroperoxide
cv.	Cultivar
Cys	Cysteine
DNA	Deoxyribonucleic acid
dpi	Days post inoculation
EDTA	Ethylenediaminetetraacetic acid
EPS	Exopolysaccharide
EtOH	Ethanol
FeMoCO	Iron molybdenum cofactor

Fix$^+$	Wild type rates of N_2 fixation
Fix$^-$	Absence of N_2 fixation
Fix^{red}	Reduced rates of N_2 fixation
gfp	Green fluorescent protein
GUS	β-glucuronidase
Gm	Gentamicin
Gm^r	Gentamicin resistance
IT	Infection thread
Km	Kanamycin
Km^r	Kanamycin resistance
LB	Luria Bertani
LPS	Lipopolysaccharide
MFP	Membrane fusion protein
MFS	Major facilitator protein
MOPS	3-(N-morpholino)propanesulfonic acid
NADPH	Nicotinamide adenine dinucleotide phosphate
NCR	Nodule-specific cysteine-rich
Neo	Neomycin
Neo^r	Neomycin resistance
OD	Optical density
ORF	Open reading frame
PCR	Polymerase chain reaction
PHB	Poly-β-hydroxybutyrate
pi	Post inoculation
PNPG	4-nitrophenyl β-D-glucuronide
Rlp4292	*Rhizobium leguminosarum* bv. phaseoli 4292
Rlv3841	*Rhizobium leguminosarum* bv. viciae 3841
RlvA34	*Rhizobium leguminosarum* bv. viciae A34
RNA	Ribonucleic acid
ROS	Reactive oxygen species
SBP	Solute binding protein
SDS	Sodium dodecyl sulphate
SEM	Standard error of the mean
Spc	Spectinomycin
Spc^r	Spectinomycin resistance

Str	Streptomycin
Str^r	Streptomycin resistance
Str^s	Streptomycin sensitive
S-XRF	Synchrotron-based X-ray fluorescence
Sym	Symbiosis
T3SS	Type III secretion system
tBOOH	t-butyl hydroperoxide
Tc	Tetracycline
Tc^r	Tetracycline resistance
TCA	Tricarboxylic acid cycle
TEM	Transmission electron microscopy
TM	Transmembrane
TY	Tryptone-yeast
UV	Ultraviolet
v/v	Volume of solute/volume of solution
w/v	Mass of solute/volume of solution
X-gal	5-bromo-4-chloro-3-indolyl-b-D-galactopyranoside

TABLE OF CONTENTS

Chapter 1: *General Introduction*

1.1 LEGUME-RHIZOBIA SYMBIOSES

1.1.1 The importance of legume-rhizobia symbioses

Plants require many nutrients but have the greatest demand for nitrogen (N), sulphur (S), phosphorus (P), magnesium (Mg), calcium (Ca) and potassium (K) (Amtmann and Blatt, 2009). Around 1.5% of plant dry weight is made up of N, most of which is incorporated into amino acids (~85%) or nucleic acids (~5%) (Maathuis, 2009). The biggest pool of N in the biosphere is atmospheric dinitrogen (N_2), but this chemically inert form is unusable for most living organisms, including plants, meaning that much of agriculture is reliant on synthetic N fertilisers (Maathuis, 2009; Seefeldt et al., 2009). The manufacture and application of synthetic N fertilisers can account for up to 50% of the costs associated with crop production and unless significant changes in agricultural practice are made, its application will triple over the next 40 years (Gutierrez, 2012; Xu et al., 2012).

N_2 fixation is the reduction of N_2 into ammonia (NH_3) and is exclusive to prokaryotes termed diazotrophs. Rhizobia are diazotrophs that can establish a symbiosis with plants in the Fabaceae family (known as legumes) by initiating and then infecting specialist organs (nodules) that typically form on the roots of legumes (Lodwig and Poole, 2003; Oldroyd and Downie, 2008). During infection, free-living rhizobia differentiate into bacteroids, which are specialists in N_2 fixation and exporting N-compounds to the plant. In return, the plant provides bacteroids with nutrients, including a source of carbon to fuel the energy-intensive process of N_2 fixation (Terpolilli et al., 2012; Udvardi and Poole, 2013). This symbiosis is essential for feeding agriculture with non-synthetic N and so research into the different aspects of legume-rhizobia interactions are of great importance.

1.1.2 Rhizobia and their plant hosts

Rhizobia are phylogenetically disparate and are spread across the α- and β-subclasses of proteobacteria (Masson-Boivin et al., 2009). Numerous genome sequences for rhizobia have now been published (Table 1.1). These genomes are typically large (5.4-9.2 Mb) and rich in transport, metabolic and regulatory genes (Mauchline et al., 2006; Masson-Boivin et al., 2009).

Genome	Reference
Azorhizobium caulinodans ORS571	Lee et al., 2008
Bradyrhizobium japonicum sp. BTAi1 and ORS278	Giraud et al., 2007
Bradyrhizobium japonicum USDA110	Kaneko et al., 2002
Mesorhizobium loti MAFF303099	Kaneko et al., 2000
Rhizobium etli CFN42	Gonzalez et al., 2006
R. leguminosarum bv. vicae 3841	Young et al., 2006
R. leguminosarum bv. trifolium WSM2304	Reeve et al., 2010
Sinorhizobium meliloti 1021	Galibert et al., 2001
Sinorhizobium sp. strain NGR234	Schmeisser et al., 2009

Table 1.1 Published genomes for rhizobia.

Some strains of rhizobia have a very narrow host range, while others are compatible with a wide variety of legumes (Table 1.2). There are several factors that determine host range (Wang et al., 2012). There is the initial dialogue between rhizobium and plant, where rhizobia must be able to identify signals secreted by the plant and the plant must be able to recognise signals exported by rhizobia. There are polysaccharides synthesised by infecting bacteria, which have been speculated to have a role in modulating plant-defences (Hotter and Scott, 1991; Parniske et al., 1994; Simsek et al., 2007; Gibson et al., 2008). Then there is the requirement of certain transporters or enzymes that are essential on some legumes-hosts but not on others, examples of which are provided in this work.

In one study on legume-rhizobia compatibility, a total of 625 strains of *R. leguminosarum* were isolated from nodules that formed on crop legumes *Pisum sativum* (pea) or *Vicia faba* (broad bean) and local, wild legumes including *Vicia hirsuta*, *Viccia cracca*, *Vicia sativa* and *Lathyrus pratensis*. These isolated-strains were tested for their ability to nodulate non-host legumes known to be nodulated by other strains of *R. leguminosarum* e.g. strains isolated from *P. sativum* were tested for their ability to nodulate *V. faba*, *V. hirsuta*, *V. cracca* etc. Collectively, a high proportion of the *R. leguminosarum* isolates were able to nodulate several wild legumes (89%) but only a third could nodulate the crop legume *Vicia faba* (34%) (Mutch and Young, 2004).

Another study characterised *Sinorhizobium* spp. isolated from the field, and focused on strains that could initiate nodulation but were ineffective at N_2 fixation on *Medicago* spp. (Crook et al., 2012). Most incompatibility was found to be host-conditioned, with strains displaying effective N_2 fixation (Fix$^+$) on some hosts and poor N_2 fixation (Fix^{red}) or no N_2 fixation (Fix$^-$) on others. Several accessory plasmids were identified as the cause of defective N_2 fixation but these plasmids were also found to give incompatible strains a competitive advantage during nodule colonisation. Indeed, there are reports of superior rhizobial inoculants being outcompeted by indigenous rhizobial strains that are less-effective at N_2 fixation (Dowling and Broughton, 1986; Triplett and Sadowsky, 1992; Crook et al., 2012). Thus, a better understanding of the factors that make rhizobia both efficient

symbionts and competitive nodule-colonisers is needed to develop more effective inoculants for crop legumes.

Strain of rhizobium	Principal legume-hosts
Azorhizobium caulinodans ORS571	*Sesbania rostrata*
B. japonicum USDA110	*Glycine max* (soybean) *Vigna unguiculata* (cowpea) *Macroptilium atropurpureum* (siratro) *Vigna radiata* (mungbean)
Mesorhizobium ciceri LMS-1	*Cicer arietinum* (chickpea)
Mesorhizobium loti MAFF303099	*Lotus* spp.
R. etli CFN42	*Phaseolus vulgaris* (common bean)
R. leguminosarum bv. viciae 3841	*Pisum* spp. (pea) *Vicia* spp. (e.g. broad-bean and vetch) *Lathyrus* spp. (e.g. meadow vetchling) *Lens* spp. (e.g. lentils)
R. leguminosarum bv. trifolium WSM2304	*Trifolium* spp. (clover)
R. leguminosarum bv. phaseoli 4292	*Phaseoli vulgaris* (common bean)
Sinorhizobium meliloti 1021	*Medicago* spp. (alfalfa and barrel medic)

Table 1.2 Host ranges of nine strains of rhizobia.

1.2 STEPS LEADING TO LEGUME-RHIZOBIA SYMBIOSIS

1.2.1 Communication in the rhizosphere: flavonoids and Nod factors

The rhizosphere is the local environment influenced by living roots, where many interactions between soil-dwelling-microorganisms and the plant take place. Early communication between rhizobia and legumes occurs in the rhizosphere and involves the secretion of flavonoids from plant roots (Fig 1.1). Flavonoids are polycyclic aromatic compounds that attract rhizobia to the rhizosphere (Cooper, 2007; Faure et al., 2009) and are released near root tips and at the emerging root hair zone i.e. the site for bacterial-infection (Hartwig et al., 1990; Graham, 1991; Zuanazzi et al., 1998; Abdel-Lateif et al., 2012).

It is generally accepted that the bacterial LysR-transcriptional regulator, NodD, is the flavonoid-receptor, although no direct biochemical binding has been reported (Peck et al., 2006). In *R. leguminosarum*, NodD is localised to the cytoplasmic membrane, where the inducing flavonoid accumulates (Recourt et al., 1989; Perret et al., 2000). The ligand-binding domain is located at the N-terminus of NodD and regulates the activity of the C-terminal DNA binding domain, which binds highly conserved *nod*-boxes found upstream of genes involved in Nod factor production (Gibson et al., 2008).

Common *nod* genes (e.g. *nodABC*) are responsible for the synthesis of the core structure of Nod factor i.e. an N-acetylated, chitin oligomeric backbone with a fatty acyl chain (Roche et al., 1996). Other *nod* gene products include enzymes that modify the core structure and thus drive Nod factor diversity (Perret et al., 2000). One example of how a Nod factor-modifying enzyme can affect host-range is the requirement of NodE by *R. leguminosarum* for nodulation of certain cultivars of *P. sativum* (Li et al., 2011).

Nod Factor Receptors (NFRs) in root cells of legumes detect Nod factor and are essential for nodule formation on *L. japonicus*, *M. truncatula*, *G. max* and *P. sativum* (Madsen et al., 2003; Oldroyd and Downie, 2008; Zhukov et al., 2008; Indrasumunar

et al., 2010; Indrasumunar et al., 2011; Broghammer et al., 2012). NFRs are receptor-like kinases with N-acetylglucosamine-binding lysine (LysM) motifs in their extracellular domain and despite their long established requirement, only recently has binding of Nod factors by NFRs been demonstrated (Broghammer et al., 2012). Perception of Nod factors by NFRs, activate signalling pathways that induce important oscillations in Ca^{2+} levels in the nuclear region of the plant cell (Oldroyd and Downie, 2008; Murray, 2011).

1.2.2 Signal transduction and nodule formation

The signalling pathway that utilises Ca^{2+} oscillations as a second messenger is known as the common symbiosis pathway and is one of the earliest responses to Nod factor (Murray, 2011). A calcium and calmodulin dependent protein kinase (CCaMK) is involved in perceiving the Ca^{2+} signal and relaying it to the downstream components (transcription factors) involved in initiating nodule formation (Oldroyd and Downie, 2008; Murray, 2011; Oldroyd et al., 2011).

Events triggered by Nod factor perception induce mitotic cell division in the root cortex or sub-epithelial cell layer, leading to formation of the nodule meristem (nodule primordium). Induction of cell division is correlated with increases in plant hormones auxin, cytokinin, gibberellins and brassinosteroid levels (Murray, 2011). There are several different types of nodules that can form, including indeterminate and determinate nodules. The best characterised legumes that form indeterminate nodules belong to galegoid clade (e.g *Medicago*, *Pisum and Vicia)*. As a consequence of a persistent meristem, indeterminate nodules have an elongated-shape and exhibit four developmental zones (Fig 1.1). The best characterised legumes that form determinate nodules belong to the phaseoloid (e.g. *G. max* and *P. vulgaris*) or robinioid clade (e.g. *Lotus japonicus*). These nodules have a transient meristem and are spherical as a consequence (Fig 1.1) (Ferguson et al., 2010; Oldroyd et al., 2011; Kondorosi et al., 2013).
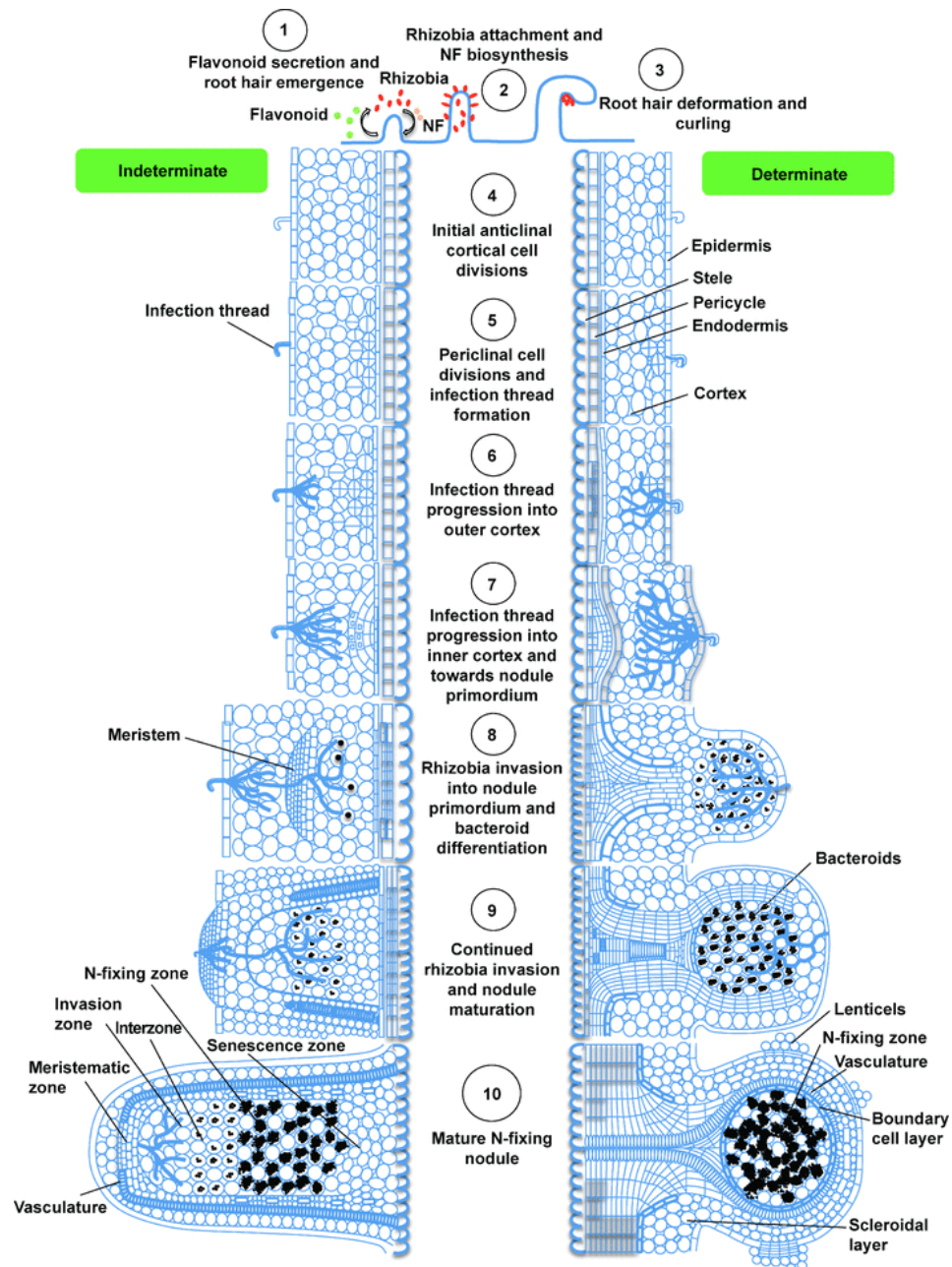
Fig 1.1 Model showing developmental stages of indeterminate and determinate nodules. Flavonoids secreted by root hairs attract rhizobia and stimulate them to produce Nod factor (1-2). Secreted Nod factor induces root hair curling, trapping the rhizobia (3). An infection thread initiates from the infection pocket and progresses towards the nodule primordium (5-7). In **indeterminate** nodules, a meristem continually develops and gives rise to new plant cells. As these new cells mature they become infected by rhizobia, leading to successive zones of rhizobial invasion and differentiation. **Determinate** nodules do not have a persistent meristem resulting in a homologous population of bacteroids. Figure reproduced from Ferguson *et al.*, 2010.

1.2.3 Infection thread formation and colonisation

To access nodule primordia, rhizobia must breach the root epidermis by passing through a plant-made structure (the infection thread) that forms inside growing root hairs (Figs 1.1 and 1.2). A parallel pathway initiated by Nod factor, independently of CCaMK, is required for root-hair deformation (Murray, 2011; Oldroyd et al., 2011). Nod factors cause growing root hairs to bend back upon themselves and this curling traps the Nod factor-producing rhizobia (Fig 1.1). Growth of the infection thread is initiated in the infection pocket by invagination of the root hair cell wall (and membrane) and localised cell wall-degradation by a plant synthesised pectate lyase (Xie et al., 2012).

Certain polysaccharides synthesised by the invading bacteria are required for infection thread formation and nodule colonisation (Gage, 2004). The exopolysaccharide (EPS) succinoglycan, is speculated to suppress the plant defence response (Hirsch, 1999; Gibson et al., 2008) and mutants that are unable to make succinoglycan are defective at initiating infection threads (Finan et al., 1985; Leigh et al., 1985; van Workum et al., 1998). Synthesis of cyclic β glucans in *M. loti* is also speculated to modulate the host defence response by reducing the production of antimicrobial phytoalexins in *L. japonicus* and may also have a role in attachment to root hairs (Dylan et al., 1990; D'Antuono et al., 2008; Gibson et al., 2008). Surface lipopolysaccharides (LPS) have also been shown to modulate the defence response by suppressing the release of reactive oxygen species (ROS) and have an important role in stabilising the membrane during exposure to stressful environments (Albus et al., 2001; Scheidle et al., 2005; Haag et al., 2013).

Extension of the infection thread structure is synchronous with the growth rate of the enclosed bacterial column (Gage, 2002). Mixed populations of bacteria in the infection thread can occur but the frequency at which this happens is unknown (reported to vary between 12-74% in laboratory conditions) (Johnston and Beringer, 1975; Denison, 2000; Gage, 2002; Friesen and Mathias, 2010). Only bacteria near the extending tips of the infection thread proliferate, with the bacteria at the base of the infection thread remaining static (Gage et al., 1996; Gage, 2004). It is feasible

that strains in mixed infection threads are in fierce competition as only the faster-growing (more competitive) strain that occupies the terminus of the infection thread will go on to populate the nodule (Gage et al., 1996).

The architecture of the infection threads change as they grow towards the nodule primordium. As the nodule grows, the infection thread chasing the growing meristem becomes highly branched and forms an infection zone (located at the nodule tip). Branching of the infection thread (Fig 1.2) during its growth increases the distribution of infected nodule cells (Gage, 2004; Monahan-Giovanelli et al., 2006).
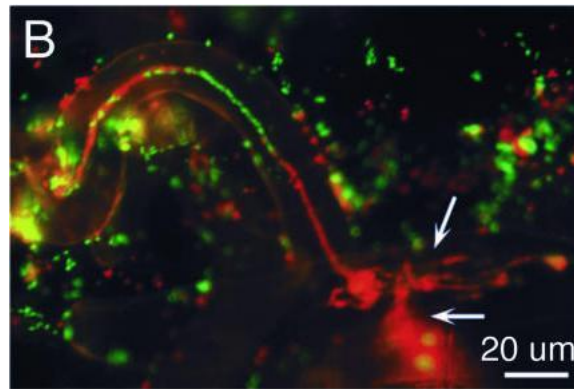
Fig 1.2 Infection thread with a mixed population of red- and green-fluorescent bacteria. Top arrow indicates infection thread branching and bottom arrow indicates penetration into the underlying cell. Reproduced from Gage, 2002.

1.2.4 Bacterial release from the infection thread

Bacteria exit the infection thread via endocytosis but what triggers this is unknown, although it must involve a remodelling of the cell wall (Brewin, 2004; Jones et al., 2007). The unwalled membrane that extends from the infection thread is known as an infection droplet and the bacteroid-containing compartment that forms is known as the symbiosome (Fig 1.3) (Brewin, 2004). In indeterminate nodules, there is typically only one bacteroid per symbiosome, in contrast to determinate nodules, where 8-12 bacteroids share the same symbiosome (Fig 1.7) (Brewin, 2004). What

bacteroids in indeterminate and determinate nodules have in common is that every nutrient they acquire must first cross the symbiosome membrane.
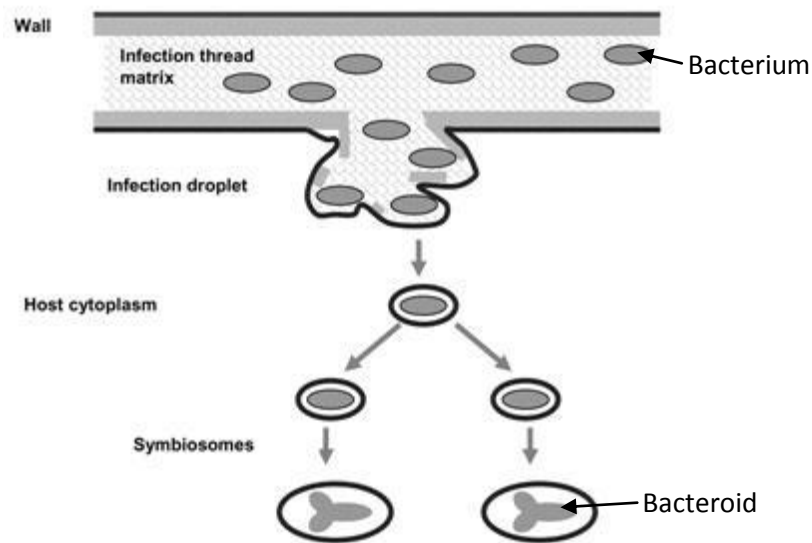
Fig 1.3 Diagram showing the release of rhizobia from the infection thread. Reproduced from Brewin, 2004.

1.3 N_2 FIXATION AND NUTRIENT SHARING

1.3.1 N_2 fixation and transport of N-compounds to the plant

The N_2 reducing enzyme, nitrogenase, consists of NifDK and NifH. NifD and NifK form a heterotetrameric complex that contains the essential iron molybdenum cofactor (FeMoCo) and a P-cluster (a [8Fe-7S] cluster). NifH is a homodimer that contains a [4Fe-4S] cluster and sites for MgATP binding and hydrolysis (Dixon and Kahn, 2004; Rubio and Ludden, 2008). N_2 reduction is an energy-intensive process requiring 16 molecules of MgATP [$N_2 + 8$ e$^-$ + 8 H$^+$ + 16 MgATP $\rightarrow$ 2 NH$_3$ + H$_2$ + 16 MgADP + 16 P$_i$]. In addition to N_2 (N≡N), additional triple-bonded molecules can serve as a substrate for nitrogenase, including acetylene (H-C≡C-H), which is widely used to measure nitrogenase activity (see methods 2.6.4) (Rubio and Ludden, 2008).

Nitrogenase is highly sensitive to oxygen, where O_2 concentrations greater than 57 nM, inhibit its activity (Kuzma et al., 1993; Dixon and Kahn, 2004). Sensitivity is partly conferred by a change in the oxidation state of the Fe centres within the NifDK complex, [8Fe-7S] cluster and FeMoCo, and inactivation of [4Fe-4S] in NifH (Gallon, 1992; Dixon and Kahn, 2004). The nodule provides protection for nitrogenase against O_2 through a cortical diffusion barrier, generating an O_2 gradient that decreases from the nodule apex to the interzone regions (where N_2 fixation takes place) (Fig 1.4) (Kuzma et al., 1993; Batut and Boistard, 1994; Soupene et al., 1995).

The necessity for a low O_2 environment must be balanced with the O_2 requirement of ATP synthesis and this balance is met by a high abundance of plant-synthesised leghamoglobins found in the cytoplasm of infected plant cells (Downie, 2005). Oxygen-binding leghaemoglobins have a fast O_2 association rate coupled with a slow dissociation, which enables them to buffer free oxygen in the nanomolar range. Consequently, inactivation of the oxygen-sensitive nitrogenase is avoided whilst an oxygen flux for respiration is maintained (Appleby, 1984; Downie, 2005; Ott et al., 2005). Rhizobia also synthesise an alternative cytochrome *cbb*$_3$-type oxidase that has a high affinity for O_2 to allow respiration under low O_2 (discussed in 1.4.6).
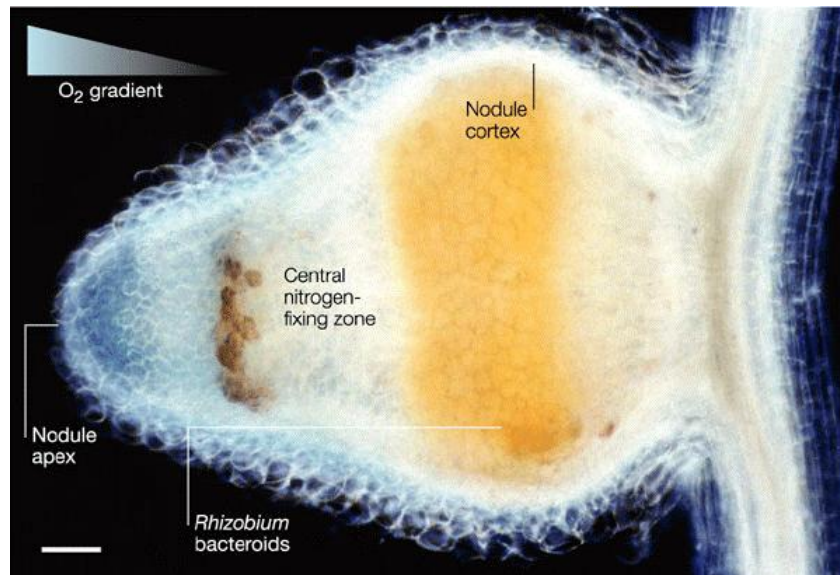
Fig 1.4 Longitudinal O_2 gradient in a nodule. The cortical diffusion barrier means the main route of O_2 is through the nodule apex. Reproduced from Dixon and Kahn, 2004.

It is not strictly known how the end product of N_2 reduction, NH_3, is exported across the bacteroid membrane (Fig 1.5). Rhizobia do encode NH_4^+ transporters belonging to the AMT (ammonium transporters) family but their expression is downregulated in bacteroids (Karunakaran et al., 2009). Instead, NH_4^+ might cross the bacteroid membrane by diffusion across the lipid bilayer or via non-selective, unidentified protein channels (Udvardi and Poole, 2013).

In plants, both an NH_4^+ channel (Niemietz and Tyerman, 2000) and a cation channel (Tyerman et al., 1995) have been reported to transport NH_4^+ across the symbiosome membrane. NH_4^+ assimilation is shutdown in bacteroids so the plant is responsible for NH_4^+ assimilation, which involves glutamine synthetase (GS), glutamate synthase (GOGAT) and aspartate amino transferase (Fig 1.5) (Udvardi and Poole, 2013). For indeterminate nodules, the amino acid asparginine is mainly exported out of the nodule and into the plant shoot (White et al., 2007).

1.3.2 Transport of nutrients to the bacteroid

The carbon used by bacteroids derives from sucrose made by the plant and metabolised into dicarboxylates in the cytoplasm of infected plant cells (Fig 1.5) (Kouchi and Yoneyama, 1984; Streeter, 1995; Udvardi and Poole, 2013). Malate is the primary dicarboxylate that is transported across the bacteroid membrane by the dicarboxylate (Dct) system (Fig 1.5) (Lodwig and Poole, 2003; Yurgel and Kahn, 2004). Dicarboxylates are then metabolised by the TCA cycle and for this reason, enzymes in TCA cycle are essential for N_2 fixation; although, there are some exceptions and variations between different species of rhizobia (reviewed in Terpolilli *et al.*, 2012).

Homocitrate is also required for N_2 fixation as it is a critical cofactor of nitrogenase (Hoover et al., 1989). Free-living diazotrophs (such as *Azotobacter vinelandii* and *Klebsiella pneumonia*) can synthesise their own homocitrate through the condensation of 2-oxoglutarate and acetyl CoA by the enzyme homocitrate synthase (NifV) (Terpolilli et al., 2012). Most symbiotic rhizobia however, do not carry a copy of *nifV* and consequently must obtain homocitrate from the plant. The

homocitrate synthase in plants is encoded by *FEN1* (Fig 1.5) (Hakoyama et al., 2009) but how homocitrate is transported across the symbiosome and bacteroid membrane is unknown.

The list of plant-encoded, nodule-specific transporters that supply bacteroids with essential nutrients is growing and includes several metal transporters (see 1.4.5). In addition to metal transporters, a plant-encoded sulphate transporter, SST1, has also been reported as essential for symbiotic N_2 fixation (Fig 1.5) (Krusell et al., 2005).

The list of bacterial-encoded transporters required for nutrient uptake during symbiosis is more extensive but still far from complete. The importance of the Dct transport system has already been discussed. Two broad-specificity ABC-type transporters, AapJQPM and BraDEFGC, which import branched-chain amino acids are also essential for N_2 fixation (Fig 1.5) (Hosie et al., 2002; Lodwig et al., 2003; Prell et al., 2010). Their requirement is a consequence of a shutdown in amino acid synthesis in bacteroids (referred to as symbiotic auxotrophy), rendering bacteroids dependent upon a supply of branched-chain amino acids from the plant (Prell et al., 2009).
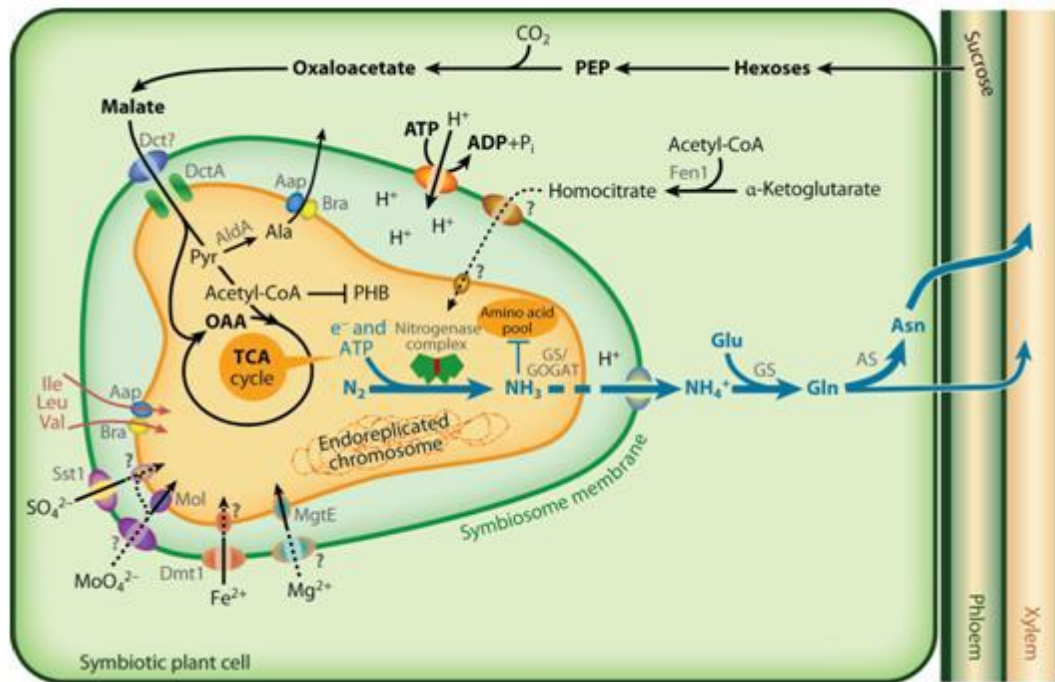
Fig 1.5 Model showing transport and metabolism of nutrients within an infected plant cell. Bacteroid (orange) contained within the symbiosome membrane. Reproduced from Udvardi and Poole, 2013.

1.4 PHYSIOLOGICAL AND REGULATORY RESPONSES OF *R. LEGUMINOSARUM* DURING BACTEROID DEVELOPMENT

Processes integral to N_2 fixation in mature bacteroids have been intensively studied (Udvardi and Poole, 2013). Less is known about how rhizobia adapt to the nodule environment during bacteroid development, the processes required for a free-living cell to differentiate into a bacteroid or how differentiation is regulated.

The remainder of this chapter will discuss what is known about the environment of the nodule and the processes that rhizobia require to colonise it. This will include: resistance to oxidative stress, organic peroxides, antimicrobial peptides and toxic metabolites; uptake and utilisation of metals and other nutrients; and adaptations to low O_2.

1.4.1 Oxidative stress

Reactive oxygen species (ROS) include superoxide anions ($O_2^{.-}$), hydrogen peroxide (H_2O_2) and hydroxyl radicals ($HO^{.}$). ROS inflicts destruction by damaging Fe-S clusters, disabling mononuclear-Fe enzymes, damaging DNA and disrupting lipids through peroxidation (Imlay, 2013). They are by-products of aerobic metabolism but also have a role as signalling molecules and as a defence response against pathogens (Nanda et al., 2010). ROS are also a prominent feature of the nodule environment (Pauly et al., 2006; Gibson et al., 2008; Soto et al., 2009; Nanda et al., 2010).

NADPH oxidases (NOx) represent the major ROS generating system in plants and play a crucial role in the oxidative burst (primarily $O_2^{.-}$ and H_2O_2) during plant-pathogen interactions (Nanda et al., 2010). ROS generation by NOx homologues in *M. truncatula* appear to be required in the early stages of symbiosis, as their inactivation suppressed root hair curling and infection thread formation (Lohar et al., 2007; Peleg-Grossman et al., 2007). Reduction of Nitroblue tetrazolium, detection of cerium perhydroxide deposits and ROS-sensitive fluorescent dyes have confirmed the presence of ROS in infection threads and roots hairs (Fig 1.6) (Santos et al., 2001; Ramu et al., 2002; Rubio et al., 2004; Pauly et al., 2006; Lohar et al., 2007; Cardenas et al., 2008). Nod factor has been reported to cause both a rapid induction of ROS production (Fig 1.6) (Ramu et al., 2002; Cardenas et al., 2008) and reduction in ROS levels at later time points (Shaw and Long, 2003; Lohar et al., 2007; Nanda et al., 2010).

The function of ROS in legume-rhizobia symbioses is not clear. They might mediate infection thread development by loosening the cell wall to allow cell expansion, or are needed for the cross-linking of glycoprotenis to stiffen cell walls and inhibit expansion (Gapper and Dolan, 2006; Gibson et al., 2008; Soto et al., 2009). Supporting this, overexpression of the catalase-encoding *katB* gene (catalases catalyse the degradation of H_2O_2 to H_2O and O_2) in *S. meliloti* delayed nodulation of *M. sativa* and resulted in enlarged infection threads (Jamet et al., 2007). ROS may also limit bacterial invasion by causing an increasing proportion of infection threads to abort after the first nodule primordia have been induced (Vasse et al., 1993). ROS

causes infection thread abortion by inducing a hypersensitive reaction (an accumulation of phenolic compounds and proteins involved in the defence response), leading to necrosis of both the plant cell and bacteria. By controlling bacterial invasion, the plant can balance its nitrogen requirements with the energy it invests into symbiosis (Reid et al., 2011). An abundance of H_2O_2 has also been reported in the senescent zone of indeterminate nodules, suggesting a role of ROS in senescence (Rubio et al., 2004)

How rhizobia defend themselves against ROS during bacteroid development is well characterised. One of the first bacterial enzymes reported as essential for ROS-resistance during symbiosis was SodA (superoxide dismutase) in *S. meliloti* (Santos et al., 1999; Santos et al., 2000). Superoxide dismutases are metalloenzymes that catalyse the conversion of superoxide into O_2 and H_2O_2. SodA in *S. meliloti* is `cambialistic', meaning it can use either Fe^{2+} or Mn^{2+} as a cofactor. In *S. meliloti*, disruption of *sodA* caused only moderate sensitivity to oxidative stress but on *M. sativa*, its absence resulted in poor nodulation and abnormal infection. Bacteroid development of the mutant was blocked in the infection zone and those bacteroids that did reach the plant cytoplasm underwent rapid senescence.

In *R. leguminosarum*, SodA was found to be exported to the periplasm and is thought to play an important role in the protection of membrane lipids and periplasmic proteins from extracellular superoxide radicals (Krehenbrink et al., 2011). However, SodA is not essential for N_2 fixation in *R. leguminosarum-P. sativum* symbiosis (personal communication, Allan Downie JIC).

The requirement of catalases has also been studied in legume-rhizobia symbioses. There are three classes of catalases: monofunctional heme-containing catalases (most common in nature), bifunctional heme-containing catalase-peroxidases and the Mn-containing catalases (Chelikani et al., 2004). *S. meliloti* encodes two monofunctional catalases (KatA and KatB) and a bifunctional catalase (KatC). A *katA katC* double mutant was released from infection threads but only fixed N_2 at ~25% compared to the wild type; this was due to a sparse distribution of bacteroids in plant cells, many of which appeared senescent (Sigaud et al., 1999; Jamet et al., 2003). In contrast, a

katB katC double mutant exhibited poor nodulation and abnormal infection, resulting in plant cells devoid of bacteroids (Jamet et al., 2003).

In *M. loti*, research into the monofunctional catalase, KatE, and bifunctional catalase, KatG, discovered that disruption of *katE* resulted in a 50-60% reduction in N_2 fixation on *L. japonicus* (Hanyu et al., 2009). The stage at which bacteroid development was impeded was not investigated but *katE* was highly expressed in the infection threads.

Bifunctional heme-containing catalase-peroxidases (KatG) have also been studied in *R. etli* and *B. japonicum*. KatG was important for H_2O_2-resistance in *R. etli* but was not required for N_2 fixation on *P. vulgaris* (and no symbiotic phenotype was reported to be caused by the disruption of *katG* in *B. japonicum*) (Vargas Mdel et al., 2003; Panek and O'Brian, 2004).
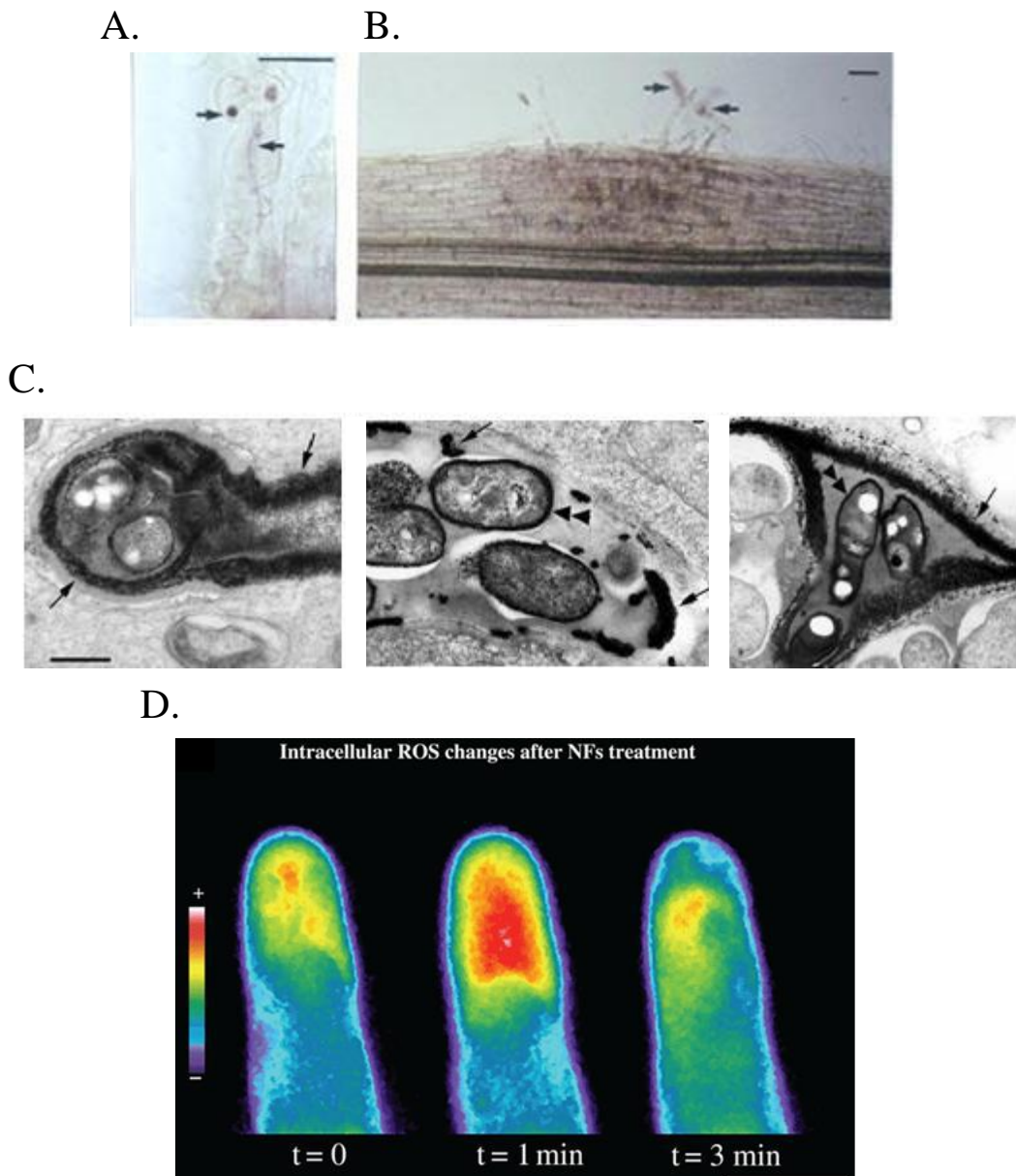
Fig 1.6 ROS shown in infection thread (A and C) and root hairs (B and D). In (A) and (B) arrows indicate the dark formazan precipitate formed by reduction of Nitroblue tetrazolium by superoxide. In (C), nodules sections were perfused with cerium chloride, which allowed H_2O_2 to be localised by the presence of electron-dense precipitates of cerium perhydroxide; cerium perhydroxides are indicated by a single arrow (when in the walls of the infection thread) or by double arrow heads (when surrounding bacteria). In (D), root hairs were loaded with ROS-sensitive fluorescent dye and treated with Nod factor after t = 0. Reproduced from Santos *et al*., 2001 (A and B), Rubio *et al*., 2004 (C) and Cardenas *et al*., 2008 (D).

1.4.2 Organic peroxides

Organic hydroperoxides (ROOH) are present as by-products of metabolism, pollutants and as antimicrobials generated by plants, fungi and bacteria (Chuchue et al., 2007; Zuber, 2009; Llewellyn et al., 2011). Enzymes that detoxify organic peroxides belong to the peroxiredoxin family or the OsmC/Ohr family.

The peroxiredoxin family (Prxs) are thiol-dependent peroxidises that catalyse the reduction of H_2O_2, organic peroxides and peroxynitrite. They are present in all kingdoms of life and the best characterised member is the alkyl hydroperoxidase reductase (Ahp), consisting of a catalaytic subunit (AhpC) and flavoprotein (AhpF) (Bsat et al., 1996; Rocha and Smith, 1999; Mongkolsuk et al., 2000; Poole, 2005; Poole et al., 2011). Despite the ability of Ahp to detoxify H_2O_2 and organic peroxides (Seaver and Imlay, 2001) little is known about their role in rhizobia accept that Ahp was not essential for H_2O_2 detoxification in *B. japonicum* (Panek and O'Brian, 2004).

The OsmC/Ohr family is exclusive to bacteria (Cussiol et al., 2003; Fontenelle et al., 2011). Genes encoding Ohr (Organic Hydroperoxide Resistance) are specifically induced by organic hydroperoxides, not by other oxidants or stresses, furthermore, disruption of *ohr* only causes hypersensitivity to organic hydroperoxides (Atichartpongkul et al., 2001). Genes encoding OsmC (Osmotically inducible) are not induced by organic peroxides but are induced by ethanol and osmotic stress instead (Fontenelle et al., 2011); disruption of *osmC* can lead to sensitivity to both H_2O_2 and organic hydroperoxides (Conter et al., 2001; Lesniak et al., 2003).

Organic peroxides are highly prominent during bacterial invasion of plant tissue (Croft et al., 1993; Jalloul et al., 2002) and defences against organic peroxides have been studied in plant pathogens *Xanthomonas campestris* (Mongkolsuk et al., 1998; Sukchawalit et al., 2001; Vattanaviboon et al., 2002; Klomsiri et al., 2005) and *Agrobacterium tumefaciens* (Chuchue et al., 2007). Organic peroxide defences have also been studied in a range of human pathogens (Fuangthong et al., 2001; Atack et al., 2008; Saikolappan et al., 2009; Wolfram et al., 2009; Llewellyn et al., 2011;

Caswell et al., 2012). To this date, only one investigation has explored the role of organic hydroperoxide resistance in legume-rhizobia symbioses (see Chapter seven).

1.4.3 Antimicrobial secondary metabolites

Plants produce an array of secondary metabolites (non-essential for the metabolic processes of the plant) to defend themselves against microbial attack or insect/mammal predation (Dixon, 2001) but the identity, variety and abundance of secondary metabolites in nodules has not been comprehensively defined (Brechenmacher et al., 2010). The phenolic metabolite salicylic acid is involved in plant defences and has been studied in legume-rhizobia symbioses. Accumulation of salicylic acid was shown to be induced by rhizobia defective for Nod factor production (Martinez-Abarca et al., 1998; van Spronsen et al., 2003) and reduction of salicylic levels in *M. truncatula* and *L. japonicus*, by overexpression of a salicylate hydroxylase, resulted in enhanced nodulation and infection (Stacey et al., 2006). Therefore, it is possible that salicylic acid has both a role in selecting compatible symbionts and limiting infection.

The system bacteria typically use to evade toxic secondary metabolites is an efflux system, which pumps antimicrobial compounds out of the cell. Several efflux systems have been reported to be important to legume-rhizobia symbioses, suggesting the presence of antimicrobial compounds in the nodule. On *G. max*, disruption of genes encoding the BdeAB efflux system in *B. japonicum*, caused a ~70% reduction in N_2 fixation compared to the wild type (Lindemann et al., 2010). Nodulation was not affected but fewer mutant bacteroids could be isolated from nodules c.f. wild type. The same mutant had no symbiotic defect on the alternative hosts *V. unguiculata* and *V. radiata*, suggesting antimicrobial compounds in the nodule vary between plants. In *S. meliloti*, *smeAB* encodes an efflux system that was required for competition during nodulation (Eda et al., 2011) and in *R. etli*, deletion of *rmrAB*, encoding an efflux system, resulted in reduced nodulation (~40%) on *P. vulgaris* (Gonzalez-Pasayo and Martinez-Romero, 2000).

1.4.4 Antimicrobial peptides

A large class of nodule-specific cysteine-rich (NCR) antimicrobial peptides are synthesised by legumes belonging to galegoid clade and are responsible for some of the profound differences seen between bacteroids that develop in nodules formed on galegoid-legumes and bacteroids that develop in nodules formed on phaseoloid- or robinioid-legumes (Mergaert et al., 2006; Van de Velde et al., 2010; Kondorosi et al., 2013). Bacteroids from galegoid-legumes are swollen (Table 1.3 and Fig 1.7), undergo endoreduplication, have increased membrane permeability and are unable to reproduce. Bacteroids from phaseoloid- or robinioid-legumes are non-swollen (Table 1.3 and Fig 1.7), do not endoreduplicate, show no increased permeability and are able to reproduce (Mergaert et al., 2006; Oono et al., 2009; Kondorosi et al., 2013).

Legume Species	Legume Clade	Nodule type	Bacteroid morphology
P. sativum	Galegoid	Indeterminate	**Swollen**
V. faba	Galegoid	Indeterminate	**Swollen**
V. hirsuta	Galegoid	Indeterminate	**Swollen**
M. sativa	Galegoid	Indeterminate	**Swollen**
M. truncatula	Galegoid	Indeterminate	**Swollen**
P. vulgaris	Phaseoloid	Determinate	**Non-swollen**
G. max	Phaseoloid	Determinate	**Non-swollen**
L. japonicus	Robinioid	Determinate	**Non-swollen**

Table 1.3 Table showing examples of legumes species belonging to the galegoid, phaseoloid or robinioid clades. Nodules formed on galegoid-legumes are indeterminate and house **swollen** bacteroids, whereas, nodules formed on phaseoloid- or robinioid- legumes are determinate and house **non-swollen** bacteroids.

Swollen bacteroids   **Non-swollen bacteroid**
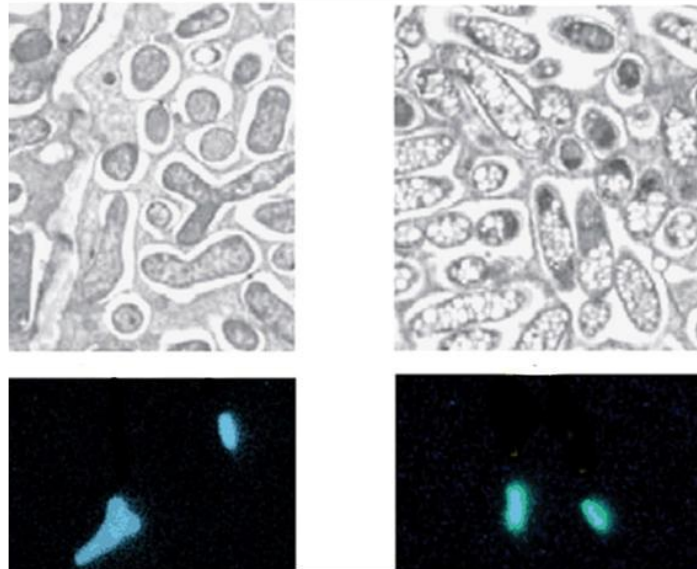
Fig 1.7 Morphology of swollen bacteroids from indeterminate and non-swollen bacteroids from determinate nodules. In indeterminate nodules there is one bacteroid per symbiosome (left) in contrast to determinate nodules, where symbiosomes contain 8-12 bacteroids (right). Reproduced from Oono *et al*., 2009.

The *M. truncatula* genome encodes 593 NCR peptides (Young et al., 2011) and more than 300 NCR peptide-encoding genes have had their expression confirmed (Mergaert et al., 2003). Genes encoding NCR peptides are differentially expressed during nodule development with an early induction of some (7 days post inoculation) and a later induction of others (13 days post inoculation) (Mergaert et al., 2003). Microdisection of nodules by laser-capture has been used to spatially define the expression of these NCR genes (Limpens et al., 2013) and identified several genes that were induced in the infection zone, with induction of some occurring in the distal infection zone (situated near the meristem) and others in the proximal infection zone (situated near the N_2 fixation zone).

NCR peptides contain an N-terminal hydrophobic signal peptide that targets them to the plant cell secretory pathway. Peptides entering this pathway have four possible

destinations: the endoplasmic reticulum (ER), the vacuole, the symbiosome or the extracellular space (Mergaert et al., 2003). A *M. truncatula dnf1-1*mutant is defective for a nodule-specific single peptidase complex (SPC), which cleaves nascent polypeptides destined for intracellular compartments or the extracellular matrix (Wang et al., 2010). NCR peptides have been shown to be targeted to bacteroids but in a *M. truncatula dnf1-1* mutant, NCR peptides were absent from the bacteroid extract and colocalised with the ER, suggesting a role of the SPC in NCR peptide targeting (Van de Velde et al., 2010). The mode of action for NCR peptides is not fully understood but they have been found to target both the membrane and the bacterial cytosol (Van de Velde et al., 2010). NCR peptides have a positive charge (cationic peptide) that has been suggested to be required for membrane permeabilisation (Haag et al., 2012; Haag et al., 2013).

BacA is predicted to form the transmembrane domain of an ABC-type transport system in bacteria and is required for protection against NCR peptides (Haag et al., 2013). An *S. meliloti* strain carrying a mutation in *bacA* was hypersensitive to NCR peptide-247 (NCR247) and other antimicrobial substances e.g. EtOH and SDS (Ichige and Walker, 1997; LeVier and Walker, 2001; Haag et al., 2011). On *M. truncatula,* a *S. meliloti bacA* mutant senesced after it was released from infection droplets (Fig 1.8) (Glazebrook et al., 1993; Haag et al., 2013). However, on the *M. truncatula dnf1-1* mutant, BacA was not required for bacterial survival (Haag et al., 2011), suggesting that *in planta*, BacA is required for resistance to NCR peptide.

Further evidence comes from a study of BacA in strains *R. leguminosarum* bv. phaseoli 4292 and *R. leguminosarum* bv. viciae A34 (Karunakaran et al., 2010). These two strains share the same core-genome but differ in their Sym plasmids (encoding genes important for host-selection) and as a consequence, one strain is able to initiate determinate nodules on *P. vulgaris* (4292) and the other strain can initiate indeterminate nodules on *P. sativum* (A34) (Downie et al., 1983). It was shown that in *R. leguminosarum* bv. phaseoli 4292, BacA was not required for N_2 fixation on *P. vulgaris* but was required in *R. leguminosarum* bv. viciae A34 for N_2 fixation on *P. sativum* (Fig 1.8). As NCR peptides were present in *P. sativum* but not in *P. vulgaris* (Table 1.3), the data agree with a BacA being required for resistance to NCR peptides. BacA has also been shown to be dispensable for bacteroid

development in other legumes that do not produce NCR peptides (Karunakaran et al., 2010; Maruya and Saeki, 2010).
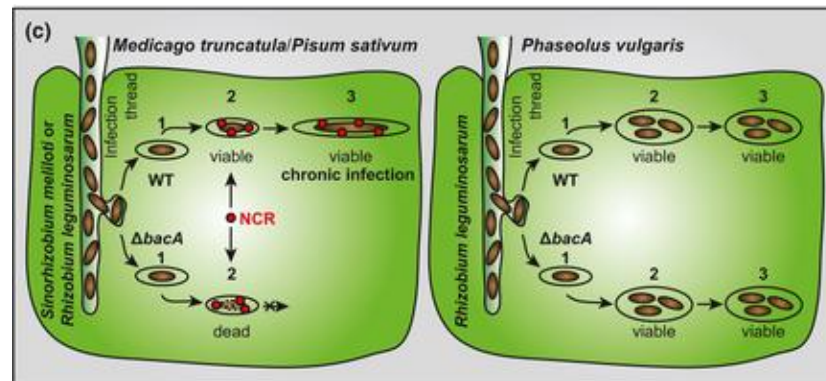
Fig 1.8 Requirement of BacA on NCR peptide-producing *M. truncataula*/*Pisum sativum* or non-NCR peptide producing *P. vulgaris*. Reproduced from Haag *et al*., 2011.

It is not known how BacA confers resistance to NCR peptides but it might provide protection via its ability to import peptides. Disruption of *bacA* in *S. meliloti* caused increased resistance to several classes of antibiotics with an intracellular target (Ichige and Walker, 1997; Ferguson et al., 2002; Karunakaran et al., 2010) and it has been shown that uptake of the peptides Bac7 and bleomycin is dependent on BacA (Marlow et al., 2009; Wehmeier et al., 2010). One model that explains how uptake of antimicrobial peptides could confer resistance has been described for the human pathogen *Haemophilus influenzae* (Shelton et al., 2011). In *H. influenzae*, the *sap* (sensitivity to antimicrobial peptides) operon encodes an inner membrane ABC-type transport system that has been shown to import and confers resistance to certain antimicrobial peptides. The same antimicrobial peptides tested for transport were also shown to be degraded by proteases in the cytoplasm of *H. influenza* and so it was proposed that the Sap transporter imports antimicrobial peptides to the cytoplasm where they can be subsequently inactivated (Shelton et al., 2011).

1.4.5 Requirement and transport of metals

Despite metals being essential to processes integral to nodule colonisation and N_2 fixation, little is known about how and when these metals are acquired. What is known about transport of iron (Fe), zinc (Zn), molybdate (Mo), manganese (Mn) and magnesium (Mg) during symbiosis is summarised below.

Since the evolution of oxygenic-photosynthesis, the predominant state of Fe switched from soluble ferrous iron (Fe^{2+}) to extremely insoluble ferric iron (Fe^{3+}) (Andrews et al., 2003). To increase the solubility of Fe^{3+}, plants produce various molecules, like nicotianamine and citrate, to form Fe-chelator complexes (Conte and Walker, 2011; Takanashi et al., 2013). A gene encoding a Fe-citrate transporter in *L. japonicus, LjMATE1*, was found to be specifically induced during nodule formation and its suppression caused a high accumulation of Fe in the nodule-root junction but low amounts of Fe in whole nodule. Suppression of this gene led to poor plant growth as a result of poor N_2 fixation (~50% reduced compared to wild type). It was suggested that LjMATE mediates Fe-citrate transport by releasing Fe-citrate into the apoplast of nodules (Takanashi et al., 2013).

One Fe^{2+} transporter (GmDmt1) belonging to the Nramp/Dmt1 family, has been found localised to the symbiosome membrane in *G. max* (Kaiser et al., 2003). Another plant-encoded transporter that is expressed in infected-nodule cells is SEN1, identified in *L. japonicus* SEN1 is a hypothetical Fe/Mn transporter (homologous to vacuolar Fe/Mn transporters in *Saccharomyces cerevisiae* and *Arabidopsis thaliana*) (Hakoyama et al., 2012). Disruption of *SEN1* caused a Fix[-] phenotype, with nodules containing small and senescent bacteroids (Hakoyama et al., 2012). Further work is needed to confirm SEN1 as a Fe transporter and to identify its precise location in the nodule. The data mentioned, together with the spatio-temporal distribution of Fe in *M. truncatula* nodules detected by synchrotron X-ray fluorescence, come together in a simple model that describes how Fe is delivered to symbiosome (Rodriguez-Haas et al., 2013). In this model Fe is released from the vasculature tissue into the apoplast of the infection zone. Infected cells subsequently import Fe from the apoplast into

the cytosol. Once in the cytosol, Fe is transported into the symbiosome (Rodriguez-Haas et al., 2013).

Fe-requiring metalloproteins in bacteroids include nitrogenase and cytochromes. Regulation of Fe homeostasis has been studied in *R. leguminosarum*, *S. meliloti* and *B. japonicum* (Hamza et al., 2000; Chao et al., 2005; Viguier et al., 2005; Rodionov et al., 2006; Todd et al., 2006; Yang et al., 2006; Johnston et al., 2007; Small et al., 2009; Hohle and O'Brian, 2010) but will not be discussed here (for a review see Johnston *et al.*, 2007). Instead, the focus will be on bacterial Fe transporters required during symbiosis.

The only Fe uptake system found to be required by bacteroids is formed by FegA and FegB in *Bradyrhizobium japonicum* 61A152 (Benson et al., 2005). The FegAB complex is an outermembrane receptor for the Fe-siderophore complex, Fe^{3+}-ferrichrome, and is dependent on the TonB energy-transducing complex (Andrews et al., 2003; Benson et al., 2005). On *G. max,* disruption of the *fegAB* operon resulted in an absence of bacteroid-containing symbiosomes despite the normal appearance of infection threads. Even though FegB was required for Fe^{3+}-ferrichrome uptake, the symbiotic phenotype could be complemented by just *fegA*-expression and disruption of *fegB* alone did not cause a symbiotic phenotype. Furthermore, ferrichrome or any related hydroxamate has not been found in *B. japonicum* 61A152 (Guerinot et al., 1990) and there is no evidence that it is produced in plants (Benson et al., 2005). Together with the experimental data, it was concluded that the requirement of FegA for symbiosis was independent of Fe^{3+}-ferrichrome uptake and is either involved in signal transduction (Schalk et al., 2004) or is the receptor for another compound (Benson et al., 2005). Consequently, the Fe transporters required by bacteroids for symbiosis remain unknown.

A Zn^{2+} transporter in *G. max*, GmZIP1, is located on the symbiosome membrane (Moreau et al., 2002) but no Zn^{2+} transporters have been characterised in rhizobia.

Molybdate (Mo) is utilised in the FeMoCo in nitrogenase. The ABC-type transporter, ModABC, has been characterised as a molybdate transporter in *B.*

japonicum and disruption of *modABC* caused a reduction in N_2 fixation (Delgado et al., 2006).

There have been several studies into the role of bacterial Mn^{2+} transporters during symbiosis. Some studies suggest that high-affinity Mn^{2+} transporters are critical during bacteroid development while others show they are dispensable (Platero et al., 2003; Chao et al., 2004; Davies and Walker, 2007a, b; Hohle and O'Brian, 2009). The role of Mn^{2+} and requirement of Mn^{2+} transporters during legume-rhizobia symbioses is discussed in detail in Chapter four.

Little is known about the transport of Mg^{2+} into bacteroids despite its importance as a cofactor for ATP and many cellular functions (Smith and Maguire, 1998; Moomaw and Maguire, 2008). Only one putative Mg^{2+} channel, found in *R. leguminosarum*, has been shown to be required for N_2 fixation (Karunakaran et al., 2009). This channel is discussed in Chapter five.

1.4.6 Low O_2

As mentioned previously, the nodule provides a low O_2 environment to allow O_2-sensitive nitrogenase to function. Plants synthesis leghemaglobin to buffer O_2 levels in the nodule but rhizobia still need to adapt to survive in the low O_2 environment. The major adaptation is the synthesis of a Cu-containing, cytochrome cbb_3-type oxidase that is essential for respiration under low O_2 (Delgado et al., 1998). The terminal oxidase has a high-affinity for O_2 and is encoded by *fixNOPQ*. The operon *fixGHIS* is in close proximity to *fixNOPQ* and encodes the machinery required for Cu-delivery to FixNOPQ (Thony-Meyer, 1997).

In *B. japonicum,* disruption of the *fixNOPQ* or *fixGHIS* operons caused a Fix[-] phenotype (Preisig et al., 1993; Preisig et al., 1996). *S. meliloti* 2011 has two copies of the *fixNOPQ* operon and both had to be deleted to cause a Fix[-] phenotype (Renalier et al., 1987); a deletion of *fixGHIS* in *S. meliloti* also caused a Fix[-] phenotype (Kahn et al., 1989). *R. leguminosarum* and *R. etli* also have two copies of *fixNOPQ*. In *R. leguminosarum*, only when both *fixNOPQ* operons were disrupted

was a Fix⁻ phenotype seen (Schluter et al., 1997). In *R. etli*, one of the *fixNOPQ* operons lies on the symbiotic plasmid (*fixNOPQ*d) and the other is located on plasmid p42f (*fixNOPQ*f); disruption of *fixNOPQ*d alone caused a Fix⁻ phenotype on *P. vulgaris* (Girard et al., 2000; Lopez et al., 2001).

Contrary to the above, deletion of *fixNO* in *A. caulinodans* only resulted in a 50% reduction in N_2 fixation on *S. rostrata*, furthermore, N_2 fixation was only mildly reduced in free-living cells (Mandon et al., 1994). This suggests that *fixNOPQ* is not as critical for *A. caulinodans* as it is for other rhizobia and is suggestive of an unidentified, alternative terminal oxidase that can partially compensate for the loss of FixNOPQ (Mandon et al., 1994). Disruption of *fixGHI* in *A. caulinodans* did not affect symbiotic N_2 fixation, and is again suggestive of an alternative assembly mechanism (Mandon et al., 1993).

Regulation of *fixNOPQ* and *fixGHIS* is complex and differs between rhizobia. For this reason, regulation will be discussed separately in Chapter six.

1.5 TRANSCRIPTOMIC PROFILING OF RHIZOBIA DURING BACTEROID DEVELOPMENT

Microarray analyses of *R. leguminosarum* bv. viciae 3841 (Rlv3841) during symbiosis with *P. sativum* has furthered our understanding of the physiological and regulatory responses of rhizobia during bacteroid development (Karunakaran et al., 2009). Transcriptomic profiles of bacteroids isolated from nodules at 7, 15, 21 and 28 days post inoculation (dpi) were compared to free-living cells grown in minimal medium. Many of the bacteria isolated from nodules 7dpi were likely to be developing bacteroids relative to the high number of mature bacteroids that would be in older nodules. Hierarchical clustering analysis (Fig 1.9) supported this and showed that bacteria isolated from nodules 7 dpi formed a separate branch from those isolated at 15, 21, and 28 dpi. This implies that the transcriptome of developing bacteroids is very different from mature bacteroids and furthermore, there are a significant number of genes that are specifically upregulated in developing

bacteroids. Many of these genes are likely to be involved in understudied processes integral to nodule colonisation or required for bacteroid development.

A similar study of the *S. meliloti-M. sativa* symbiosis revealed that bacteroids isolated from young nodules (5 dpi) again formed a separate branch from those isolated from older nodules (8-18 dpi), highlighting a strong distinction between the gene expression profiles of developing and mature bacteroids (Capela et al., 2006).
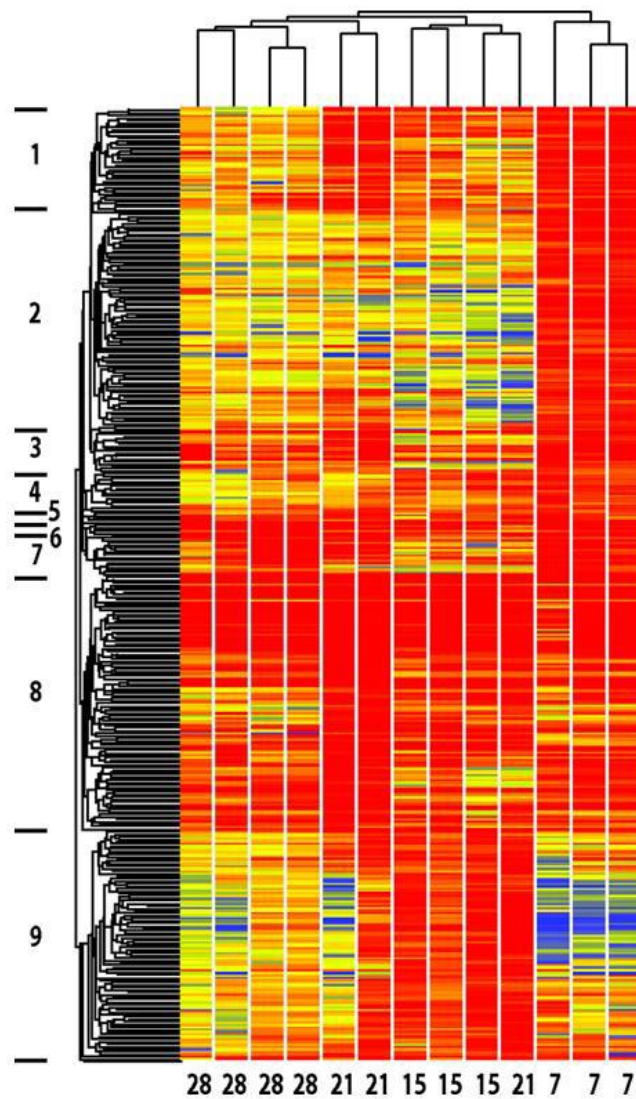
Fig 1.9 Tree showing hierarchal clustering of gene expression in developing and mature bacteroids isolated from nodules at 7, 15, 21 and 28 dpi. Red indicates highly expressed, yellow intermediate and blue low. Reproduced from Karunakaran *et al.*, 2009.

1.6 RESEARCH OBJECTIVES

The organism used in this study was primarily *R. leguminosarum* bv. viciae 3841 due to the wealth of transcriptomic data available for this strain (compiled by the Philip Poole lab) and its compatibility with two important crop legumes: *P. sativum* (pea) and *V. faba* (broad bean). The preliminary objective was to determine the requirement of genes specifically upregulated in developing bacteroids. This was achieved by targeted mutagenesis and the screening of mutants on *P. sativum*.

After screening, five aspects of bacteroid development were selected for further investigation. The requirement of two types of Mn^{2+} transport systems during the colonisation of both indeterminate and determinate nodules is explored in Chapter four. Chapter five focuses on the characterisation of a Mg^{2+} channel and its requirement on different legume-hosts. In Chapter six, the regulatory pathways that govern the expression of genes essential to N_2 fixation are investigated. Chapter seven looks at organic peroxide resistance and the function of two organic peroxidases. Chapter eight examines the role of two plasmid-encoded proteases in bacteroids. Thus, this study aims to provide a holistic insight into bacteroid development and enhance our understanding of what is required for an effective symbiosis.

Chapter 2: *Materials and Methods*

2.1 MEDIA, ANTIBIOTICS AND OTHER CHEMICALS

2.1.1 Media

For routine growth, *R. leguminosarum* strains were grown at 28°C in tryptone-yeast (TY) broth [5 g.l^{-1} tryptone, 3 g.l^{-1} yeast, 6 mM CaCl$_2$] (Beringer, 1974) with shaking at 250 rpm. For solid TY medium, agar (1.75% w/v) was added prior to autoclaving. Solid TY medium was supplemented with 50 μM MnSO$_4$ when growing the double manganese mutants i.e. LMB466 (*sitA*:pK19mob *mntH*ΩSpc), LMB539 (RlvA34 *sitA*:pK19mob *mntH*ΩSpc) and LMB630 (Rlp4292 *sitA*ΩKm *mntH*ΩSpc).

When a defined medium was required, *R. leguminosarum* strains were grown on acid minimal salts (AMS). One litre of AMS contains 0.5 ml 1 M K$_2$HPO$_4$, 0.5 g MgSO$_4$.7H$_2$O, 0.2 g NaCl, 4.19 g MOPS buffer, 1 ml *Rhizobium* solution A (containing 15 g EDTA-Na$_2$, 0.16 g ZnSO$_4$.7H$_2$O, 0.2 g NaMoO$_4$, 0.25 g H$_3$BO$_3$, 0.2 g MnSO$_4$.4H$_2$O, 0.02 g CuSO$_4$.5H$_2$O, 0.001 g CoCl$_2$.6H$_2$O per litre) and 2 ml *Rhizobium* solution B (containing 1.28 g CaCl$_2$.2H$_2$O, 0.33 g FeSO$_4$.7H$_2$O per 100 ml) adjusted to pH 7.0. After autoclaving, 1 ml *Rhizobium* solution C (containing 1 g thiamine hydrochloride, 2 g D-Pantothenic acid Ca salt, 0.001 g Biotin per litre) was added (Poole et al., 1994). Glucose (10 mM) and NH$_4$Cl (10 mM) were filter sterilised using a 0.22 μm filter (Millipore) and added to AMS medium. Modifications made to AMS to test growth of mutant *R. leguminosarum* strains are stated in Chapters four and five.

E. coli strains were grown at 37°C in Luria Bertani (LB) broth [10 g.l^{-1} tryptone, 5 g.l^{-1} yeast extract, 5 g.l^{-1} NaCl], with shaking at 250 rpm. For solid medium, agar (1.4% w/v) was added prior autoclaving. Solid LB medium was supplemented with 100 mM MgSO$_4$ when growing the *E. coli* triple gene knock-out strain (Δ*mgtA* Δ*corA* Δ*yhiD*) (Hattori et al., 2009).

All bacterial strains constructed in this study were stocked in 15% v/v glycerol, snap frozen in liquid nitrogen and stored at -80°C.

2.1.2 Antibiotics and other chemicals

Where appropriate, antibiotics were added to media at the concentrations listed in Table 2.1. For *R. leguminosarum* bv. phaseoli, antibiotics were added at the same concentration as they were for *R. leguminosarum* bv. viciae, with the omission of streptomycin; instead of streptomycin, rifampicin was used a 10 µg/ml.

Where blue-white screening could be used for screening *E. coli* transformants, X-gal (5-bromo-4-chloro-3-indolyl-β-D-galactopyranoside) was added to solid LB medium at 40 µg/ml.

Antibiotic	Concentrations (µg/ml)	
	E. coli	*R. leguminosarum* bv. viciae
Ampicillin (Amp)	100	-
Gentamicin (Gm)	10	20
Kanamycin (Km)	20	-
Neomycin (Neo)	-	80[a]
Spectinomycin (Spc)	50	100
Streptomycin (Str)	-	500
Tetracycline (Tc)	10	2

Table 2.1 Concentrations of antibiotics used for *E. coli* and *R. leguminosarum*.
[a] Neomycin was added at 250 µg/ml when used to select for pRU877- and pK19mob-integration.

2.2 BACTERIAL STRAINS, PLASMIDS, BACTERIOPHAGE AND PRIMERS

2.2.1 Strains

All *R. leguminosarum* strains used for this thesis are listed and referenced in Table 2.2. Nomenclature for mutations can be found in Abbreviations.

Strain	Description	Reference
Rlv300	Wild type *R. leguminosarum* bv. viciae; Str^s	Johnston and Beringer, 1975
Rlv3841	Wild type *R. leguminosarum* bv. viciae; Str^r derivative of strain Rlv300; Str^r	Johnston and Beringer, 1975
J325	*R. leguminosarum* bv. viciae J251; *mur*ΩSpc; Spc^r	Wexler et al., 2001
RlvA34	*R. leguminosarum* bv. *viciae* formerly known as 8401/pRL1JI	Downie et al., 1983
Rlp4292	Derivative of field bean isolate 8002 with sym plasmid pRP2J1; Rif^r	Lamb et al., 1982
LMB338	pLMB305 integrated into Rlv300; pRL100224:pRU877; Neo^r	This study
LMB340	pLMB176 integrated into Rlv300; RL3152:pRU877; Neo^r	This study
LMB343	pLMB212 integrated into Rlv300; RL1485:pRU877; Neo^r	This study
LMB347	pLMB208 integrated into Rlv3841; pRL90266:pRU877; Neo^r	This study
LMB348	pLMB209 integrated into Rlv3841; pRL90226:pRU877; Neo^r	This study
LMB349	pLMB211 integrated into Rlv3841; RL3273:pRU877; Neo^r	This study
LMB351	pLMB187 integrated into Rlv3841; pRL120695:pRU877; Neo^r	This study
LMB354	pLMB216 integrated into Rlv3841; pRL90056:pRU877; Neo^r	This study
LMB360	pLMB469 integrated into Rlv3841; RL2022:pK19mob; Neo^r	This study
LMB361	pLMB246 integrated into Rlv3841; RL0447:pRU877; Neo^r	This study
LMB363	pLMB440 integrated into Rlv3841; RL0940:pK19mob; Neo^r	This study
LMB364	pLMB452 integrated into Rlv3841; RL3884:pK19mob;	This study

	Neo^r	
LMB365	pLMB186 integrated into Rlv3841; pRL80012:pRU877; Neo^r	This study
LMB366	pLMB306 integrated into Rlv3841; RL1317:pRU877; Neo^r	This study
LMB367	pLMB248 integrated into Rlv3841; RL0262:pRU877; Neo^r	This study
LMB369	pLMB502 integrated into Rlv3841; pRL80060:pK19mob; Neo^r	This study
LMB372	pLMB202 integrated into Rlv3841; RL1302:pRU877; Neo^r	This study
LMB374	pLMB185 integrated into Rlv3841; pRL90025:pRU877; Neo^r	This study
LMB375	pLMB206 integrated into Rlv3841; RL0472:pRU877; Neo^r	This study
LMB376	pLMB329 integrated into Rlv3841; RL2307:pRU877; Neo^r	This study
LMB377	pLMB177 integrated into Rlv3841; RL2927:pRU877; Neo^r	This study
LMB378	pLMB189 integrated into Rlv3841; pRL110033:pRU877; Neo^r	This study
LMB385	pLMB215 integrated into Rlv3841; pRL110377:pRU877; Neo^r	This study
LMB391	pLMB433 integrated into Rlv3841; pRL110287:pK19mob; Neo^r	This study
LMB392	pLMB430 integrated into Rlv3841; RL1880:pK19mob; Neo^r	This study
LMB396	pLMB434 integrated into Rlv3841; RL4103:pK19mob; Neo^r	This study
LMB397	pLMB428 integrated into Rlv3841; RL2925:pK19mob; Neo^r	This study
LMB398	pLMB432 integrated into Rlv3841; RL1631:pK19mob; Neo^r	This study
LMB400	pLMB454 integrated into Rlv3841; RL2924:pK19mob; Neo^r	This study
LMB401	pLMB456 integrated into Rlv3841; RL0390:pK19mob; Neo^r	This study
LMB402	pLMB457 integrated into Rlv3841; pRL120362:pK19mob; Neo^r	This study
LMB403	pLMB441 integrated into Rlv3841; RL1879:pK19mob; Neo^r	This study
LMB404	pLMB427 integrated into Rlv3841; RL1226:pK19mob; Neo^r	This study
LMB410	pLMB467 integrated into Rlv3841; RL3688:pK19mob; Neo^r	This study
LMB411	pLMB429 integrated into Rlv3841; pRL90060:pK19mob; Neo^r	This study
LMB421	pLMB207 integrated into Rlv3841; pRL90278:pK19mob; Km^r	This study

LMB423	RL4272:pRU877 transduced from LMB384 into Rlv3841; Neo^r	This study
LMB425	pLMB243 integrated into Rlv3841; pRL110623:pK19mob; Neo^r	This study
LMB440	pLMB245 integrated into Rlv3841; pRL110055:pK19mob; Neo^r	This study
LMB441	pLMB335 integrated into Rlv3841; RL3783:pK19mob; Neo^r	This study
LMB448	*mgtE*::mTn5 transduced from RU4107 into Rlv3841; Neo^r	This study
LMB449	pRL100036:mTn5 transduced from RU4067 into Rlv3841; Neo^r	This study
LMB457	pLMB540 integrated into Rlv3841; pRL100035:pK19mob; Neo^r	This study
LMB458	pLMB541 integrated into Rlv3841; pRL80013:pK19mob; Neo^r	This study
LMB549	pLMB542 integrated into Rlv3841; pRL100112:pK19mob; Neo^r	This study
LMB460	pLMB546 conjugated into Rlv3841; *mntH*ΩSpc; Spc^r	This study
LMB466	*mntH*ΩSpc transduced from LMB460 into LMB364 (*sitA*:pK19mob); Neo^r Spc^r	This study
LMB472	pLMB568 (pJP2pRL100036) conjugated in RU4067; Neo^r Tc^r	This study
LMB481	pLMB576 (pJP2*mgtE*) conjugated into RU4107; Neo^r Tc^r	This study
LMB482	pLMB578 conjugated into Rlv3841; ΔpRL100036-35ΩSpc; Spc^r	This study
LMB489	pLMB455 integrated into Rlv3841; RL1107:pK19mob; Neo^r	This study
LMB495	pLMB590 conjugated into Rlv3841; *fixL*ΩSpc; Spc^r	This study
LMB496	pLMB441 integrated into LMB495; RL1879:pK19mob *fixL*ΩSpc; Neo^r Spc^r	This study
LMB497	pLMB596 integrated into Rlv3841; *oxyR*:pK19mob; Neo^r	This study
LMB498	pLMB597 conjugated into Rlv3841; *sitA-gusA*; Tc^r	This study
LMB505	pLMB600 conjugated into Rlv3841; *mntH-gusA*; Tc^r	This study
LMB506	pLMB599 conjugated into Rlv3841; *pspA*ΩSpc; Spc^r	This study
LMB511	pLMB597 conjugated into LMB497; *sitA-gusA*; Tc^r	This study
LMB512	pLMB600 conjugated into LMB497; *mntH-gusA*; Tc^r	This study
LMB519	Rlv3841; RL1329ΩSpc	Unpublished
LMB523	Rlv3841; pRL90059:pK19mob RL1329ΩSpc	Unpublished
LMB525	*sitA*:pK19mob transduced from LMB364 into RlvA34; Neo^r	This study
LMB526	*mntH*ΩSpc transduced from LMB460 into RlvA34; Spc^r	This study
LMB539	*sitA*:pK19mob transduced from LMB364 into LMB526; Neo^r Spc^r	This study

LMB541	pLMB546 integrated into Rlp4292; *mntH*ΩSpc; Spc^r	This study
LMB550	pLMB597 conjugated into J325; *sitA-gusA*; Tc^r	This study
LMB551	pLMB600 conjugated into J325; *mntH-gusA*; Tc^r	This study
LMB571	ΔpRL100036-35ΩSpc transduced from LMB482 into LMB458 (pRL80013:pK19mob); Neo^r Spc^r	This study
LMB603	pLMB692 conjugated into Rlv3841; RL1302ΩSpc; Spc^r	This study
LMB620	RL2927:pRU877 transduced from LMB377 into LMB603; Neo^r Spc^r	This study
LMB624	pLMB694 conjugated into 4292; *sitA*ΩKm; Neo^r	This study
LMB630	pLMB694 conjugated into LMB541; *sitA*ΩKm *mntH*ΩSpc; Neo^r Spc^r	This study
LMB648	pLMB733 conjugated into Rlv3841; *fnrN*ΩTc; Tc^r	This study
LMB673	*fnrN*ΩTc transduced from LMB648 into LMB496; RL1879:pK19mob *fixL*ΩSpc *fnrN*ΩTc; Km^r Spc^r Tc^r	This study
LMB683	pLMB766 (pJP2*mntH*) conjugated into LMB466 (*sitA*:pK19mob *mntH*ΩSpc); Neo^r Spc^r Tc^r	This study
LMB730	pLMB733 conjugated into LMB403; RL1879:pK19mob *fnrN*ΩTc; Neo^r Tc^r	This study
LMB731	pLMB733 conjugated into LMB495; *fixL*ΩSpc *fnrN*ΩTc; Spc^r Tc^r	This study
RU4040	Rlv3841 (*bacA*:pK19mob); Neo^r	Karunakaran et al., 2010
RU4067	Rlv3841 pRL100036::mTn5; Neo^r	Karunakaran et al., 2009
RU4107	Rlv3841 *mgtE*::mTn5; Neo^r	Karunakaran et al., 2009
RU4260	Rlv300; RL4274:pK19mob; Neo^r	Ramachandran et al., 2011
RU4314	Rlv3841; pRL90059:pK19mob	Unpublished

Table 2.2 *R. leguminosarum* strains. All strains referenced as unpublished were constructed by the Philip Poole group.

All *E. coli* K-12 strains used for this thesis are listed and referenced in Table 2.3

Strain	Description	Reference
DH5α	F⁻ *deoR* *end*A1 *rec*A1 *rel*A1 *gyr*A96 *hsd*R17(r$_k$⁻, m$_k$⁺) *sup*E44 *thi*-1 *pho*A Δ(*lac*ZYA-*arg*F)U169 Φ80*lac*ZΔM15 λ⁻	Bioline
Mg Triple KO strain	Δ*mgtA* Δ*corA* Δ*yhiD*	Hattori et al., 2009
LMB469	pRK415 transformed into Mg Triple KO strain; Tc^r	This study
LMB470	pLMB562 (pRK415*mgtE*) transformed into Mg Triple KO strain; *mgtE* in same orientation as *lac* promoter; Tc^r	This study
LMB471	pLMB565 (pRK415*mgtE*) transformed into Mg Triple KO strain; *mgtE* in reverse orientation as *lac* promoter; Tc^r	This study

Table 2.3 *E. coli* strains.

2.2.2 Plasmids

All plasmids used for this thesis are listed and referenced in Table 2.4.

Plasmid	Description	Reference
pJET 1.2/Blunt	PCR product cloning vector; Amp^r	Fermentas
pK19mob	Mobilisable vector used for integration mutagenesis; pMB1 replicon, RP4 mob, *lacZα*. Km^r Neo^r	Schafer et al., 1994
pRU877	*gusA* in pK19mob; Km^r	Lodwig et al., 2004
pRK2013	Helper plasmid; triparental conjugation; Km^r	Ditta et al., 1980
pRK415	Broad-host-range plasmid	Keen et al., 1988
pJP2	Wide-host-range stable *gusA* transcriptional promoter probe vector; Tc^r	Prell et al., 2002
pHP45Ω-Spc	pBR322 derivative carrying Ω interposon spectinomycin resistance cassette, pHP45 replicon; Amp^r Spc^r	Fellay et al., 1987
pHP45Ω-Km	pBR322 derivative carrying Ω interposon kanamycin resistance cassette pHP45 replicon; Amp^r Km^r	Fellay et al., 1987
pHP45Ω-Tc	pBR322 derivative carrying Ω interposon tetracycline resistance cassette pHP45 replicon; Amp^r, Tc^r	Fellay et al., 1987
pJQ200SK	pACYC derivative, P15A origin of replication; Gm^r	Quandt and Hynes, 1993
pLMB176	Internal fragment of RL3152 PCR amplified with primers pr0426-27 cloned into pRU877 at *Xba*I; Km^r	This study
pLMB177	Internal fragment of RL2927 PCR amplified with primers pr0429-30 cloned into pRU877 at *Xba*I; Km^r	This study
pLMB185	Internal fragment of pRL90025 PCR amplified with primers pr0516-17 cloned into pRU877 at *Xba*I; Km^r	This study
pLMB186	Internal fragment of pRL80012 PCR amplified with primers pr0519-20 cloned into pRU877 at *Xba*I; Km^r	This study
pLMB187	Internal fragment of pRL120695 PCR amplified with primers pr0522-23 cloned into pRU877 at *Xba*I; Km^r	This study
pLMB189	Internal fragment of pRL110033 PCR amplified with primers pr0537-38 cloned into pRU877 at *Xba*I; Km^r	This study

pLMB202	Internal fragment of RL1302 PCR amplified with primers pr0483-84 cloned into pRU877 at *Xba*I; Km^r	This study
pLMB206	Internal fragment of RL0472 PCR amplified with primers pr0498-99 cloned into pRU877 at *Xba*I; Km^r	This study
pLMB207	Internal fragment of pRL90278 PCR amplified with primers pr0504-05 cloned into pRU877 at *Xba*I; Km^r	This study
pLMB208	Internal fragment of pRL90266 PCR amplified with primers pr0507-08 cloned into pRU877 at *Xba*I; Km^r	This study
pLMB209	Internal fragment of pRL90226 PCR amplified with primers pr0510-11 cloned into pRU877 at *Xba*I; Km^r	This study
pLMB211	Internal fragment of RL3273 PCR amplified with primers pr0546-47 cloned into pRU877 at *Xba*I; Km^r	This study
pLMB212	Internal fragment of RL1485 PCR amplified with primers pr0549-50 cloned into pRU877 at *Xba*I; Km^r	This study
pLMB215	Internal fragment of pRL110377 PCR amplified with primers pr0561-62 cloned into pRU877 at *Xba*I; Km^r	This study
pLMB216	Internal fragment of pRL90056 PCR amplified with primers pr0564-65 cloned into pRU877 at *Xba*I; Km^r	This study
pLMB243	Internal fragment of pRL110623 PCR amplified with primers pr0528-29 cloned into pRU877 at *Xba*I; Km^r	This study
pLMB245	Internal fragment of pRL110055 PCR amplified with primers pr0534-35 cloned into pK19mob at *Xba*I; Km^r	This study
pLMB246	Internal fragment of RL0447 PCR amplified with primers pr0543-44 cloned into pRU877 at *Xba*I; Km^r	This study
pLMB248	Internal fragment of RL0262 PCR amplified with primers pr0610-11 cloned into pRU877 at *Xba*I; Km^r	This study
pLMB305	Internal fragment of pRL100224 PCR amplified with primers pr0552-53 cloned into pRU877 at *Xba*I; Km^r	This study
pLMB306	Internal fragment of RL1317 PCR amplified with primers pr0613-14 cloned into pRU877 at *Xba*I; Km^r	This study
pLMB329	Internal fragment of RL2307 PCR amplified with primers pr0540-41 cloned into pRU877 at *Xba*I; Km^r	This study
pLMB335	Internal fragment of RL3783 PCR amplified	This study

	with primers pr0355-56 cloned into pRU877 at *Xba*I; Km[r]	
pLMB427	Internal fragment of RL1226 PCR amplified with primers pr0990-91 cloned into pK19mob at *Xba*I; Km[r]	This study
pLMB428	Internal fragment of RL2925 PCR amplified with primers pr0976-77 cloned into pK19mob at *Xba*I; Km[r]	This study
pLMB429	Internal fragment of pRL90060 PCR amplified with primers pr1000-01 cloned into pK19mob at *Xba*I; Km[r]	This study
pLMB430	Internal fragment of RL1880 PCR amplified with primers pr0986-97 cloned into pK19mob at *Xba*I; Km[r]	This study
pLMB432	Internal fragment of RL1631 PCR amplified with primers pr1016-17 cloned into pK19mob at *Xba*I; Km[r]	This study
pLMB433	Internal fragment of pRL110287 PCR amplified with primers pr1008-09 cloned into pK19mob at *Xba*I; Km[r]	This study
pLMB434	Internal fragment of RL4103 PCR amplified with primers pr0968-69 cloned into pK19mob at *Xba*I; Km[r]	This study
pLMB440	Internal fragment of RL0940 PCR amplified with primers pr0996-97 cloned into pK19mob at *Xba*I; Km[r]	This study
pLMB441	Internal fragment of RL1879 PCR amplified with primers pr0988-89 cloned into pK19mob at *Xba*I; Km[r]	This study
pLMB452	Internal fragment of RL3884 PCR amplified with primers pr0970-71 cloned into pK19mob at *Xba*I; Km[r]	This study
pLMB454	Internal fragment of RL2924 PCR amplified with primers pr0978-79 cloned into pK19mob at *Xba*I; Km[r]	This study
pLMB455	Internal fragment of RL1107 PCR amplified with primers pr0992-93 cloned into pK19mob at *Xba*I; Km[r]	This study
pLMB456	Internal fragment of RL0390 PCR amplified with primers pr0998-99 cloned into pK19mob at *Xba*I; Km[r] This study	This study
pLMB457	Internal fragment of pRL120362 PCR amplified with primers pr1004-05 cloned into pK19mob at *Xba*I; Km[r]	This study
pLMB467	Internal fragment of RL3688 PCR amplified with primers pr0972-73 cloned into pK19mob at *Xba*I; Km[r]	This study
pLMB469	Internal fragment of RL2022 PCR amplified with primers pr0984-85 cloned into pK19mob	This study

	at *Xba*I; Km[r]	
pLMB502	Internal fragment of pRL80060 PCR amplified with primers pr1115-16 cloned into pK19mob at *Xba*I; Km[r]	This study
pLMB540	Internal fragment of pRL100035 PCR amplified with primers pr1189-90cloned into pK19mob at *Xba*I; Km[r]	This study
pLMB541	Internal fragment of pRL80013 PCR amplified with primers pr1192-93 cloned into pK19mob at *Xba*I; Km[r]	This study
pLMB542	Internal fragment of pRL100112 PCR amplified with primers pr1195-96 cloned into pK19mob at *Xba*I; Km[r]	This study
pLMB543	*mntH* (RL0940) PCR amplified with primers pr1186-87 cloned into pJET1.2/Blunt; Amp[r]	This study
pLMB544	pHP45 ΩSpc (SmaI fragment) cloned into pLMB543 (pJET1.2/Blunt- *mntH*) at *Eco*RV; Amp[r] Spc[r]	This study
pLMB546	*mntH*ΩSpc from *Xba*I/*Xho*I digested pLMB544 cloned into pJQ2OOSK; Gm[r] Spc[r]	This study
pLMB553	*mgtE* (RL1461) PCR amplified with primers pr1241 and pr1242 cloned into pJET1.2/Blunt; Amp[r]	This study
pLMB554	Internal fragment of pRL100036 PCR amplified with primers pr1247 and pr1248 cloned into pJET1.2/Blunt; Amp[r]	This study
pLMB555	Internal fragment of pRL100035 PCR amplified with primers pr1249 and pr1250 cloned into pJET1.2/Blunt; Amp[r]	This study
pLMB562	*mgtE*-containing BglII fragment cut from pLMB553 cloned into pRK415 at *Bam*HI; *mgtE* in same orientation as *lac* promoter; Tc[r]	This study
pLMB565	*mgtE*-containing *Bgl*II fragment cut from pLMB553 cloned into pRK415 at *Bam*HI; *mgtE* in reverse orientation as *lac* promoter; Tc[r]	This study
pLMB566	*Xho*I/*Bam*HI fragment containing internal fragment of pRL100036 cut from pLMB554 and cloned into *Xho*I/*Bam*HI digested pJQ200SK; Gm[r]	This study
pLMB567	*Bam*HI/*Xba*I fragment containing internal fragment of pRL100035 cut from pLMB555 and cloned into *Bam*HI/*Xba*I digested pLMB566; Gm[r]	This study
pLMB569	*mgtE* (RL1461) PCR amplified with primers pr1240 and pr1265 cloned into pJET1.2/Blunt; Amp[r]	This study
pLMB576	*mgtE* from *Xba*I/*Kpn*I diegested pLMB569 cloned into pJP2 *Xba*I/*Kpn*I; Tc[r]	This study

pLMB578	*Bam*HI fragment containing ΩSpc cloned into *Bam*HI digested pLMB567; Gm^r Spc^r	This study
pLMB581	*fixL* PCR amplified with primers pr1270-71 cloned into pJET1.2/Blunt; Amp^r	This study
pLMB585	*fixL* from *Xba*I/*Xho*I digested pLMB581 cloned into pJQ2OOSK *Xba*I/*Xho*I; Gm^r	This study
pLMB590	ΩSpc from *Sma*I digested pHP45 cloned into pJQ200SK- *fixL* at *Stu*I (blunted); Gm^r Spc^r	This study
pLMB592	Internal fragment of *oxyR* PCR amplified with primers pr1286-87 cloned into pJET1.2/Blunt; Amp^r	This study
pLMB596	Internal fragment of *oxyR* from *Xba*I/*Bgl*II digested pLMB592 cloned into pK19mob *Xba*I/*Bam*HI; Km^r	This study
pLMB597	*sitA* promoter PCR amplified with pr1292-93 cloned into pJP2 *Xba*I/*Hin*dIII; Tc^r	This study
pLMB600	*mntH* promoter PCR amplified with pr1290-91 cloned into pJP2 *Xba*I/*Hin*dIII; Tc^r	This study
pLMB677	RL1302 PCR amplified with pr1385-86 cloned into pJET1.2/Blunt; Amp^r	This study
pLMB679	*sitA* PCR amplified from 4292 with primers pr1378 and pr1394 cloned into pJET1.2/Blunt; Amp^r	This study
pLMB688	ΩSpc from *Sma*I digested pHP45 cloned into pLMB677 (pJET1.2/Blunt- RL1302) at *Bmg*BI; Amp^r Spc^r	This study
pLMB691	ΩKm from *Eco*RI digested pHP45ΩKm (blunted) cloned into pLMB679 *Sma*I; Amp^r Km^r	This study
pLMB692	RL1302ΩSpc from *Xba*I/*Xho*I digested pLMB688 cloned into pJQ2OOSK *Xba*I/*Xho*I; Gm^r Spc^r	This study
pLMB694	*sitA*ΩKm from *Xba*I/*Not*I digested pLMB691 cloned into pJQ200SK (*Xba*I/*Not*I); Km^r Gm^r	This study
pLMB732	*fnrN* PCR amplified with primers pr1381-82 cloned into pJQ200SK at *Xba*I/*Xho*I; Gm^r	This study
pLMB733	ΩKm from EcoRI digested pHP45ΩTc cloned into pLMB732 (pJQ200SK- *fnrN*) *Mfe*I; Gm^r Tc^r	This study
pLMB766	*mntH* PCR amplified with primers pr1290 and pr1462 cloned into pJP2 at *Xba*I/*Hin*dIII; Tc^r	This study

Table 2.4 Plasmids.

2.2.3 Bacteriophages

R. leguminosarum bv. viciae was transduced using bacteriophage RL38 (Buchanan-Wollaston, 1979) .

2.2.4 Primers

All primers used for this thesis are listed and referenced in Table 2.5.

Primers	Sequence	Description
M13uni (-21)	TGTAAAACGACGGCCAGT	Mapping/sequencing primer; pK19mob and pRU877
M13rev (-29)	CAGGAAACAGCTATGACC	Mapping/sequencing primer; pK19mob and pRU877
pK19/18A	ATCAGATCTTGATCCCCTGC	Mapping primer for pK19mob and pRU877 integration
pK19/18B	GCACGAGGGAGCTTCCAGGG	Mapping primer for pK19mob integration
pr0095	TGCATCGGCGAACTGATCGTTA	Mapping primer for pRU877 integration
pOT forward	CGGTTTACAAGCATAAAGC	Mapping primer; intersposon mutagenesis
pOT forward_far	GACCTTTTGAATGACCTTTA	Mapping primer; intersposon mutagenesis
pJET 1.2 For	CGACTCACTATAGGGAGAGCGGC	Mapping/sequencing primer; pJET 1.2/Blunt
pJET 1.2 Rev	AAGAACATCGATTTTCCATGGCAG	Mapping/sequencing primer; pJET 1.2/Blunt
p611	GCGATCCAGACTGAATGCCC	Mapping primer; pJP2
pr0096	TCGTAAATGCTGGACCCGATGG	Mapping primer; pJP2
pr0355	CTTCTCGAGCTCTAGATTGCGCAATCACTGAACCAG	Forward primer; BD cloning of RL3783
pr0356	ATTACCTCAGTCTAGAGAACAGCTTCGGGTTCACGA	Reverse primer; BD cloning of RL3783
pr0413	GGGCGGCGTTCGGTTGCCGAG	Mapping primer for RL4103 mutagenesis
pr0416	GGGACGGACAAGATTGCC	Mapping primer for RL3884 mutagenesis
pr0419	GGCGGCCTGGCTCATGGCGGA	Mapping primer for RL3688 mutagenesis
pr0426	CTTCTCGAGCTCTAGATCGCATTGATGACCGACCCG	Forward primer; BD cloning of RL3152

pr0427	ATTACCTCAGTCTAGAGCAGGCCGCTATGGGTGAGC	Reverse primer; BD cloning of RL3152
pr0428	ACCGCTGTTGTCGCAACGGC	Mapping primer for RL3152 mutagenesis
pr0429	CTTCTCGAGCTCTAGAGGCAAAACCCACATCTCCGG	Forward primer; BD cloning of RL2927
pr0430	ATTACCTCAGTCTAGAGAAGAAGGAGCCGTTGTCGG	Reverse primer; BD cloning of RL2927
pr0431	ACGGCTGGGTCGAGCACGA	Mapping primer for RL2927 mutagenesis
pr0434	ATGCTCGCTGAAGACCCGTTCA	Mapping primer for RL2925 mutagenesis
pr0437	CTATGTCAGTAGCTACCAAC	Mapping primer for RL2924 mutagenesis
pr0446	ATCCGACGGACAGCCGGCGCCG	Mapping primer for RL2022 mutagenesis
pr0479	GTTGGCGCCGTCGAACATGC	Mapping primer forRL1880 mutagenesis
pr0482	AGTTCGATGTTCGTATCCGAAC	Mapping primer for RL1879 mutagenesis
pr0483	CTTCTCGAGCTCTAGAGTTTCCGAAAACGGCGTTCT	Forward primer; BD cloning of RL1302
pr0484	ATTACCTCAGTCTAGAAAGGGCAGACGATGTGGGCT	Reverse primer; BD cloning of RL1302
pr0485	GAAGACAGAAGCTGCTCCCG	Mapping primer for RL1302 mutagenesis
pr0488	GGCCCGCCACGGCCGGGAAA	Mapping primer for RL1226 mutagenesis
pr0491	CAAAAGTTGAATGCGGGAACA	Mapping primer for RL1107 mutagenesis
pr0497	ACGGCCGGGCGGCCTATGC	Mapping primer for RL0940 mutagenesis
pr0498	CTTCTCGAGCTCTAGAAGGCGGCGATGACCCTCTTT	Forward primer; BD cloning of RL0472
pr0499	ATTACCTCAGTCTAGATGACGATTGCCGCAAGGACG	Reverse primer; BD cloning of RL0472
pr0500	GAGCGGAAACATCGACATCGAG	Mapping primer for RL0472 mutagenesis
pr0503	AAAGGCGGCCTTTCGACCG	Mapping primer for RL0390 mutagenesis
pr0504	CTTCTCGAGCTCTAGACTTCGATGTGGTCTTCAACC	Forward primer; BD cloning of pRL90278
pr0505	ATTACCTCAGTCTAGAAGATCATGGCCGAGATCCTC	Reverse primer; BD cloning of pRL90278
pr0506	GTTTCATAGTCGATGAGTTC	Mapping primer for pRL90278 mutagenesis
pr0507	CTTCTCGAGCTCTAGAGAGAACACGATCGCCGCCTT	Forward primer; BD cloning of pRL90266
pr0508	ATTACCTCAGTCTAGAACC	Reverse primer; BD cloning of

	AGATCCTGCGGACGTTC	pRL90266
pr0509	ACGTCGAAGGAGGTTACCTT	Mapping primer for pRL90266 mutagenesis
pr0510	CTTCTCGAGCTCTAGAGAGCAGGCGGCCGATGAAAA	Forward primer; BD cloning of pRL90226
pr0511	ATTACCTCAGTCTAGAATGGCGATCTCGTCGGAGCT	Reverse primer; BD cloning of pRL90226
pr0512	TCATCCTCTTTTGGTTTTTG	Mapping primer for pRL90226 mutagenesis
pr0515	CGGAAAGCGCTCGCCGGCAA	Mapping primer for pRL90060 mutagenesis
pr0516	CTTCTCGAGCTCTAGAAGCAGCCAGTCGAACATCTG	Forward primer; BD cloning of pRL90025
pr0517	ATTACCTCAGTCTAGAATCATTCGCGACACAGTTTC	Reverse primer; BD cloning of pRL90025
pr0518	TGCTTTAGGCGTTCTGGCTT	Mapping primer for pRL90025 mutagenesis
pr0519	CTTCTCGAGCTCTAGACCAGGAACAGGCAAGTCTCT	Forward primer; BD cloning of pRL80012
pr0520	ATTACCTCAGTCTAGAGTTACGCGACTCATGAACGG	Reverse primer; BD cloning of pRL80012
pr0521	GATCCATCTGAAGGCTCAGAA	Mapping primer for pRL80012 mutagenesis
pr0522	CTTCTCGAGCTCTAGATGGATGCCGCCTTCGAGGAA	Forward primer; BD cloning of pRL120695
pr0523	ATTACCTCAGTCTAGATGTTGTCGTCAGGATGGGCG	Reverse primer; BD cloning of pRL120695
pr0524	ATCTACGTGTTTGGCGCGGAAT	Mapping primer for pRL120695 mutagenesis
pr0527	GCCCGGGCAAAATGCTGTCG	Mapping primer for pRL120362 mutagenesis
pr0528	CTTCTCGAGCTCTAGAATCGGCTATCACGCTGTCGG	Forward primer; BD cloning of pRL110623
pr0529	ATTACCTCAGTCTAGATTTCTCTGAGCTCATGGCCG	Reverse primer; BD cloning of pRL110623
pr0530	AATGATGGAATTCCATCATTG	Mapping primer for pRL110623 mutagenesis
pr0533	GGAAAGCTTGATGTCTTCGC	Mapping primer for pRL110287 mutagenesis
pr0534	CTTCTCGAGCTCTAGAGGCGTTACCATCGAGGGCTT	Forward primer; BD cloning of pRL110055
pr0535	ATTACCTCAGTCTAGATGTCGATATAGGCCTGCCGG	Reverse primer; BD cloning of pRL110055
pr0536	AGACGCGCGAATTATCACA	Mapping primer for pRL110055 mutagenesis
pr0537	CTTCTCGAGCTCTAGATGCTCTTCGGCATCGTCTTC	Forward primer; BD cloning of pRL110033
pr0538	ATTACCTCAGTCTAGAACGTCGAGCACTTCGGTCAG	Reverse primer; BD cloning of pRL110033

pr0539	CGGACGCACAAAGGTCGCTT	Mapping primer for pRL110033 mutagenesis
pr0540	CTTCTCGAGCTCTAGAGATTGGAATCGTGTCGAAGG	Forward primer; BD cloning of RL2307
pr0541	ATTACCTCAGTCTAGAATGTCGCGTTTAACACGATC	Reverse primer; BD cloning of RL2307
pr0542	CAGACAGCAAAAACCCGGCT	Mapping primer for RL2307 mutagenesis
pr0543	CTTCTCGAGCTCTAGAGCGGTGCTGCGATGTTCGAT	Forward primer; BD cloning of RL0447
pr0544	ATTACCTCAGTCTAGAGTCACATGGGAGACGCCGCC	Reverse primer; BD cloning of RL0447
pr0545	GGAGCGCCCCAATGCGTCTG	Mapping primer for RL0447 mutagenesis
pr0546	CTTCTCGAGCTCTAGAGAAACAGGGCCTTCGTCGAA	Forward primer; BD cloning of RL3273
pr0547	ATTACCTCAGTCTAGAGCAGAACATCACGGCCTTCG	Reverse primer; BD cloning of RL3273
pr0548	GTCGGCCCCCTCGAATAATA	Mapping primer for RL3273 mutagenesis
pr0549	CTTCTCGAGCTCTAGACATGGGTCGTGGTCTGCAAC	Forward primer; BD cloning of RL1485
pr0550	ATTACCTCAGTCTAGATCCAGGGAGATCGCTGCTTG	Reverse primer; BD cloning of RL1485
pr0551	GCCGTTCGACCCGCGTTCAC	Mapping primer for RL1485 mutagenesis
pr0552	CTTCTCGAGCTCTAGACGCCTCGATCGATCTCATCA	Forward primer; BD cloning of pRL100224
pr0553	ATTACCTCAGTCTAGATACTTGGCGTCCGCCTCTTC	Reverse primer; BD cloning of pRL100224
pr0554	TGTTCATTGCGGTTCGTCAG	Mapping primer for pRL100224 mutagenesis
pr0557	GAAAGCGAGCGGATGGCGCT	Mapping primer for pRL80060 mutagenesis
pr0561	CTTCTCGAGCTCTAGAGACGACATGCCCGACCTCAT	Forward primer; BD cloning of pRL110377
pr0562	ATTACCTCAGTCTAGACGCGCAGGATGTCGTATTCC	Reverse primer; BD cloning of pRL110377
pr0563	TACTGTTCGGGCAGCGGGAG	Mapping primer for pRL110377 mutagenesis
pr0564	CTTCTCGAGCTCTAGACGCCATCTACGATCGCCTCT	Forward primer; BD cloning of pRL90056
pr0565	ATTACCTCAGTCTAGACGGTCGATCTGCACCTTGAC	Reverse primer; BD cloning of pRL90056
pr0566	CTTCCCTCTCGCTTTTCGTT	Mapping primer for pRL90056 mutagenesis
pr0610	CTTCTCGAGCTCTAGAGAGGCGGAGATGCGGGAAAT	Forward primer; BD cloning of RL0262
pr0611	ATTACCTCAGTCTAGACGTT	Reverse primer; BD cloning of

	GGCGCGATATCGTCAA	RL0262
pr0612	TAGAAAAGTGTCAGCGTTT T	Mapping primer for RL0262 mutagenesis
pr0613	CTTCTCGAGCTCTAGACCTG AGCGGATGGCTAGAAG	Forward primer; BD cloning of RL1317
pr0614	ATTACCTCAGTCTAGAGAA CTGCCTTTTCGAACGGG	Reverse primer; BD cloning of RL1317
pr0615	ATCTTGTCGATGTTACGGCC	Mapping primer for RL1317 mutagenesis
pr0621	ACGCGTGAAGGCGCTCGAT CA	Mapping primer forRL1631 mutagenesis
pr0706	TTCGTCCGGAATTGCGCGA A	Mapping primer for RL3783 mutagenesis
pr0968	GCAGGTCGACTCTAGACCG GCGGCGGCTGGGACCAG	Forward primer; BD cloning of RL4103
pr0969	CCGGGGATCCTCTAGACCA GCCCTTGGTCTTCAGCG	Reverse primer; BD cloning of RL4103
pr0970	GCAGGTCGACTCTAGAACA GACAACCAATTCGAAGT	Forward primer; BD cloning of RL3884
pr0971	CCGGGGATCCTCTAGATAA AGCACGCCTCCATAGTG	Reverse primer; BD cloning of RL3884
pr0972	GCAGGTCGACTCTAGAAGT TGCTGGAGGTCGCCGCG	Forward primer; BD cloning of RL3688
pr0973	CCGGGGATCCTCTAGATGG CTTTCCAACGTATCTGC	Reverse primer; BD cloning ofRL3688
pr0976	GCAGGTCGACTCTAGAAGT TCCAGGCGCAAGGTGCA	Forward primer; BD cloning of RL2925
pr0977	CCGGGGATCCTCTAGAAGG TAACGCCAATTCGGCTT	Reverse primer; BD cloning of RL2925
pr0978	GCAGGTCGACTCTAGAGAA TTTCCTGTGCTTCGCGG	Forward primer; BD cloning of RL2924
pr0979	CCGGGGATCCTCTAGATTC TGCACGACGGGAAAGTC	Reverse primer; BD cloning of RL2924
pr0984	GCAGGTCGACTCTAGACTG TTTGCACCGGCAGCTTT	Forward primer; BD cloning of RL2022
pr0985	CCGGGGATCCTCTAGAGTA TTTGAAGATCTCGGGAT	Reverse primer; BD cloning of RL2022
pr0986	GCAGGTCGACTCTAGAAGA CCGTCGAGACAGCACAG	Forward primer; BD cloning of RL1880
pr0987	CCGGGGATCCTCTAGAAAC CGGCTCGCAACCTTGAA	Reverse primer; BD cloning of RL1880
pr0988	GCAGGTCGACTCTAGATGG AAGAGCTTCGGACCGAA	Forward primer; BD cloning of RL1879
pr0989	CCGGGGATCCTCTAGAATA TCTCGATCGTCAGACGG	Reverse primer; BD cloning of RL1879
pr0990	GCAGGTCGACTCTAGAGCT GACGCGCTATTACTTCA	Forward primer; BD cloning of RL1226
pr0991	CCGGGGATCCTCTAGAGAA ATAGAAGGCGCCGAGGC	Reverse primer; BD cloning of RL1226

pr0992	GCAGGTCGACTCTAGAACA TCTCCTTCGGCTCGGCC	Forward primer; BD cloning of RL1107
pr0993	CCGGGGATCCTCTAGAGCG GATCAGCTTCTCGGATT	Reverse primer; BD cloning of RL1107
pr0996	GCAGGTCGACTCTAGAGCT CGAAATTCGGCTATGCG	Forward primer; BD cloning of RL0940
pr0997	CCGGGGATCCTCTAGAATA CCAGATGGTGACGATCG	Reverse primer; BD cloning of RL0940
pr0998	GCAGGTCGACTCTAGATAT TCGCCTCCGCCGTACGA	Forward primer; BD cloning of RL0390
pr0999	CCGGGGATCCTCTAGAGCG AACCTTGGGATCGGAAA	Reverse primer; BD cloning of RL0390
pr1000	GCAGGTCGACTCTAGACTG ACGGCCTATTTCAGCAA	Forward primer; BD cloning of pRL90060
pr1001	CCGGGGATCCTCTAGAATT GCGCAGCATGTTGGTCA	Reverse primer; BD cloning of pRL90060
pr1004	GCAGGTCGACTCTAGATTT TGCGCCGCTCAACAGCT	Forward primer; BD cloning of pRL120362
pr1005	CCGGGGATCCTCTAGAAAT GTCCTTGTCGTCGACAA	Reverse primer; BD cloning of pRL120362
pr1008	GCAGGTCGACTCTAGATGA TCGGTGGTTTTGGTGGC	Forward primer; BD cloning of pRL110287
pr1009	CCGGGGATCCTCTAGAAAC AGTGACGACGCGGTCGA	Reverse primer; BD cloning of pRL110287
pr1016	GCAGGTCGACTCTAGAGCC GAAAGCCTTGGGATGAA	Forward primer; BD cloning of RL1631
pr1017	CCGGGGATCCTCTAGATTG ACGACATTGCGAATATT	Reverse primer; BD cloning of RL1631
pr1115	GCAGGTCGACTCTAGATCG TCCGGTACGCTCACAAT	Forward primer; BD cloning of pRL80060
pr1116	CCGGGGATCCTCTAGACAT TTCAGCTGAGGCCTTGT	Reverse primer; BD cloning of pRL80060
pr1186	CGTATAGACGCGGCGTTCG A	Forward primer; *mntH* (RL0940)
pr1187	AGGGCATGAGCGTGCTGGA A	Reverse primer; *mntH* (RL0940)
pr1189	GCAGGTCGACTCTAGATCG CCGGGCGGTTGAATATT	Forward primer; BD cloning of pRL100035
pr1190	CCGGGGATCCTCTAGAACA TTGGGTCGGTAGTACGT	Reverse primer; BD cloning of pRL100035
pr1191	GCCAGATATCGGAGTGCAC A	Mapping primer for pRL100035 mutagenesis
pr1192	GCAGGTCGACTCTAGATCC GCACCGGAAGATGATGA	Forward primer; BD cloning of pRL80013
pr1193	CCGGGGATCCTCTAGACCT GAGATTCGAAAACCACG	Reverse primer; BD cloning of pRL80013
pr1194	CGTCCGAACAATTTTCCGTC	Mapping primer for pRL80013 mutagenesis
pr1195	GCAGGTCGACTCTAGATGT	Forward primer; BD cloning of

	GAGGAATGCATACGCGG	pRL100112
pr1196	CCGGGGATCCTCTAGACCT TGCAGATCGCCGATGGC	Reverse primer; BD cloning of pRL100112
pr1197	GCTGCATTCGGAACGAAAT T	Mapping primer for pRL100112 mutagenesis
pr1225	GCAGCACCTTCGAGCGAGA C	Mapping primer for *mntH* (RL0940) mutagenesis
pr1226	CCTTAGACAGAATGAGCTG G	Mapping primer for *mntH* (RL0940) mutagenesis
pr1240	TTTTCTAGAGAAGCTGCCC GAGGGAAAAT	Forward primer; *mgtE* (RL1461)
pr1241	TTTGAATTCAGTCGATTGCC TTTGCCGTA	Forward primer; *mgtE* (RL1461)
pr1242	TTTGAATTCTGCCCGAGGG AAAATAATTC	Reverse primer; *mgtE* (RL1461)
pr1247	TTTCTCGAGCGACGTACAA GGAATTGTTA	Forward primer; pRL100036
pr1248	TTTGGATCCTAGTTCGTACG CGATGACAT	Reverse primer; pRL100036
pr1249	TTTGGATCCAATATCCCGAT CGAAATGAT	Forward primer; pRL100035
pr1250	TTTTCTAGAGAAGACGCCA ATCGCATCAC	Reverse primer; pRL100035
pr1265	AAAGGTACCCATTCTGGCG TTAAGCATTT	Reverse primer; *mgtE* (RL1461)
pr1270	CTCGAGGCTACATCGACCA CTATCTC	Forward primer; *fixL*
pr1271	TCTAGAACACGGGCGTCAT CTTCGAC	Reverse primer; *fixL*
pr1272	CGGAAGAGCTTCCACGATG A	Mapping primer for *fixL* mutagenesis
pr1273	GCCGTCCGCACCTGTCGTTC	Mapping primer for *fixL* mutagenesis
pr1286	AGATCTATCTCCCAGCCGG CATTGTC	Forward primer; *oxyR*
pr1287	TCTAGAGGCCATCGGTGTC GAATTGC	Reverse primer; *oxyR*
pr1288	GCTTGATAGGCCACAGCAG G	Mapping primer for *oxyR* mutagenesis
pr1289	GCGATGCCCACGCCGTTGG C	Mapping primer for *oxyR* mutagenesis
pr1290	AAGCTTTCAGGCGCGACTG GACGGGC	Forward primer; *mntH* (RL0940) promoter
pr1291	TCTAGATCGCCATGCCGAG CTGTGAC	Reverse primer; *mntH* (RL0940) promoter
pr1292	AAGCTTCCTATCTGGTCTTC AAGGCC	Forward primer; *sitA* (RL3884) promoter
pr1293	TCTAGATTGGTTGTCTGTTG GGCAGC	Reverse primer; *sitA* (RL3884) promoter

pr1378	CGAGCTTTCCGGCGGCCAGA	Forward primer; Rlp4292 *sitA*
pr1381	GCCTAAAGCGCGTCTGGTTC	Forward primer; *fnrN*
pr1382	AATAAGCCTGCGGCGCATCC	Reverse primer; *fnrN*
pr1385	GCTAATTCCGGGCGTGGCAT	Forward primer; RL1302
pr1386	GACCTTTACCCAGGGCATCG	Reverse primer; RL1302
pr1387	GGTGAATCTCCGTCGAGGGC	Mapping primer for RL1302 mutagenesis
pr1388	GGGTGCCGATCAGTTCTTCC	Mapping primer for RL1302 mutagenesis
pr1394	GCGTCACCGCCGTCGTCGGC	Reverse primer; Rlp4292 *sitA*
pr1432	CTGGGCCATGGTCTCGATCA	Mapping primer for *fnrN* mutagenesis
pr1433	CATAATCTCGGCACCATGGC	Mapping primer for *fnrN* mutagenesis
pr1457	CGTTGAGCTGATCGACCATG	Mapping primer for Rlp4292 *sitA* mutagenesis
pr1462	TCTAGAGCTGCGTGCGCCTCTCGTCA	Reverse primer; *mntH*

Table 2.5 Primers.

2.3 MOLECULAR TECHNIQUES

2.3.1 DNA isolation

Genomic DNA (gDNA) was isolated from bacterial cultures using the DNeasy Blood and Tissue kit (Qiagen), following instructions provided by the manufacturer (Pre-treatment for Gram-Negative bacteria and Purification of total DNA from Animal Tissues).

Plasmid DNA was isolated from *E. coli* DH5α using the Spin Miniprep kit (Qiagen), following instructions provided by the manufacturer (Plasmid DNA Purification using the QIAprep Spin Miniprep Kit and a Microcentrifuge).

2.3.2 Polymerase chain reaction (PCR)

PCR primers were designed using Vector NTI 11.0 or the Clontech online tool for creating primers used for In-Fusion® cloning (Clontech). Primers were synthesised by Eurofins MWG Operon.

PCR reactions (10 µl or 50 µl) were made using GoTaq® Green master mix (Promega) or Phusion® High-fidelity PCR master mix (Finnzymes). Thermocycler conditions were set using instructions provided by the manufacturer of the master mix and Tm calculations of primers provided by Eurofins MWG Operon. Both gDNA and plasmid DNA were used as templates for PCR. Colony PCR was used for large screens of transformants, where *E. coli* cells were transferred from a single colony to the PCR reaction using a sterile pin. For large screens of *R. leguminosarum* strains (i.e. screening for mutagenesis), cells were transferred to 500 µl sterile H_2O using a sterile loop and pelleted by centrifugation (6000 rpm for 4 minutes). Following centrifugation, 490 µl of the supernatant was removed and 100 µl alkaline poly(ethylene) (PEG) reagent was added. To make the alkaline PEG reagent, 60g PEG200 (Sigma) was combined with 0.93 ml 2M KOH and 39 ml water. Pelleted bacteria were incubated in the alkaline PEG reagent at room

temperature for 15 minutes. For a 10 µl PCR reaction, 1 µl of bacteria suspended in alkaline PEG was added.

When PCR product was to be used for cloning, PCR products were purified using the QIAquick PCR purification kit (Qiagen), following the manufacturer's instructions.

2.3.3 Agarose gel electrophoresis

PCR products, restriction digests and GeneRuler^{TM} 1 kb DNA ladder (Thermo Scientific) were separated by agarose gel electrophoresis on 1% agarose (Sigma) in TAE buffer [400 mM Tris acetate, 1 mM EDTA] at 120 mV for 45-75 minutes. For PCR reactions using Phusion® High-fidelity PCR master mix (Finnzymes), 1X DNA loading dye (Qiagen) was added to samples. After electrophoresis, DNA was stained in ethidium bromide (0.5 µg/ml^{-1}) for 30 minutes and analysed using a UV transilluminator.

2.3.4 Restriction digests

Restriction digests of purified DNA were conducted using restriction endonucleases and buffers (Fermentas or Roche) following the manufacturer's instructions. Fragmented DNA was analysed by agarose gel electrophoresis. When required for cloning, fragmented DNA was purified using the QIAquick PCR purification kit (Qiagen) or QIAquick gel extraction kit (Qiagen) following instructions provided by the manufacturer.

2.3.5 Ligations

DNA ligations were performed using enzymes and buffers provided in the CloneJET PCR Cloning kit (Fermentas) or T4 DNA ligase supplied with the 10X T4 DNA ligase buffer (Fermentas). Ligations for pJET cloning were performed at room temperature for 20 minutes, or for all other ligations, overnight at 16°C.

2.3.6 BD In-Fusion™ cloning

A BD In-Fusion™ cloning kit (clontech) was used for high-throuput cloning following the manufactures instructions. An online tool (Clontech) was used to design primers with 16 bp extensions homologous to vector ends. Cloning enhancer (Clontech) was added to PCR product before the In-Fusion™ cloning reaction to achieve optimal results. A second online tool was used to calculate the optimal molar ratio of PCR product to vector for the cloning reaction. After the In-Fusion reaction, recombinant plasmids were used to transform competent E. coli DH5α cells.

2.3.7 Transformations

Chemically competent *E. coli* DH5α cells (Bioline) were used for transformations. Competent cells (50 µl) were thawed on ice and 2 µl ligation mix or purified plasmid was added. Cells were then incubated for 30 minutes on ice, heat shocked at $42^{o}C$ for 45 seconds and then transferred back to ice. After three minutes, 250 µl SOC medium (2% w/v tryptone, 0.5% w/v yeast extract, 10 mM NaCl, 2.5 mM KCl, 10 mM $MgSO_4$ 10 mM $MgCl_2$, 20 mM glucose) was added and cells were incubated for 1 hour at $37^{o}C$ with shaking at 250 rpm. Cells were then plated on LB agar containing the appropriate antibiotic selection and incubated overnight at $37^{o}C$.

2.3.8 Conjugation from *E. coli* to *R. leguminosarum*

Plasmids were transferred from *E. coli* to *R. leguminosarum* by tri-parental conjugation using a helper *E. coli* strain that carried pRK2013 (Ditta et al., 1980). *E. coli* strains carrying either the plasmid of interest or pRK2013 were grown in LB (containing the appropriate antibiotics) overnight at $37^{o}C$ with shaking at 250 rpm. Overnight cultures were then subcultured (200-500 µl inoculum) in fresh LB containing appropriate antibiotics and grown for 6-8 hours at $37^{o}C$ with shaking at 100 rpm (to OD_{600} 0.4-0.6). When grown, *E. coli* strains were pelleted by centrifugation at 6000 rpm for 4 minutes and then re-supsended in TY; a washing step was included to remove traces of antibiotics.

Recipient *R. leguminosarum* strains were grown on TY slopes containing appropriate antibiotics at 28°C. After 3 weeks, 5 ml TY was added to slopes to obtain a rhizobial suspension. To make the conjugation mix, the rhizobial suspension was added to 400 µl of washed *E. coli* culture carrying the plasmid of interest and 200 µl of washed *E. coli* culture carrying the pRK2013 plasmid. The conjugation mix was then spun down at 6000 rpm for 4 minutes, resuspended in 30-50 µl TY and then spotted onto a sterile nitrocellulose filter placed on solid TY medium. Conjugation mix was incubated overnight at 28°C, suspended in 1 ml TY, plated out on TY agar containing appropriate antibiotics and incubated at 28°C. To select against *E. coli*, streptomycin (500 µg/ml) or in the case of *R. leguminosarum* bv. phaseoli, rifampicin (10 µg/ml) was used.

2.4 MUTAGENESIS TECHNIQUES

2.4.1 Mutagenesis of *R. leguminosarum* by pRU877- and pK19mob-integration (single-crossover)

High-throughput, site-directed mutagenesis of *R. leguminosarum* was achieved by pRU877- (Lodwig et al., 2004) or pK19mob-integration (Schafer et al., 1994).

PCR primers were designed to amplify the internal fragment (300-900 bp) of the targeted gene. A 16 bp extension homologous to the vector ends of *Xba*I-digested pRU877 or *Xba*I-digested pK19mob was added to the 5' end of the primers. These primers were used to amplify the internal fragment of genes from *R. leguminosarum* gDNA. The PCR products were then cloned directly into *Xba*I-digested pRU877 or *Xba*I-digested pK19mob using the BD In-Fusion™ cloning kit (Clontech) (2.3.6). Recombinant plasmids were transformed into competent DH5α cells (2.3.7). *E. coli* cells carrying the pRU877 or pK19mob plasmid were selected for using kanamycin on solid LB medium. For pK19mob recombinant plasmids, blue/white screening could be used to check for an insert by the addition of X-gal to the solid LB medium.

To confirm that the correct sequence had been cloned into pRU877 or pK19mob, sizes of the inserts were determined by colony PCR using the vector-mapping

primers M13uni (-21) and M13 (-29). Plasmids with the correctly sized inserts were sent to Eurofins MWG Operon for sequencing (at a concentration of 50-100 ng/µl) using M13 primers. Sequences were then checked against the Rlv3841 genome sequence (Young et al., 2006) using Vector NTI 11 Align X.

Recombinant plasmids with the correct sequence were transferred into *R. leguminosarum* by tri-parental conjugation (2.3.8). To select against *E. coli*, streptomycin (500 µg/ml) or in the case of *R. leguminosarum* bv. phaseoli, rifampicin (10 µg/ml) was used. To select for pRU877 or pK19mob integration, neomycin was used at 250 µg/ml. Colonies that grew on solid TY medium containing these antibiotics were screened for pRU877/pK19mob integration by colony PCR using a mapping primers specific to pRU877 (pr0095) or pK19mob (pK19/18A or pK19/18B) and a primer binding ~500bp upstream of the disrupted gene. Mapping primers along with primers used to amplify the internal fragments of the targeted genes can be found in Table 2.5.

In this thesis, the nomenclature used to denote mutations created by pRU877- or pK19mob-integration is :pRU877 or :pK19mob e.g. *sitA*:pRU877 means mutation of *sitA* by pRU877-integration.

2.4.2 Mutagenesis of *R. leguminosarum* by Ω intersposon insertion (double-crossover)

When an alternative marker was required (e.g. for the construction of double mutants), genes were disrupted with by insertion of an Ω intersposon carrying spectomycin resistance (ΩSpc), an Ω intersposon carrying tetracycline resistance (ΩTc) or an Ω intersposon carrying kanamycin resistance (ΩKm) (Fellay et al., 1987).

The general strategy involved cloning a DNA region that contained the target gene with ~1 kb either side into pJET1.2/blunt. The Ω interspsosons carrying antibiotic resistance were cut from pHP45Ω plasmids (Fellay et al., 1987) and inserted into the cloned gene at a unique restriction site. When necessary, linearised-plasmid was

blunted by a Klenow Fragment (Thermo Scientific). The pJET1.2/blunt insert was then cloned into the mobilisable, suicide vector pJQ200SK (Quandt and Hynes, 1993). Alternatively, the gene of interest with the 1 kb flanking regions was cloned into pJQ200SK, and in this vector, the Ω intersposon was inserted. Recombinant pJQ200SK plasmids were transferred into *R. leguminosarum* by tri-parental conjugation (2.3.8) and pJQ200SK- integration was selected for with the appropriate antibiotics. Approximately ten antibiotic-resistant colonies were grown on a TY slope containing the appropriate antibiotics. After three days' growth, 5 ml TY was added to the slope and the suspension was plated out on solid AMS medium containing 10 mM NH_4Cl and 10% sucrose. Due to the presence of the lethal sucrose-inducible *sacB* gene on pJQ200SK, addition of 10% sucrose selected for double-crossover events that result in the replacement of the host DNA with the pJQ200SK-insert. To confirm the loss of the pJQ200SK vector and presence of the Ω intersposon insertion, sucrose-resistant colonies were then patched on a TY plate containing gentamicin and a replicate TY plate containing the antibiotic that the Ω intersposon confered resistance to i.e. spectinomycin, tetracycline or kanamycin. Colonies sensitive to gentamicin but resistant to the second antibiotic were screened by PCR for double-crossover events using a mapping primer specific to the Ω intersposon (pOT forward_far) and mapping primers designed to bind >1 kb downstream and upstream of the disrupted gene. Mapping primers and cloning primers used for Ω intersposon insertions can be found in Table 2.5.

In this thesis, the nomenclature used to denote a mutation created by Ω intersposon insertion is ΩSpc, ΩKm or ΩTc (depending on the antibiotic resistance) e.g. *sitA*ΩSpc.

2.4.3 Generalised transduction in *R. leguminosarum*

The bacteriophage RL38 (Buchanan-Wollaston, 1979) was used to transduce genetic regions carrying mutations (and antibiotic resistance markers) from one strain of *R. leguminosarum* to another.

Phage were propagated in the donor strain (i.e. the strain that carries the genetic region that is to be transferred). The donor strain was grown on a TY slope carrying the appropriate antibiotics. After two days' growth, bacteria were resuspended in 3 ml sterile H_2O and 0.1 ml aliquots of this suspension were added to 0.1 ml of a serial dilution of phage (1 x 10^{-2} to 1 x 10^{-6}). In addition, for controls, one sample contained just bacteria and another sample just contained phage. All samples were used to inoculate 3 ml melted TY agar (0.9% w/v agar) incubated at 42°C, which was then poured over the surface of a TY plate. Plates were incubated at 28°C.

After 2-3 days, the bacterial/phage dilution that produced a lawn, that was just before complete confluence, was eluted by the addition of 10 ml sterile H_2O to the plate. Bacteria and phage were eluted by gentle rocking. After 2 hours, the bacteria/phage suspension was recovered using a 10 ml syringe and passed through a 0.22 µM filter (Millipore) to remove bacteria. After filter sterilisation, 2-4 drops of chloroform were added to the phage to ensure that the phage solution was free from bacteria. Phage solution was stored at 4°C.

For transductions, the recipient strain (i.e. the strain that will receive the genetic region that is to be transferred by the phage) was grown on a TY slope at 28°C. After 2-3 days' growth, 3 ml TY was added to obtain a bacterial suspension. 200 µl aliquots of this suspension were mixed with 0.1, 1.0, 10 and 100 µl of phage solution prepared from the donor strain. Controls that contained just the phage or bacteria were made. Bacteria/phage mixtures were incubated at 28°C and after 1 hour, were plated out on solid TY medium containing the appropriate antibiotics. Plates were incubated for 3-5 days at 28°C and colonies were isolated using a sterile plastic loop. Colonies were checked for correct transductions by colony PCR.

2.5 ASSAYS

2.5.1 Testing growth of *R. leguminosarum* strains in modified AMS medium containing varying levels of MnSO$_4$ (96-well plate)

Growth of *R. leguminosarum* strains was tested in modified AMS medium containing 0.05 μM or 25 μM MnSO$_4$ using the following protocol. Strains were first grown on TY slopes with the appropriate antibiotics and for the growth of LMB466 (*sitA*:pK19mob *mntH*ΩSpc) solid TY medium was supplemented with 50 μM MnSO$_4$. After 2 days' growth, 5 ml AMS was added to the slopes to obtain a bacterial suspension, which was then used to inoculate 100 ml AMS glucose (or modified AMS glucose containing 25 μM MnSO$_4$ for growth of LMB466 (*sitA*:pK19mob *mntH*ΩSpc)) to an OD$_{600}$ of 0.01. Cultures were incubated at 28°C with shaking at 220 rpm. When exponential phase was reached (OD$_{600}$ 0.2-0.6), 10 ml samples x2 were taken from each culture, centrifuged at 4000 rpm (revolutions per minute) for 5 minutes and then resuspended in modified AMS (omitting MnSO$_4$). This washing-step was repeated twice to remove extracellular traces of MnSO$_4$. After the third wash, for each stain, one sample was resuspended in modified AMS glucose containing 0.05 μM MnSO$_4$ and the second sample was resuspended in AMS glucose containing 25 μM MnSO$_4$. Both were resupended to an OD$_{600}$ of 0.1. Samples were then transferred to a 96-well plate as 200 μl aliquots and read at OD$_{600}$ by a BioTek EON^{TM} plate reader. Growth was measured for 24 hours at 30 minute intervals between linear-shaking.

2.5.2 Testing growth of *R. leguminosarum* strains in modified AMS medium containing varying levels of MnSO$_4$ (conical flask)

Growth of *R. leguminosarum* strains was tested in 50 ml of modified AMS glucose containing 0.05 or 10 μM MnSO$_4$ using the following protocol. Strains were grown first on TY slopes with the appropriate antibiotics and for the growth of the double mutants LMB466 (*sitA*:pK19mob *mntH*ΩSpc), LMB539 (RlvA34 *sitA*:pK19mob *mntH*ΩSpc) and LMB630 (Rlp4292 *sitA*ΩKm *mntH*ΩSpc), solid TY medium was supplemented with 50 μM MnSO$_4$. After 2 days' growth, 5 ml modified AMS

(omitting $MnSO_4$) was added to the slopes to obtain a bacterial suspension; this suspension was used to inoculate both 50 ml modified AMS glucose containing 0.05 μM $MnSO_4$ and 50 ml modified AMS glucose containing 10 μM $MnSO_4$ to an $\sim OD_{600}$ of 0.005. Cultures were incubated at 28°C with shaking at 220 rpm. After 14 hours, samples were taken every 3-4 hours and used to measure OD_{600}.

2.5.3 Testing growth of *R. leguminosarum* strains in AMS medium containing varying levels of $MgSO_4$ at pH 7.0 or pH 5.75 (conical flask)

Strains were grown on TY slopes with the appropriate antibiotics and after 2 days' growth, 5 ml modified AMS (omitting $MgSO_4$) was added to obtain a bacterial suspension. The bacterial suspension was used to inoculate both 50 ml modified AMS glucose containing 0.01 mM $MgSO_4$ or 50 ml AMS glucose containing 2 mM $MgSO_4$. Cultures were incubated at 28°C with shaking at 220 rpm. After 14 hours, samples were taken every 3 hours and used to measure OD_{600}. When measuring growth at low pH, pH of AMS was adjusted to pH 5.75.

2.5.4 Testing growth of *R. leguminosarum* strains in the presence of 5% EtOH (96-well plate)

Growth of *R. leguminosarum* strains was tested in AMS glucose containing 5% EtOH using the following protocol. Strains were first grown on TY slopes with the appropriate antibiotics. After 2 days' growth, 5 ml AMS was added to the slopes to obtain a bacterial suspension, which was then used to inoculate 100 ml AMS glucose to an OD_{600} of 0.01. Cultures were incubated at 28°C with shaking at 220 rpm. When exponential phase was reached (OD_{600} 0.2-0.6), 10 ml samples x2 were taken from each culture and centrifuged at 4000 rpm for 5 minutes. One pellet was resupended in AMS glucose containing 5% EtOH and the other was resuspended in AMS glucose (negative control) to an OD_{600} 0.1. Samples were then transferred to a 96-well plate as 200 μl aliquots and read at OD_{600} by a BioTek EON^{TM} plate reader. Growth was measured for 40 hours at 30 minute intervals between linear-shaking.

2.5.5 H$_2$O$_2$ sensitivity assay

To measure sensitivity of Rlv3841, LMB364 (*sitA*:pK19mob) and LMB460 (*mntH*ΩSpc) to H$_2$O$_2$, strains were pre-cultured in 100 ml AMS glucose to stationary phase (OD$_{600}$ 0.9-1.1). Cultures were washed x3 in modified AMS (omitting MnSO$_4$) and diluted with modified AMS glucose (omitting MnSO$_4$) to a final OD$_{600}$ 0.1. Diluted cultured were split into 2 x 50 ml cultures and 0.5 mM H$_2$O$_2$ was added to one and the other was used as a negative control. Cultures were incubated at 28°C with shaking at 220 rpm and at 0, 2, 4 and 6 hours, samples were taken and serially diluted (1 x 10^{-1} to 1 x 10^{-8}) in modified AMS (omitting MnSO$_4$). All dilutions were spotted (15 µl aliquots) onto solid AMS glucose medium (3 spots for each dilution). Plates were incubated at 28°C and after two days, colony forming units/ml for each sample was determined.

2.5.6 β-glucuronidase (GUS) activity

To study expression of *sitA* and *mntH* in response to MnSO$_4$, GUS activity was measured in strains carrying *sitA-gusA* or *mntH-gusA*. Cells were grown overnight at 28°C with shaking at 220 rpm, in modified AMS glucose containing either 0.05 µM or 0.9 µM MnSO$_4$. When OD$_{600}$ 1-1.2 was reached, 1.5 ml samples were taken, centrifuged at 6500 rpm for 5 minutes and resuspended in 1.5 ml Z buffer (0.06 M Na$_2$HPO$_4$, 0.04 M NaH$_2$PO$_4$, 0.01 M KCl, 0.001 M MgSO$_4$, pH 7.0). In duplicate, 350 µl of resupended cells was taken and added to 280 µl Z buffer and 70 µl lysozyme-solution (0.05 g lysozyme and 350 µl mercaptoethanol in 10 ml of 10 mM phosphate buffer, pH 7.8). To make 10 mM phosphate buffer, 0.1 M phosphate buffer was made (90.8 ml 1 M K$_2$HPO$_4$ added to 9.2 ml 1 M KH$_2$PO$_4$) and diluted to 10 mM ; pH was tested before and after dilution. The final concentration of lysozyme equates to 0.5 mg/ml. Samples were inverted several times and incubated at 30°C for five minutes. Remainder of cells suspended in Z buffer was used to determined the OD$_{600}$.

After five minutes, 15 µl 0.5 M ethylenediaminetetraacetic acid (EDTA), pH 8.0, was added, samples were mixed by inverting several times and then left to incubate

at 30°C. After 15 minutes, 0.5 µl of 20% sodium dodecyl sulfate (SDS) was added, samples were mixed by inverting and then incubated at 30°C. After 30 minutes, 140 µl of 4-nitrophenyl β-D-glucuronide (PNPG) solution (0.08g PNPG (Sigma) and 70 µl mercaptoethanol in 20 ml of Z buffer) was added and incubated at 30°C. After 5 minutes, the reaction was stopped by the addition of 350 µl of 1 M Na_2CO_3. Samples were mixed by inverting several times, centrifuged at 13000 rpm for 30 minutes to pellet cell debris and the supernatant was measured at OD_{420}. The assumption that 1 ml of an OD_{600} 1.0 culture contains 0.22 mg of protein and the extinction co-efficient of 4.012 x 10^3 mol^{-1} cm^{-1} was used to calculate the rate at which p-nitrophenyl was released from PNPG by β-glucuronidase hydrolysis (Lodwig et al., 2004).

To study expression of *sitA-gusA* and *mntH-gusA* in response to oxidative stress, cells were grown in 100 ml AMS glucose to OD_{600} 0.2-0.4. Cultures were then split into 2x 50 ml, where to one, 100 µM H_2O_2 was added and the other was used as a negative control. Following treatment, samples were taken at 0, 2, 4 and 6 hours. GUS activity was measured for all samples as described above.

2.5.7 Disk assays

Strains were grown on TY slopes containing the appropriate antibiotics. After two days' growth, 5 ml TY was added to obtain a bacterial suspension, which was diluted with TY to OD_{600} 0.2. A volume of 200 µl was taken from this diluted bacterial suspension and used to inoculate 3 ml melted TY agar (0.9% w/v agar) incubated at 42°C. Immediately after inoculation, the melted TY agar was poured over solid TY medium and left to solidify at room temperature. After 30 minutes, a sterile filter disc (Whatman Grade AA 6 mm discs; GE Healthcare, Life Sciences) was placed on the top layer of agar and 15 µl of the experimental compound was added directly to the disc. Plates were incubated at 28°C and after 2 days, the zone of inhibition was measured. Disk assays testing the sensitivities of Rlv3841 and RU4107 (*mgtE*::mTn5) to toxic-concentrations of metals (Chapter five) were conducted on solid AMS glucose instead of TY.

2.6 PLANT EXPERIMENTS

2.6.1 Growth of *P. sativum* and *V. faba*

P. sativum cv. Avola or scarified *V. faba* cv. Sutton seeds were surface sterilised by immersing them in 70% EtOH. After 1 minute, the EtOH was poured away and the seeds were immersed in sterile H_2O. After 1 minute, H_2O was poured away and seeds were immersed in 2% sodium hypochlorite for 5 minutes and then washed with sterile H_2O for 1 minute. Washing with sterile H_2O was repeated 5 times to remove traces of sodium hypochlorite. After washing, seeds were transferred to a sterile flask and the washing step was repeated another 5 times. Surface sterilised seeds were then placed in a sterile Petri dish.

Surface sterilised seeds were sown in 1 l^{-1} pots (2 seeds per pot) containing autoclaved vermiculite and 400 ml N-free rooting solution (4 mM Na_2HPO_4, 3.7 mM K_2PO_4, 1 mM $CaCl_2$, 800 μM $MgSO_4$, 100 μM KCl, 35 μM H_3BO_3, 10 μM Fe EDTA, 9 μM $MnCl_2$, 0.8 μM $ZnCl_2$, 0.5 μM Na_2MoO_4, 0.3 μM $CuSO_4$). To make the inoculants, *R. leguminosarum* strains were grown on TY slopes containing the appropriate antibiotics. After 3 days' growth, 5 ml of sterile H_2O was added to slopes and 1 ml of the bacterial suspension was diluted with 19 ml sterile H_2O. At time of sowing, seeds were inoculated with 1 ml of the diluted bacterial suspension and pots were covered with Clingfilm to reduce water loss and contamination when being transported to the controlled growth room.

Plants were grown in a controlled growth room at 22^oC with a 16 hour light cycle. After 5-7 days, above the emerging shoots an opening was made in the Clingfilm using a sterile blade and seedlings were thinned to one plant per pot. Plants were harvested 3 weeks post inoculation (p.i.).

When necessary, nodules from 3 week plants were sectioned and stained with toluidine blue by Sue Bunnewell (BioImaging, JIC). Sections were then visualised under a Leica DM6000 light microscope. For visualisation by electron microscopy,

ultrathin sections were taken and stained with uranyl acetate and lead citrate by Kim Findlay (BioImaging, JIC).

2.6.2 Growing *V. hirsuta*

V. hirsuta seeds were scarified with sandpaper for 10 seconds. Seeds were then surface sterilised by immersion in 1% sodium hypochlorite for 5 minutes. Sodium hypochlorite was poured away, seeds were washed 5 times with sterile H_2O, transferred to a sterile flask and then washed another 5 times. Seeds were then placed on H_2O agar (agar 3% w/v) and incubated at 4^oC. After 3 days, seeds were moved to room temperature and kept in the dark to germinate. After two days, germinated seeds were sown into 1 l^{-1} pots (6 seeds per pot) containing autoclaved vermiculite and 400 ml N-free rooting solution. Seeds were inoculated with *R. leguminosarum* strains (as described in 2.6.1). Following seed inoculation, pots were covered with Clingfilm.

Plants were grown in a controlled growth room at 22^oC with a 16 hour light cycle. After 5-7 days, above the emerging shoots an opening was made in the Clingfilm using a sterile blade. Plants were harvested 3 weeks p.i.

2.6.3 Growing *P. vulgaris*

P. vulgaris cv. Tendergreen seeds were surface sterilised by immersion in 70% EtOH for 30 seconds and then washed in sterile H_2O for 5 seconds. Seeds were then immersed in 2% sodium hypochlorite for 2 minutes, and quickly washed with sterile H_2O 5 times, only leaving the seeds in the H_2O for a maximum of 5 seconds. Seeds were transferred to a sterile flask and washed another 3 times. After the final wash, seeds were placed in a sterile Petri dish. Seeds were sown in 1 l^{-1} pots (2 seeds per pot) containing autoclaved vermiculite and 400 ml N-free rooting solution. Seeds were then inoculated with *R. leguminosarum* bv. phaseoli strains (as described in 2.6.1). Following seed inoculation, pots were covered with Clingfilm.

Plants were grown in a controlled growth room at 22$^{\text{o}}$C with a 16 hour light cycle. After 5-7 days, above the emerging shoots an opening was made in the Clingfilm using a sterile blade and seedlings were thinned to one plant per pot. Plants were harvested 4 weeks p.i.

2.6.4 Acetylene reduction assays

Rates of N$_2$ fixation were determined by measuring the reduction of acetylene to ethylene (Hardy et al., 1973; Trinick et al., 1976). Harvested plants (3 weeks p.i. for *P. sativum*, *V. faba* and *V. hirsuta* or 4 weeks p.i. for *P. vulgaris*) were placed in 250 ml Schott bottles lined with moistened paper and neoprene lids to ensure an airtight seal. Once sealed, 8 ml of air was removed and 6.5 ml of acetylene was added by syringe. Plants were incubated at room temperature and after 1 hour, 1 ml gas samples were collected by syringe. Samples were analysed by a Shimadzu GC-14B gas chromatograph and rates of acetylene reduction were calculated based on the ratio of ethylene to acetylene.

2.6.5 Nodule counts and re-isolation of nodule bacteria

After rates of acetylene reduction were determined, plants were removed from Schott bottles and nodules were counted. After the nodules had been counted, approximately 5-10 nodules for each inoculation were removed from the roots and placed in an Eppendorf tube. Nodules were immersed in 70% EtOH and after 1 minute washed in sterile H$_2$O. Nodules were washed in sterile H$_2$O 10 times, placed in a 96-well plate and then immersed in 100 µl sterile H$_2$O. Nodules were crushed with a sterile rod and the resulting bacterial suspension was streaked onto a solid TY medium. Plates were incubated at 28$^{\text{o}}$C for 3-4 days. From these TY plates, 5-10 colonies were randomly selected and patched onto a TY plate and replica TY plates containing antibiotics to verify the presence of the antibiotic resistance marker.

2.6.6 Shoot dry weights

P. sativum or *V. faba* seeds were sown and inoculated (2.6.1) in 2 l^{-1} pots containing autoclaved vermiculite and 800 ml N-free rooting solution. After 4 weeks p.i., 400 ml of sterile H_2O was added to each pot and after 6 weeks p.i., plants were harvested. Shoots were removed, placed in pre-weighed envelopes and dried at $60^{o}C$. After 3 days, weights of dried shoots were determined.

2.6.7 Histochemical staining of nodule sections

To detect *sitA*-g*usA* and *mntH*-g*usA* expression *in planta*, nodules were taken from 3 week plants and sectioned under H_2O into 80-100 μM sections using a vibratome. Sections were then incubated in staining buffer (50 mM sodium phosphate buffer pH 7.0; 0.1% Triton X-100, 5 mM $K_3[Fe(CN)_6]$; 5 mM $K_4[Fe(CN)_6]$) containing 0.02% 5-bromo-4-chloro-3-indoyl-β-D-glucuronide (X-GlcA, Sigma). After 18 minutes, the reaction was stopped by fixing the sections in 1.25% glutaraldehyde in 50 mM sodium phosphate buffer (pH 7.0). Sections were visualised under a Leica DM6000 light microscope.

2.6.8 Dry weights of bacteroids, plant cytosol, nodules and quantification of Mg by Atomic Absorption Spectroscopy

Atomic absorption spectroscopy (AAS) was used to quantify Mg associated with the plant cytosol and bacteroids isolated from nodules. Rlv3841 or RU4107 (*mgtE*::mTn5) was used to inoculate 32 *P. sativum* seeds sown in 1 l^{-1} pots (2x seeds per pot) (2.6.1). This was done in triplicate e.g. 3 cultures of Rlv3841 were used to inoculate x3 batches, each batch containing 32 seeds. After 5-7 days, seedlings were thinned to 1 seedling per pot. This was repeated for *V. faba*.

Plants were harvested after 3 weeks; all nodules were collected from each batch of plants and transferred to separate beakers. Nodules were macerated with a clean mortar and pestle in 10 ml of 10 mM phosphate buffer (pH 7.0). The macerated nodule-mix was transferred to a 15 ml Falcon tube and centrifuged at 1000 rpm for 5

minutes to remove traces of vermiculite and plant debris. The supernatant was transferred to a new 15 ml Falcon tube and centrifuged at 4000 rpm. After 10 minutes, the supernatant (plant cytosol) was transferred to a new 15 ml Falcon tube; the pellet was also kept (bacteroid).

Samples were prepared for AAS following the Perkin Elmer guide for Analytical Methods for Atomic Absorption Spectroscopy; Analysis of Plant Tissue: Dry Ashing protocol. Plant cytosol and bacteroid fractions were transferred to a pre-weighed crucible (bacteroid pellet was resupended in deionized H_2O to transfer) and dried at 100^oC overnight. Crucibles containing the dried samples were weighed and sample weight was determined. Nodule dry weight could be calculated by combining the dry weights of the bacteroid and plant cytosol fractions. Weighed-samples were then transferred to a muffle furnace, where they were ashed at 250^oC for 2 hours (with the temperature increasing by 10^oC/minute) and then at 550^oC for 20 hours (increasing by 10^oC/minute). Ashed samples were weighed and then dissolved in 1 ml^{-1} 2% HCl acid. Samples were then diluted 1/100 with deionized H_2O or in the case of RU4107 bacteroid pellet, 1/50. Samples were mixed by vortexing.

Mg was quantified with assistance from Dave Hart (IFR) using a Perkin Elmer Model 3300 Atomic Absorption instrument with an air-acetylene flame. The Mg standard was an Mg AAS solution 1000 mg/l^{-1} (Sigma). A non-linear standard curve was created by measuring AU for the following concentrations of the Mg AAS standard: 0.5 mg/l^{-1}, 1.5 mg/l^{-1} and 3.0 mg/l^{-1}. Using the standard curve, samples were analysed by the atomic absorption instrument and Mg was quantified (Mg mg/l^{-1}). Each sample was measured in triplicate for 1 second^{-1} at 1 second^{-1} intervals and then averaged. After every 10 readings, dilutions of the Mg AAS solution were analysed to verify the reliability of the standard curve. Mg concentrations (mg/l^{-1}), dilution factor and dry weights of samples were used to determine Mg mg/g^{-1} dry weight.

Chapter 3: *Mutagenesis of Genes Upregulated during nodule-colonisation and bacteroid development*

3.1 INTRODUCTION

Microarrays that compared Rlv3841 grown in minimal medium to bacteria isolated from *P. sativum* nodules at four different time points, provided an insight into bacteroid development (Karunakaran et al., 2009). Genes upregulated (≥3-fold) in developing bacteroids (isolated from nodules 7 dpi) but not in mature bacteroids (isolated from nodules 15, 21 and 28 days dpi.) were identified. Forty-eight of these genes were selected for mutagenesis to discover genes required for nodule colonisation and bacteroid development.

3.2 RESULTS AND DISCUSSION

3.2.1 Construction of mutants

Targeted mutagenesis utilised the integration plasmids pRU877 and pK19mob (2.4.1) (Fig 3.1). Plasmid pRU877 (Lodwig et al., 2004) is derived from pK19mob (Schafer et al., 1994), with the addition of *gusA* (from pJP2) cloned into pK19mob as a *Kpn*I/*Pst*I fragment to combine integration mutations with *gusA* chromosomal fusions. Plasmid pK19mob was used because a number of genes could not be mutated using pRU877; this may have been the result of incorrect integrations caused by a low level of homology between *gusA* and an unknown region(s) in the Rlv3841 genome.

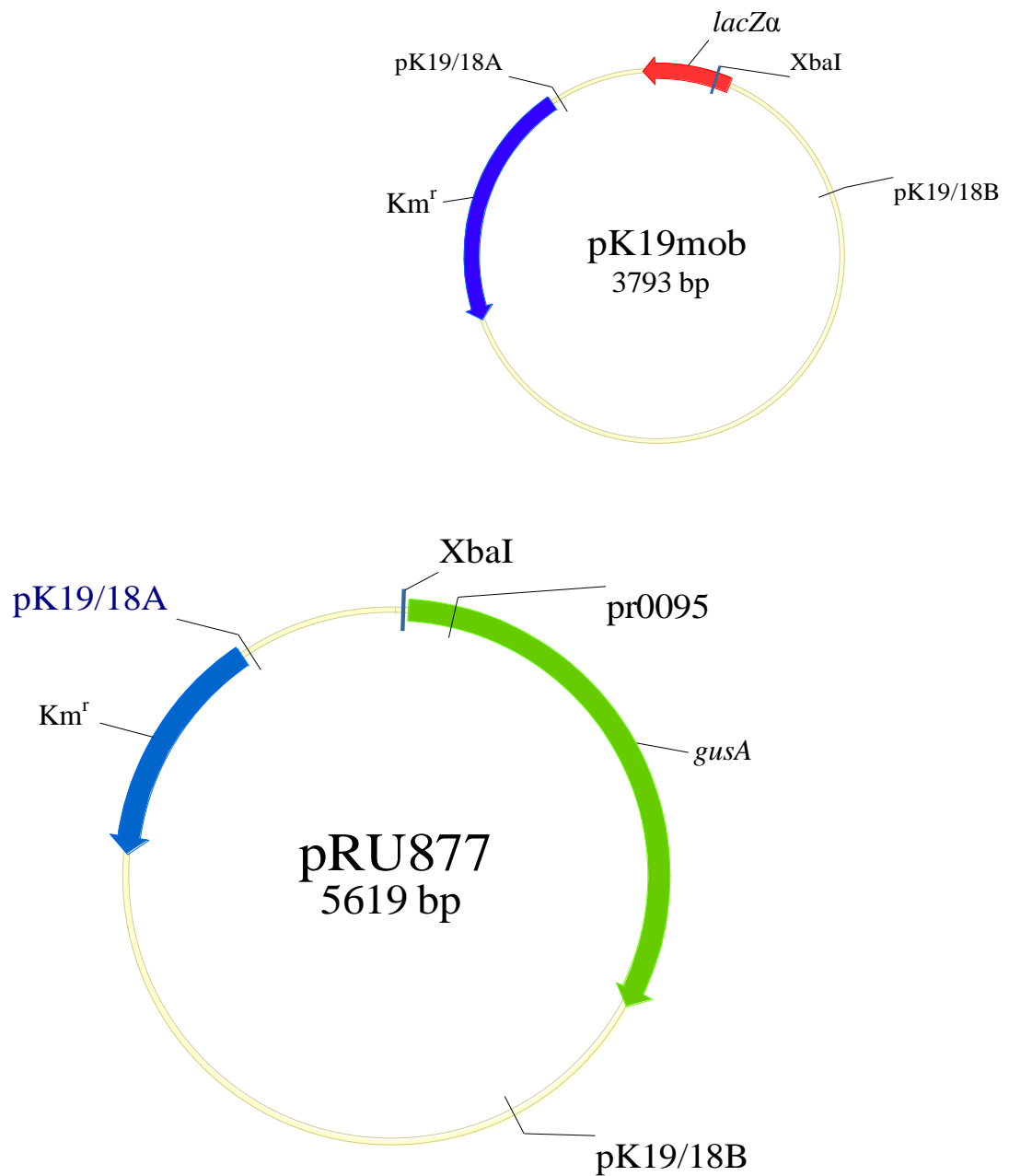**Fig 3.1** Maps of integration plasmids pK19mob (top) and pRU877 (bottom) showing location of *Xba*I in the multiple cloning site and binding sites for primers (pK19/18A, pK19/18B and pr0095) used for mapping integrated-plasmids to Rlv3841 genome.

3.2.2 Analysis of upregulated genes and their requirement for bacteroid development

Forty-eight genes were selected for mutagenesis and ultimately, forty-two of these genes were successfully mutated (Table 3.1). The forty-two genes could be separated into seven classes based on their putative roles during bacteroid development. These classes were: transport, efflux systems, resistance to oxidative stress, resistance to membrane stress, metabolism, regulation and unknowns (Table 3.1). In this section, genes and results are discussed for each separate class.

To test their abilities to nodulate and fix N_2 on *P. sativum*, the forty-two mutants were used to inoculate seeds that were subsequently grown for three weeks (2.6.1). After three weeks, N_2 fixation was measured by acetylene reduction (2.6.4), nodules were counted and then crushed to confirm the presence of the integrated plasmid (2.6.5). Due to space constraints in the controlled growth room, plants were tested in 13 batches with each batch including uninoculated plants and plants inoculated with Rlv3841 (wild type). Rates of acetylene reduction for mutant-inoculated plants were compared to both Rlv3841-inoculated plants in the same batch (batch Rlv3841) and the average rate for all Rlv3841-inoculated plants across the 13 batches (combined Rlv3841). The same was done for nodule counts. Combining the Rlv3841-inoculated plants helped deal with the issue of some batches containing Rlv3841-inoculated plants that had low rates of acetylene reductions due to slow germinating seeds or poor plant growth.

Gene	Exp. at 7dpi	Description	Strain
RL0262	3.1	Putative oxygen-binding heme protein	LMB367
RL0390	3.9	PraR; regulator involved in quorum sensing	LMB401
RL0447	7.0	Conserved hypothetical exported protein	LMB361
RL0472	3.0	Putative TetR family transcriptional regulator	LMB375
RL0940	5.7	Putative MntH protein; Mn^{2+} transporter	LMB363
RL1106	20.0	Putative PspA (phage shock response protein)	LMB506
RL1107	27.6	Putative YiaAB superfamily protein;	LMB489
RL1226	11.3	Conserved hypothetical protein	LMB404
RL1302	9.3	Putative OsmC/Ohr organic peroxide	LMB372
RL1317	3.7	Putative TM protein; CBS containing ion transporter	LMB366
RL1485	4.6	Putative protein required for attachment to host cells	LMB343
RL1631	12.8	Putative hypothetical protein	LMB398
RL1879	3.2	Putative FixL-homologue; FixLJ hybrid protein	LMB403
RL1880	3.3	Putative FixK-like protein; CRP/FNR family	LMB392
RL2022	8.4	Putative cobalamin/Fe3+-siderophore transporter	LMB360
RL2307	4.4	Putative CsbD superfamily protein; general stress response	LMB376
RL2924	3.9	Putative MarR regulator	LMB400
RL2925	4.1	Putative MutT; hydrolyzes mutagenic nucleotides	LMB397
RL2927	5.6	Putative OsmC/Ohr organic peroxide	LMB377
RL3152	3.1	Putative regulator	LMB340
RL3273	4.1	Putative protein of unknown function	LMB349
RL3688	3.2	Putative TetR family transcriptional regulator;	LMB410
RL3783	8.5	Putative MFS transporter; efflux system	LMB441
RL3884	4.8	Putative SitA protein; Mn^{2+} transport	LMB364
RL4103	7.5	Putative protein; extra-cytoplasmic solute receptors	LMB396
RL4274	14.2	Putative MFP component of efflux system	LMB384
pRL80060	3.5	Putative solute-binding component of ABC transporter	LMB369
pRL80012	5.4	Putative AAA+ protein; proposed protease interaction	LMB365
pRL90025	5.4	Putative FixK-like protein; CRP/FNR family	LMB374
pRL90056	3.9	Putative GntR family transcriptional regulator	LMB354
pRL90060	11.6	Putative MFS transporter; efflux system	LMB411
pRL90226	3.2	Putative regulator; contains receiver and effector domain	LMB348
pRL90266	3.3	Putative glycerophosphodiester phosphodiesterase	LMB347
pRL90278	4.4	Putative cytochrome bd-II oxidase subunit 1	LMB421
pRL100224	4.5	Putative nitrilotriacetate monooxygenase component	LMB338
pRL110033	5.1	Putative ABC efflux system	LMB378
pRL110055	3.3	Putative protein containing mononucleotidyl cyclase domain	LMB440
pRL110287	6.6	Putative 3-oxoadipate CoA-transferase subunit A (PcaI)	LMB391
pRL110377	6.9	Putative Kdp operon transcriptional regulatory protein	LMB385
pRL110623	4.3	Putative sugar-binding protein containing DNA binding domain	LMB425
pRL120362	4.0	Putative catalase-peroxidase; KatG	LMB402
pRL120695	6.3	Putative TetR family transcriptional regulator	LMB351

■Transport   ■ Efflux system   ■ Resistance to oxidative stress   ■ Resistance to membrane stress

■ Metabolism   ■ Regulator   □ Unknown or other

Table 3.1 Mutated genes and their fold-induction in bacteroids isolated from nodules 7 dpi relative to free-living cells (Exp. at 7dpi) (Karunakaran et al., 2009). Putative functions of genes are colour coded (see legend). Where abbreviated, TM = transmembrane, AAA = ATPase family associated with various cellular activities, MFP = membrane fusion protein, MFS = major facilitator superfamily, SBP = solute binding protein and CBS = cystathionine-β-synthase.

Transport

Putative transport systems were identified using the sequenced-genome of Rlv3841 (Young et al., 2006), searching for homology to characterised-transporters using the basic local alignment search tool (BLAST) (Altschul et al., 1990) and identifying conserved domains (Marchler-Bauer et al., 2009). Substrates for the putative transporter systems were also considered using a transport database that predicts substrates based on the family the putative transporter has been assigned to (Ren et al., 2007).

Five genes encoding putative transporters or components of transport systems were mutated. Two of these genes encode putative proteins involved in the transport of Mn^{2+}. The gene *mntH* (RL0940) encodes a putative H^+-dependent transporter belonging to the natural resistance-associated macrophage protein (Nramp) family (Kehres et al., 2000; Makui et al., 2000) that shows 60% amino acid identity to *B. japonicum* MntH (Altschul et al., 1990; Hohle and O'Brian, 2009). The gene *sitA* (RL3884) encodes a solute binding protein (SBP) for the Mn^{2+} ABC-type transport system (SitABCD) (Diaz-Mireles et al., 2004). Mn^{2+} transport has been shown to be required for *S. meliloti-M. sativa* symbiosis but neither disruption of *mntH* or *sitA* in Rlv3841 caused an obvious symbiotic defect on *P. sativum* (Table 3.2).

Genes RL2022 and pRL80060 encode putative SBPs that are predicted to belong to ABC-transport systems that import amino acids (Ren et al., 2007). However, neither gene was required for bacteroid development (Table 3.2).

The mutated gene RL1317, encodes a protein with a transporter associated domain and two conserved CBS (cystathionine β-synthase) domains, which are associated with the gating of ion channels (Ignoul and Eggermont, 2005; Ishitani et al., 2008). Plants inoculated with the mutant strain LMB366 (RL1317:pRU877) did have significantly (p= 0.01) fewer nodules relative to plants inoculated with Rlv3841 but the mutant reduced acetylene at the same rate as the batch Rlv3841 (p= 0.36) (Table 3.2). More replicates are needed to confirm this reduction in nodulation.

		Acetylene Reductions			Nodule Counts		
Strain	*Disrupted gene*	*Acetylene reduction (μmol h^{-1} plant^{-1})*	*% of batch Rlv3841[a]*	*% of combined Rlv3841[b]*	*Nodule count (n= 3)*	*% of batch Rlv3841[a]*	*% of combined Rlv3841[b]*
LMB360	RL2022	**3.96 ± 0.56 (n= 5)**	92 ± 13	80 ± 11	**94 ± 10**	104 ± 11	97 ± 10
LMB363	RL0940 (*mntH*)	**4.02 ± 0.5 (n= 5)**	93 ± 97	82 ± 10	**107 ± 10**	117 ± 12	110 ± 11
LMB364	RL3884 (*sitA*)	**6.30 ± 0.68 (n= 5)**	117 ± 13	128 ± 14	**78 ± 6**	102 ± 8	81 ± 6
LMB366	RL1317	**3.51 ± 0.63 (n= 4[c])**	76 ± 14	71 ± 13	**54 ± 7**	57 ± 8	56 ± 7
LMB369	pRL80060	**4.01 ± 0.28 (n= 5)**	122 ± 8	81 ± 6	**111 ± 5**	101 ± 4	114 ± 5

Table 3.2 Rates of acetylene reduction and nodule counts (± SEM) for *P. sativum* inoculated with strains carrying mutations in genes that encode putative transport systems. n= number of plants tested.

[a] Batch Rlv3841 refers to average measurement recorded for Rlv3841-inoculated plants sown and harvested on the same day as the mutant strain.

[b] Combined Rlv3841 refers to average measurement recorded for all Rlv3841-inoculated plants across all batches.

[c] For the majority of inoculations, five biological replicates were used to measure rates of acetylene reduction. A seed not germinating was the cause for when less than five replicates were used.

Efflux

Several efflux systems were upregulated in developing bacteroids agreeing with the research on efflux systems in *B. japonicum*, *S. meliloti* and *R. etli*. There are five families of efflux systems: (1) resistance nodulation cell division (RND), (2) major facilitator superfamily (MFS), (3) small multidrug resistance (SMR), (4) multidrug and toxic compound extrusion (MATE) and (5) ATP-binding cassette (ABC). Six putative RND-type and six putative MFS-type efflux systems were found to be encoded by Rlv3841 (Table 3.3).

RL4274 (Table 3.3) was selected for mutagenesis because of its strong induction during bacteroid development and in the rhizosphere of *P. sativum* (Ramachandran et al., 2011). It encodes a putative membrane fusion protein (MFP) that is predicted to function as part of a tripartite RND efflux system. MFPs are lipoproteins that bridge the periplasm, forming a tunnel that connects the efflux pump with an outermembrane channel (Lewis, 2000; Blair and Piddock, 2009). The cognate pump for this system is likely to be encoded by RL4275.

Two MFS-type efflux systems were also targeted for mutagenesis: RL3783 and pRL90060 (Table 3.3). The product of pRL90060 is an ortholog of RmrB in *R. etli* (1.4.3), sharing 88% amino acid identity (Gonzalez-Pasayo and Martinez-Romero, 2000). The gene pRL110033 was also mutated as it encodes a putative ABC-type efflux system (polypeptide that contains both the ABC and transmembrane domains). Some efflux system-encoding genes were upregulated in developing bacteroids but were not selected for mutagenesis due to a high p-value or because they had been investigated previously (see section 3.2.5).

None of the mutations in genes encoding for efflux systems caused an obvious symbiotic defect except disruption of RL4274, which resulted in a Fix$^-$ phenotype (incapable of N_2 fixation) (Table 3.4). Nodules initiated by the mutant strain LMB384 (RL4272:pRU877) were small, white and spherical. It was possible to isolate bacteria from nodule crushes.

Efflux Type	Locus Tag	Component	7 dpi bacteroid	21 dpi bacteroid	Pea rhizospere
RND	RL4274	MFP	14.2	2.6	135.0
RND	RL4275	Pump	0.6	1.6	1.2
RND	RL1454	MFP	10.5	1.7	2.0
RND	RL1453	Pump	2.3	1.4	1.8
RND	RL4224	MFP	4.6	1.4	1.0
RND	RL4223	Pump	2.2	1.3	0.6
RND	RL3269	Pump	2.6	0.7	1.2
RND	RL3270	MFP	1.7	0.7	0.9
RND	pRL120696	MFP	2.3	0.6	1.5
RND	pRL120697	MFP	2.1	0.9	1.1
RND	pRL120698	Pump	2.5	0.5	0.9
RND	RL2666	Pump	2.4	1.4	1.5
RND	RL2667	MFP	1.7	0.7	0.4
MFS	pRL90059	MFP	27.5	3.3	5.5
MFS	pRL90060	Pump	11.6	0.8	1.4
MFS	RL3784	MFP	13.0	0.9	1.6
MFS	RL3783	Pump	8.5	0.7	1.4
MFS	RL4180	MFP	8.3	1.0	1.7
MFS	RL4179	Pump	2.9	1.2	1.3
MFS	RL4612	Pump	7.3	3.2	0.8
MFS	RL0996	Pump	4.8	2.7	4.6
MFS	RL1330	Pump	2.1	1.0	1.7
MFS	RL1329	MFP	1.6	2.1	1.8

Table 3.3 Putative RND- and MFS-type efflux systems and their fold-induction in bacteria isolated from nodules 7 dpi, 21 dpi or pea rhizosphere relative to free-living cells grown on minimal medium (Karunakaran et al., 2009; Ramachandran et al., 2011). Green highlights genes >3-fold upregulated. Genes written in red were mutated in this study.

		Acetylene Reductions			Nodule Counts		
Strain	Disrupted gene	Acetylene reduction ($\mu mol\ h^{-1}\ plant^{-1}$)	% of batch Rlv3841	% of combined Rlv3841	Nodule count (n= 3)	% of batch Rlv3841	% of combined Rlv3841
LMB378	pRL110033	**4.53 ± 0.76** **(n= 5)**	78 ± 13	92 ± 15	**68** **± 11**	62 ± 10	70 ± 11
LMB384	RL4274	**0.02 ± 0.00** **(n= 5)**	0 ± 0	0 ± 0	**106** **± 8**	111 ± 8	109 ± 8
LMB411	pRL90060 (*rmrB*)	**6.92 ± 0.36** **(n=5)**	129 ± 7	140 ± 7	**84** **± 11**	110 ± 14	87 ± 11
LMB441	RL3783	**7.20 ± 1.24** **(n= 5)**	94 ± 16	146 ± 25	**84** **± 14**	83 ± 14	86 ± 14

Table 3.4 Rates of acetylene reduction and nodule counts (± SEM) for *P. sativum* inoculated with strains carrying mutations in genes that encode putative efflux systems. n= number of plants tested.

Resistance to oxidative stress

Agreeing with the presence of ROS in infection threads, several genes predicted to have a role in resistance to oxidative stress were upregulated in developing bacteroids.

Gene pRL120362 encodes a putative bi-functional heme-dependent catalase-peroixdase (KatG). Disruption of this gene did cause a decrease in acetylene reduction relative to the combined Rlv3841-incoulated plants (Table 3.5) but this experiment needs to be repeated due to low rates of acetylene reduction for the batch-Rlv3841 (2.27 $\mu mol\ h^{-1}\ plant^{-1}$ ± 0.18).

RL1302 and RL2927 encode putative organic peroxidases belonging to the OsmC/Ohr family. Clustered with RL2927, RL2925 encodes a putative pyrophosphohydrolase (MutT), which prevents errors in DNA replication by hydrolysing mutagenic mispairing nucleotides (e.g. 8-oxo-dGTP) caused by oxidative damage (Fowler and Schaaper, 1997). These genes however, were not essential for bacteroid development (Table 3.5).

		Acetylene Reductions			Nodule Counts		
Strain	*Disrupted gene*	*Acetylene reduction* ($\mu mol\ h^{-1}\ plant^{-1}$)	*% of batch Rlv3841*	*% of combined Rlv3841*	*Nodule count* (n= 3)	*% of batch Rlv3841*	*% of combined Rlv3841*
LMB372	RL1302 (*osmC/ohr*)	**3.99 ± 0.62** (n= 3)	86 ± 14	81 ± 13	**92 ± 4**	96 ± 4	94 ± 4
LMB377	RL2927 (*osmC/ohr*)	**5.81 ± 0.59** (n =5)	100 ± 10	118 ± 12	**72 ± 3**	66 ± 3	74 ± 3
LMB397	RL2925 (*mutT*)	**4.21 ± 0.20** (n= 5)	73 ± 3	85 ± 4	**92 ± 9**	79 ± 8	95 ± 9
LMB400	RL2924	**4.12 ± 0.50** (n= 5)	88 ± 11	84 ± 10	**95 ± 8**	92 ± 7	97 ± 8
LMB402	pRL120362 (*katG*)	**2.76 ± 0.24** (n= 5)	121 ± 11	56 ± 5	**76 ± 5**	84 ± 6	78 ± 6

Table 3.5 Rates of acetylene reduction and nodule counts (± SEM) for *P. sativum* inoculated with strains carrying a mutation in genes encoding proteins with a putative role in oxidative stress resistance. n= number of plants tested.

Resistance to membrane stress

Three upregulated genes were predicted to have a role in resistance to membrane stress. RL1106 encodes a putative PspA (Phage Shock Protein) and is likely to share an operon with RL1107, which encodes a putative transmembrane protein. PspA was discovered when found in high abundance in *E. coli* upon infection by filamentous phage (Brissette et al., 1990; Joly et al., 2010). Since this discovery, PspA has been reported to respond to a multitude of conditions that perturb the integrity of the membrane e.g. salt stress (Bidle et al., 2008; Vrancken et al., 2008), ethanol (Vrancken et al., 2008), osmotic stress (Vrancken et al., 2008), proton ionophores (Weiner and Model, 1994; Becker et al., 2005), organic solvents (Kobayashi et al., 1998), heat shock (Brissette et al., 1990) and stationary-phase at alkaline pH (Weiner and Model, 1994). PspA is speculated to provide protection by binding to the membrane in response to stress and maintaining the proton motive force (pmf) by forming a homomultimeric scaffold that covers the inner membrane, suppressing proton leakage (Kobayashi et al., 2007; Joly et al., 2010). Despite this, disruption of *pspA* or RL1107 did not cause any obvious symbiotic defects (Table 3.6).

Gene pRL80012 encodes a putative AAA+ (ATPase associated with diverse cellular activities) protein and is likely to share an operon with pRL80013, which encodes a

putative protease. The putative products of these two genes typically form a complex known as AAA+ protease, which can degrade damaged or misfolded proteins (Sauer and Baker, 2011). Surprisingly, plants inoculated with the mutant LMB365 (pRL80012:pRU877) had a higher rate of acetylene reduction relative to the batch Rlv3841-inoculated plants (p ≤0.05) (Table 3.6). However, when this experiment was repeated with 12 biological replicates for both Rlv3841 and LMB365 (pRL80012:pRU877), there was no significant difference between the rates of acetylene reduction (LMB365= 7.45 ± 0.34 c.f. Rlv3841= 7.19 ± 0.19; p= 0.46).

		Acetylene Reductions			Nodule Counts		
Strain	*Disrupted gene*	*Acetylene reduction ($\mu mol\ h^{-1}\ plant^{-1}$)*	*% of batch Rlv3841*	*% of combined Rlv3841*	*Nodule count (n= 3)*	*% of batch Rlv3841*	% of combined Rlv3841
LMB365	pRL80012	**6.39 ± 0.45 (n= 5)**	182 ± 13	130 ± 9	**108 ± 5**	86 ± 4	111 ± 6
LMB489	RL1107	**5.33 ± 0.73 (n= 5)**	116 ± 16	108 ± 15	**78 ± 3**	94 ± 4	80 ± 3
LMB506	RL1106 (*pspA*)	**5.93 ± 0.74 (n= 5)**	107 ± 13	120 ± 15	**100 ± 4**	105 ± 4	103 ± 4

Table 3.6 Rates of acetylene reduction and nodule counts (± SEM) for *P. sativum* inoculated with strains carrying mutations in genes encoding proteins with putative roles in membrane stress resistance. n= number of plants tested.

Metabolism

Three genes were predicted to have a metabolic function. The gene pRL90266 encodes a putative glycerophosphodiester phosphodiesterase (GDPD), which hydrolyses glycerophosphodiesters formed by the deacylation of phospholipids; it is involved in membrane recycling and nutrient scavenging (Patton-Vogt, 2007; Santos-Beneit et al., 2009). Products of glycerophosphodiesterases breakdown can be fed into pathways utilised for glycerol metabolism. Recently, genes essential for glycerol utilisation were identified in *R. leguminosarum* bv. viciae VF39 and their disruption caused a reduced ability to compete with the wild type during colonisation of *P. sativum* nodules (Ding et al., 2012). Orthologs of these genes can be found in Rlv3841 between loci pRL90074-pRL90081; some of these genes were moderately

upregulated (≥1.5-fold) in developing bacteroids. Disruption of pRL90266 did not cause a significant decrease in acetylene reduction or nodule number (Table 3.7) but it remains to be determined if LMB347 (pRL90266:pRU877) is defective for competition.

Aromatic compounds can be metabolised to tricarboxylic acid intermediates by the β-ketoadipate pathway (MacLean et al., 2006). The gene pRL110287 (*pcaI*) forms part of the putative *pcaIJF* operon that is required for the conversion of β-ketoadipate to succinate and acetyl-coenzyme A (MacLean et al., 2006). However, no noticeable phenotype was caused by disruption of pRL110287 (Table 3.7).

Strain	Disrupted gene	Acetylene Reductions			Nodule Counts		
		Acetylene reduction ($\mu mol\ h^{-1}\ plant^{-1}$)	% of batch Rlv3841	% of combined Rlv3841	Nodule count (n= 3)	% of batch Rlv3841	% of combined Rlv3841
LMB347	pRL90266	**6.19 ± 0.86** **(n= 4)**	107 ± 15	126 ± 17	**86** **± 16**	79 ± 15	89 ± 16
LMB391	pRL110287 (*pcaI*)	**3.50 ± 0.29** **(n= 3)**	81 ± 7	71 ± 6	**79** **± 8**	87 ± 9	82 ± 9
LMB421	pRL90278	**3.77 ± 0.46** **(n=5)**	88 ± 11	77 ± 9	**87** **± 3**	95 ± 3	89 ± 3

Table 3.7 Rates of acetylene reduction and nodule counts (± SEM) for *P. sativum* inoculated with strains carrying mutations in genes encoding proteins with a putative metabolic function. n= number of plants tested.

Regulation

Twelve genes encoding putative regulators were mutated, including one gene (RL1879) that encodes a FixL-homologue. FixL is an O_2-sensing regulator essential for N_2 fixation in *S. meliloti*, *B. japonicum* and *A. caulinodans* (David et al., 1988; Anthamatten and Hennecke, 1991; Kaminski and Elmerich, 1991) but not in *R. leguminosarum* bv. viciae VF39 (Patschkowski et al., 1996). Two of the other genes encode FixK-homologues (RL1880 and pRL90025), which are also involved in regulating genes essential for N_2 fixation (Terpolilli et al., 2012). However, disruption of these putative regulators did not cause any obvious symbiotic defects (Table 3.8).

The protein encoded by RL0390 was originally annotated as a putative pH-regulated regulator (PhrR) but has since been identified as a repressor (PraR) of two *N*-acyl-homoserine lactone (AHL)-based quorum sensing systems (Frederix et al., 2011). In agreement with the thesis of Marijke Frederix, 2010 (Allan Downie lab), *P. sativum* inoculated with the *praR* mutant formed pink nodules and showed no reduction in nodule number (Table 3.8).

Rates of acetylene reduction or nodule number were not affected by any of the other mutations in genes encoding for putative regulators (Table 3.8).

Strain	Disrupted gene	Acetylene Reductions			Nodule Counts		
		Acetylene reduction ($\mu mol\ h^{-1}\ plant^{-1}$)	% of batch Rlv3841	% of combined Rlv3841	Nodule count (n= 3)	% of batch Rlv3841	% of combined Rlv3841
LMB340	RL3152	**4.90 ± 0.48** (n= 5)	85 ± 8	99 ± 10	**123 ± 11**	113 ± 10	127 ± 11
LMB348	pRL90226	**3.08 ± 0.09** (n= 5)	88 ± 3	63 ± 2	**74 ± 1**	59 ± 0	76 ± 1
LMB351	pRL120695	**4.75 ± 0.75** (n= 4)	103 ± 16	96 ± 15	**76 ± 7**	79 ± 7	78 ± 7
LMB354	pRL90056	**3.85 ± 0.56** (n= 3)	83 ± 12	78 ± 11	**87 ± 7**	91 ± 7	89 ± 7
LMB374	pRL90025 (*fixK*-like)	**6.17 ± 0.23** (n= 4)	134 ± 5	125 ± 5	**94 ± 22**	99 ± 23	97 ± 22
LMB375	RL0472	**4.74 ± 0.53** (n= 5)	82 ± 9	96 ± 11	**73 ± 11**	66 ± 10	75 ± 11
LMB385	pRL110377	**4.29 ± 0.43** (n= 5)	93 ± 9	87 ± 9	**102 ± 11**	107 ± 12	105 ± 12
LMB392	RL1880 (*fixL*-like)	**5.71 ± 0.50** (n= 5)	122 ± 11	116 ± 10	**84 ± 11**	82 ± 11	86 ± 11
LMB401	RL0390 (*praR*)	**5.48 ± 0.40** (n= 5)	127 ± 9	111 ± 8	**110 ± 3**	110 ± 3	103 ± 3
LMB403	RL1879 (*fixK*-like)	**4.18 ± 0.14** (n= 5)	90 ± 3	85 ± 3	**93 ± 2**	90 ± 2	95 ± 2
LMB410	RL3688	**4.85 ± 0.55** (n= 5)	85 ± 10	98 ± 11	**93 ± 4**	80 ± 4	95 ± 5
LMB425	pRL110623	**4.4 ± 0.35** (n= 5)	125 ± 10	89 ± 7	**80 ± 1**	63 ± 1	82 ± 1

Table 3.8 Rates of acetylene reduction and nodule counts (± SEM) for *P. sativum* inoculated with strains carrying a mutation in genes encoding putative regulators. n= number of plants tested.

Unknowns or other

Six of the genes mutated encoded hypothetical conserved proteins and four encoded putative proteins that could not be assigned a putative function. *P. sativum* inoculated with LMB343 (RL1485:pRU877), LMB376 (RL2307:pRU877) and LMB404 (RL1226:pK19mob) showed moderate decreases in acetylene reduction that were statistically significant (p ≤0.05) (Table 3.9) but more replicates are needed to confirm this. All other mutations caused no differences in acetylene reduction or nodule number (Table 3.9).

Strain	Disrupted gene	Acetylene Reductions			Nodule Counts		
		Acetylene reduction (μmol h⁻¹ plant⁻¹)	*% of batch Rlv3841*	*% of combined Rlv3841*	*Nodule count (n= 3)*	*% of batch Rlv3841*	*% of combined Rlv3841*
LMB338	pRL100224	**3.23 ± 0.36 (n= 5)**	98 ± 11	66 ± 7	**103 ± 5**	94 ± 4	106 ± 5
LMB343	RL1485	**3.64 ± 0.34 (n= 5)**	63 ± 6	74 ± 7	**94 ± 4**	86 ± 4	97 ± 5
LMB349	RL3273	**4.83 ± 0.81 (n= 4)**	83 ± 14	98 ± 16	**69 ± 7**	63 ± 7	71 ± 8
LMB361	RL0447	**3.52 ± 0.12 (n= 5)**	107 ± 4	71 ± 2	**90 ± 10**	82 ± 9	93 ± 11
LMB367	RL0262	**3.69 ± 0.36 (n= 5)**	86 ± 8	75 ± 7	**80 ± 13**	88 ± 14	83 ± 13
LMB376	RL2307	**4.07 ± 0.15 (n= 3)**	70 ± 3	83 ± 3	**70 ± 4**	64 ± 4	72 ± 4
LMB396	RL4103	**4.35 ± 0.44 (n= 5)**	93 ± 9	88 ± 9	**92 ± 10**	89 ± 9	95 ± 10
LMB398	RL1631	**3.30 ± 0.23 (n= 5)**	100 ± 7	67 ± 5	**80 ± 3**	73 ± 3	83 ± 3
LMB404	RL1226	**4.21 ± 0.27 (n= 5)**	73 ± 5	85 ± 6	**122 ± 17**	105 ± 15	126 ± 18
LMB440	pRL110055	**7.94 ± 1.25 (n= 5)**	104 ± 16	161 ± 25	**95 ± 15**	94 ± 15	98 ± 16

Table 3.9 Rates of acetylene reduction and nodule counts (± SEM) for *P. sativum* inoculated with strains carrying mutations in genes encoding proteins with an unknown function. n= number of plants tested.

3.2.3 Genes that could not be mutated

Despite multiple attempts, it was not possible to isolate strains carrying mutations in six genes, including three genes (RL2578, RL2582 and RL2580) thought to share an operon that encodes proteins predicted to be involved in Fe-S cluster biogenesis (Young et al., 2006). Fe-S clusters are used as cofactors by a wide range of proteins, participating in electron transfer, catalysis and regulatory processes (Beinert et al., 1997; Lill, 2009). There are three types of Fe-S assembly systems in bacteria: ISC (iron sulphur cluster), SUF (sulphur formation) and NIF (nitrogen fixation) (Lill, 2009). Typically, the ISC system is used for housekeeping cluster assembly, SUF is used during oxidative stress and NIF is used to assemble clusters into nitrogenase (Takahashi and Tokumoto, 2002; Tokumoto et al., 2004; Ayala-Castro et al., 2008).

The genes *sufS* (RL2578), *sufB* (RL2582) and *sufC* (RL2580) encode a putative cysteine desulfurase, Fe-S scaffold protein and a transfer protein, respectively, that operate as part of the SUF assembly system (Table 3.10). Some bacteria encode more than one Fe-S cluster biogenesis system e.g. *E. coli* (Tokumoto et al., 2004; Xu and Moller, 2008) but Rlv3841 only seems to encode the SUF system (Table 3.10) (it does contain a weak orthologue for *nifS* but all other components of the NIF system are absent) (Altschul et al., 1990; Young et al., 2006). This offers an explanation to why it was not possible to mutate *sufC*, *sufB* and *sufS*, as their loss would be lethal. It also implies that the SUF system delivers the Fe-S cluster to nitrogenase.

Another gene that could not be mutated is *mraZ* (RL3316), which has been associated with cell wall biosynthesis and cell division. The gene *mraW*, downstream of *mraZ*, has been shown to be essential in *E. coli* (Carrion et al., 1999; Adams et al., 2005).

	Rlv3841	**Amino acid identity %**
Cysteine desulphurase	*sufS* (RL2578)	46
	nifS (RL2583)	36
Scaffold	*sufA* (RL2576)	41
	sufB (RL2582)	61
	sufD (RL2579)	30
Fe-S transfer	*sufC* (RL2580)	58

Table 3.10 Putative Fe-S cluster biogenesis system in Rlv3841. Genes identified by the homology of their products to SUF components present in *E. coli* K12 or NIF components present in *Azotobacter vinelandii DJ*.

3.2.4 Disruption of RL4274 does not cause a Fix⁻ phenotype on *P. sativum*

LMB384 (RL4274:pRU877) was the only mutant strain to show a Fix⁻ phenotype on *P. sativum*. To ascertain whether the Fix⁻ phenotype was caused by the mutation RL4274:pRU877 or was the result of a secondary mutation, RL4274:pRU877 was transduced using RL38 phage (2.4.3) from LMB384 into Rlv3841, resulting in strain LMB423. The presence of the RL4274:pRU877 mutation in LMB423 was confirmed by PCR using pK19/18A and pr0560. *P. sativum* was inoculated with LMB423 and after three weeks, rates of acetylene reduction were measured. In strong contrast to LMB384 (RL4274:pRU877), LMB423 reduced acetylene at the same rate as Rlv3841 (Fig 3.2), implying that the Fix⁻ phenotype observed with LMB384 was the result of an unknown, secondary mutation.
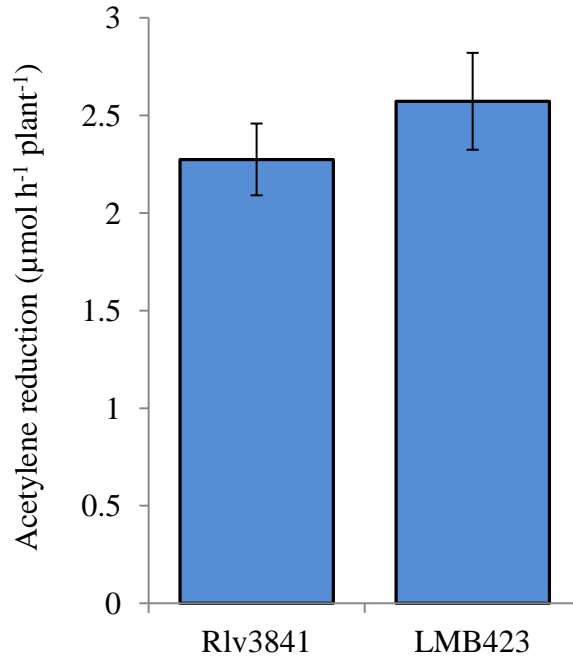
Fig 3.2 Rates of acetylene reduction for *P. sativum* inoculated with Rlv3841 and LMB423. Averaged from five plants ± SEM.

Further proof that RL4274 is not essential for N_2 fixation came from mutant strain RU4260 (RL4274:pK19mob) (Ramachandran et al., 2011). As a result of an overlap between this project and a project that focussed on genes important to colonisation of the *P. sativum* rhizosphere, RL4274 had been selected for mutagenesis twice. RU4260 (RL4274:pK19mob) had not previously been tested for its ability to fix N_2, but when inoculated onto *P. sativum*, in agreement with LMB423, this strain reduced acetylene at the same rate as Rlv3841 (Fig 3.3).
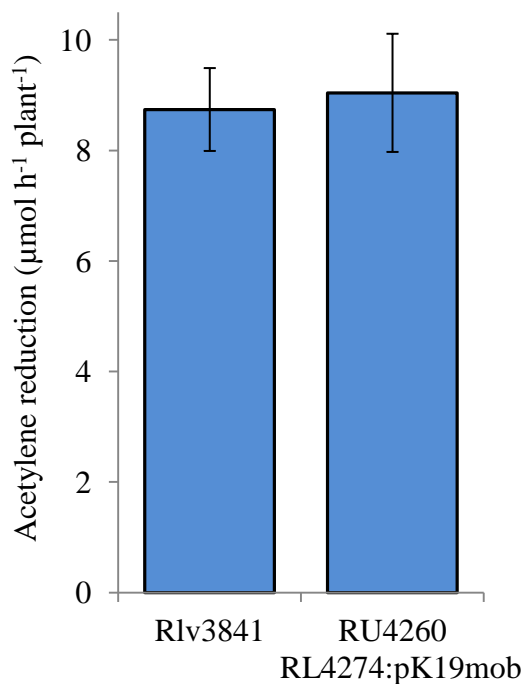
Fig. 3.3 Rates of acetylene reduction for *P. sativum* inoculated Rlv3841 and RU4260. Averaged from five plants ± SEM.

3.2.5 Requirement of efflux systems on *Vicia faba*

The efflux system BdeAB is required by *B. japonicum* for efficient symbiosis on *G. max* but not on *V. radiata* or *V. unguiculata* (Lindemann et al., 2010). This implies that the requirement of some efflux systems depends on the legume-host i.e. toxic compounds endogenous to the plant. For this reason, all Rlv3841 strains carrying a mutation in a gene encoding for an efflux system-component were screened on *V. faba* (an alternative legume-host for Rlv3841). In addition to mutants made in this study, strains RU4260 (RL4274:pK19mob), RU4314 (pRL90059:pK19mob), LMB519 (RL1329ΩSpc) and double mutant LMB523 (pRL90059:pK19mob RL1329ΩSpc) were also tested; additional mutants were constructed by Adrian Tett and Karunakaran Ramakrishnan and were Fix[+] on *P. sativum* (unpublished data from the Philip Poole lab).

V. faba seeds were inoculated with the mutant strains (2.6.1) and harvested after three weeks. All strains were able to nodulate and reduce acetylene on *V. faba* (Figs 3.4 and 3.5). LMB523 (pRL90059:pK19mob RL1329ΩSpc) was the only strain that showed a decrease in acetylene reduction and nodulation relative to Rlv3841 (Figs 3.4 and 3.5). This experiment needs to be repeated with more replicates to confirm these differences.
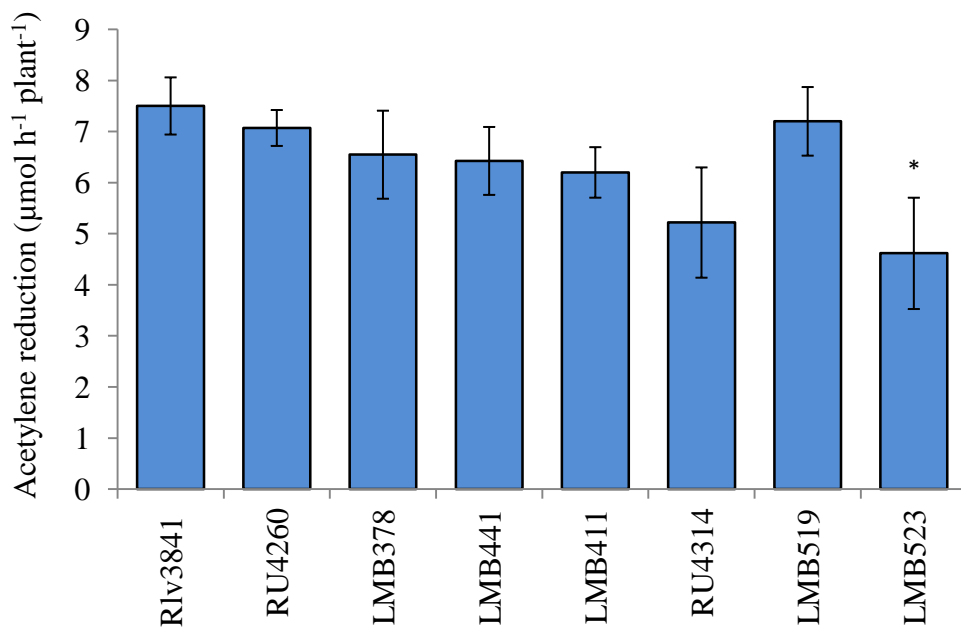
Fig 3.4 Rates of acetylene reduction for *V. faba* plants inoculated with Rlv3841 and strains carrying mutations in genes encoding for putative efflux systems. Averaged from five plants ± SEM. * indicates a statistically significant (p ≤ 0.05) difference relative to Rlv3841-inoculated plants.
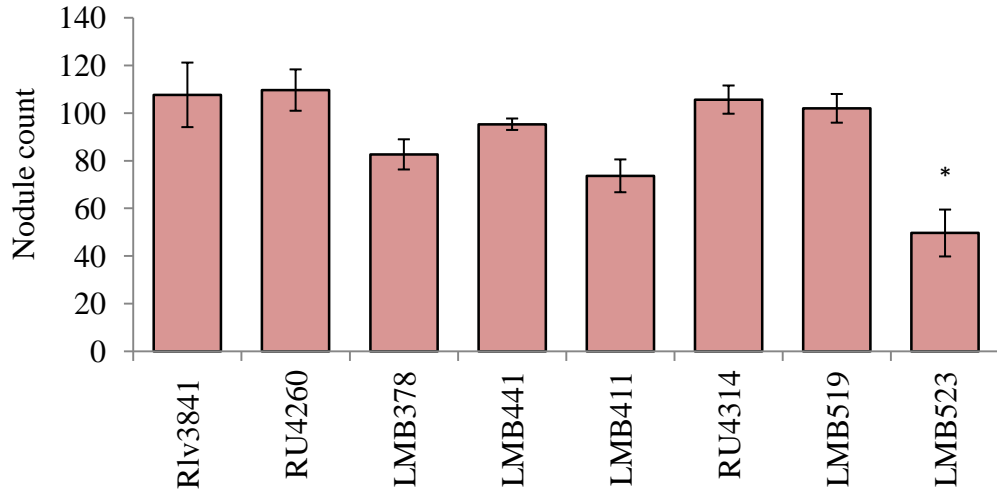
Fig 3.5 Nodule counts recorded from *V. faba* plants inoculated with Rlv3841 and strains carrying mutations in genes encoding for putative efflux systems. Averaged from three plants ± SEM. * indicates a statistically significant (p ≤ 0.05) difference relative to Rlv3841-inoculated plants.

3.3 CONCLUSION

This preliminary investigation was vital for identifying functional classes of genes and processes required during bacteroid development. None of the mutations severely impaired bacteroid development which is likely to be the result of functional redundancy between the upregulated genes. The two putative Mn^{2+} transport systems encoded by *mntH* and *sitABCD* are a clear example of this. SitABCD could apparently compensate for the loss of MntH and vice versa.

The efflux systems could be another example of functional redundancy as there were eight efflux systems upregulated in developing bacteroids (Table 3.3). Furthermore, it is known that efflux systems have a broad specificity for a diverse range of compounds (Higgins, 2007). Therefore, the loss of one efflux system could easily be compensated by another.

There is also likely to be some functional redundancy between genes involved in resistance to oxidative stress. In addition to the mutated catalase-encoding gene,

katG (Table 3.5), Rlv3841 encodes a second putative heme-dependent catalase, KatE (encoded by RL2024). Furthermore, *katE* is >3-fold upregulated in mature bacteroids, 1.7-fold upregulated in developing bacteroids (Karunakaran et al., 2009) and shares 77% amino acid identity with a catalase (KatE) required by *M. loti* for N_2 fixation on *L. japonicus* (Hanyu et al., 2009). In addition to the two catalases, there could also be a degree of functional redundancy between the two OsmC/Ohr organic peroxidases encoded by RL1302 and RL2927 (Table 3.5).

There may also be functional redundancy amongst the regulators upregulated in developing bacteroids, particularly between *fixL* and RL1879 (encoding a FixL-homologue) (Table 3.8).

Five of the mutants were moderately reduced in their ability to reduce acetylene or initiated less nodules relative to Rlv3841: LMB366 (RL1317:pRU877) (Table 3.2), LMB402 (*katG*:pK19mob) (Table 3.5), LMB343 (RL1485:pRU877) (Table 3.8), LMB376 (RL2307:pRU877) (Table 3.8), LMB404 (RL1226:pK19mob) (Table 3.8) and LMB523 (pRL90059:pK19mob RL1329ΩSpc) (Figs 3.4 and 3.5). However, because these were only moderate phenotypes it was decided that further investigation into the functional redundancy between genes would have a greater chance of unearthing processes critical to bacteroid development.

The remainder of this thesis will therefore focus on four different aspects of bacteroid development: the transport of metals (Chapters four and five), regulation of genes essential to N_2 fixation (Chapter six), resistance to organic peroxides (Chapter seven) and the role AAA+ proteases (Chapter eight) in developing bacteroids. The efflux systems were not investigated further due to the number of systems encoded by Rlv3841 (Table 3.3). The hypothesised redundancy between the two catalases was also not pursued as their role in bacteroid development has already been well-characterised in *S. meliloti* and *M. loti* (Jamet et al., 2003; Hanyu et al., 2009).

Chapter 4: *Mn^{2+} transport*

4.1 INTRODUCTION

Manganese (Mn^{2+}) is a trace metal maintained at a concentration of 10-100 μM in the cell (Finney and O'Halloran, 2003). Mn^{2+} has been found to be critical for numerous processes but the most common physiological role attributed to Mn^{2+} is resistance to oxidative stress (Kehres and Maguire, 2003). In Mn^{2+}-dependent superoxide dismutases (SodA), Mn^{2+} operates as a redox catalyst in the detoxification of O$_2^-$ into H$_2$O$_2$ and O$_2$. Mn^{2+} is also a cofactor for non-haem catalases that detoxify H$_2$O$_2$ into H$_2$O and O$_2$ (McEwan, 2009). Furthermore, Mn^{2+} has a protective role during oxidative stress that is independent of both superoxides and catalases (McEwan, 2009). It has been speculated that Mn complexed to polyphosphate and pyrophosphate can quench O$_2^-$, while Mn complexed to bicarbonate can quench H$_2$O$_2$ (Archibald and Fridovich, 1982; Berlett et al., 1990). However, the physiological relevance of this scavenging property has been disputed in a study conducted by Anjem *et al*., 2009, which proposes the protective effect of Mn^{2+} instead stems from its ability to replace Fe^{2+} as a cofactor for mononuclear enzymes. The replacement of Fe^{2+} with Mn^{2+} would make these proteins less vulnerable to H$_2$O$_2$ and O$_2^-$ (Anjem and Imlay, 2012) and suppresses the Fe^{2+}-dependent formation of HO$^·$ radicals (Anjem et al., 2009; Imlay, 2013).

Mn^{2+} is also utilised as a cofactor for enzymes in unstressed cells, for example, pyruvate kinase in *B. japonicum* (PykA) (Hohle and O'Brian, 2012), malic enzymes in *P.aeruginosa* (Eyzaguir.J et al., 1973) and a certain class of ribonucleotide reductase in *E. coli* (required under Fe-limitation) (Andrews, 2011; Martin and Imlay, 2011). In *B. japonicum*, Mn^{2+} also has a role in Fe-homeostasis through binding the global Fe-regulator Irr (positively regulates genes encoding Fe-transporters), altering its structure and subsequently, making it less vulnerable to degradation (Puri et al., 2010). However, like other metals, Mn^{2+} can be toxic in excess, which is supported by the recent discoveries of Mn^{2+} efflux systems in bacteria (Rosch et al., 2009; Sun et al., 2010; Li et al., 2011; Waters et al., 2011).

To enter a Gram-negative cell, Mn^{2+} must first cross the outer membrane, which can be achieved via a selective outer membrane pore (MnoP) (Hohle et al., 2011). Mn^{2+} is then transported across the inner membrane by an ABC-type transporter encoded by the *sitABCD* operon or an H^+-coupled symporter (belonging to Nramp protein family) encoded by *mntH* (Fig 4.1).
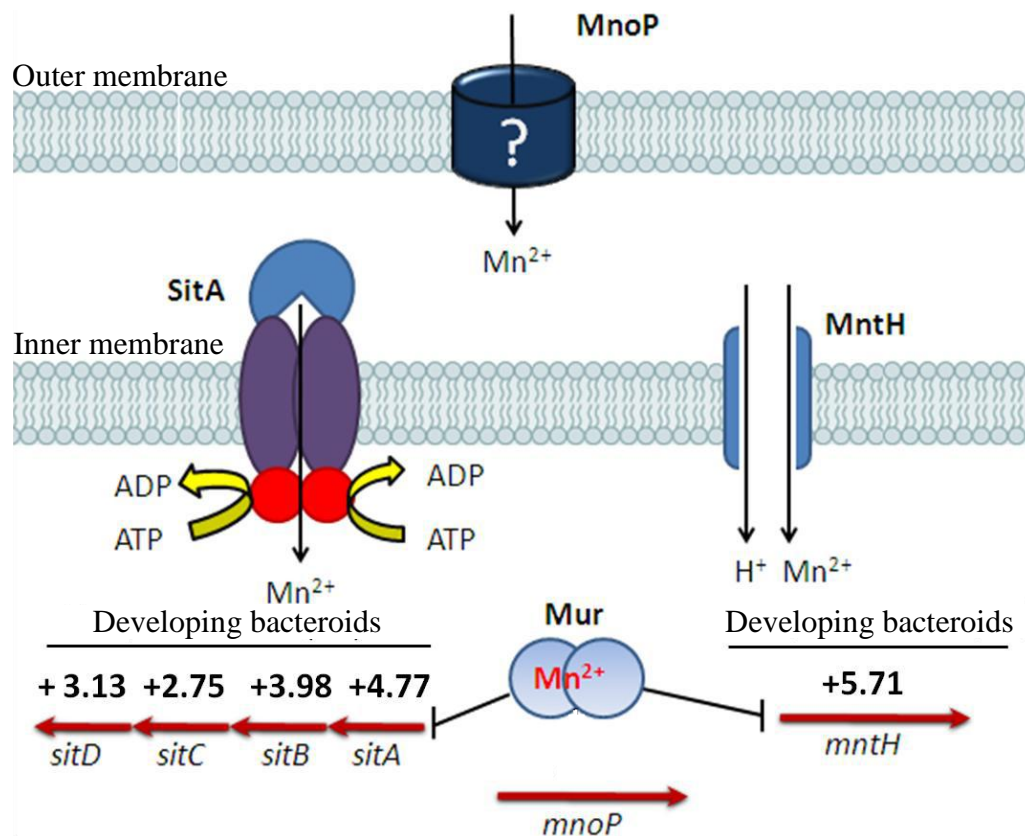

Fig 4.1 Scheme showing importation of Mn^{2+} into a Gram-negative bacterium via an outer membrane protein (MnoP) and inner membrane transporters SitABCD and MntH. Encoding genes are represented by red arrows. Values correspond to fold-induction of genes in developing bacteroids isolated from nodules 7 dpi relative to free-living cells grown in minimal medium (Karunakaran et al., 2009).

The requirement of Mn^{2+} transport for bacteroid development in indeterminate nodules has been demonstrated in *M. sativa-S. meliloti* symbiosis. *S. meliloti* encodes a SitABCD transport system that was required for growth in medium limited for Mn^{2+} (Platero et al., 2003; Chao et al., 2004; Davies and Walker, 2007a, b). On *M. sativa*, deletion of *sitA* (Δ *sitA*) (Chao et al., 2004) or mutation by mTn5-integration (*sitA*::mTn5) (Davies and Walker, 2007b) caused a ~50-75% decrease in acetylene reduction relative to the wild type (Table 4.1). *M. sativa* inoculated with *sitA*::mTn5, formed either small white nodules (Fig 4.2B) or elongated white nodules (Fig 4.2C). Electron microscopy revealed that *sitA*::mTn5 bacteroids were present within plant cells of both nodule-types but the mutant could only be isolated from the elongated white nodules, which contained 1000-fold fewer bacteria relative to nodules containing the wild type.
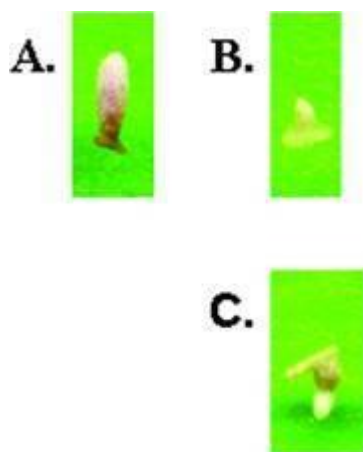
Fig 4.2 Nodules formed on *M. sativa* inoculated with *S. meliloti* 1021 (A) or *S. meliloti* (*sitA*::mTn5) (B and C). Reproduced from Davies and Walker, 2007b.

In contrast to the above, a third study reported that there were no difference between the dry weight of *M. sativa* inoculated with *S. meliloti* wild type and *M. sativa* inoculated with *S. meliloti* strains carrying Tn5-mutations in either *sitB* or *sitD* (Platero et al., 2003); however, acetylene reduction assays were not conducted. Furthermore, the strain of *S. meliloti* and cultivar of plant used by Platero *et al* were

different from those used in the other two studies (Chao et al., 2004; Davies and Walker, 2007a) (Table 4.1).

The requirement of Mn^{2+} transport for bacteroid development in determinate nodules has been investigated using *B. japonicum* and *G. max*. *B. japonicum* does not encode a *sitABCD* operon and instead contains a MntH transporter that is essential for Mn^{2+} uptake and growth in Mn^{2+} limited medium. However, MntH was shown not to be essential for *G. max-B. japonicum* symbiosis as confirmed by nodule weights and rates of acetylene reduction (Table 4.1) (Hohle and O'Brian, 2009).

The Rlv3841 genome is predicted to encode both putative MntH and SitABCD transport systems. MntH is encoded by *mntH* (RL0940) and shows 60% amino acid identity to *B. japonicum* MntH (Altschul et al., 1990; Hohle and O'Brian, 2009). Expression of the *sitABCD* operon from *R. leguminosarum* was previously shown to rescue the growth phenotype of *S. meliloti sitB*::Tn5 (Platero et al., 2003; Diaz-Mireles et al., 2004) and its expression in *R. leguminosarum* is regulated in response to Mn^{2+} by the Fur-like repressor, Mur (manganese uptake regulator) (Fig 4.1) (Diaz-Mireles et al., 2004; Diaz-Mireles et al., 2005). When bound to Mn^{2+}, Mur binds to conserved sites upstream of *sitABCD* and represses transcription by occluding RNA polymerase access to the promoter (Diaz-Mireles et al., 2005). Mur-binding sites have also been identified upstream of *mntH* in Rlv3841, but regulation of *mntH* by Mur has not been demonstrated (Rodionov et al., 2006). In Rlv3841, expression of both *sitABCD* and *mntH* is strongly induced during bacteroid development (Fig 4.1) (Karunakaran et al., 2009) but single mutations in *sitA* or *mntH* did not prevent bacteroid development in indeterminate nodules formed on *P. sativum* (Table 4.1).

This investigation determines whether there is functional redundancy between the two Mn^{2+} transport systems encoded by Rlv3841 and subsequently, establishes whether Mn^{2+} transport is required for bacteroid development in nodules formed by *P. sativum*. It also addresses whether the requirement of Mn^{2+} transporters differs between legume-hosts, including both plants that form indeterminate nodules (e.g. *M. sativa*, *P. sativum*, *V. faba* and *V. hirsuta*) and plants that form determinate nodules (*G. max* and *P. vulgaris*).

Organism	Mutation	Symbiotic phenotype	Legume-host	Nodule Type	Reference
S. meliloti 242	*sitB*::Tn5	Plant dry weights equivalent to wild type inoculated	*M. sativa* cv. Creola	Indeterminate	Platero *et al.*, 2003
S. meliloti 242	*sitD*::Tn5	Plant dry weights equivalent to wild type inoculated	*M. sativa* cv. Creola	Indeterminate	Platero *et al.*, 2003
S. meliloti 1021	Δ *sitA*	Decreased plant wet weight and ~50% decrease in acetylene reduction	*M. sativa* cv. Europe	Indeterminate	Chao *et al.*, 2004
S. meliloti 1021	*sitA*::mTn5	~75% decrease in acetylene reduction and small white or intermediate-sized nodules	*M. sativa*	Indeterminate	Davies and Walker 2007a, b
B. japonicum USDA110	Δ *mntH*	Nodule weight and rates of acetylene reduction equivalent to wild type	*G. max* cv. Essex	Determinate	Hohle and O'Brian 2009
Rlv3841	*sitA*:pK19mob	Nodule number and acetylene reduction equivalent to wild type	*P. sativum* cv. Avola	Indeterminate	This study
Rlv3841	*mntH*:pK19mob	Nodule number and acetylene reduction equivalent to wild type	*P. sativum* cv. Avola	Indeterminate	This study

Table 4.1 Symbiotic phenotypes for rhizobial strains carrying mutation in *sitABCD* or *mntH*.

4.2 RESULTS

4.2.1 Expression of *sitA-gusA* and *mntH-gusA* is induced in response to Mn^{2+} limitation and during symbiosis

Reporter *gusA*-fusions, where *gusA* encodes β-glucuronidase (GUS), were used to study the expression of *sitABCD* and *mntH* in free-living cells and during symbiosis. To construct *sitA-gusA* and *mntH-gusA*, promoter regions were PCR amplified from Rlv3841 gDNA using *sitA* primers pr1292 and pr1293 and *mntH* primers pr1290 and pr1291. The PCR products were cloned into the broad-host range plasmid pJP2 (Prell et al., 2002) at the *Xba*I/*Hin*dIII site to make plasmids pLMB597 (*sitA-gusA*) and pLMB600 (*mntH-gusA*). Plasmids were then conjugated into Rlv3841 (2.3.8) to make LMB498 (*sitA-gusA*) and LMB505 (*mntH-gusA*).

To investigate expression of *sitA-gusA* and *mntH-gusA* in response to Mn^{2+} limitation, LMB498 (*sitA-gusA*) and LMB505 (*mntH-gusA*) were grown in modified AMS glucose containing 0.05 µM or 0.9 µM MnSO$_4$. Samples were taken from the cultures and used to measure GUS activity (2.5.6). For both LMB498 (*sitA-gusA*) and LMB505 (*mntH-gusA*), GUS activity was approximately 2-fold higher when grown in 0.05 µM relative 0.9 µM MnSO$_4$ (Fig 4.3). A 2-fold induction of *sitABCD* and *mntH* may seem a weak response to Mn-limitation but this can be explained by the fact that both *sitA-gusA* and *mntH-gusA* were encoded by a multi-copy plasmid. More specifically, in medium containing 0.9 µM, some expression of *sitA-gusA* and *mntH-gusA* may have been due to inadequate numbers of the chromosome-encoded, repressor Mur, consequently, obscuring the true affect of Mn^{2+} on the expression of both *gusA*-fusions.

To determine whether the induction of *sitA-gusA* and *mntH-gusA* is dependent upon Mur, plasmids pLMB597 (*sitA-gusA*) and pLMB600 (*mntH-gusA*) were conjugated into *R. leguminosarum* bv. viciae strain J325 (*mur*ΩSpc) (Wexler et al., 2001) to make LMB550 (*mur*ΩSpc *sitA-gusA*) and LMB551 (*mur*ΩSpc *mntH-gusA*). In the *mur*ΩSpc background, expression of both *gusA*-fusions was increased and

differential expression between MnSO$_4$-concentrations was lost (Fig 4.3). This confirms that both *sitABCD* and *mntH* are repressed by Mur.
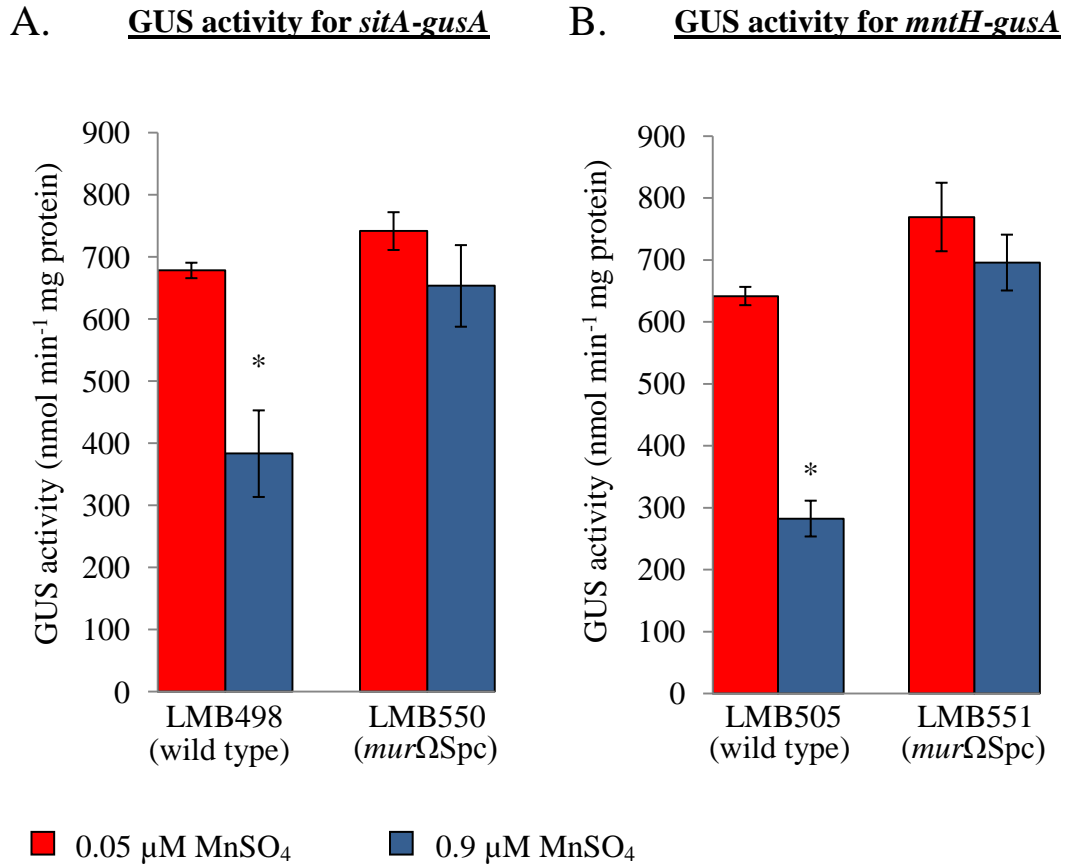
A. **GUS activity for *sitA-gusA*** **B.** **GUS activity for *mntH-gusA***

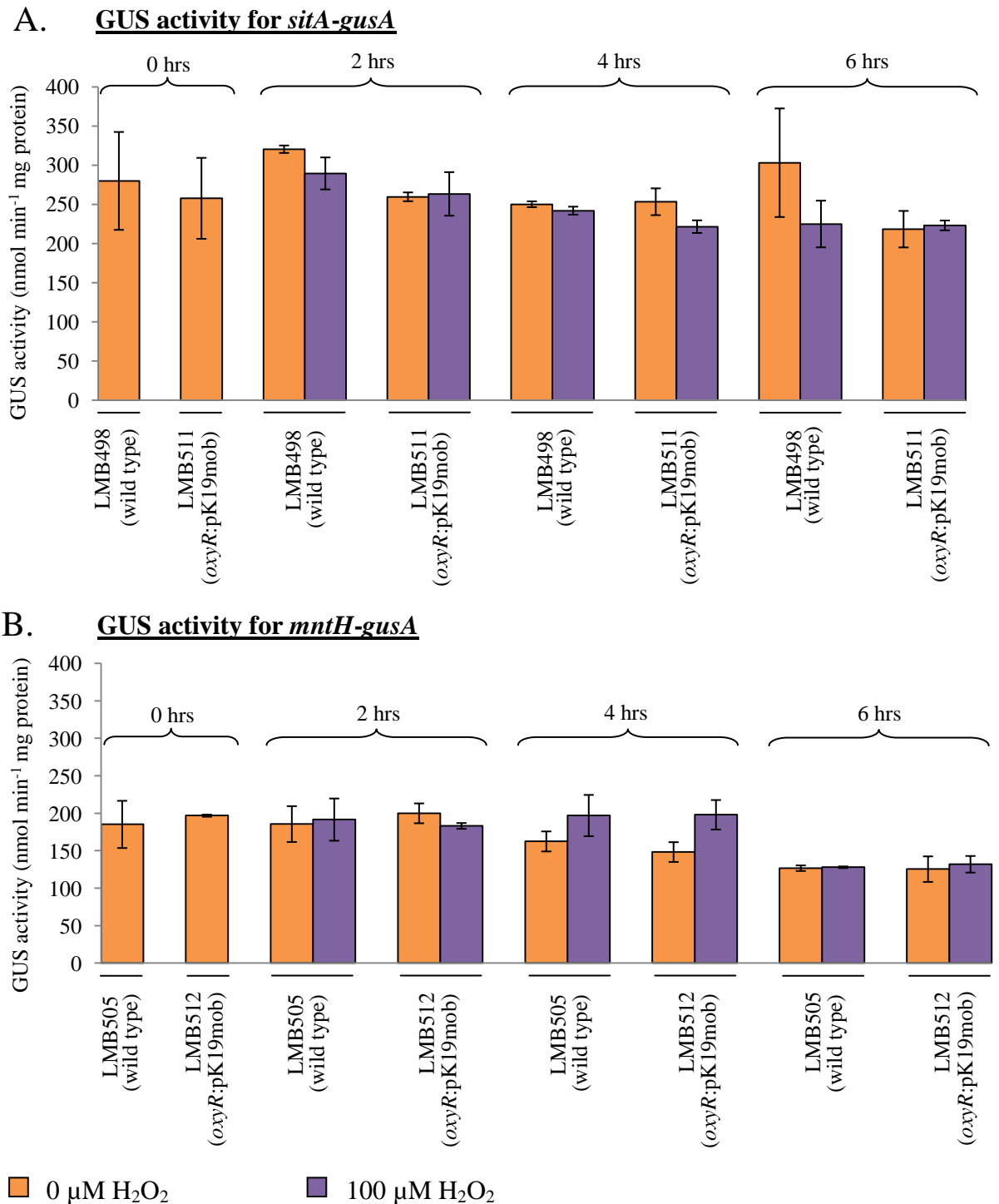**Fig 4.3** GUS activity measured for (A) LMB498 (*sitA-gusA*), LMB550 (*mur*ΩSpc *sitA-gusA*), (B) LMB505 (*mntH-gusA*) and LMB551 (*mur*ΩSpc *mntH-gusA*) grown in modified AMS glucose containing 0.05 μM or 0.9 μM MnSO$_4$. Averaged from three independent experiments ± SEM. * indicates statistically significant difference (p ≤ 0.05).

In addition to Mn^{2+} limitation, studies on other bacteria have found the expression of Mn^{2+} transporter-encoding genes to be regulated by OxyR in response to oxidative stress (Kehres et al., 2000; Kehres et al., 2002a; Runyen-Janecky et al., 2006). To investigate if this holds true for Rlv3841, *gusA*-fusions were tested in a strain carrying a mutation in *oxyR*.

To mutate *oxyR*, its internal fragment was PCR amplified using primers pr1286 and pr1287. The PCR product was cloned into pJET1.2/blunt to make pLMB592. An *Xba*I/*Bgl*II fragment containing the internal fragment of *oxyR* was cut from pLMB592 and cloned into *Xba*I/*Bam*HI-digested pK19mob, resulting in pLMB596. Plasmid pLMB596 was conjugated into Rlv3841 to make LMB497 (*oxyR*:pK19mob). Plasmids pLMB597 and pLMB600 were then conjugated into LMB497 (*oxyR*:pK19mob), resulting in strains LMB511 (*oxyR*:pK19mob *sitA-gusA*) and LMB512 (*oxyR*:pK19mob *mntH-gusA*).

To measure expression in response to oxidative stress, cultures were grown and split into two samples. To one sample, 100 μM H_2O_2 was added, while the other sample was treated as a negative control. GUS activity was measured at 0, 2, 4 and 8 hours (2.5.6). However, disruption of *oxyR* did not cause a change in GUS activity and GUS activity did not differ between samples treated and not treated with H_2O_2 (Fig 4.4).

The *gusA*-fusions were also used to analyse expression of the Mn^{2+} transporters during symbiosis. *P. sativum* was inoculated with LMB498 (*sitA-gusA*) or LMB505 (*mntH-gusA*). After three weeks, sections were taken from nodules and stained for GUS activity (2.6.7). Both *sitA-gusA* and (Fig 4.5A) and *mntH-gusA* (Fig 4.5B) were expressed throughout the nodule, highlighting the probable importance of Mn^{2+} uptake during symbiosis.

Fig 4.4 GUS activity measured for (A) LMB498 (*sitA-gusA*), LMB511 (*oxyR*:pK19mob *sitA-gusA*), (B) LMB505 (*mntH-gusA*) and LMB512 (*oxyR*:pK19mob *mntH-gusA*) grown in AMS glucose containing 0 μM or 100 μM H₂O₂. H₂O₂ added at 0 and samples taken at 2, 4 and 6 hrs. Averaged from three independent experiments ± SEM.
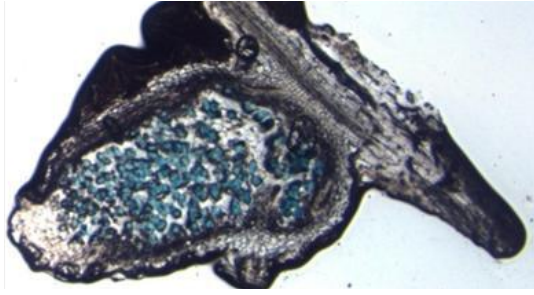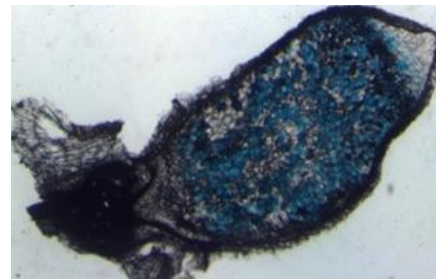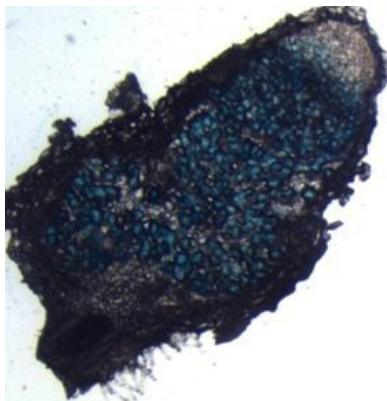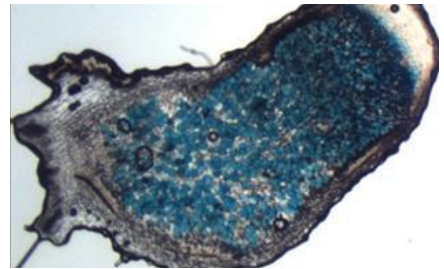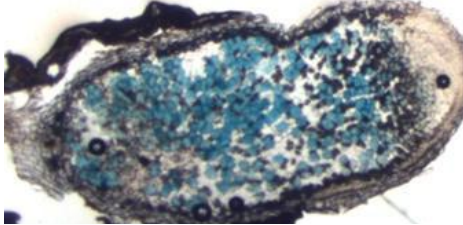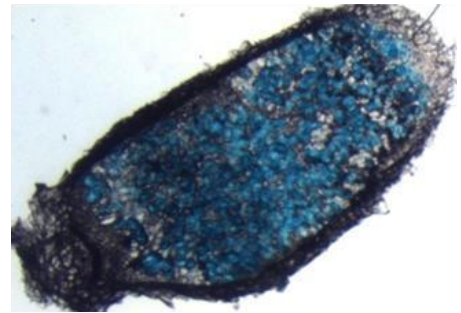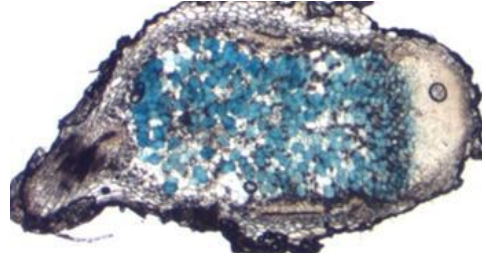
Fig 4.5 Histochemical staining of longitudinal sections of three week *P. sativum* nodules for GUS activity. Plants were inoculated with (A) LMB498 (*sitA-gusA*) or (B) LMB505 (*mntH-gusA*). Four nodules shown for each inoculation.

4.2.2 A *sitA mntH* double mutant cannot grow in Mn^{2+}-limited medium

A double mutant was constructed to test if there is any functional redundancy between *sitABCD* and *mntH*. To make the double mutant, *mntH* was first mutated by insertion of a Ω intersposon carrying Spc[r] (*mntHΩSpc*). Primers pr1186 and pr1187 were used to amplify a 3 kb region containing *mntH* from Rlv3841 gDNA. The PCR product was subcloned into pJET1.2/blunt to make pLMB543. A *Sma*I fragment containing the ΩSpc cassette was cloned into pLMB543 at *Eco*RV to make pLMB544. A 5 kb *Xba*I/*Xho*I fragment from pLMB544 was cloned into *Xba*I/*Xho*I-digested pJQ200SK resulting in pLMB546. Plasmid pLMB546 was conjugated into Rlv3841 to make LMB460 (*mntHΩSpc*) (2.4.2). To construct the double mutant, *mntHΩSpc* was transduced from LMB460 (*mntHΩSpc*) into LMB364 (*sitA*:pK19mob) to make LMB466 (*sitA*:pK19mob *mntHΩSpc*). TY was supplemented with 50 μM $MnSO_4$ when selecting for and for routine growth of LMB466 (*sitA*:pK19mob *mntHΩSpc*).

Strains were tested for growth in modified AMS medium containing 0.05 (Mn^{2+}-limited) or 25 μM $MnSO_4$ (non-limited) (2.5.1). Both single mutants were able to grow in AMS glucose containing 0.05 μM $MnSO_4$ but LMB364 (*sitA*:pK19mob) had a longer mean generation time (5.5 hrs c.f. 4.5 hrs) (Fig 4.6). Growth of LMB466 (*sitA*:pK19mob *mntHΩSpc*) however, was severely reduced in AMS glucose containing 0.05 μM $MnSO_4$. Growth phenotypes for both LMB364 (*sitA*:pK19mob) and LMB466 (*sitA*:pK19mob *mntHΩSpc*) could be rescued by the addition of 25 μM $MnSO_4$ (Fig 4.6). The growth defect of LMB466 (*sitA*:pK19mob *mntHΩSpc*) could be reproduced in flask cultures (Fig 4.25) and on solid medium (Fig 4.7).
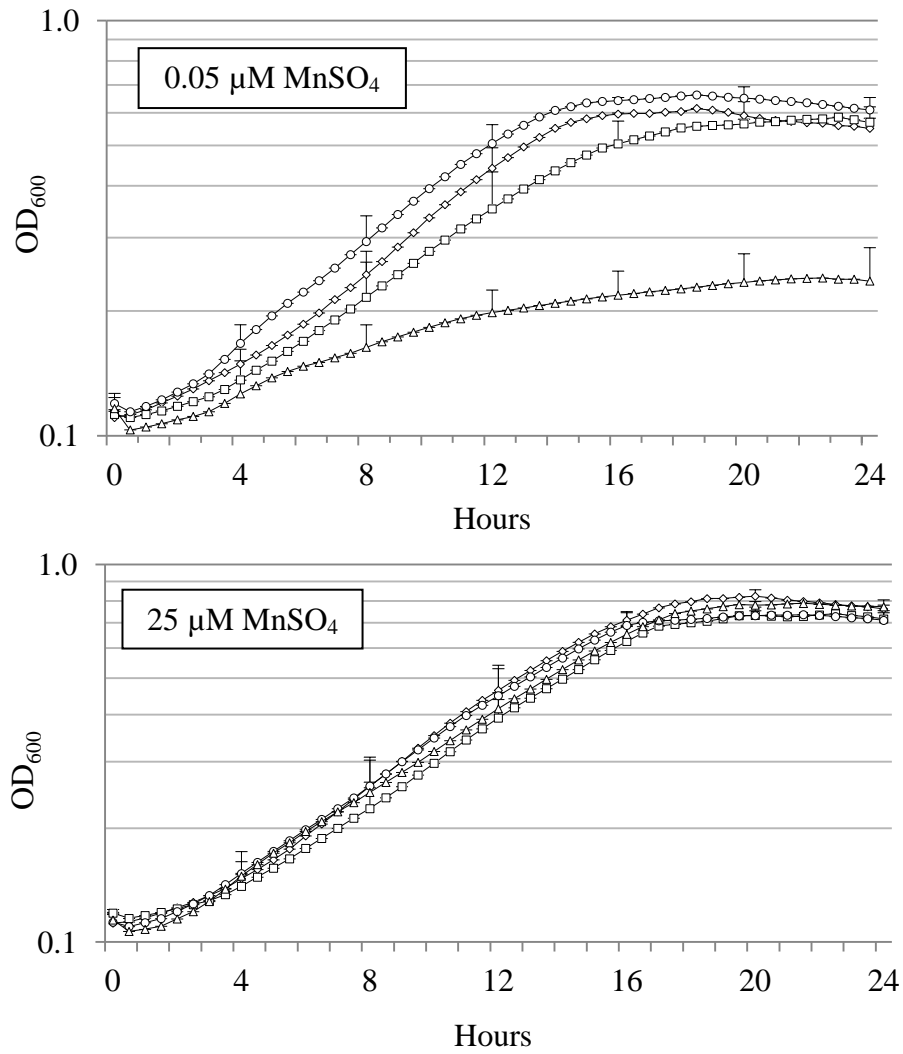
Fig 4.6 Growth of Rlv3841 [diamonds], LMB364 (*sitA*:pK19mob) [squares], LMB460 (*mntH*ΩSpc) [circles] and LMB466 (*sitA*:pK19mob *mntH*ΩSpc [triangles] in modified AMS glucose containing either 0.05 μM $MnSO_4$ or 25 μM $MnSO_4$. Averaged from three independent experiments ± SEM.
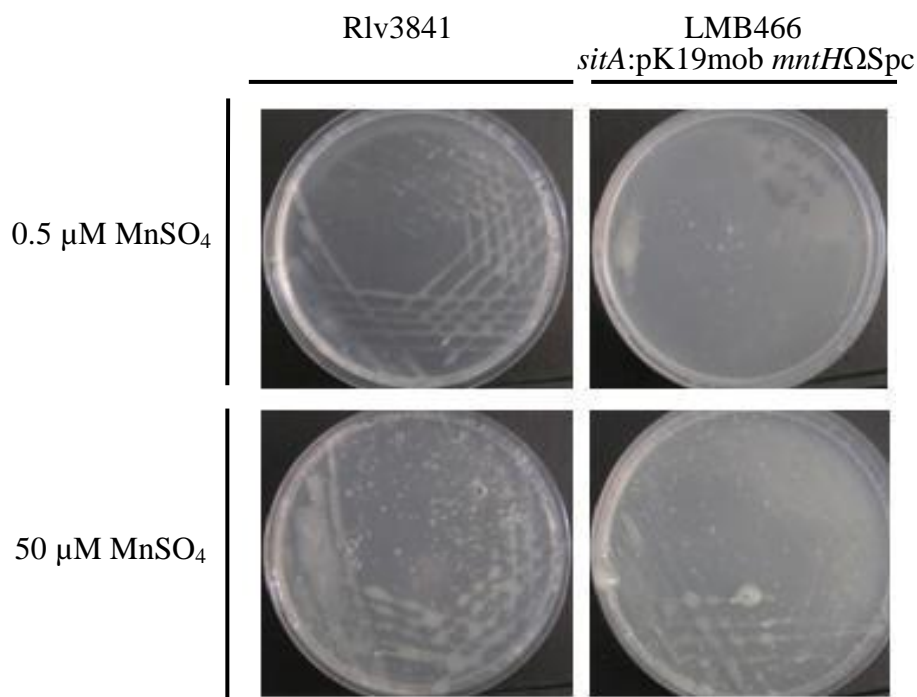
Fig 4.7 Rlv3841 and LMB466 (*sitA*:pK19mob *mntH*ΩSpc) grown on solid modified AMS glucose medium containing either 0.5 μM or 50 μM $MnSO_4$.

4.2.3 SitABCD and MntH are required for H_2O_2-resistance

Even though no change in expression for *sitA-gusA* and *mntH-gusA* was seen in response to H_2O_2 (Fig 4.4), the requirement of SitABCD and MntH for resistance to oxidative stress was tested. To measure H_2O_2-sensitivity, Rlv3841, LMB364 (*sitA*:pK19mob) and LMB460 (*mntH*ΩSpc) were first grown in AMS glucose. Cultures were then washed with and resuspended in modified AMS (omitting $MnSO_4$); resuspended cultures were split into two samples and 0.5 mM H_2O_2 was added to one, while the other culture was used as a negative control. Samples were taken at 0, 2, 4 and 6 hrs and used to determine number of colony forming units (CFU) (2.5.5).

Both LMB364 (*sitA*:pK19mob) and LMB460 (*mntH*ΩSpc) were more sensitive to H_2O_2 relative to Rlv3841 (Fig 4.8). The hypersensitivity of LMB364 (*sitA*:pK19mob) to H_2O_2 agrees with the slow growth phenotype seen in Mn^{2+}-

limited medium (Fig 4.6). LMB460 (*mntH*ΩSpc) does not show a growth phenotype (Fig 4.6) and so its hypersensitivity might suggest a greater demand for Mn^{2+} under oxidative stress, consistent with the [54]Mn data published by Anjem *et al* 2009.
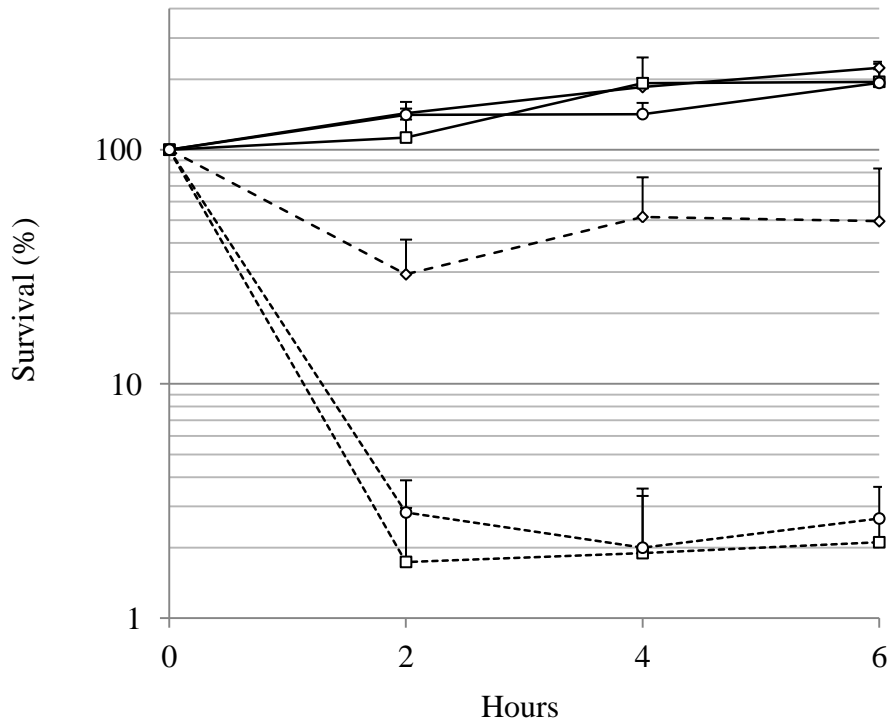

Fig 4.8 Sensitivity of Rlv3841 [diamonds], LMB364 (*sitA*:pK19mob) [squares] and LMB460 (*mntH*ΩSpc) [circles] to H_2O_2. Strains incubated in $MnSO_4$-free AMS glucose containing either 0 mM H_2O_2 (solid line) or 0.5 mM H_2O_2 (broken line). Survival (%) corresponds to number of colony forming units (CFU) relative to the number of CFUs at time 0 hrs. Averaged from three independent experiments ± SEM.

In order to test sensitivity of LMB466 (*sitA*:pK19mob *mntH*ΩSpc), cultures had to be grown in modified AMS glucose containing 25 μM $MnSO_4$. The cultures were then tested for sensitivity to H_2O_2 as described previously. When grown in 25 μM $MnSO_4$ however, no difference in sensitivity was seen between the single mutants and Rlv3841 (Fig 4.9). Furthermore, LMB466 (*sitA*:pK19mob *mntH*ΩSpc) did not show any increased sensitivity to H_2O_2 relative to the other strains (Fig 4.9). It is

speculated that when grown in 25 μM MnSO$_4$, none of the mutants were limited for Mn^{2+} and so exhibited the same sensitivity as Rlv3841. Therefore, the sensitivity of LMB466 (*sitA*:pK19mob *mntH*ΩSpc) to H$_2$O$_2$ still needs to be determined and the experiment is likely to involve growing LMB466 (*sitA*:pK19mob *mntH*ΩSpc) in a Mn^{2+}-rich medium and then starving the culture of Mn^{2+} for a period of time before treating with H$_2$O$_2$.
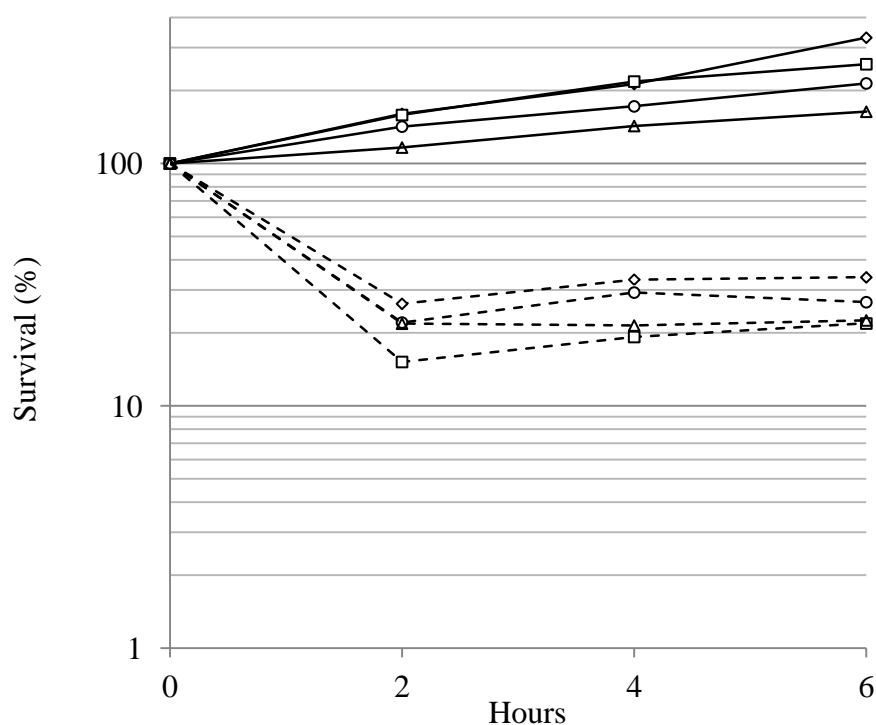

Fig 4.9 Sensitivity of Rlv3841 [diamonds], LMB364 (*sitA*:pK19mob) [squares], LMB460 (*mntH*ΩSpc) [circles] , LMB466 (*sitA*:pK19mob *mntH*ΩSpc) [triangles] to H$_2$O$_2$. Strains were grown in modified AMS (containing 25 μM MnSO$_4$) glucose and then incubated in MnSO$_4$-free AMS glucose containing either 0 mM H$_2$O$_2$ (solid line) or 0.5 mM H$_2$O$_2$ (broken line). Survival (%) corresponds to number of colony forming units (CFU) relative to the number of CFUs at time 0 hrs. Data from one experiment.

4.2.4 A *sitA mntH* double mutant is Fix⁻ on *P. sativum*

To test whether Mn^{2+} transport is required for bacteroid development, *P. sativum* was inoculated with Rlv3841, the single mutants or double mutant. After three weeks, *P. sativum* inoculated with LMB364 (*sitA*:pK19mob) or LMB460 (*mntH*ΩSpc), had nodules that were similar in colour and morphology to nodules on Rlv3841-inoculated plants. Plants inoculated with LMB466 (*sitA*:pK19mob *mntH*ΩSpc) however, formed small, white and spherical nodules, which are typical of an ineffective symbiosis (Fig 4.10). Rates of acetylene reduction suggest that LMB364 (*sitA*:pK19mob) and LMB460 (*mntH*ΩSpc) fix N$_2$ at wild type rates but in concurrence with the nodule morphology, no N$_2$ fixation could be detected for plants inoculated with LMB466 (*sitA*:pK19mob *mntH*ΩSpc) (Fig 4.11). It was possible to recover LMB466 (*sitA*:pK19mob *mntH*ΩSpc) from the Fix⁻ nodules.
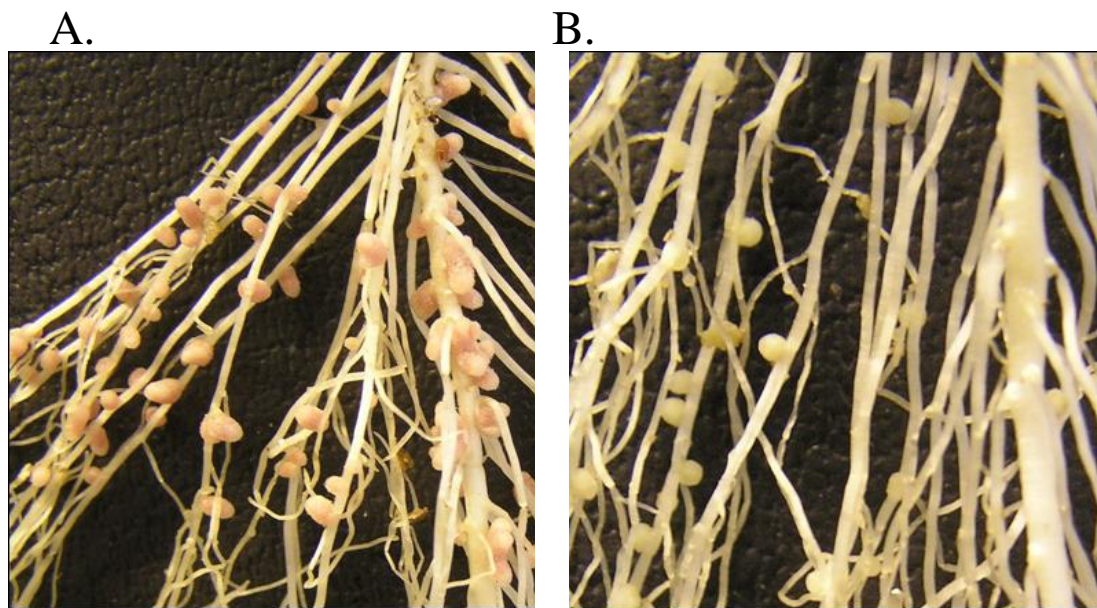
A.   B.

Fig 4.10 Nodules on *P. sativum* inoculated with (A) Rlv3841 or (B) LMB466 (*sitA*:pK19mob *mntH*ΩSpc).
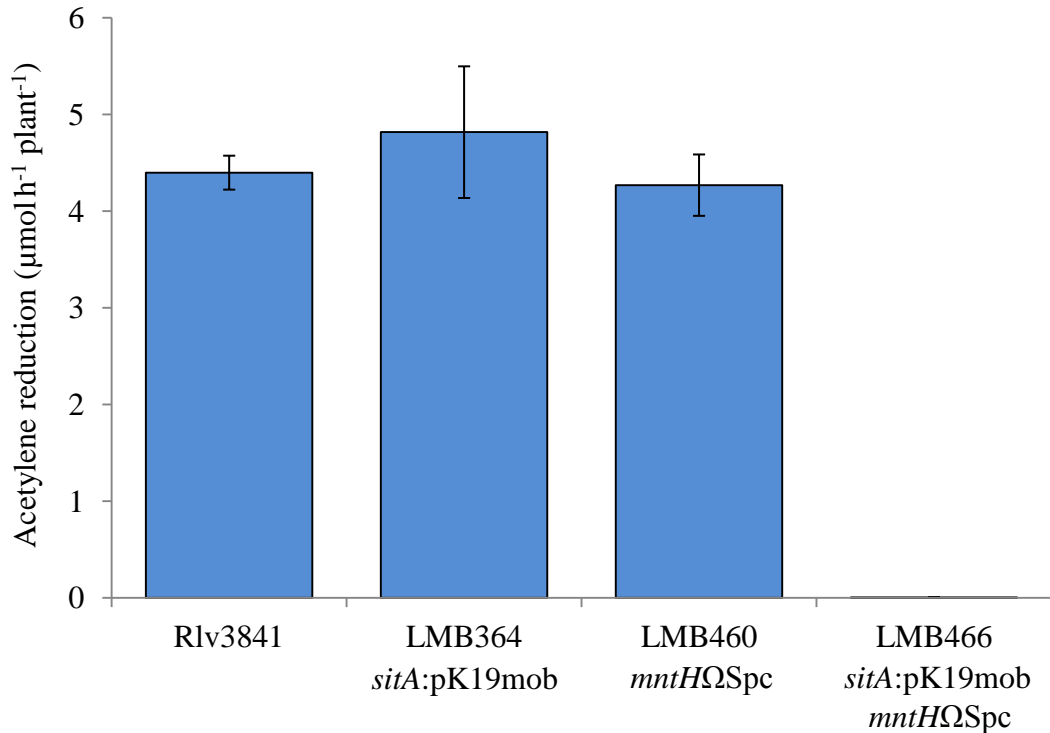
Fig 4.11 Rates of acetylene reduction for Rlv3841, LMB364 (*sitA*:pK19mob), LMB460 (*mntH*ΩSpc) and LMB466 (*sitA*:pK19mob *mntH*ΩSpc) on *P. sativum*. Averaged from five plants ± SEM.

P. sativum inoculated with LMB466 (*sitA*:pK19mob *mntH*ΩSpc) were also grown for six weeks alongside Rlv3841-inoculated and uninoculated plants. Plants inoculated with LMB466 (*sitA*:pK19mob *mntH*ΩSpc) were indistinguishable from the uninoculated controls in both appearance (Fig 4.12) and shoot dry weight (2.6.6) (Table 4.2) confirming the absence of N_2 fixation.
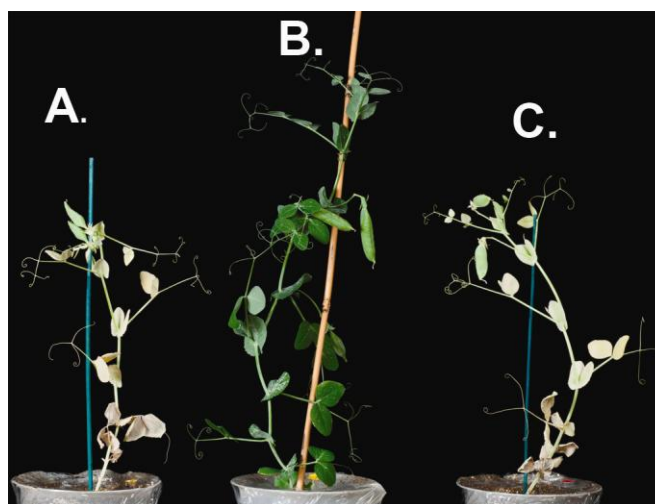
Fig 4.12 Photo showing (A) uninoculated, (B) Rlv3841-incoulated and (C) LMB466 (*sitA*:pK19mob *mntH*ΩSpc)-inoculated *P. sativum*. All plants were grown for six weeks.

Inoculation	Shoot dry weight (g)
Uninoculated	0.87 ± 0.07
Rlv3841	3.0 ± 0.23
LMB466 (*sitA*:pK19mob *mntH*ΩSpc)	0.9 ± 0.06

Table 4.2 Shoot dry weights for (A) uninoculated, (B) Rlv3841-inoculated and (C) LMB466 (*sitA*:pK19mob *mntH*ΩSpc)-inoculated *P. sativum*. All plants were grown for six weeks. Averaged from ten plants ± SEM.

The ability of *mntH* to rescue the symbiotic phenotype of LMB466 (*sitA*:pK19mob *mntH*ΩSpc) was tested. Primers pr1290 and pr1462 were used to PCR-amplify a 1.9 kb region containing *mntH* from Rlv3841 gDNA. The PCR product was digested with *Xba*I/*Hin*dIII and cloned into *Xba*I/*Hin*dIII-digested pJP2, to make pLMB766. The plasmid pLMB766 was conjugated into LMB466 (*sitA*:pK19mob *mntH*ΩSpc) to make LMB683 (*sitA*:pK19mob *mntH*ΩSpc pJP2*mntH*). LMB683 (*sitA*:pK19mob *mntH*ΩSpc pJP2*mntH*) was able to reduce acetylene at wild type rates (Fig 4.13)

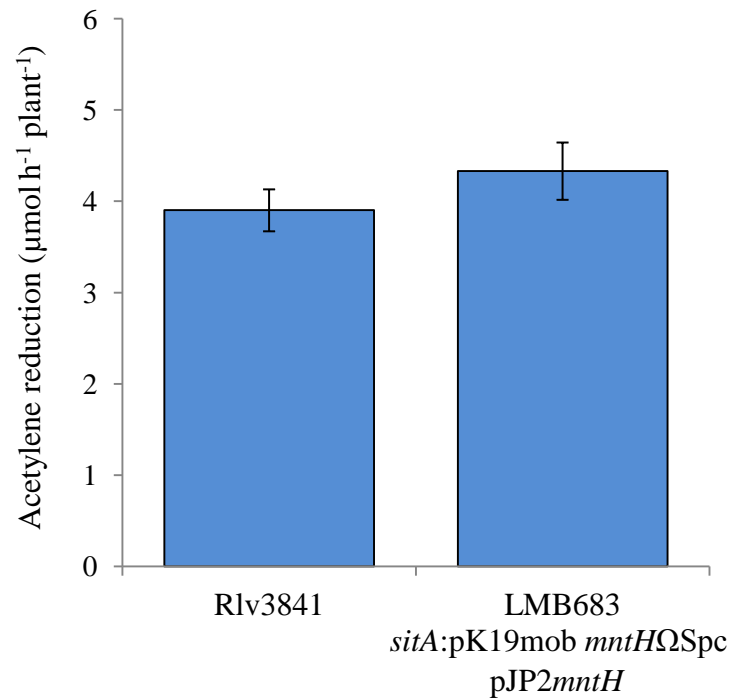demonstrating that pJP2*mntH* can rescue the symbiotic phenotype of the double mutant.

Fig 4.13 Rates of acetylene reduction for Rlv3841 and LMB683 (*sitA*:pK19mob *mntH*ΩSpc pJP2*mntH*). Averaged from five plants ± SEM.

Sections taken from nodules (2.6.1) formed on Rlv3841- or LMB466 (*sitA*:pK19mob *mntH*ΩSpc)-inoculated *P. sativum* were visualised by light microscopy (Figs 4.14 and 4.15) and transmission electron microscopy (TEM) (Fig 4.16). Even though infection thread-like structures could be seen in both nodules containing Rlv3841 and LMB466 (*sitA*:pK19mob *mntH*ΩSpc) (Fig 4.14), only a few plant cells were infected by LMB466 (*sitA*:pK19mob *mntH*ΩSpc) (Fig 4.15). The few plant cells that were infected, were sparsely packed with LMB466 (*sitA*:pK19mob *mntH*ΩSpc) bacteroids, relative to the densely-packed plant cells containing Rlv3841 (Fig 4.16). Furthermore, nodules from LMB466 (*sitA*:pK19mob *mntH*ΩSpc)-inoculated plants contained many starch granules (Fig 4.16), which is typical of an infective symbiosis (Udvardi and Poole, 2013).
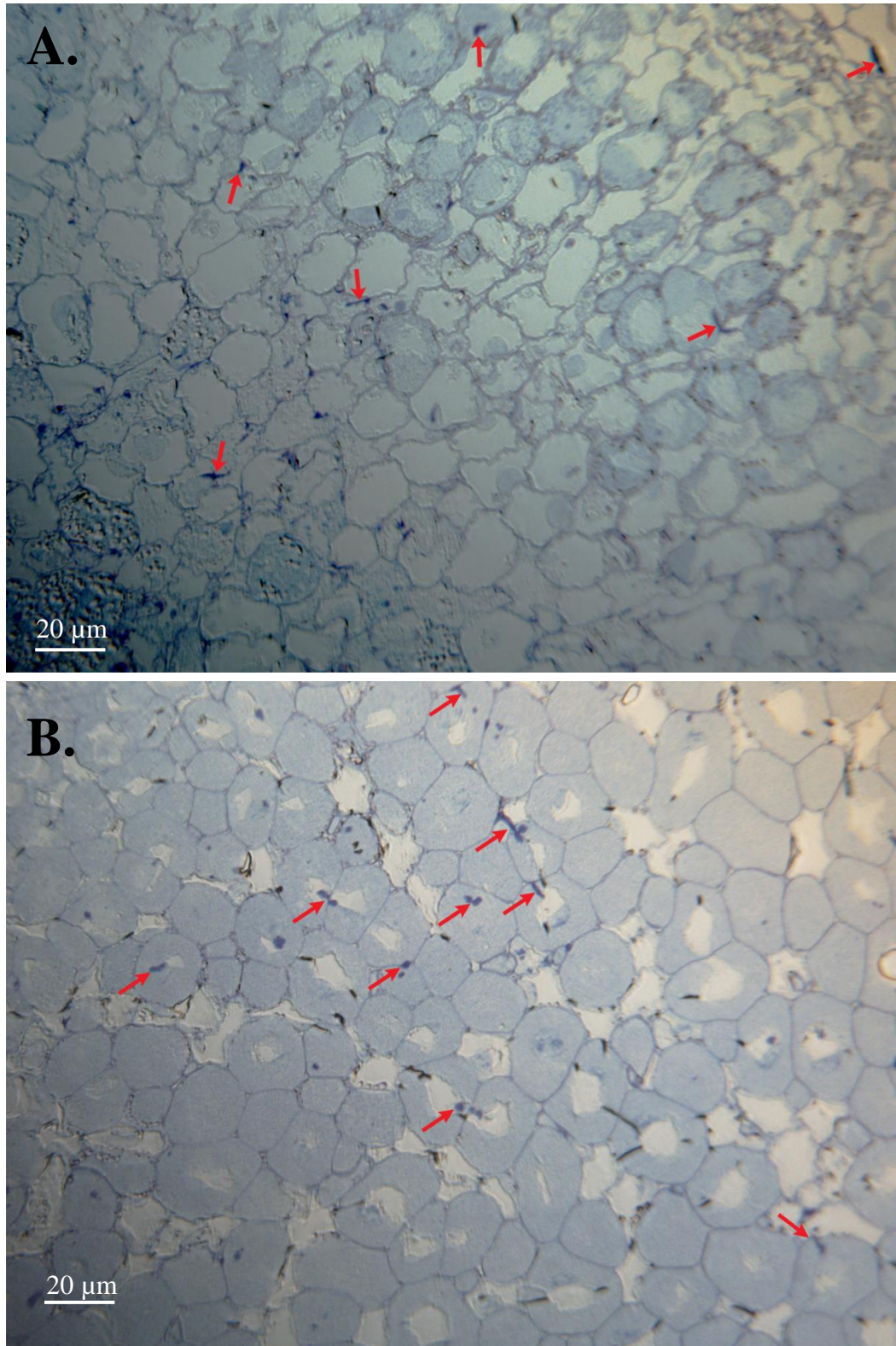
Fig 4.14 Sections of nodules taken from *P. sativum* inoculated with (A) Rlv3841 or (B) LMB466 (*sitA*:pK19mob *mntH*ΩSpc). Arrows indicate infection thread-like structures. Sections stained with toluidine blue. Visualised by light microscopy at magnification x 20.
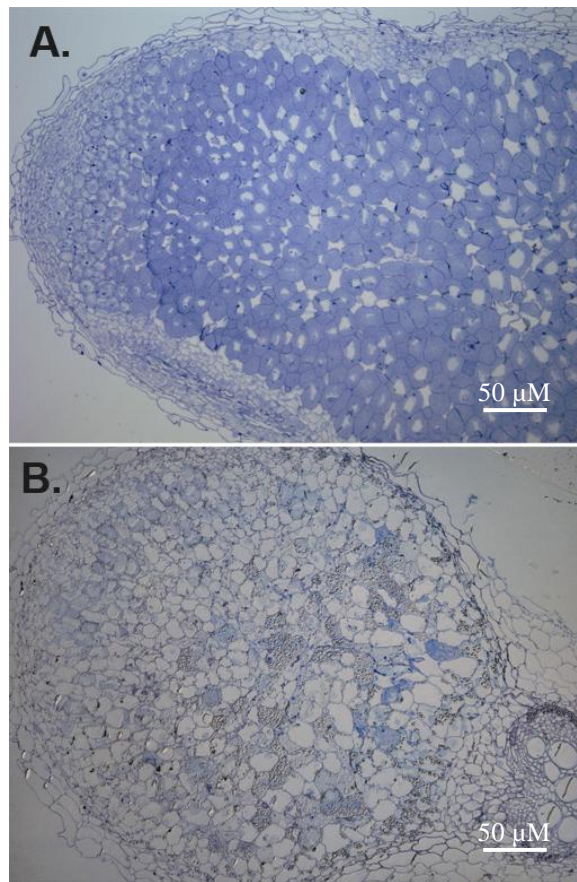
Fig 4.15 Sections of nodules taken from *P. sativum* inoculated with (A) Rlv3841 or (B) LMB466 (*sitA*:pK19mob *mntH*ΩSpc). Sections stained with toluidine blue. Visualised by light microscopy at magnification x 10.
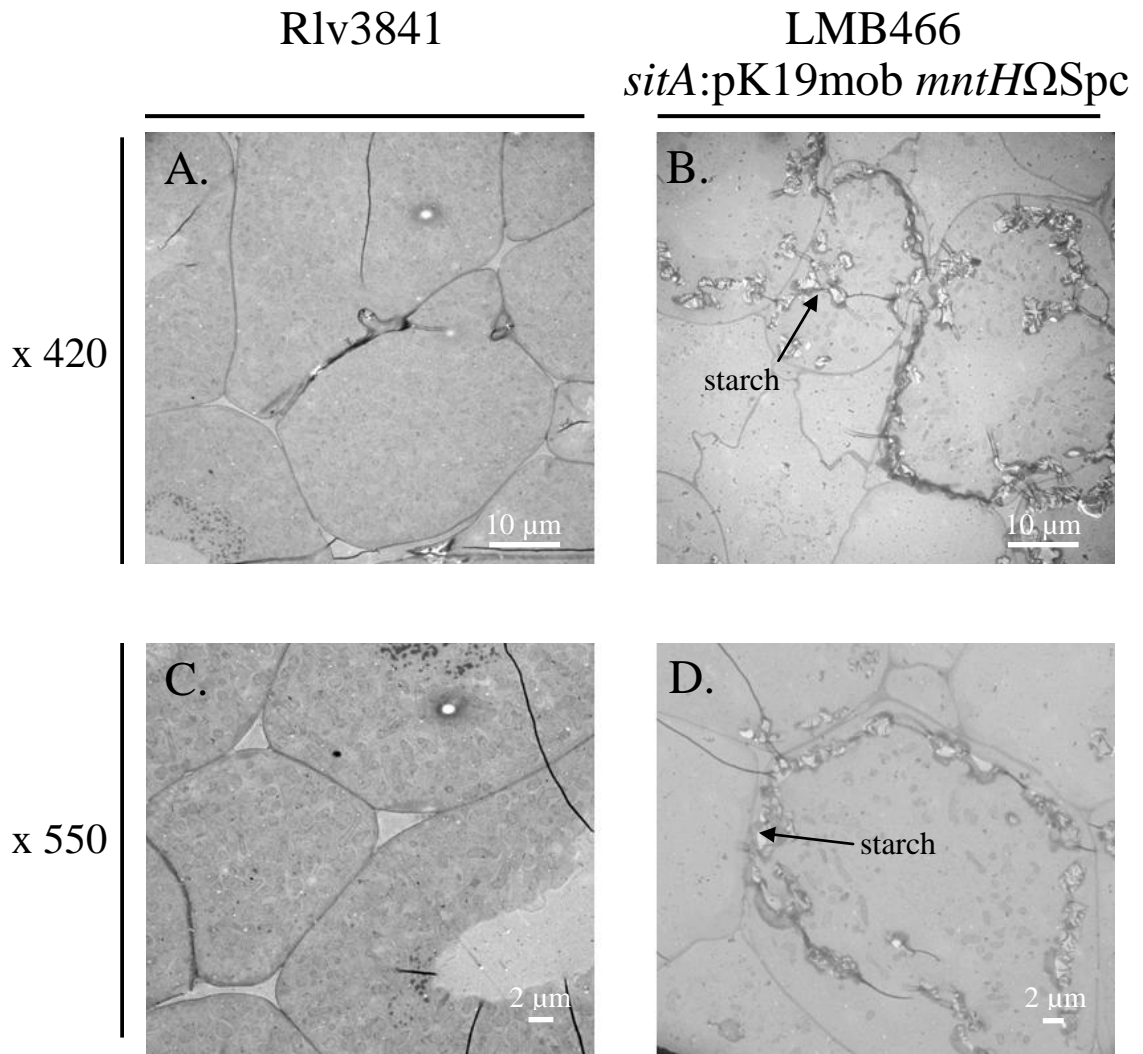
Fig 4.16 Ultrathin sections of nodules taken from *P. sativum* inoculated with Rlv3841 (A and C) or LMB466 (*sitA*:pK19mob *mntH*ΩSpc) (B and D). Visualised by TEM at magnfication x 420 (A and B) or x 550 (C and D).

4.2.5 A *sitA mntH* double mutant is Fix⁻ on *V. faba* and *V. hirsuta*

The requirement of SitABCD and MntH for symbiosis with other indeterminate legumes within the host range of Rlv3841 was investigated. As with *P. sativum*, inoculating *V. faba* with LMB466 (*sitA*:pK19mob *mntH*ΩSpc) resulted in small, white spherical nodules (Fig 4.17) and an absence of acetylene reduction (Fig 4.18).

Furthermore, both LMB364 (*sitA*:pK19mob) and LMB460 (*mntH*ΩSpc) initiated pink nodules on *V. faba* and reduced acetylene at a rate similar to Rlv3841 (Fig 4.18).
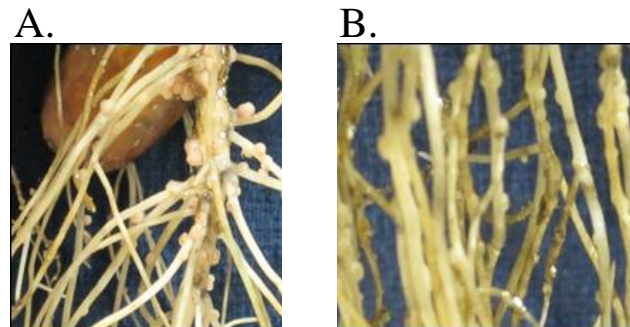

Fig 4.17 Nodules on *V. faba* inoculated with (A) Rlv3841 or (B) LMB466 (*sitA*:pK19mob *mntH*ΩSpc).
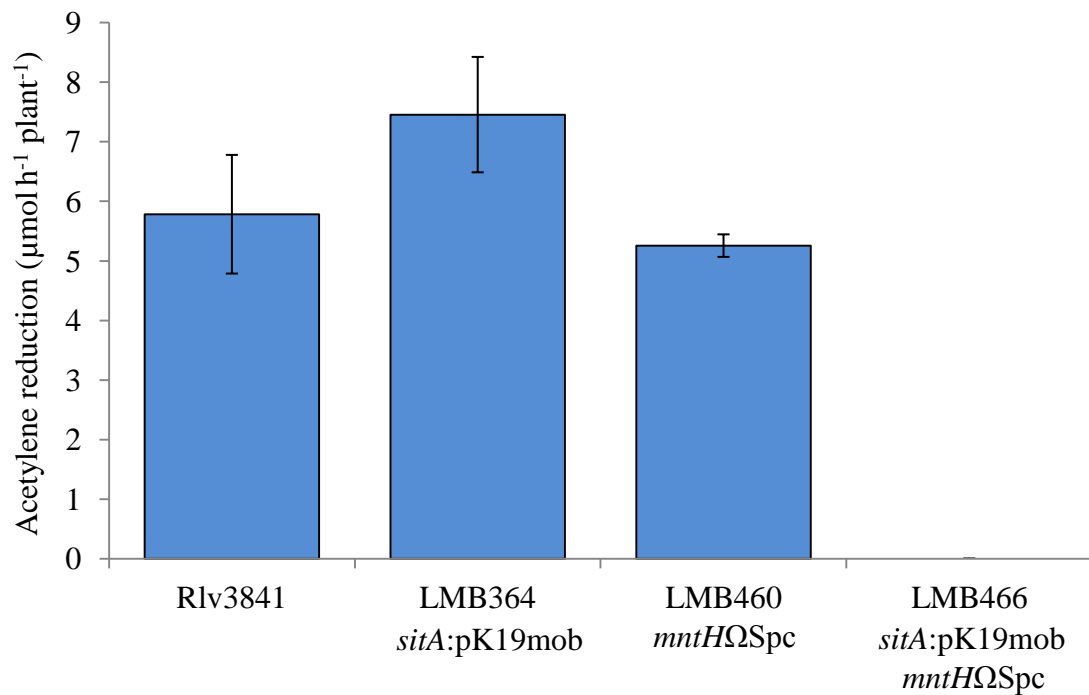

Fig 4.18 Rates of acetylene reduction for Rlv3841, LMB364 (*sitA*:pK19mob), LMB460 (*mntH*ΩSpc) and LMB466 (*sitA*:pK19mob *mntH*ΩSpc) on *V. faba*. Averaged from five plants ± SEM.

Consistent with *P. sativum*, infection thread-like structures could be seen in sections taken from *V. faba* nodules containing LMB466 (*sitA*:pK19mob *mntH*ΩSpc) (Fig 4.19) and there were few infected plant cells (Figs 4.19 and 4. 20). Furthermore, plant cells that were infected by LMB466 (*sitA*:pK19mob *mntH*ΩSpc) appeared to contain a low number of bacteroids compared to cells densely packed with Rlv3841bacteroids (Fig 4.19).

The requirement of SitABCD and MntH was also tested with *V. hirsuta* After three weeks, *V. hirsuta* inoculated (2.6.2) with LMB466 (*sitA*:pK19mob *mntH*ΩSpc) were stunted in growth and showed signs of chlorosis, as seen with the uninoculated control (Fig 4.21). Acetylene reduction assays confirm that LMB466 (*sitA*:pK19mob *mntH*ΩSpc) was unable to fix N_2 on *V. hirsuta* (Fig 4.22).

Fig 4.19 Sections of nodules taken from *V. faba* inoculated with (A) Rlv3841 or (B) LMB466 (*sitA*:pK19mob *mntH*ΩSpc). Arrows indicate infection thread-like structures. Sections stained with toluidine blue visualised by light microscopy at magnification x 20.

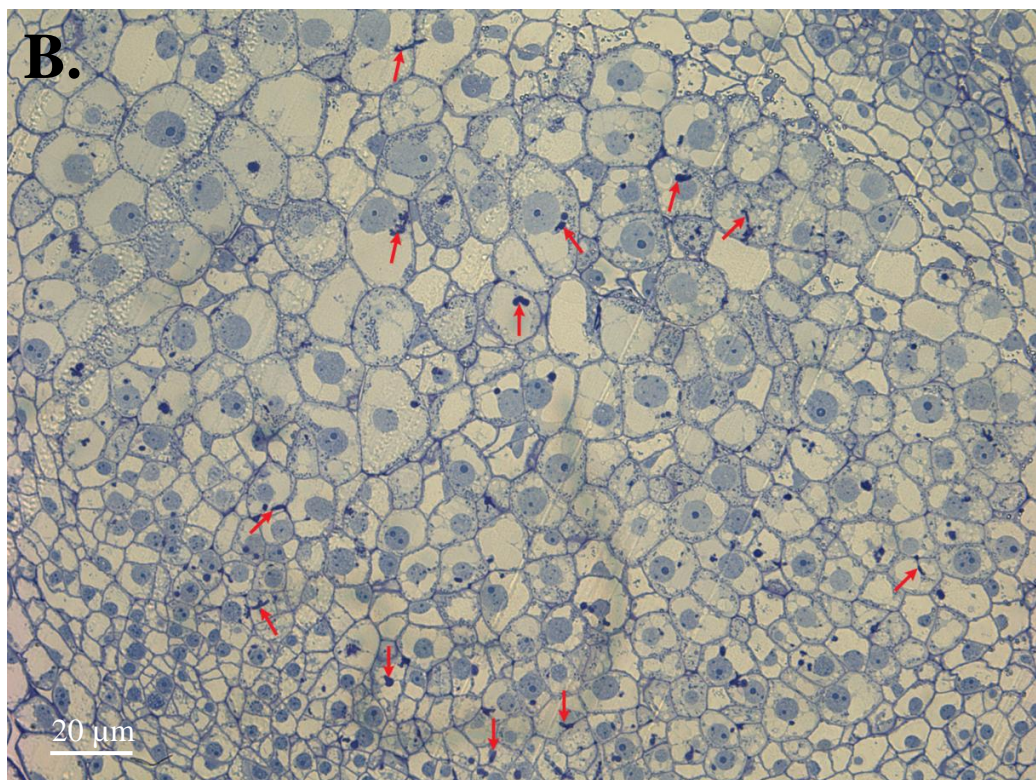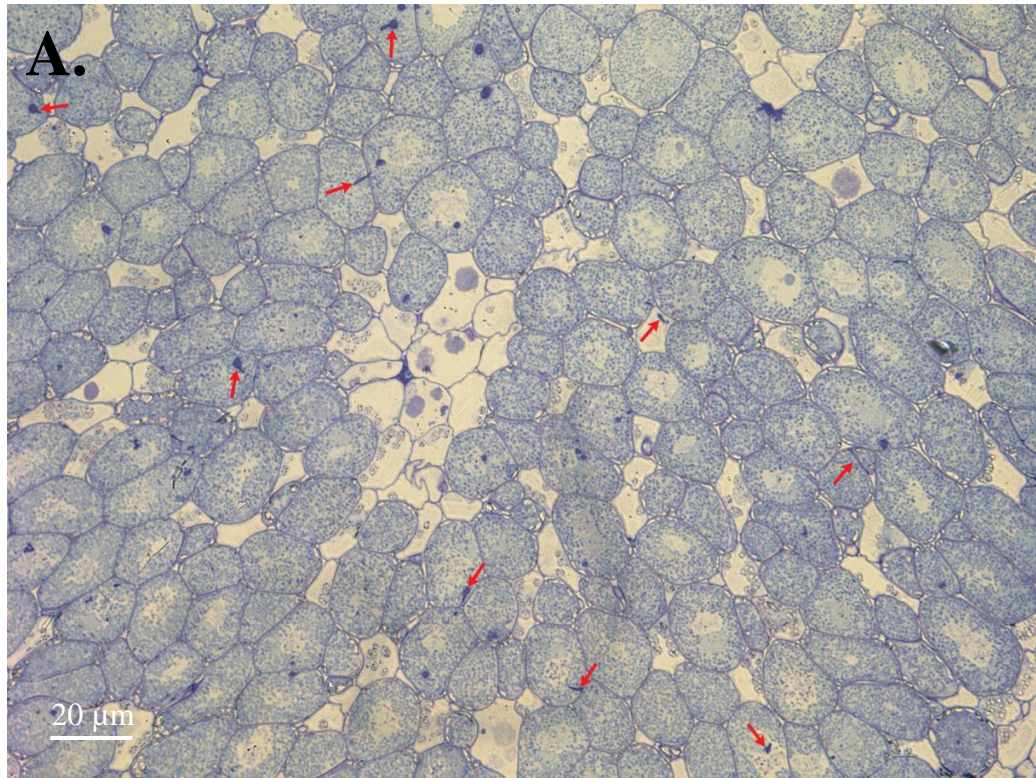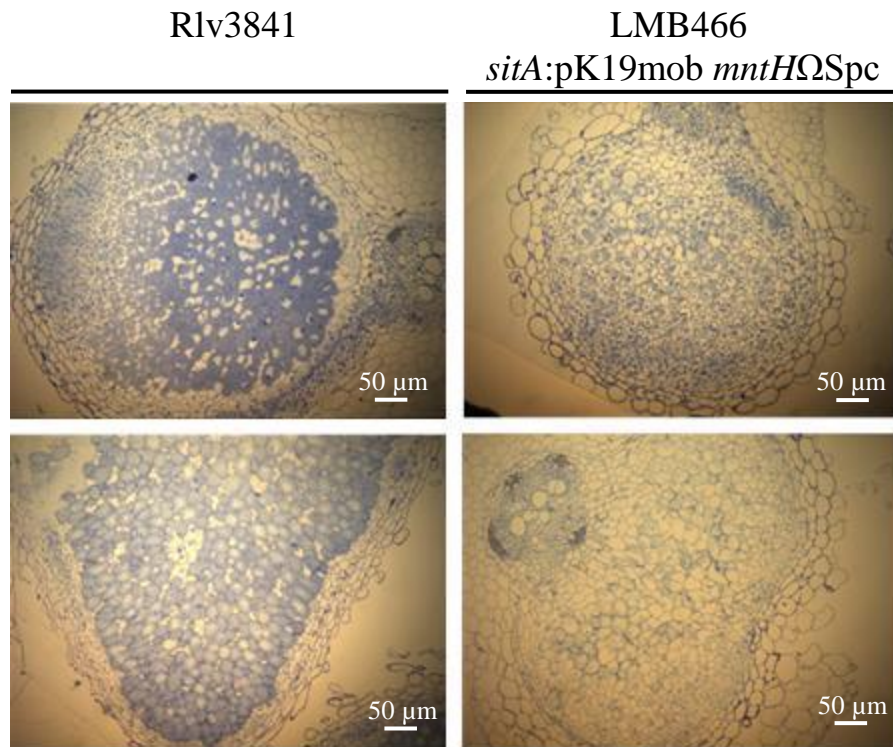**Fig 4.20** Sections of nodules taken from *V. faba* inoculated with Rlv3841 or LMB466 (*sitA*:pK19mob *mntH*ΩSpc). Sections stained with toluidine blue. Visualised by light microscopy at magnification x10.

Fig 4.21 Photo showing (A) uninoculated, (B) Rlv3841-inoculated and (C) LMB466 (*sitA*:pK19mob *mntH*ΩSpc)-inoculated *V. hirsuta*. All plants were grown for three weeks.
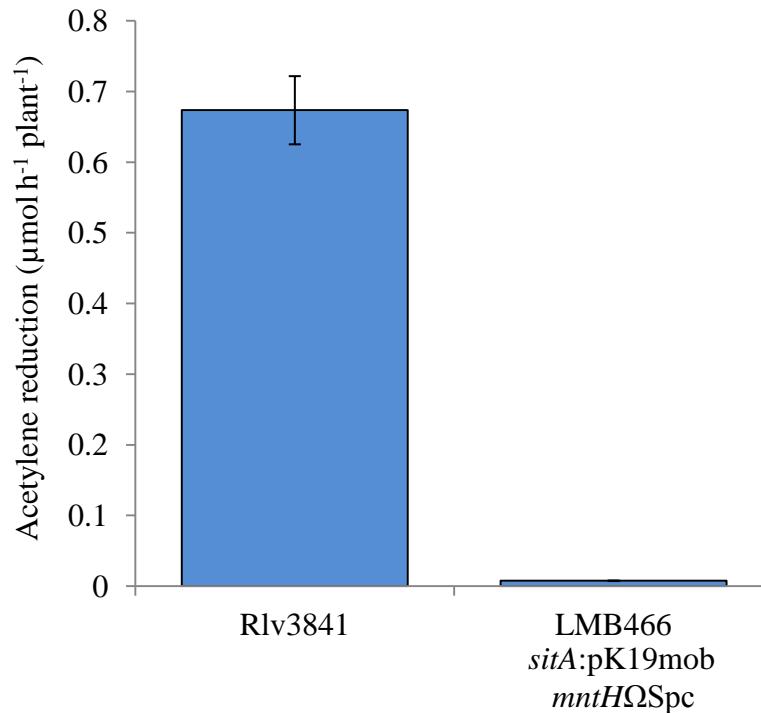
Fig 4.22 Rates of acetylene reduction for Rlv3841 and LMB466 (*sitA*:pK19mob *mntH*ΩSpc) on *V. hirsuta*. Averaged from twenty-four plants ± SEM.

4.2.6 High affinity Mn^{2+} transporters are not essential for bacteroid development in determinate nodules formed by *P. vulgaris*

Strains, *R. leguminosarum* bv. phaseoli 4292 (Rlp4292) and *R. leguminosarum* bv. viciae A34 (RlvA34) were used to test if SitABCD and MntH are required for symbiosis with a legume that forms determinate nodules. These two strains share the same genetic background with the exception of their Sym plasmids (encoding genes important for host selection) (Fig 4.23); consequently, one strain initiates determinate nodules on *P. vulgaris* (Rlp4292), whereas the other initiates indeterminate nodules on *P. sativum* (RlvA34) (Lamb et al., 1982; Downie et al., 1983).
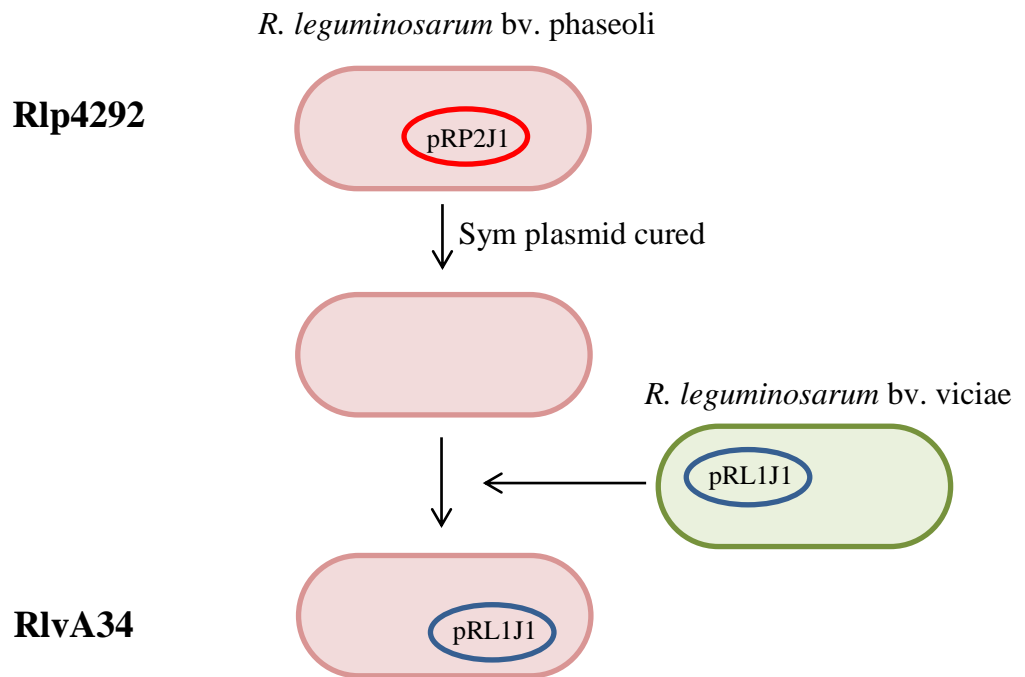
Fig 4.23 Rlp4292 and RlvA34. RlvA34 was engineered by curing Rlp4292 of its Sym plasmid (pRP2J1) and conjugating the Sym plasmid from *R. leguminosarum* (pRL1J1) into the cured strain (Lamb et al., 1982; Downie et al., 1983).

Mutations made in Rlv3841 were remade in both RlvA34 and Rlp4292. To remake the mutations in RlvA34, *sitA*:pK19mob and *mntH*ΩSpc were transduced from LMB364 and LMB460 (respectively) into RlvA34, resulting in LMB525 (RlvA34 *sitA*:pK19mob) and LMB526 (RlvA34 *mntH*ΩSpc). To create the double mutant, *sitA*:pK19mob was transduced from LMB364 into LMB526, to make LMB539 (RlvA34 *sitA*:pK19mob *mntH*ΩSpc). TY was supplemented with 50 μM MnSO$_4$ when selecting for and for routine growth of LMB539 (RlvA34 *sitA*:pK19mob *mntH*ΩSpc).

Bacteriophage RL38 is incapable of infecting Rlp4292 so mutations were remade by conjugation. To make *mntH*ΩSpc in Rlp4292, pLMB546 was conjugated into Rlp4292, resulting in LMB541 (Rlp4292 *mntH*ΩSpc). To make *sitA*ΩKm, a 3 kb region containing *sitA* was PCR-amplified from Rlp4292 gDNA using primers pr1378 and pr1394. The PCR product was subcloned into pJET1.2/blunt to make

pLMB679. A blunted *Eco*RI fragment containing ΩKm was then cloned into *Sma*I-digested pLMB679 to make pLMB691. A 5 kb *Xba*I/*Not*I fragment from pLMB691 was cloned into *Xba*I/*Not*I digested pJQ200SK, resulting in pLMB694. Plasmid pLMB694 was conjugated into Rlp4292 to make LMB624 (Rlp4292 *sitA*Ωkm). To make the double mutant, pLMB694 was conjugated into LMB541, resulting in LMB630 (Rlp4292 *sitA*ΩKm *mntH*ΩSpc). TY was supplemented with 50 μM MnSO$_4$ when selecting for and for routine growth of LMB630 (Rlp4292 *sitA*ΩKm *mntH*ΩSpc).

P. sativum was inoculated with RlvA34, LMB525 (RlvA34 *sitA*:pK19mob), LMB526 (RlvA34 *mntH*ΩSpc) or LMB539 (RlvA34 *sitA*:pK19mob *mntH*ΩSpc). The double mutant LMB539 (RlvA34 *sitA*:pK19mob *mntH*ΩSpc) did not reduce acetylene on *P. sativum*, consistent with what was seen with LMB466 (Rlv3841 *sitA*:pK19mob *mntH*ΩSpc) (Fig 4.24).

P. vulgaris was then inoculated with Rlp4292, LMB541 (Rlp4292 *mntH*ΩSpc), LMB624 (Rlp4292 *sitA*ΩKm) or LMB630 (Rlp4292 *sitA*ΩKm *mntH*ΩSpc) (2.6.3). In contrast to the Fix$^-$ phenotype seen with *P. sativum*, double mutant LMB630 (Rlp4292 *sitA*ΩKm *mntH*ΩSpc) reduced acetylene at a rate equal to Rlp4292 (Fig 4.24).

Following these results, the ability of LMB539 (RlvA34 *sitA*:pK19mob *mntH*ΩSpc) and LMB630 (*mntH*ΩSpc *sitA*ΩKm) to grow in Mn^{2+}-limited medium was tested (2.5.2). Conforming with the growth phenotype of LMB466 (*sitA*:pK19mob *mntH*ΩSpc), LMB539 (RlvA34 *sitA*:pK19mob *mntH*ΩSpc) and LMB630 (Rlp4292 *mntH*ΩSpc *sitA*ΩKm) grew poorly in modified AMS glucose containing 0.05 μM MnSO$_4$ (Fig 4.25). This implies that the difference in symbiotic phenotypes is not due to an unidentified Mn^{2+} transporter encoded on the Sym plasmid of Rlp4292.
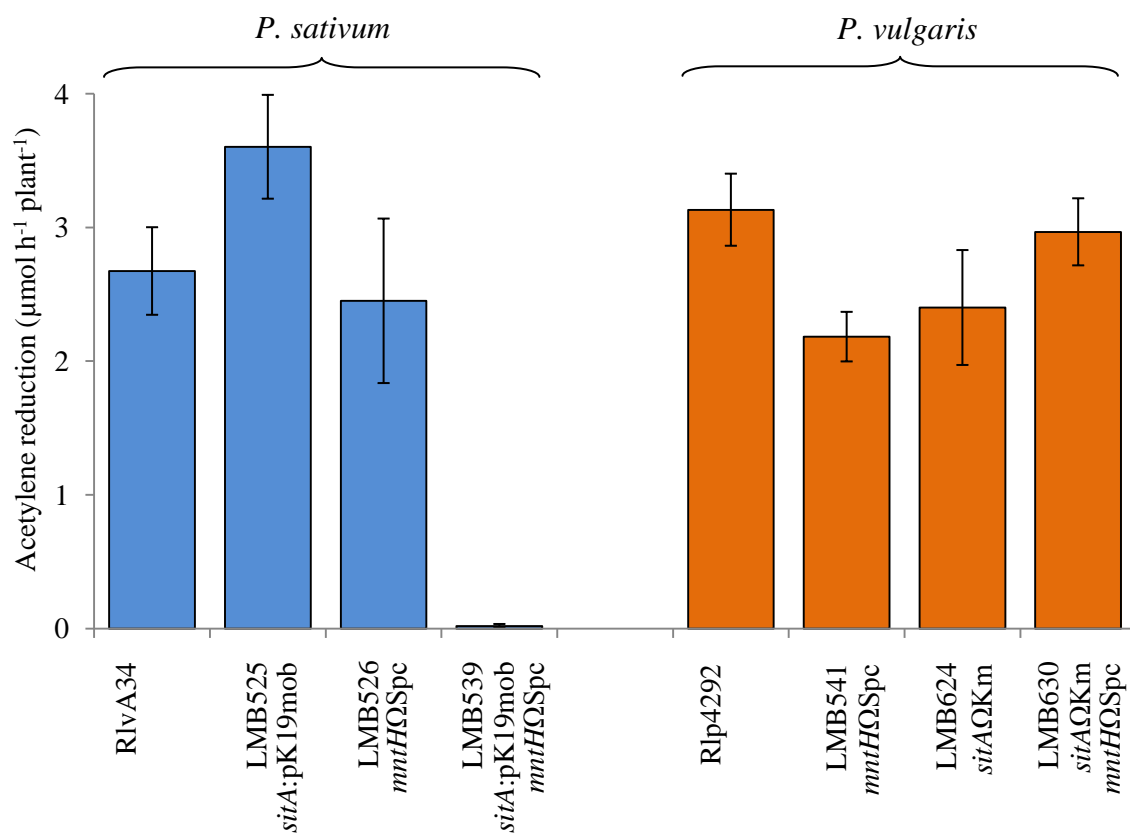
Fig 4.24 Rates of acetylene reduction for *P. sativum* (blue bars) inoculated with RlvA34, LMB525 (RlvA34 *sitA*:pK19mob), LMB526 (RlvA34 *mntH*ΩSpc) or LMB539 (RlvA34 *sitA*:pK19mob *mntH*ΩSpc) and *P. vulgaris* (orange bars) inoculated with Rlp4292, LMB541 (Rlp4292 *mntH*ΩSpc), LMB624 (*sitA*ΩKm) or LMB630 (*mntH*ΩSpc *sitA*ΩKm).
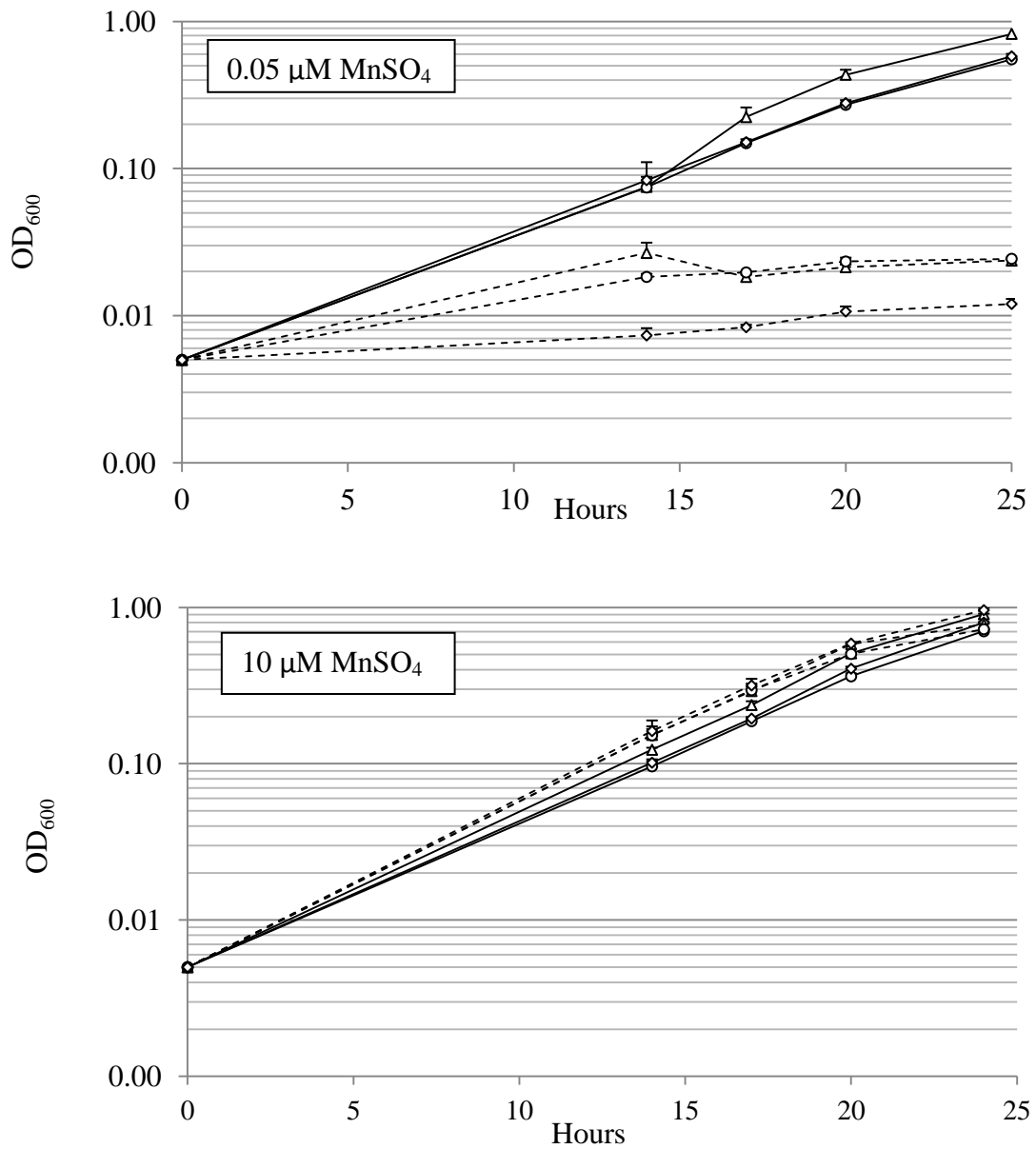
Fig 4.25 Growth of Rlv3841 (solid line with triangles), double mutant LMB466 (broken line with triangles), RlvA34 (solid line with circles), double mutant LMB539 (broken line with circles), Rlp4292 (solid line with diamonds) and double mutant LMB630 (broken line with diamonds) grown in modified AMS containing either 0.05 μM MnSO$_4$ or 10 μM MnSO$_4$.

4.3 DISCUSSION

The homology of SitABCD and MntH to characterised Mn^{2+} transporters, the regulation of *sitABCD* and *mntH* by Mur in response to Mn^{2+} (Fig 4.3) and the growth phenotype of LMB466 (*sitA*:pK19mob *mntH*ΩSpc) (Fig 4.6), strongly suggest that *sitABCD* and *mntH* encode Mn^{2+} transporters. However, transport assays using $^{54}Mn^{2+}$ are still required to confirm this. Furthermore, because some Mn^{2+} transporters are also capable of Fe^{2+} transport, the ability of unlabelled Fe^{2+} to inhibit $^{54}Mn^{2+}$-uptake should also be tested (Hohle and O'Brian, 2009). Indeed, the possibility that SitABCD and MntH may also be capable of a level of Fe^{2+} transport is particularly relevant to symbiosis because, despite Fe have a clear role in N_2 fixation, it is not known how Fe is imported into the bacteroid.

It is not unusual for bacteria to encode both types of Mn^{2+} transporter but only a few studies have eliminated both transport systems within the same strain (Zaharik et al., 2004; Runyen-Janecky et al., 2006; Sabri et al., 2008; Perry et al., 2012). One reason for having two Mn^{2+} transporters would be if the abilities of SitABCD and MntH to transport Mn^{2+} differed according to the environment. For example, *Salmonella enterica* encodes both MntH and SitABCD. In *S. enteria*, MntH can transport Mn^{2+} at a high rate at both an acidic and slightly alkaline pH, whereas SitABCD, is almost inactive in acidic environments, and optimally transports Mn^{2+} at slightly alkaline pH (Kehres et al., 2002b). If this is also the case for Rlv3841, it would enable Rlv3841 to effectively compete for Mn^{2+} in both alkaline and acidic soils. It would be intriguing to measure growth of the single mutants at different pH, to see if the disruption of *mntH* would cause a growth phenotype at low pH, like disruption of *sitA* did at neutral pH (Fig 4.6).

Both single mutants exhibited hypersensitivity to H_2O_2 relative to Rlv3841 (Fig 4.8). Although it is well know that disruption of Mn^{2+} transport causes sensitivity to oxidative stress (Davies and Walker, 2007b; Anderson et al., 2009; Anjem et al., 2009), this result differs from what was seen for *Shigella flexneri* and an avian pathogenic *E. coli* strain , where both *sitABCD* and *mntH* had to be mutated to cause H_2O_2-hypersensitivity (Runyen-Janecky et al., 2006; Sabri et al., 2006). However,

the fore mentioned studies used disk assays to determine H_2O_2-sensitivity, whereas in this study, sensitivity was determined in liquid medium.

The symbiotic phenotype of LMB466 (*sitA*:pK19mob *mntH*ΩSpc) on *P. sativum, V. faba* and *V. hirsuta* differed from the symbiotic phenotype of *S. meliloti sitA*::mTn5 (and Δ *sitA*) on *M. sativa* (Fig 4.2) (Chao et al., 2004; Davies and Walker, 2007b). Only small white nodules were initiated by LMB466 (*sitA*:pK19mob *mntH*ΩSpc) (Figs 4.10 and 4.17) in contrast to the mixture of small white and intermediate-sized nodules initiated by *S. meliloti sitA*::mTn5 on *M. sativa* (Davies and Walker, 2007b). Furthermore, LMB466 (*sitA*:pK19mob *mntH*ΩSpc) was incapable of N_2 fixation, whereas some acetylene reduction could be detected for *S. meliloti sitA*::mTn5 and Δ *sitA* (Chao et al., 2004; Davies and Walker, 2007b). One explanation could be that *S. meliloti* encodes another Mn^{2+} transporter. *S. meliloti* does contain an uncharacterised gene (SMa1115) that encodes a putative Nramp transporter that shares 26% amino acid identity with MntH from *E. coli* and 24% with MntH from Rlv3841 (93% and 67% coverage respectively) (Patzer and Hantke, 2001; Platero et al., 2007). If SMa1115 does encode a functional Mn^{2+} transporter it would explain why mutations in the *S. meliloti sitABCD* operon either caused partial symbiotic phenotypes (Chao et al., 2004; Davies and Walker, 2007b) or no phenotype (Platero et al., 2003) on *M. sativa* cultivars.

It is not know at what stage LMB466 (*sitA*:pK19mob *mntH*ΩSpc) is blocked in bacteroid development. The presence of normal-looking infection threads (Figs 4.14 and 4.19), low number of infected cells (Figs 4.15 and 4.20) and small number of bacteroids in infected cells (Figs 4.16 and 4.19) suggest that development is blocked at a late stage of infection thread progression or possibly during the release stage. A similar phenotype was seen for RU4040 (*bacA*:pK19mob) on *P. sativum*, where infection threads could be seen but the mutant was unable to infect plant cells and develop into bacteroids (Karunakaran et al., 2010).

What causes the block in the release of bacteria from the infection thread is also unknown. A likely explanation is an inability to survive the oxidative stress imposed by the presence of H_2O_2 in the infection threads (Santos et al., 2001; Rubio et al., 2004; Cardenas et al., 2008; Montiel et al., 2012). In one strain of *S. meliloti*

(Rm5000), a Mn-dependent SodA has been shown to be essential for infection and bacteroid development (Santos et al., 2000), however, disruption of *sodA* in the parent strain of *S. meliloti sitA*::mTn5 (*S. meliloti* 1021) did not cause a symbiotic defect (note: *sodA* is annotated as *sodB* in *S. meliloti* 1021). Furthemore, a *sitA sodA* double mutant exhibited the same level of symbiotic deficiency as a *sitA*::mTn5 mutant (Davies and Walker, 2007b). Indeed, disruption of *sodA* in Rlv3841 was also found not to affect acetylene reduction or nodulation on *P. sativum* (personal communication, Allan Downie JIC). Therefore, the requirement of SitABCD and MntH for symbiosis cannot be attributed to the activity of SodA. Alternatively, importation of Mn^{2+} might provide protection against oxidative stress by replacing Fe^{2+} in certain mononuclear enzymes (Anjem et al., 2009).

For some bacteria however, the requirement of Mn^{2+} is not restricted to oxidative stress resistance and is utilised by enzymes central to metabolism e.g. pyruvate kinase (PykA), NAD^+ malic enzyme (Dme) and $NADP^+$ malic enzyme (Tme) (Eyzaguir.J et al., 1973; Hohle and O'Brian, 2012). Dme has been shown to be essential in *S. meliloti* for N_2 fixation (Driscoll and Finan, 1993) and a *dme pykA* double mutant in Rlv3841 is Fix⁻ (Mulley et al., 2010). However, the *dme pykA* double mutant was not defective for bacteroid formation (unpublished data, Philip Poole lab) and so the symbiotic phenotype of LMB466 (*sitA*:pK19mob *mntH*ΩSpc) cannot be attributed to an absence of a Mn^{2+} cofactor for metabolic enzymes Dme and PykA.

SitABCD and MntH were not required for bacteroid development in determinate nodules formed on *P. vulgaris* as acetylene reductions for the double mutant LMB630 (Rlp4292 *sitA*ΩKm *mntH*ΩSpc) were equivalent to wild type Rlp4292 (Fig 4.24). This agrees with the symbiotic phenotype of *B. japonicum* Δ *mntH*, which was severely defective for $^{54}Mn^{2+}$ uptake but not for bacteroid development in determinate nodules on *G. max* (Hohle and O'Brian, 2009). A simple explanation could be that there are higher levels of bioavailable Mn^{2+} in *P. vulgaris* and *G. max* nodules relative to *P. sativum*, *V. faba*, *V. hirsuta* and *M. sativa*; this may or may not be a general feature of determinate nodules. Alternatively, developing bacteroids in indeterminate nodules may have a higher requirement for Mn^{2+} relative to developing bacteroids in determinate nodules, for example, if the infection threads in

indeterminate nodules contain higher levels of ROS. However, ROS have never been accurately quantified in the infection threads of either nodule-type.

Another alternative explanation could be the presence of NCR peptides in nodules formed on legumes belonging to the galegoid clade (e.g. *P. sativum*, *V. hirsuta*, *V. faba* and *M. sativa*) but absence in nodules formed on legumes in belonging to the phaseoloid (e.g. *G. max* and *P. vulgaris*) (see 1.4.4). These plant-derived antimicrobial peptides increase membrane permeability (Van de Velde et al., 2010) and disruption of the membrane by other antimicrobial peptides leads to loss of K^+ ions, amino acids, ATP and Mg^{2+} ions from the cell (Galvez et al., 1991; Okereke and Montville, 1992; Maftah et al., 1993; Matsuzaki et al., 1997; Xu et al., 1999; Brogden, 2005; Bolintineanu et al., 2010). It is therefore feasible, that NCR peptides present in galegoid nodules may cause a loss of ions from the bacterial cell, including Mn^{2+}, explaining the requirement of high-affinity Mn^{2+} transporters during infection of *P. sativum*, *V. faba* etc.

Some antimicrobial peptides can also disrupt the proton motive force (pmf) of the membrane and the functionality of some divalent metal transporters has been shown to depend on pmf-conservation (Karlinsey et al., 2010). Therefore, in phaseoloid nodules, divalent transporters with a low-affinity for Mn^{2+} might be able to compensate for the absence of SitABCD or MntH, however, if the functionality of these low-affinity transporters is compromised by the presence of NCR peptides, the rate of Mn^{2+} uptake might not be enough to compensate for the loss of high-affinity Mn^{2+} transporters.

A third reason explaining why the presence of NCR peptides might cause a requirement of high-affinity Mn^{2+} transport is that antimicrobial peptides have been reported to stimulate $HO^{\cdot}$ formation via the Fenton reaction (via the damage of Fe-S clusters) (Kohanski et al., 2007). Consequently, there could be a higher demand for Mn^{2+} to suppress the Fenton reaction by replacing Fe^{2+} in mononuclear enzymes and as a cofactor for SodA (Davies and Walker, 2007b; Krehenbrink et al., 2011; Anjem and Imlay, 2012). However, this common mechanism of $HO^{\cdot}$ induced cell death caused by antimicrobial peptides has been since disputed by Ezraty *et al*., 2013.

Contrasting phenotypes resulting from elimination of Mn^{2+} transporters has also been seen in the human pathogen *Yersinia pestis*, where a *sitA mntH* double mutant (note: *sitABCD* in *Y. pestis* is annotated as *yfeABCD*), caused reduced virulence in the lymph nodes (bubonic plague) but no loss of virulence in the lungs (pneumonic plague) (Perry et al., 2012). However, for plant-infecting bacteria, this is the first demonstration that the requirement of metal transporters depends upon the species of the plant-host.

Chapter 5: *Mg^{2+} transport*

5.1 INTRODUCTION

5.1.1 Magnesium

Magnesium (Mg^{2+}) is the most abundant divalent cation inside many living cells and essential for a broad range of cellular functions, including stabilising ribosomal subunits, a cofactor for ATP, establishing the secondary structure of nucleic acids and stabilising membranes (Smith and Maguire, 1998; Moomaw and Maguire, 2008). Despite this, very little is known about how Mg^{2+} is transported during legume-rhizobia symbioses.

One study found that *M. sativa* grown in Mg^{2+}-limited conditions nodulated poorly, were small, chlorotic and exhibited poor rates of N$_2$ fixation (<25% compared to plants grown in the normal growth medium) (Miller and Sirois, 1983). In the same study, the rate of acetylene reduction for bacteroids isolated from *M. sativa* nodules (taken from plants grown in the normal growth medium), could be improved by ~ 10% by the addition of Mg^{2+}. Furthermore, addition of the chelating agent ethyleneglycol-bis-(aminoethyl ether)-N, N'-tetraacetic acid (EGTA) to the isolated bacteroids caused a 28% decrease in acetylene reduciton, which could be partially restored by the addition of Mg^{2+}. One requirement of Mg^{2+} for N$_2$ fixation is providing energy to nitrogenase because reduction of N$_2$ by this enzyme requires sixteen MgATP molecules [N$_2$+8H$^+$+16MgATP+8e$^-$ $\rightarrow$ 2NH$_3$+H$_2$+16MgADP+16P$_i$] (Seefeldt et al., 2009).

5.1.2 Magnesium importers

Three types of Mg^{2+} importers have been identified in prokaryotes: (1) P-type ATPase, (2) the CorA channel and (3) the MgtE channel (Maguire, 2006; Moomaw and Maguire, 2008).

The P-type ATPases MgtA and MgtB are unusual transporters because they utilise ATP for Mg^{2+}-uptake with, rather than against, the electrochemical gradient (Moncrief and Maguire, 1999; Maguire, 2006). MgtA and MgtB in *Salmonella typhimurium* are capable of Mg^{2+} (and Ni^{2+}) influx but not efflux (Smith and Maguire, 1998). Disruption of *mgtB* has been shown to hinder long-term survival of *S. typhimurium* in macrophages (Blanc-Potard and Groisman, 1997; Smith and Maguire, 1998).

The second type of Mg^{2+} importer, the CorA (cobalt resistance) channel, is ubiquitous amongst prokaryotes and can mediate both uptake and efflux of Mg^{2+} (in addition to Co^{2+} and Ni^{2+}) (Smith and Maguire, 1995; Moncrief and Maguire, 1999; Moomaw and Maguire, 2008). The CorA-channel has been studied in the human pathogens *S. enterica* and *Helicobacter pylori*; disruption of *corA* attenuated virulence of *S. enterica* in mice and resulted in defective invasion of and replication within epithelial cells (Pfeiffer et al., 2002; Papp-Wallace et al., 2008). CorA has also been investigated in the plant pathogen *Pectobacterium carotovorum*, where mutation of *corA* caused a decrease in the production of cell-wall degrading enzymes i.e. pectate lyase, proteases, polygalacturonase and cellulase (Kersey et al., 2012). Consequently, the mutant had attenuated virulence as it macerated less host tissue compared to the wild type and multiplied poorly *in planta*. CorA-type channels have also been indentified in plants and are annotated as MRS2. In *A. thaliana*, eight MRS2-like genes have been shown to encode functional CorA channels (Schock et al., 2000; Li et al., 2001; Gebert et al., 2009).

The third type of Mg^{2+} importer, the MgtE channel, was first discovered in *Bacillus firmus* OR4 (Smith et al., 1995) but is now known to be commonly present in all kingdoms of life (Moomaw and Maguire, 2008; Hattori et al., 2009). *In vivo* complementation of a mutant *E. coli* strain deficient for Mg^{2+}-uptake together with *in vitro* patch-clamp analysis, characterised MgtE as a highly selective Mg^{2+} channel (but also capable of low levels of Co^{2+}-uptake) (Hattori et al., 2009). A crystal structure of MgtE from *Thermus thermophilus* identified MgtE as a homodimer in the presence of Mg^{2+} (Hattori et al., 2007). Cystathionine β-synthase (CBS) domains that reside in the cytosolic region of MgtE are thought to be involved in ion sensing

and regulation of a gating-mechanism for the ion-conducting pore in response to Mg^{2+} levels (Fig 5.1) (Ishitani et al., 2008; Hattori et al., 2009).
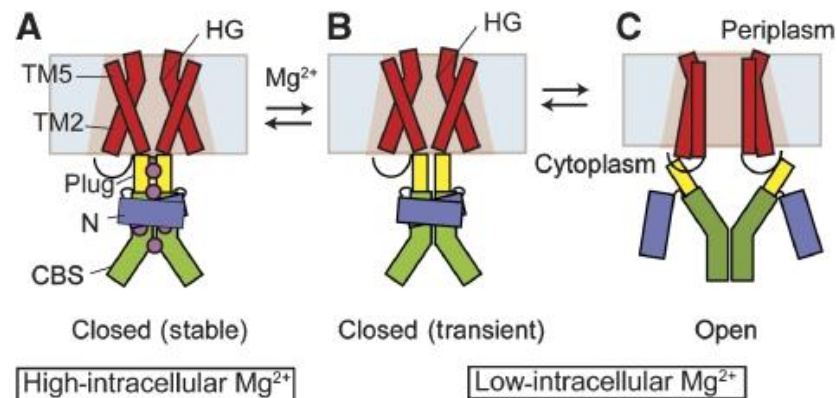

Fig 5.1 Model for Mg^{2+}-dependent gating of MgtE channel. Model shows the N-terminal (blue), CBS domains (green), the plug helix (yellow) and transmembrane domains (red). When intracellular levels of Mg^{2+} are high, Mg^{2+} ions (purple circles) bind between the interface of the CBS domains or the interface between the CBS domains and the N-terminal, stabilising the closed state of the channel. When intracellular levels of Mg^{2+} are low, the interface between the cytosolic domains is destabalised. This in turn destabalises the closed state of the transmembrane domains, resulting in an open formation that allows the passage of Mg^{2+} ions into the cell. Reproduced from Hattori *et al*., 2009.

Only a few studies on MgtE in bacteria have been reported and typically focus on the structure, mechanism or function of the channel (Smith et al., 1995; Merino et al., 2001; Hattori et al., 2007; Anderson et al., 2009; Ragumani et al., 2010). Only three studies have investigated the physiological role of MgtE. In *Aeromonas hydrophilia*, disruption of *mgtE* resulted in a reduced ability to adhere to Hep-2 cells, decreased swarming on semisolid agar and reduced its ability to form biofilms (Merino et al., 2001). In *Pseudomonas aeruginosa*, disruption of *mgtE* caused increased cytotoxicity on epithelial cells (Anderson et al., 2010). Overexpression of *mgtE* from *Bacillus subtillis* in *S. enterica*, enhanced thermotolerance of *S. enterica* as did overexpression of a gene encoding its native transporter MgtA (O'Connor et al., 2009). The increased thermotolerance may have been due to accumulated levels of

intracellular Mg^{2+} caused by the overexpresion of *mgtE*, which stabilised proteins and increased membrane integrity. Mg^{2+} has also been shown to inhibit Fe^{2+} transport by an unknown mechanism therefore, hyperaccumulation of Mg^{2+} might have lessened oxidative damage by preventing Fe^{2+} uptake   (levels of oxygen radicals increase with above-optimal temperatures) (Papp and Maguire, 2004; O'Connor et al., 2009).

5.1.3 Regulation of genes encoding Mg^{2+} importers

Regulation of genes encoding Mg^{2+} importers occurs at the transcriptional level, post-transcriptional level and post-translational level (Cromie et al., 2006; Dann et al., 2007; Hattori et al., 2009; Zhao et al., 2011; Lim et al., 2012). In *S. enterica, mgtA* and *mgtB* are regulated by the PhoQ-PhoP two-component system. Under low levels of Mg^{2+}, PhoQ phosphorylates the DNA binding protein PhoP; PhoP~P then activates *mgtA* and *mgtB* expression (Groisman, 2001; Cromie et al., 2006).

Expression of *mgtA* has an additional level of control, which is dependent on a 5' untranslated region (5'UTR) (Cromie et al., 2006). When Mg^{2+} levels are above a certain threshold, Mg^{2+} will bind to the 5'UTR of *mgtA*, which promotes the formation of a stem-loop structure, causing transcription to terminate before the coding-region of *mgtA* is reached. In contrast, when Mg^{2+} levels are below a certain threshold, the 5'UTR is not bound to Mg^{2+} and consequently, an alternative stem-loop structure is formed, allowing transcription of the *mgtA* coding region (Cromie et al., 2006). More recently, an ORF encoding a 17-residue peptide, MgtL, was identified within the 5'UTR of *mgtA* (Zhao et al., 2011). High levels of Mg^{2+} stimulate the translation of *mgtL* and this translation is essential for the premature termination of *mgtA*-transcription. The mechanism behind MgtL-dependent termination of *mgtA*-transcription is unknown (Zhao et al., 2011).

Regulation of *mgtE* from *B. subtillis* is also reliant on a riboswitch, "M-box", that binds and responds to Mg^{2+}; however, the 5'UTR of *mgtA* and the M-box of *mgtE* share no similarities in sequence or secondary structure (Dann et al., 2007). The model for M-box regulation is as follows: when Mg^{2+} levels are low, a stem-loop

structure forms in the M-box and acts as an anti-terminator, thereby preventing the formation of an additional stem-loop that can terminate transcription. When Mg^{2+} levels are high, Mg^{2+} binds to the M-box, the secondary structure changes and the anti-terminator is lost, allowing the formation of the terminator (Dann et al., 2007; Helmann, 2007).

Regulation of *corA* from *E. coli* is also reliant on a 5'UTR (Lim et al., 2012). The 5'UTR is targeted and cleaved by Mg^{2+}-dependent RNaseIII. It has been suggested that loss of the 5'UTR makes the *corA* transcript highly vulnerable to attack by RNases, the action of which is inhibited by hairpin structures in the 5'UTR.

5.1.4 A Putative MgtE channel in Rlv3841 is required for symbiosis on *P. sativum*

Isolated from a random-mutagenesis screen of Rlv3841, the strain RU4107 carries a mTn5 in *mgtE* (RL1461) and was shown to be symbiotically defective on *P. sativum* (Karunakaran et al., 2009). However, rates of acetylene reduction were never measured and infection was never analysed. Furthermore, it was not experimentally proven that *mgtE* encoded a Mg^{2+} channel and there was no characterisation of RU4107 (*mgtE*::mTn5) in a free-living state.

No other Mg^{2+} importer has been identified to have a role in legume-rhizobia symbioses so it was important to further investigate the role of the putative MgtE channel in free-living cells and during symbiosis. This investigation aimed to determine the stage at which bacteroid development of RU4107 (*mgtE*::mTn5) is impeded i.e. in the infection threads as with LMB466 (*sitA*::pK19mob *mntH*ΩSpc) or at a later developmental stage. Furthermore, following the discovery that the requirement of Mn^{2+} transporters depends upon the plant-host, the requirement of MgtE was also tested on *V. faba* and *V. hirsuta*.

5.2 RESULTS

5.2.1 The gene *mgtE* encodes a Mg^{2+} channel

The TransportDB database (Ren et al., 2007) and searches on the Rlv3841 genome using the BLAST (Altschul et al., 1990; Young et al., 2006), identified three genes encoding putative CorA and two genes encoding putative MgtE channels (Table 5.1). It is not unusual for bacteria to encode multiple Mg^{2+} importers, in fact, multiple genes encoding putative Mg^{2+} importers were also identified in other rhizobia (Table 5.1). In contrast to the Mn^{2+} transporters, according to microarray data, genes encoding the putative Mg^{2+} channels were not upregulated in developing bacteroids (Table 5.2) (Karunakaran et al., 2009).

Genome	Number of *corA*	Number of *mgtE*	Number of *mgtA/B*
R. leguminosarum 3841	3	2	0
S. meliloti 1021	3	1	0
R. etli CFN 42	3	2	0
M. loti MAFF303099	6	2	0
B. japonicum USDA110	4	1	1

Table 5.1 Distribution of genes encoding putative Mg^{2+} importers across five species of rhizobia (Ren et al., 2007).

Locus Tag	Putative Family	7 day bacteroid	15 day bacteroid	21 day bacteroid
RL1461 (*mgtE*)	MgtE	0.7	0.5	0.8
RL2551	MgtE	0.5	1.1	0.9
RL0921	CorA	0.4	0.6	0.6
RL0964	CorA	1.3	1.8	1.0
pRL120701	CorA	0.6	0.7	0.5

Table 5.2 Genes encoding putative Mg^{2+} channels in Rlv3841. Values correspond to fold-induction of genes in Rlv3841 isolated from from nodules 7, 15 or 21 dpi relative to free-living cells grown in minimal medium (Karunakaran et al., 2009). The highlighted row indicates the *mgtE* required for symbiosis on *P. sativum*.

In Rlv3841, the gene *mgtE* encodes a putative MgtE channel that shares 37% amino acid identity with the characterised MgtE from *T. thermophilus* (Altschul et al., 1990; Hattori et al., 2007). To confirm that *mgtE* did encode a Mg^{2+} channel, a 1.6 kb fragment containing *mgtE* was cloned into the broad-host-range vector pRK415 (Keen et al., 1988) to see if it could complement an *E. coli* triple gene knock-out strain (Δ*mgtA* Δ*corA* Δ*yhiD*), hereafter denoted as MgKO, for growth on LB (Hattori et al., 2009). Primers pr1241 and pr1242 were used to amplify *mgtE* from Rlv3841 gDNA. The PCR product was subcloned into pJET1.2/blunt to make plasmid pLMB553. A *Bgl*II fragment from pLMB553 containing *mgtE* was cloned into *Bam*HI-digested pRK415, in the same orientation of and downstream of the *lac* promoter, resulting in plasmid pLMB562 (p*lac-mgtE*). This fragment was also cloned into *Bam*HI-digested pRK415 in the reverse orientation, resulting in pLMB565 (*mgtE*). *E. coli* MgKO was then transformed with the empty plasmid pRK415, pLMB562 (p*lac-mgtE*) and pLMB565 (*mgtE*) to make LMB469, LMB470 and LMB471, respectively.

The *E. coli* MgKO strain could only grow on LB when supplemented with 100 mM $MgSO_4$ (Fig 5.2). Expression of *mgtE* from the *lac* promoter (LMB470) was able to complement growth of *E. coli* MgKO on unsupplemented LB, whereas the vector by

itself (LMB469) or *mgtE* in the reverse orientation of the *lac* promoter (LMB471) was unable to do so. From this complementation assay, it was concluded that *mgtE* did encode a Mg^{2+} channel.
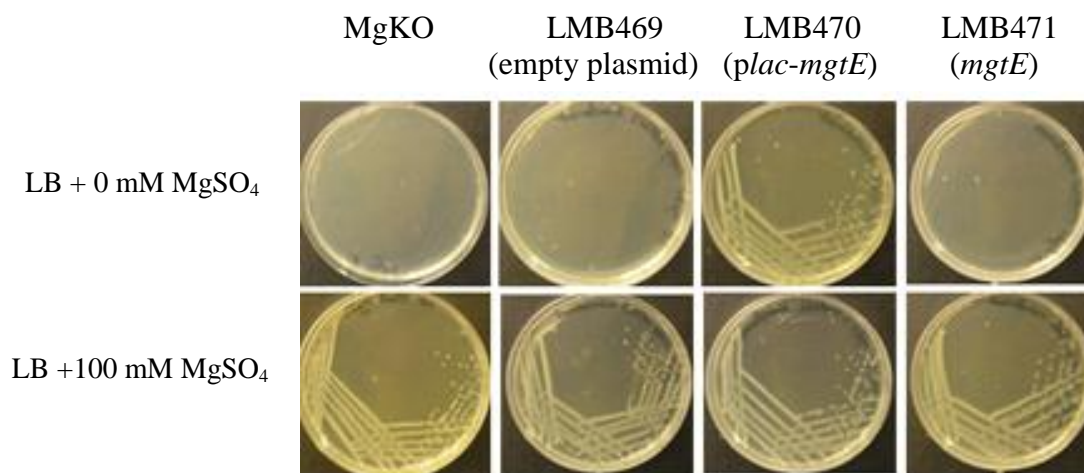

Fig 5.2 Complementation of *E. coli* Δ*mgtA* Δ*corA* Δ*yhiD* strain (MgKO) for growth on LB with Rlv3841 *mgtE*. *E. coli* MgKO strain was transformed with empty plasmid (LMB469), plasmid containing *mgtE* under the control of the *lac* promoter (LMB470) and plasmid containing *mgtE* in the reverse orientation of the *lac* promoter (LMB471).

To determine if the MgtE channel was permeable to other metals, disk assays (2.5.7) were used to test the sensitivity of RU4107 (*mgtE*::mTn5) to toxic levels of $CoCl_2$, $NiSO_4$ and $ZnCl_2$. Agreeing with the permeability of MgtE from *T. thermophilus* to Co^{2+} (Hattori et al., 2009), RU4107 (*mgtE*::mTn5) was less sensitive to a toxic concentration of $CoCl_2$ relative to Rlv3841 (Fig 5.3), implying that MgtE is capable of a level of Co^{2+}-uptake in addition to Mg^{2+}. RU4107 (*mgtE*::mTn5) was not more sensitive to toxic concentrations of $NiSO_4$ and $ZnCl_2$, indicating that MgtE is impermeable to these metals.
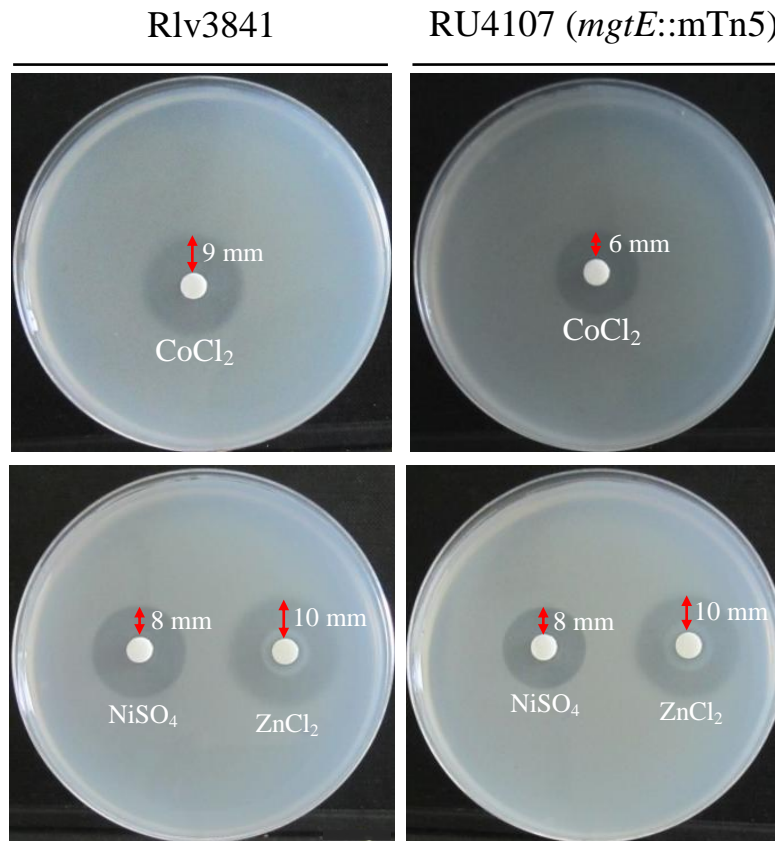
Fig 5.3 Sensitivity of Rlv3841 and RU4107 (*mgtE*::mTn5) to 50 mM CoCl$_2$, 50 mM NiSO$_4$ and 100 mM ZnCl$_2$. Zone of inhibition averaged from three experiments.

5.2.2 RU4107 (*mgtE*::mTn5) grows poorly at low pH in Mg^{2+}-limited medium

Growth of RU4107 (*mgtE*::mTn5) in modified AMS containing either 0.01 mM or 2 mM $MgSO_4$ (2.5.3) was found to be similar to Rlv3841 (Fig 5.4). The absence of a growth phenotype for RU4107 (*mgtE*::mTn5) was not surprising due to the presence of other putative Mg^{2+} importers encoded by Rlv3841 (Table 5.2). Indeed, studies on other bacteria have reported that more than one gene encoding a Mg^{2+} importer needs to be disrupted to cause a growth defect (Hmiel et al., 1989; Snavely et al., 1989; Hattori et al., 2009). However, because RU4107 (*mgtE*::mTn5) is symbiotically defective on *P. sativum*, it was hypothesised that conditions associated with the nodule might affect the requirement of MgtE. Level of pH was a strong candidate because pH has been shown to change functionality of other transporters (Hicks et al., 2003; Mahmood et al., 2009; Hirano et al., 2011; Lu et al., 2011) and rhizobia are exposed to low levels of pH during symbiosis (Pierre et al., 2013). This hypothesis was proven to be correct because at low pH (5.75), growth of RU4107 (*mgtE*::mTn5) was greatly reduced in modified AMS containing 0.01 mM $MgSO_4$ (Fig 5.4). Growth of RU4107 (*mgtE*::mTn5) could be rescued by the addition of $MgSO_4$ (Fig 5.4) (2.5.3)

A plasmid containing *mgtE* was constructed to test whether *mgtE* could rescue growth of RU4107 (*mgtE*::mTn5) at pH 5.75 in Mg^{2+}-limited medium. Plasmid pJP2 was selected for the cloning of *mgtE* because it is highly stable and therefore could be used for *in planta*, in addition to growth complementation studies. Primers pr1240 and pr1265 were used to amplify a 1.6 kb fragment from Rlv3841 gDNA containing *mgtE*. The PCR product was subcloned into pJET1.2/blunt to make pLMB569. A *Xba*I/*Kpn*I fragment from pLMB569 containing *mgtE* was cloned into *Xba*I/*Kpn*I digested pJP2, yielding pLMB576 (pJP2*mgtE*). Plasmid pLMB576 (pJP2*mgtE*) was then conjugated into RU4107 (*mgtE*::mTn5) to make LMB481 (*mgtE*::mTn5 pJP2*mgtE*). As with Rlv3841, at pH 5.75 LMB481 (*mgtE*::mTn5 pJP2*mgtE*) could grow in modified AMS medium containing 0.01 mM $MgSO_4$ (Fig 5.4), demonstrating that *mgtE* can complement the growth of RU4107 (*mgtE*::mTn5).
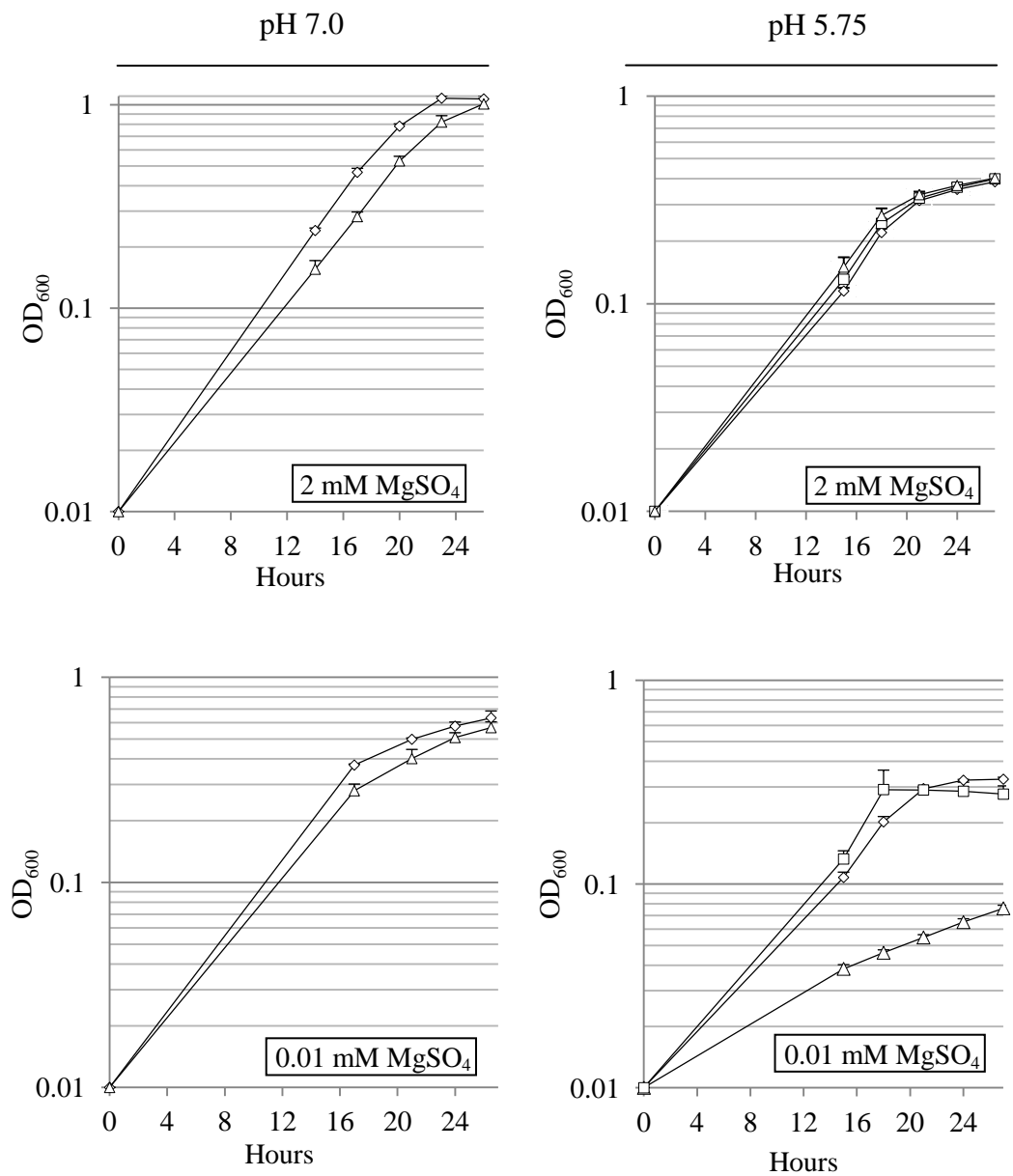
Fig 5.4 Growth of Rlv3841 [diamonds], RU4107 (*mgtE*::mTn5) [triangles] and LMB481 (*mgtE*::mTn5 pJP2*mgtE*) [squares] at pH 7.0 or pH 5.75 in modified AMS glucose containing 0.01 mM or 2 mM MgSO4. Averaged from three independent experiments ± SEM.

Microarrays that compared free-living Rlv3841 grown at pH 5.75 to cells grown at pH 7.0 have been conducted in the Philip Poole lab (unpublished) but expression of *mgtE* was not upregulated at pH 5.75 (Table 5.3). This implies that expression of *mgtE* is not regulated in response to pH.

Locus Tag	Putative Family	pH 5.75
mgtE	MgtE	1.0
RL2551	MgtE	0.6
RL0921	CorA	0.4
RL0964	CorA	1.6
pRL120701	CorA	0.7

Table 5.3 Fold-induction of Rlv3841 genes encoding putative Mg^{2+} channels in cells grown in minimal medium at pH 5.75 compared to cells grown pH 7.0. The highlighted row indicates the *mgtE* required for symbiosis on *P. sativum*.

5.2.3 RU4107 (*mgtE*::mTn5) forms bacteroids on *P. sativum*

To determine the stage at which bacteroid development of RU4107 (*mgtE*::mTn5) is impeded, *P. sativum* was inoculated with RU4107 (*mgtE*::mTn5). After three weeks, nodules containing RU4107 (*mgtE*::mTn5) were small and white, in contrast to the elongated, pink nodules containing Rlv3841. Dry weights revealed that nodules containing RU4107 (*mgtE*::mTn5) weighed <50% the weight of nodules containing Rlv3841 (Fig 5.5A) (2.6.8). Acetylene reduction assays suggest that N_2 fixation was <10% for RU4107 (*mgtE*::mTn5) compared to Rlv3841 and this could be complemented by plasmid pJP2*mgtE* (LMB481) (Fig 5.5B).
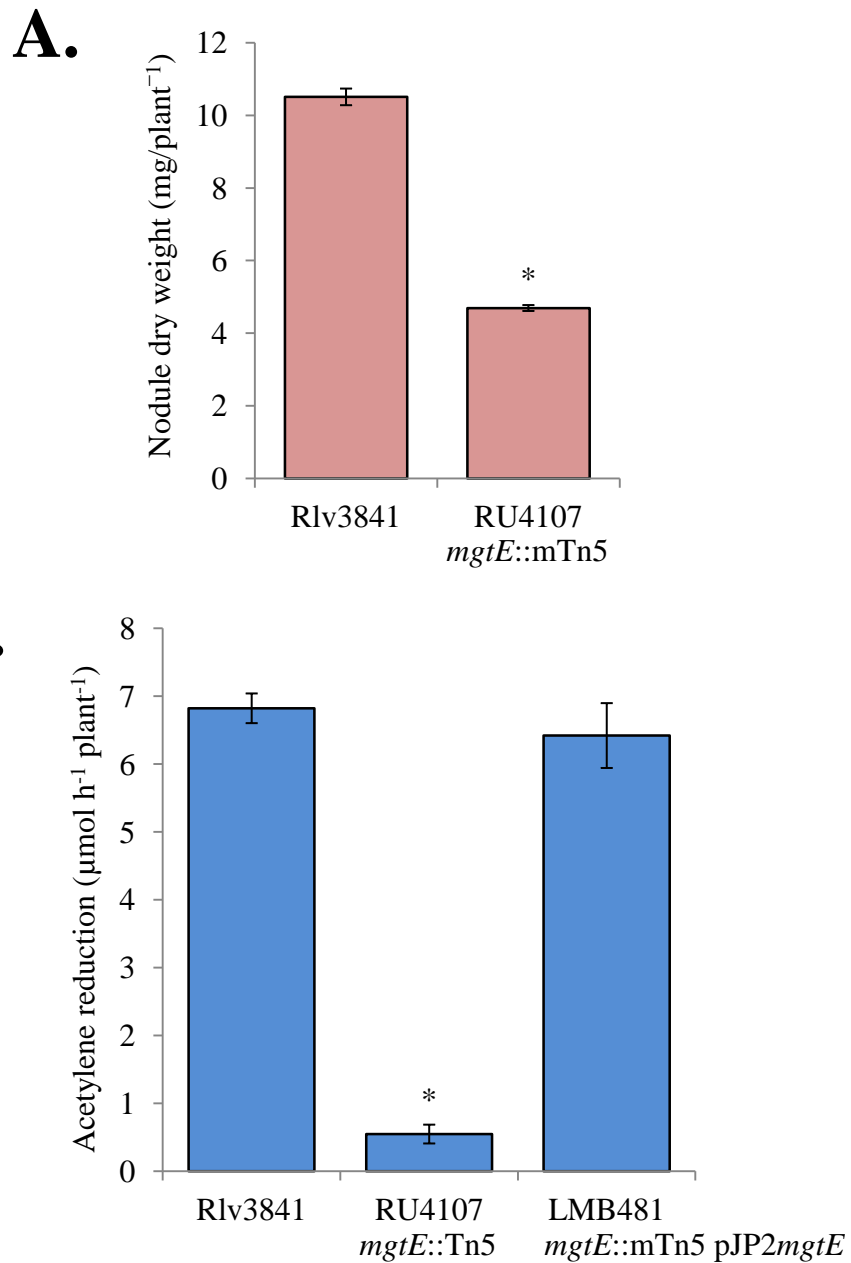
Fig 5.5 Nodule dry weights (A) and rates of acetylene reduction (B) for Rlv3841, RU4107 (*mgtE*::mTn5) or LMB481 (*mgtE*::mTn5 pJP2*mgtE*) on *P. sativum*. Averaged from forty-eight (A) or five (B) plants ± SEM. * indicates a statistically significant (p ≤ 0.05) difference relative to Rlv3841-inoculated plants.

Nodule sections revealed that bacteria carrying the *mgtE*::mTn5 mutation could infect plant cells but there was a higher proportion of uninfected plant cells relative to nodules containing Rlv3841 (Fig 5.6). Electron microscopy revealed that RU4107 (*mgtE*::mTn5) did form classical branch-shaped bacteroids, however, many of the RU4107 (*mgtE*::mTn5) bacteroids had accumulated poly-β-hydroxybutyrate (PHB) granules, in contrast to Rlv3841 bacteroids where PHB was mostly absent (Fig 5.7). This implies that RU4107 (*mgtE*::mTn5) bacteroids do not fully mature on *P. sativum* (Trainer and Charles, 2006; Terpolilli et al., 2012; Udvardi and Poole, 2013). Electron micrographs also show that those plant cells infected with RU4107 (*mgtE*::mTn5), contain fewer bacteroids relative to cells infected with Rlv3841 (Fig 5.7). Furthermore, by measuring dry weights (2.6.8), it was observed that the weight of RU4107 bacteroids/nodule dry weight measured ~30% less than Rlv3841 bacteroids (Fig 5.8).

Rlv3841   RU4107 (*mgtE*::mTn5)
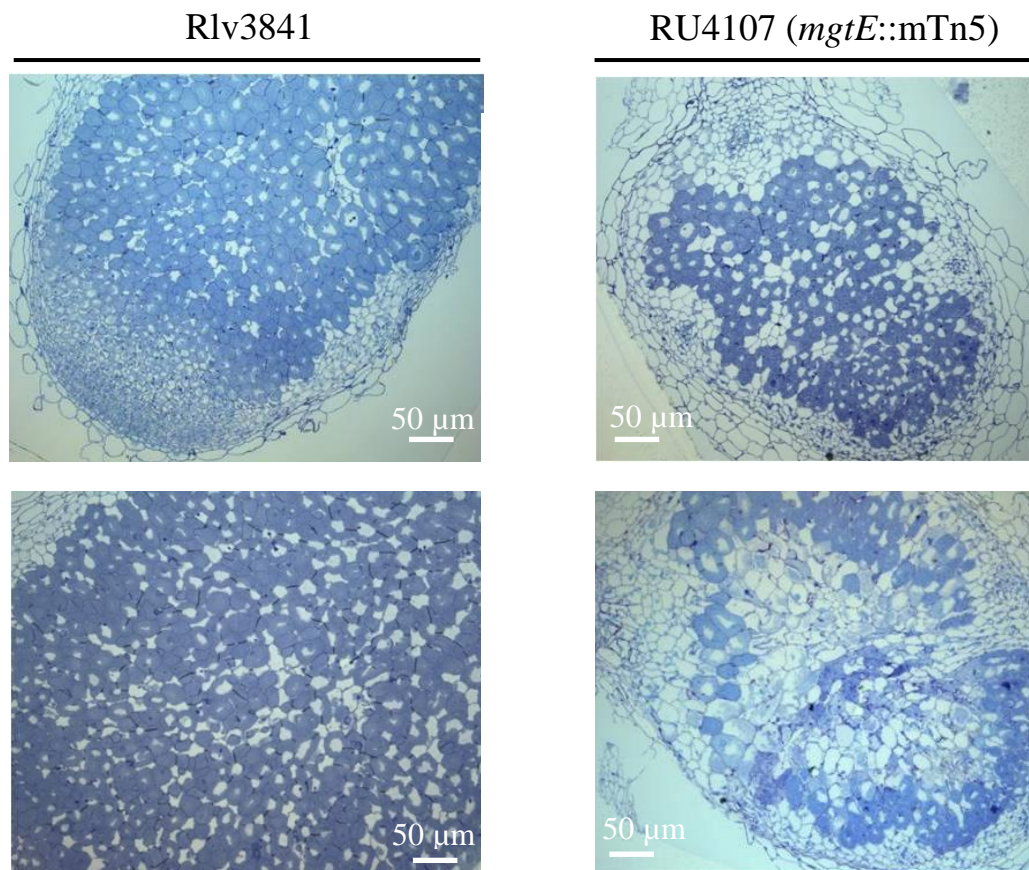
Fig 5.6 Sections of nodules taken from *P. sativum* inoculated with Rlv3841 or RU4107 (*mgtE*::mTn5). Sections stained with toluidine blue. Visualised by light microscopy at magnification x 10.
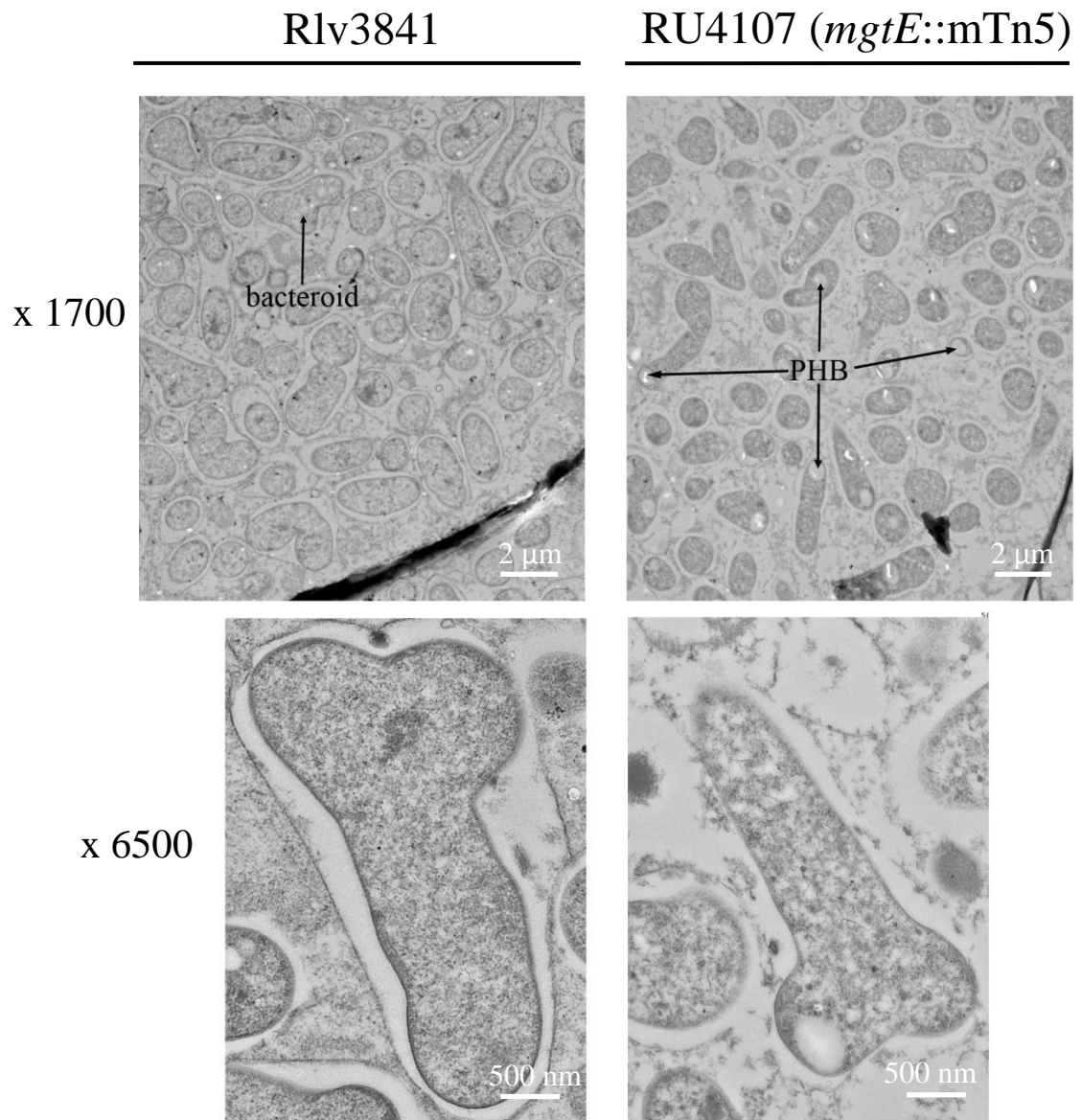
Fig 5.7 Ultrathin sections of nodules taken from *P.sativum* inoculated with Rlv3841 or RU4107 (*mgtE*::mTn5). Arrows indicate bacteroids or poly-β-hydroxybutyrate (PHB). Visualised by TEM at magnification x 1700 (top) or x 6500 (bottom).
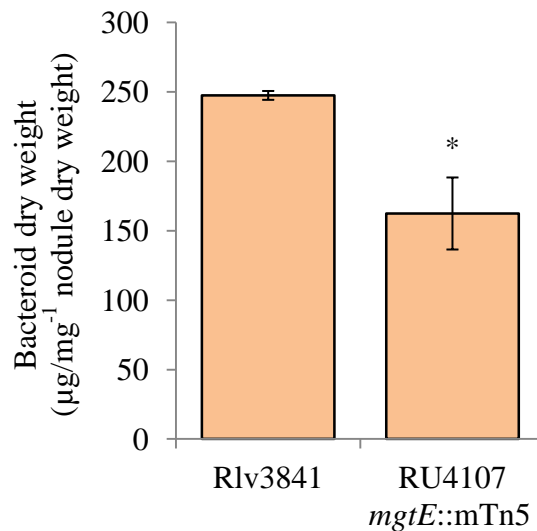
Fig 5.8 Dry weights of Rlv3841 and RU4107 (*mgtE*::mTn5) bacteroids isolated from *P. sativum* nodules. Averaged from forty-eight plants ± SEM. * indicates a statistically significant (p ≤ 0.05) difference relative to Rlv3841-inoculated plants.

P. sativum inoculated with RU4107 (*mgtE*::mTn5) were also grown for six weeks. After six weeks, plants inoculated with RU4107 (*mgtE*::mTn5) looked similar to uninoculated plants (Fig 5.9) and the shoots weighed a third of *P. sativum* inoculated with Rlv3841 (Table 5.4).
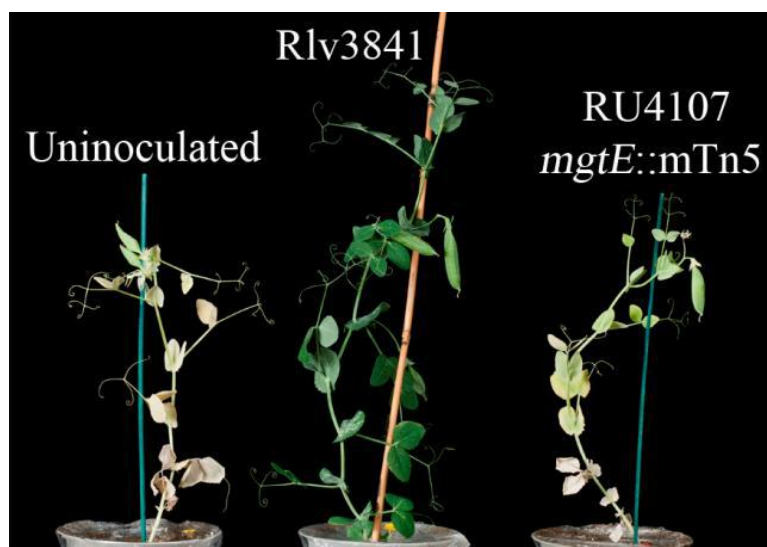
Fig 5.9 Photo showing (A) uninoculated, (B) Rlv3841-inoculated and (C) RU4107 (*mgtE*::mTn5)-inoculated *P. sativum*. All plants were grown for six weeks.

Inoculation	Shoot dry weight (g)
Uninoculated	0.87 ± 0.07
Rlv3841	3.0 ± 0.23
RU4107 (*mgtE*::mTn5)	1.0 ± 0.03

Table 5.4 Shoot dry weights for (A) uninoculated, (B) Rlv3841-inoculated and (C) RU4107 (*mgtE*::mTn5)-inoculated *P. sativum*. All plants were grown for six weeks. Averaged from ten plants ± SEM.

5.2.4 RU4107 (*mgtE*::mTn5) is symbiotically defective on *V. hirsuta* but not on *V. faba*

The symbiotic efficiency of RU4107 (*mgtE*::mTn5) was tested on other legumes within the host-range of Rlv3841 to determine whether the requirement of MgtE extends to other plant-hosts. On *V. hirsuta*, RU4107 (*mgtE*::mTn5) showed a similar phenotype to what was seen with *P. sativum* i.e. rates of acetylene reduction were <5% compared to Rlv3841 (Fig 5.10). Consequently, *V. hirsuta* inoculated with RU4107 (*mgtE*::mTn5) were small and showed signs of chlorosis (Fig. 5.11).

In contrast, *V. faba* plants inoculated with RU4107 (*mgtE*::mTn5) formed elongated, pink nodules and reduced acetylene at the same rate as Rlv3841 (Fig 5.12). Dry weights of *V. faba* nodules containing RU4107 (*mgtE*::mTn5) were similar to nodules containing Rlv3841 (Fig 5.13A) and the dry weight of RU4107 (*mgtE*::mTn5) bacteroids weighed the same as Rlv3841 bacteroids (per nodule dry weight) (Fig 5.13B). Six week *V. faba* inoculated with RU4107 (*mgtE*::mTn5) were indistinguishable, in both appearance (Fig 5.14) and shoot dry weight (Table 5.5), from *V. faba* inoculated with Rlv3841.
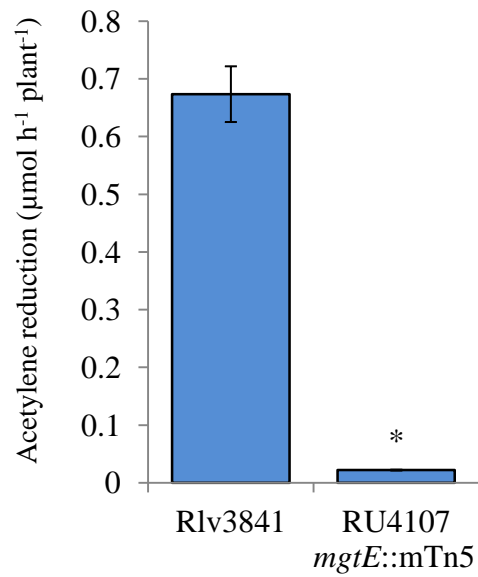
Fig 5.10 Rates of acetylene reduction for *V. hirsuta* inoculated with Rlv3841 or RU4107 (*mgtE*::mTn5). Averaged from twenty-four plants ± SEM. * indicates a statistically significant (p ≤ 0.05) difference relative to Rlv3841-inoculated plants.

Fig 5.11 Photo showing (A) uninoculated, (B) Rlv3841-inoculated and (C) RU4107 (*mgtE*::mTn5)-inoculated *V. hirsuta*. All plants were grown for three weeks.
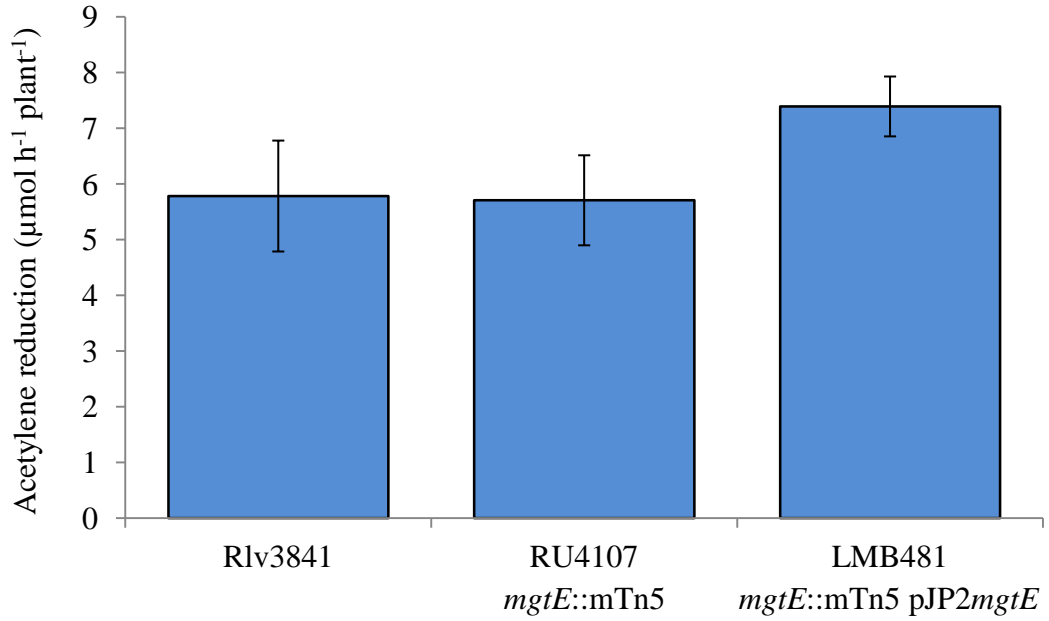
Fig 5.12 Rates of acetylene reduction for *V. faba* inoculated with Rlv3841, RU4107 (*mgtE*::mTn5) or LMB481 (*mgtE*::mTn5 pJP2*mgtE*). Averaged from five plants ± SEM.
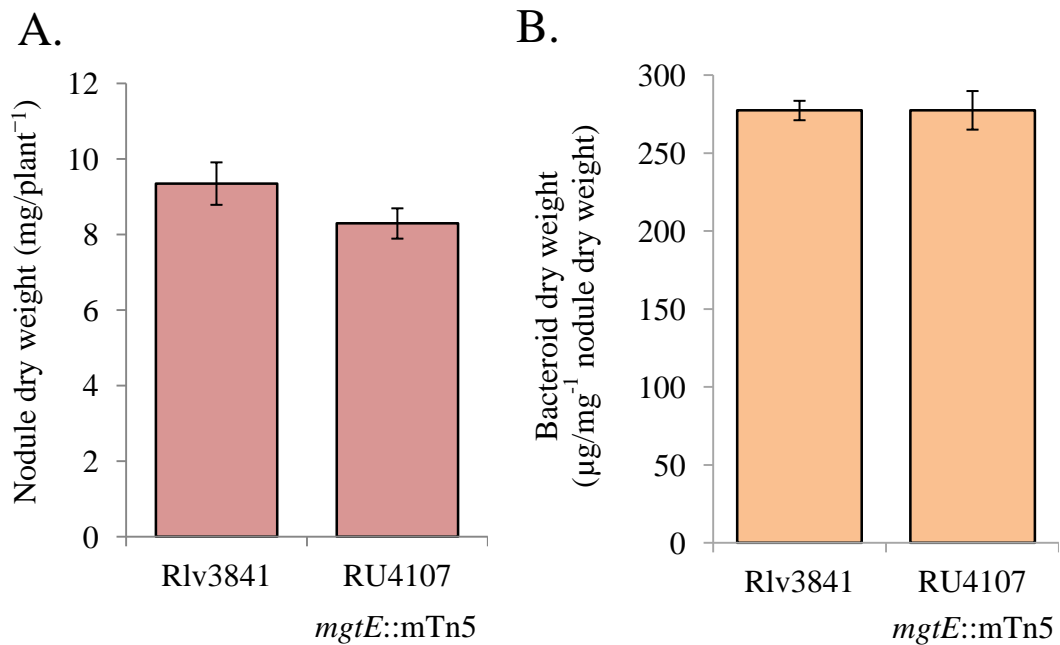
Fig 5.13 Dry weights of nodules (A) and bacteroids (B) from *V. faba* plants inoculated with Rlv3841, RU4107 (*mgtE*::mTn5) or LMB481 (*mgtE*::mTn5 pJP2*mgtE*). Averaged from 44-48 plants ± SEM.
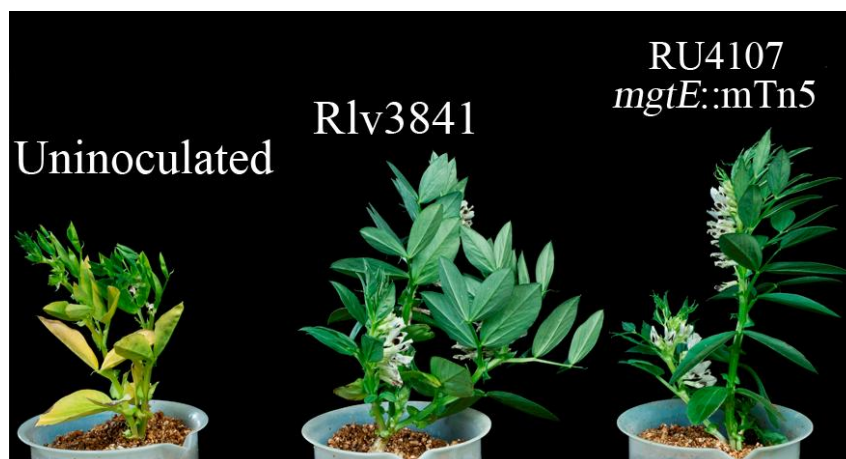
Fig 5.14 Photo showing (A) uninoculated, (B) Rlv3841-inoculated and (C) RU4107 (*mgtE*::mTn5)-inoculated *V. faba*. All plants were grown for six weeks.

Inoculation	Shoot dry weight (g)
Uninoculated	1.71 ± 0.13
Rlv3841	3.5 ± 0.33
RU4107 (*mgtE*::mTn5)	3.61 ± 0.22

Table 5.5 Shoot dry weights for (A) uninoculated, (B) Rlv3841-inoculated and (C) RU4107 (*mgtE*::mTn5)-inoculated *V. faba*. All plants were grown for six weeks. Averaged from ten plants ± SEM.

5.2.5 Quantification of Mg associated with bacteroids and plant cytosol from *P. sativum* and *V. faba* nodules

It was hypothesised that RU4107 (*mgtE*::mTn5) bacteroids in *P. sativum* nodules were starved of Mg^{2+} and that this caused the poor rates of acetylene reduction (Fig 5.5). Furthermore, RU4107 (*mgtE*::mTn5) bacteroids from *V. faba* were not starved of Mg^{2+}, explaining why no decrease in acetylene reduction was observed (Fig 5.12). A difference in the bioavailability of Mg^{2+} between *P. sativum* and *V. faba* nodules would explain this. To test these hypotheses, atomic absorption spectroscopy (AAS)

was used to quantify Mg levels associated with Rlv3841 and RU4107 (*mgtE*::mTn5) bacteroids isolated from both *P. sativum* and *V. faba* nodules. In addition, Mg was quantified in the plant cytosol of nodules formed on *P. sativum* and *V. faba*.

Three replicate samples were obtained for each inoculation where each sample was derived from nodules collected from 13-16 plants. Bacteroids were separated from the plant ctyosol by centrifugation and dry weights of both were measured (Table 5.6). The weighed bacteroid and plant cytosol fractions were then used to quantify Mg as described in 2.6.8.

	Weight of bacteroid sample (mg) ± SEM		Weight of plant cytosol sample (mg) ± SEM	
	Rlv3841	**RU4107**	**Rlv3841**	**RU4107**
P. sativum	41.6 ± 1	12.3 ± 2	126.5 ± 2	62.8 ± 1
V. faba	41.5 ± 3	33.6 ± 2 [a]	108 ± 6	87.4 ± 2 [a]

Table 5.6 Dry weights of bacteroid and plant cytosol samples used for AAS. Weights averaged from three independent samples, where each sample was derived from nodules taken from 13-16 plants.

[a] fewer *V. faba* inoculated with RU4107 (*mgtE*::mTn5) germinated [n= 13, 15, 16) relative to *V. faba* inoculated with Rlv3841 [n= 16, 16, 16), explaining the difference in sample weights.

Surprisingly, for bacteroids isolated from *P. sativum*, there was more Mg associated with RU4107 (*mgtE*::mTn5) than there was with Rlv3841 (per g^{-1} dried bacteroids) (Fig 5.15A). There was no difference between Mg levels associated with RU4107 (*mgtE*::mTn5) and Rlv3841 bacteroids isolated from *V. faba* (per g^{-1} dried bacteroid) (Fig 5.15A). A similar pattern was observed for the plant cytosol, as plant cytosol isolated from *P. sativum* nodules containing RU4107 (*mgtE*::mTn5) was associated with higher levels of Mg relative to the plant cytosol isolated from nodules containing Rlv3841 (per g^{-1} dried plant cytosol) (Fig 5.15B). Again, no difference was observed for *V. faba* (per g^{-1} dried plant cytosol) (5.15B). It was also observed

that there were lower amounts of Mg associated with both bacteroids and plant cytosol isolated from *V. faba* relative to *P. sativum* (per g^{-1} dried nodule) (Fig 5.15).
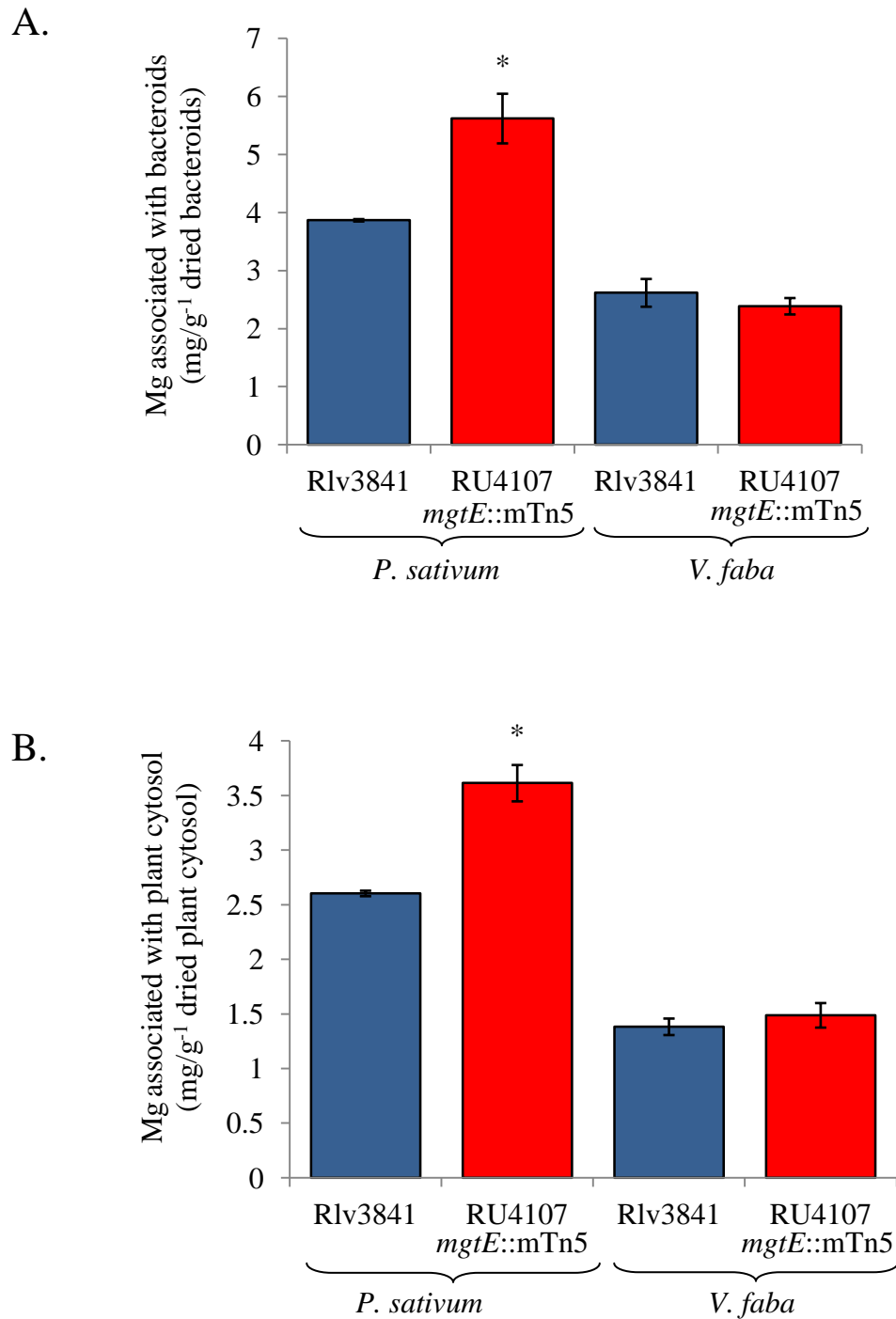
A.

B.

Fig 5.15 Quantification of Mg associated with (A) bacteroids and (B) plant cytosol isolated from nodules formed on *P. sativum* or *V. faba* inoculated with Rlv3841 (blue bars) or RU4107 (*mgtE*::mTn5) (red bars). Averaged from three samples ± SEM. * indicates a statistically significant (p ≤ 0.05) difference relative to sample isolated from nodules containing Rlv3841.

5.3 DISCUSSION

The ability of RU4107 (*mgtE*::mTn5) to grow in medium limited for Mg^{2+} depended on pH (Fig 5.4), implying that MgtE is sensitive to changes in pH. MgtE may be similar to KcsA, a channel for potassium-transport, in the way it is regulated by pH (Hirano et al., 2011). The model for pH-regulated gating of KcsA relies on electrostatic charges between clusters of charged amino acids. Upon a lowering of the pH, these clusters become positively charged, causing a repulsion that brings about a conformational change in the ion-conducting pore (Fig 5.16). Clusters important to regulating the gating of the KcsA in response to pH have been located at both the transmembrane and cytoplasmic domains of KcsA (Hirano et al., 2011). Alternatively, a lowering of the pH might increase the demand for Mg^{2+}, for example, the requirement of MgATP to energise proton pumps (P-type ATPases and F-ATPases) needed to maintain the intracellular pH. It is feasible that a change in pH might alter the availability of free-Mg^{2+}, however, a decrease in pH would favour the release of Mg^{2+} from metabolites (Igamberdiev and Kleczkowski, 2011) and therefore cannot explain the poor growth of RU4107 (*mgtE*::mTn5) at low pH. It should also be noted that a buffer was not used in growth experiments conducted at low pH (Fig 5.4) and that, although it was measured prior, pH was not measured after the experiment. Consequently, although a strong phenotype was observed for RU4107 (*mgtE*::mTn5), the experiment does need to be repeated with an appropriate buffer and the pH should be measured after the experiment to confirm that the pH of the medium has not changed.

MgtE is essential for efficient symbiosis with *P. sativum* and *V. hirsuta* (Figs 5.5 and 5.10) but not on *V. faba* (Fig 5.12). Three possible explanations for this are (1) there is a difference in the requirement of Mg^{2+}, (2) the activity of other Mg^{2+} transporters differs between hosts or (3) there is a difference in the bioavailability of Mg^{2+}. It is unlikely that bacteroids from *P. sativum* and *V. faba* differ in their requirement for Mg^{2+} because it is fundamental for N_2 fixation and many other cellular processes. The functionality of other putative Mg^{2+} importers (Table 5.2) might be the cause if the environment provided by *P. sativum* and *V. hirsuta* nodules is different from *V. faba* nodules. For example, if the nodules from *V. faba* provide a less acidic

environment than nodules from *P. sativum*, the requirement for a low pH Mg^{2+} transporter would be less and the functionality of other Mg^{2+} importers might be higher. Proving this would involve testing the functionality of the other putative Mg^{2+} importers encoded by Rlv3841 (Table 5.2) at range of pH levels.
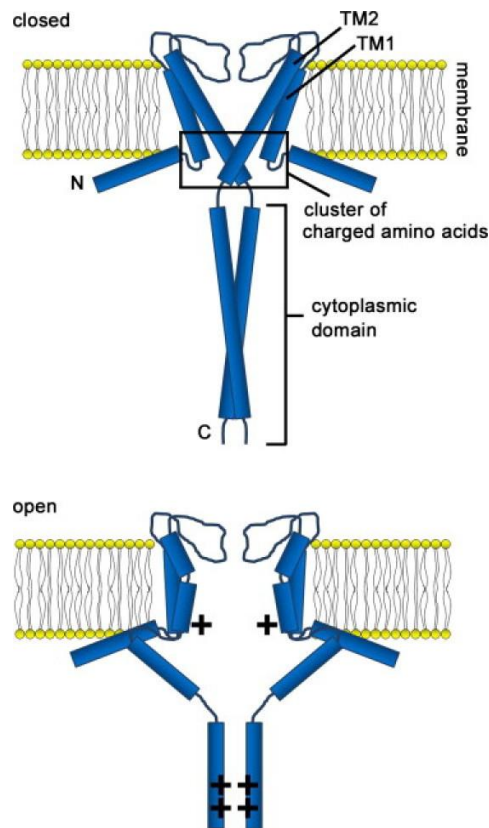
Fig 5.16 Model for pH-dependent gating of KcsA. At pH 7.0 (top), the cytoplasmic domains and the cluster of charged amino acids situated between the transmembrane domains have a neutral charge, resulting in a closed formation of the channel. At pH 4.0 (bottom), the cytoplasmic domains and the cluster of charged amino acids, become positively charged, causing a repulsion that opens the channel. Reproduced from Hirano *et al*., 2011.

A difference in the bioavailability of Mg^{2+} would be an obvious explanation for the contrasting phenotypes but less Mg was found to be associated with the plant cytosol isolated from *V. faba* relative to *P. sativum* (per g^{-1} dried plant cytosol) (Fig 5.15B). This however, does not disprove the bioavailability hypothesis as the difference in the bioavailability of Mg^{2+} could be specifically localised to the symbiotic space.

Such an occurrence could arise from a plant-encoded Mg^{2+} transporter located in the symbiosome membrane, which would supply the enclosed bacteroids with Mg^{2+}. This transporter would have to be present in *V. faba* but not in *P. sativum* or *V. hirsuta*. Several plant-encoded, nodule-specific transporters have been identified and supply bacteroids with metal ions (Moreau et al., 2002; Kaiser et al., 2003; Hakoyama et al., 2012). Furthermore, AAS does not show how much Mg is freely available. The concentration of Mg^{2+} in plant tissues has been reported to be around 10 mM, however, much of this Mg^{2+} is complexed with metabolites; as a result, the steady cytosolic concentration of free-Mg^{2+} could be as low as 0.2-0.4 mM (Igamberdiev and Kleczkowski, 2001, 2011). Thus, although there is more Mg in *P. sativum* nodules, *V. faba* nodules could still contain more Mg^{2+} that is freely-available to bacteroids.

Intriguingly, *P. sativum* nodules containing RU4107 (*mgtE*::mTn5) bacteroids had higher levels of Mg associated with the plant cytosol (per g^{-1} dried plant cytosol) relative to nodules containing Rlv3841 (Fig 5.15B). If correct, the plant may be delivering more Mg^{2+} to the inefficient nodules, which may be specific to RU4107 (*mgtE*::mTn5) or a general feature of ineffective symbiosis. However, the data could be misleading; the nodules taken from *P.sativum* inoculated with RU4107 (*mgtE*::mTn5) had a lower mass relative to nodules containing Rlv3841 (Fig 5.5A). Thus, caution should be taken when comparing the two.

It was predicted that the symbiotically-defective RU4107 (*mgtE*::mTn5) bacteroids on *P. sativum* were starved of Mg^{2+}, however, more Mg was found associated with RU4107 (*mgtE*::mTn5) than with Rlv3841 bacteroids (per g^{-1} dried bacteroid) (Fig 5.15A). If correct, this would imply that the requirement of MgtE during symbiosis is independent of its ability to import Mg^{2+}. Phenotypes caused by the disruption of *mgtE* in other bacteria have been found to be independent of the cell's ability to import Mg^{2+}. In *P. aeruginosa*, disruption of *mgtE* led to increased cytotoxicity in epithelial cells (Anderson et al., 2008). Further investigation revealed this was due to the induction of genes encoding for the type III secretion system (T3SS). Intriguingly, the authors proposed that modulation of T3SS expression by MgtE was independent of the transport function of MgtE, as MgtE variants defective for Mg^{2+} transport (where MgtE was altered at its Mg^{2+} binding sites) could still complement

the cytotoxicity effect (Anderson et al., 2010). Similarly, disruption of *corA* in *S. enterica* attenuated virulence but this loss of virulence was found to be independent of intracellular Mg^{2+} levels (Papp-Wallace and Maguire, 2008). Therefore, further work is required to determine whether the requirement of MgtE on *P. sativum* and *V. hirsuta* is dependent on its transport function or dependent on an unknown function of MgtE. An additional role of MgtE could depend on the presence of the CBS pair within the cytosolic region. In addition to ion channels, CBS-containing proteins have been found to interact with thioredoxins and consequently, are important to cellular redox homeostasis; for example, the chloroplast-localised CBS-containing protein CBSX1 was found to regulate H_2O_2 levels via thioredoxin-interactions (Yoo et al., 2011). Alternatively, it is likely that there was some contamination of the bacteroid samples with Mg from the plant cytosol sticking to the EPS and LPS on the bacterial surface. Therefore, the higher levels of Mg in RU4107 (*mgtE*::mTn5) bacteroids could be explained by the higher levels of Mg in the plant cytosol of nodules containing RU4107 (*mgtE*::mTn5) bacteroids (Fig 5.15B).

Nevertheless, *mgtE* has been shown to encode a Mg^{2+} importer that is required for N_2 fixation on some but not all legumes compatible with Rlv3841. Along with the Mn^{2+} transporters studied in Chapter four, there are now two examples of the requirement of metal transporters differing between legume-hosts.

Chapter 6: *Switching on Genes Required for N₂ Fixation*

6.1 INTRODUCTION

6.1.1 O_2-responsive regulators

There is a multitude of regulators in bacteria that utilise either a [4Fe-4S] cluster or haem to sense O_2 (Green et al., 2009). The sensory domain of FNR (Fumarate and Nitrate Reduction) for example, contains essential cysteine residues that coordinate a [4Fe-4S] cluster (Sutton et al., 2004). In the absence of O_2, the $[4Fe-4S]^{2+}$ cluster permits dimerisation of FNR, which is optimal for the regulatory domain to bind DNA. In the presence of O_2 however, the $[4Fe-4S]^{2+}$ is converted to $[2Fe-2S]^{2+}$, causing a conformational change in FNR that promotes the inactive-monomeric state (Moore and Kiley, 2001; Moore et al., 2006; Jervis and Green, 2007). FNR has been characterised in *R. leguminosarum* and *R. etli* where it is encoded by *fnrN* (Gutierrez et al., 1997; Colombo et al., 2000; Clark et al., 2001; Lopez et al., 2001; Boesten and Priefer, 2004; Moris et al., 2004; Granados-Baeza et al., 2007).

A second type of O_2-responsive regulator is FixL, which consists of a C-terminal transmitter domain and a N-terminal sensory component that is dependent upon an O_2-sensing haem contained within a PAS domain (Taylor and Zhulin, 1999; Green et al., 2009). The presence of O_2 can change the co-ordination state of the Fe atom within the haem and subsequently cause a conformational change in FixL. Only in the absence of oxygen does the conformation of FixL allow autophosphorylaiton of its C-terminal transmitter domain (Tuckerman et al., 2001).

A less well-characterised O_2-responsive regulator is NifA, an enhancer-binding protein that, in conjunction with σ^{54}, activates the transcription of *nifHDK* and other genes required for N₂ fixation (Salazar et al.; Bobik et al., 2006; Hauser et al., 2007; Sullivan et al., 2013). In *B. japonicum*, NifA is directly inactivated by O_2 and subsequently degraded (Morett et al., 1991). Conserved cysteine residues and metal

ions, Fe^{2+} in particular, are essential for NifA-activity (Fischer et al., 1988; Morett et al., 1991; Dixon and Kahn, 2004). In *S. meliloti*, NifA has also been shown to be sensitive to O_2 and degraded upon inactivation (Huala and Ausubel, 1989). In *E. coli*, degradation of inactive *S. meliloti* NifA was found to be dependent on Lon protease (Huala et al., 1991).

6.1.2 Regulation of *fixNOPQ*

The nodule provides a low O_2-environment to enable O_2-sensitive nitrogenase to function. To maintain respiration under low O_2, rhizobia synthesise a cytochrome cbb_3 terminal oxidase, encoded by *fixNOPQ* and assembled by FixGHIS. The number of copies and regulation of *fixNOPQ* differs between rhizobia but activation typically requires FixL, FnrN or both. Regulation of *fixNOPQ* also involves CRP/FNR homologues, termed FixK, that act downstream of FixL and FnrN (Terpolilli et al., 2012).

In *S. meliloti*, expression of *fixNOPQ* is regulated by a FixLJ-FixK regulatory cascade (Fig 6.1). In the absence of oxygen, the membrane-anchored FixL autophosphorylates and subsequently phosphorylates the receiver domain of the transcriptional regulator, FixJ (Lois et al., 1993). Phosphorylation promotes dimerisation of FixJ, disrupting the inhibitory interface between the receiver domain and the transcriptional activator domain (Da Re et al., 1999). Activated FixJ~P then induces the expression of *fixK* and FixK activates expression of *fixNOPQ*. Consequently, disruption of either *fixL* or *fixK* in *S. meliloti* caused a Fix⁻ phenotype on *M. sativa* (Forrai et al., 1983; David et al., 1988; Virts et al., 1988; Batut et al., 1989; Terpolilli et al., 2012).

The *fixNOPQ* operon in *A. caulinodans* is also regulated by a FixLJ-FixK cascade (Fig 6.1). As with *S. meliloti*, mutation of either *fixL* or *fixK* in *A. caulinodans* prohibited symbiotic-N_2 fixation on *Sesbania rostrata* and also N_2 fixation in free-living cells (Kaminski and Elmerich, 1991; Kaminski et al., 1991).

Fig 6.1 Regulation of *fixNOPQ* in *S. meliloti* and *A. caulinodans*. Grey arrows represent genes, black arrows denote DNA binding, blue arrows indicate transcription, +/- specifies positive/negative regulation and dotted arrows show phosphorylation.

Regulation of the *fixNOPQ* operon in *B. japonicum* is under the control of a FixLJ-FixK$_2$ cascade. Unlike the membrane-anchored FixL in *S. meliloti*, FixL from *B. japonicum* lacks the transmembrane segments and is cytosolic as a consequence (Gilles-Gonzalez et al., 1994; Rodgers, 1999). In addition to being transcriptionally regulated by FixJ~P, FixK$_2$ is post-translationally regulated by ROS, where the oxidation of a critical single cysteine residue near the DNA-binding domain causes its inactivation (Mesa et al., 2009). This post-translational control might prevent FixK$_2$-activating *fixNOPQ* and other symbiotic genes prematurely (e.g. in the infection thread where ROS are present) and also cause the shutdown of symbiotic processes during senescence (when ROS are also present). Disruption of *fixL* or *fixK$_2$* caused a severe reduction (90-99%) in N$_2$ fixation (Anthamatten and Hennecke, 1991; Nellen-Anthamatten et al., 1998).

Fig 6.2 Regulation of *fixNOPQ* in *B. japonicum*. Grey arrows represent genes, black arrows denote DNA binding, blue arrows indicate transcription, +/- specifies positive/negative regulation and dotted arrows show phosphorylation.

Studies suggest that in *R. etli* CFN42, two parallel pathways, governed by FixL and FnrN, regulate expression of the two *fixNOPQ* operons (Fig 6.3) (Granados-Baeza et al., 2007). There is no FixJ in *R.* etli so FixL regulates expression of *fixK* via FxkR, a regulator that belongs to the OmpR/PhoB family (Zamorano-Sanchez et al., 2012). FixL post-translationally regulates FxkR but it is not known whether a phoshorelay is involved. FxkR is required for microaerobic expression of both *fixNOPQ* operons (Girard et al., 2000; Zamorano-Sanchez et al., 2012). In the second pathway, expression of *fixNOPQ* is regulated by two FNR-regulators, FnrNchr (encoded on the chromosome) and FnrNd (encoded on the symbiotic plasmid) (Lopez et al., 2001; Terpolilli et al., 2012). Under low oxygen, *fixNOPQ*d expression is under the positive control of FnrNchr (and also FnrNd to a lesser extent). A severe reduction in N$_2$ fixation was only seen when *fixL, fnrN*chr and *fnrN*d were mutated in the same background (Lopez et al., 2001). There is also a degree of crosstalk between these regulators, which is reviewed in Terpololli *et al.*, 2012.
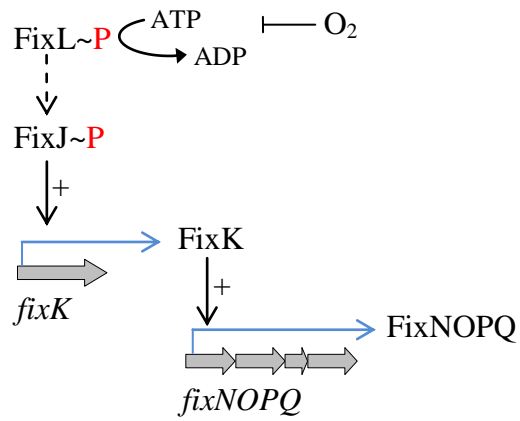

Fig 6.3 Regulation of *fixNOPQ*d and *fixNOPQ*f in *R. etli*. Grey arrows represent genes, black arrows denote DNA binding, blue arrows indicate transcription, +/- specifies positive/negative regulation and dotted arrows show phosphorylation.

Regulation of the both *fixNOPQ* operons in *R. leguminosarum* bv. viciae VF39 might also be dependent on both FixL and FnrN (Fig 6.4) (Schluter et al., 1997). As in *R. etli*, there is no FixJ but there is a FxkR-orthologue that was able to complement the loss of *fxkR* in a *R. etli* background (Zamorano-Sanchez et al., 2012). FixL is required for induction of *fnrN* and *fixNOPQ* under O_2 limitation (Schluter et al., 1997; Boesten and Priefer, 2004). Single mutations in *fixL* and *fixK* resulted in a Fix$^+$ phenotype, whereas disruption of *fnrN* caused a ~70% reduction in N_2 fixation (Colonna-Romano et al., 1990; Patschkowski et al., 1996). When *fixK* and *fnrN* are disrupted in the same background, a Fix$^-$ phenotype was observed (Patschkowski et al., 1996). However, the phenotype of a *fixL fnrN* double mutant was never reported in *R. leguminosarum*, leaving uncertainty about the requirement of FixL.
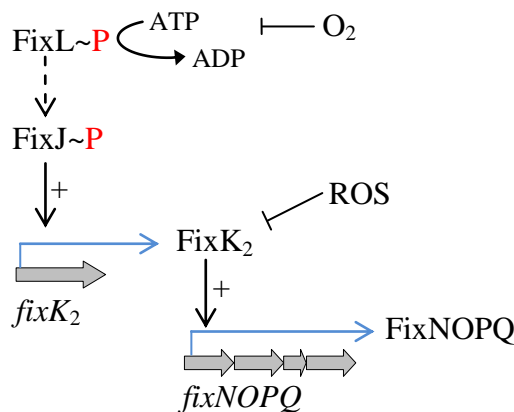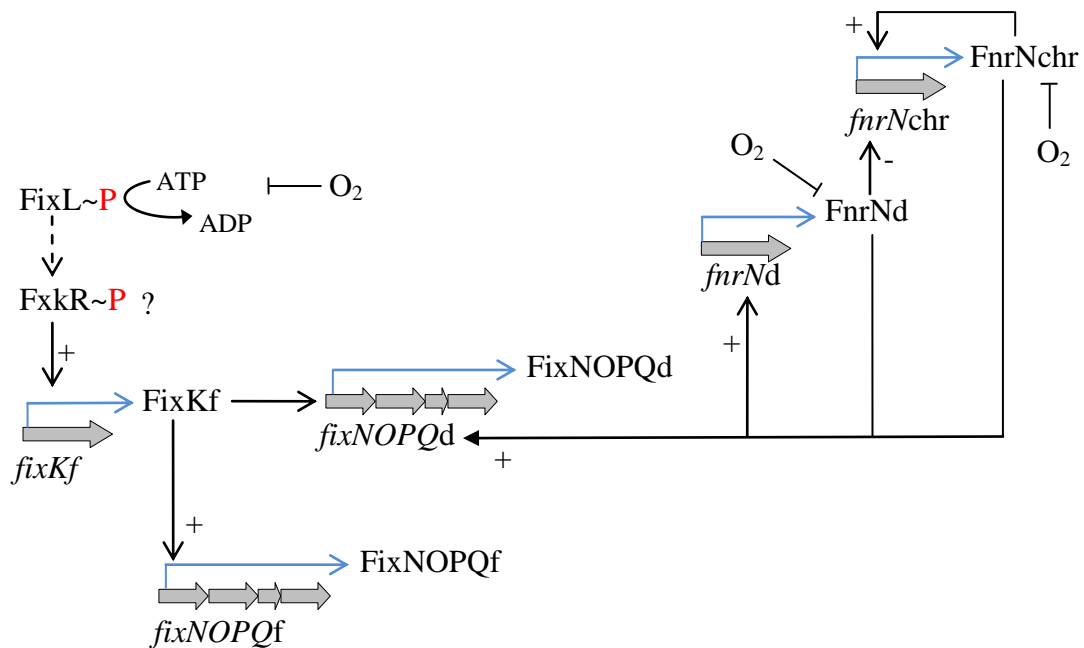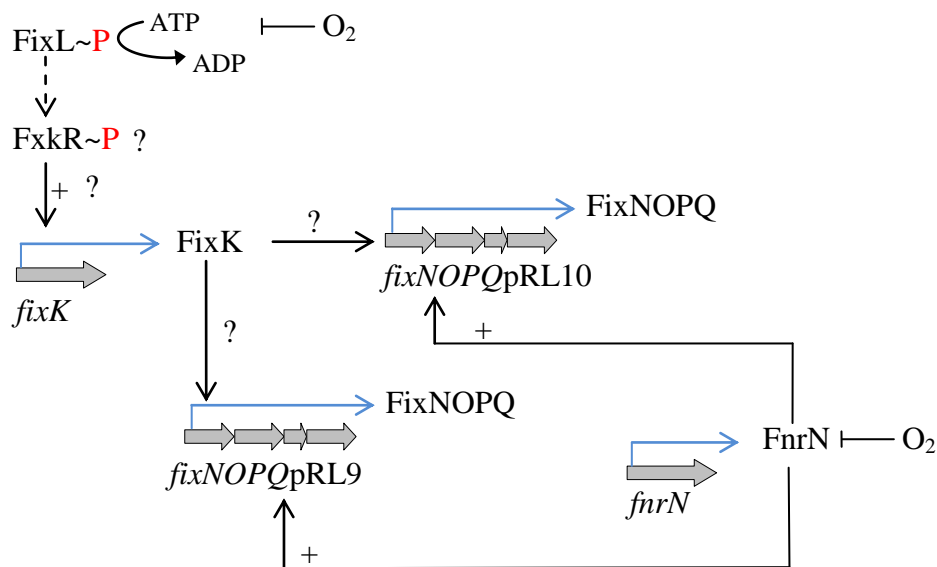

Fig 6.4 Incomplete model showing regulation of *fixNOPQ*pRL9 and *fixNOPQ*pRL10 in *R. leguminosarum*. Grey arrows represent genes, black arrows denote DNA binding, blue arrows indicate transcription, +/- specifies positive/negative regulation and dotted arrows show phosphorylation.

6.2 RESULTS

6.2.1 Identification and expression of three *fixK*-like regulators, *fnrN* and two *fixL*-homologues in Rlv3841

The Rlv3841 genome (Young et al., 2006), BLAST (Altschul et al., 1990) and a comparative genomic analysis conducted by Dufour *et al* 2010, were used to identify putative regulators of the *fixNOPQ* operons in Rlv3841 (Table 6.1). Three CRP/FNR regulators belonging to the FixK subfamily were identified and provisionally annotated FixK, FixKb and FixKc, where pRL90019 encodes the FixK characterised in *R. leguminosarum* bv. viciae VF39 (Patschkowski et al., 1996; Li et al., 2003; Dufour et al., 2010). The gene encoding FixKb (pRL90025) is also located on pRL9 and is proximal to the *fxkR*-orthologue, whereas the gene encoding FixKc (RL1880), is located on the chromosome, upstream of a *fixL*-homolgue (Fig 6.5). The FixL-homologue has been provisionally annotated FixLc (where c denotes chromosome) as it shares 57% amino acid identity with FixL (Fig 6.6) and contains the conserved PAS domain, haem binding pocket, histidine kinase domain and C-terminal receiver domain (Marchler-Bauer et al., 2011). However, FixKb (pRL90025), FixLc (RL1879) and FixKc (RL1880) were shown not to be essential for N_2 fixation on *P. sativum* (Table 3.8).

Two other regulators in Rlv3841 that belong to the CRP/FNR family, StoR10 and StoR9 (see Table 6.1), are orthlogues of StroRd and StoRf in *R. etli* (Granados-Baeza et al., 2007). In *R. etli*, both are involved in negative regulation of the two *fixNOPQ* operons but may also have additional roles as disruption of *stoR*d causes an increase in N_2 fixation, while disruption of *stoR*f caused a reduction in N_2 fixation (Granados-Baeza et al., 2007).

Once identified, expression of the putative regulators of *fixNOPQ* were examined in developing bacteroids (Karunakaran et al., 2009) and at pH 5.75 (unpublished data from the Philip Poole lab) (Table 6.1). Expression of both *fixL*-homologues and their neighbouring *fixK* genes was upregulated during bacteroid development (Karunakaran et al., 2009), implying that synthesis of the cytochrome cbb_3 terminal

oxidase is an early feature of nodule colonisation. Intriguingly, all three *fixK*-like genes and both *fixL*-homologues were also upregulated at pH 5.75, suggesting that low pH could be another signal for the switch on of N_2 fixation.

Gene Designation	Locus Tag	Product	7d bacteroid	21d bacteroid	pH 5.75
fixL	pRL90020	FixL	2.6	0.8	2.4
fixK	pRL90019	FixK	15.8	2.4	50.4
fixN	pRL90018	FixN	21.9	38.1	1.7
fixO	pRL90017	FixO	47.8	54.7	1.6
fixP	pRL90016A	FixP	49.6	53.3	1.8
fixQ	pRL90016	FixQ	67.4	63.9	1.0
fixG	pRL90015	FixG	18.7	9.3	1.4
fixH	pRL90014	FixH	11.3	4.1	1.3
fixI	pRL90013	FixI	9.4	3.2	1.1
fixS	pRL90012A	FixS	18.7	8.7	1.0
*stoR*9	pRL90012	Putative StoR	11.5	4.6	0.9
fxkR	pRL90026	FxkR	0.5	0.5	0.5
fixKb	pRL90025	Putative FixK	5.4	1.0	38.7
fixN	pRL100205	FixN	80.4	119.7	1.5
fixO	pRL100206	FixO	65.8	69.3	1.1
fixP	pRL100206A	FixP	39.9	71.3	1.1
fixQ	pRL100207	FixQ	87.7	85.3	0.8
fixG	pRL100208	FixG	5.5	3.5	1.6
fixH	pRL100209	FixH	19.9	5.0	1.1
fixI	pRL100210	FixI	5.9	1.8	0.9
fixS	pRL100210A	FixS	9.5	13.8	1.0
*stoR*10	pRL100211	Putative StoR	8.7	3.5	0.9
nifA	pRL100196	NifA	11.6	11.9	5.4
fnrN	RL2818	FnrN	13.4	4.9	1.7
*fixL*c	RL1879	Putative FixL	3.2	1.5	3.3
*fixK*c	RL1880	Putative FixK	3.3	1.6	9.1

Table 6.1 Genes encoding putative regulators of *fixNOPQ* and *fixGHIS* operons in Rlv3841. Values for 7d bacteroid and 21d bacteroid correspond to fold-induction of genes in Rlv3841 isolated from nodules 7 and 21 dpi relative to free-living cells grown in minimal medium (Karunakaran et al., 2009). Values for pH 5.75 correspond to fold-induction of genes in Rlv3481 grown in minimal medium at pH 5.75 relative to Rlv3841 grown at pH 7.0 (unpublished data from the Philip Poole lab). Green highlights genes >3-fold upregulated.
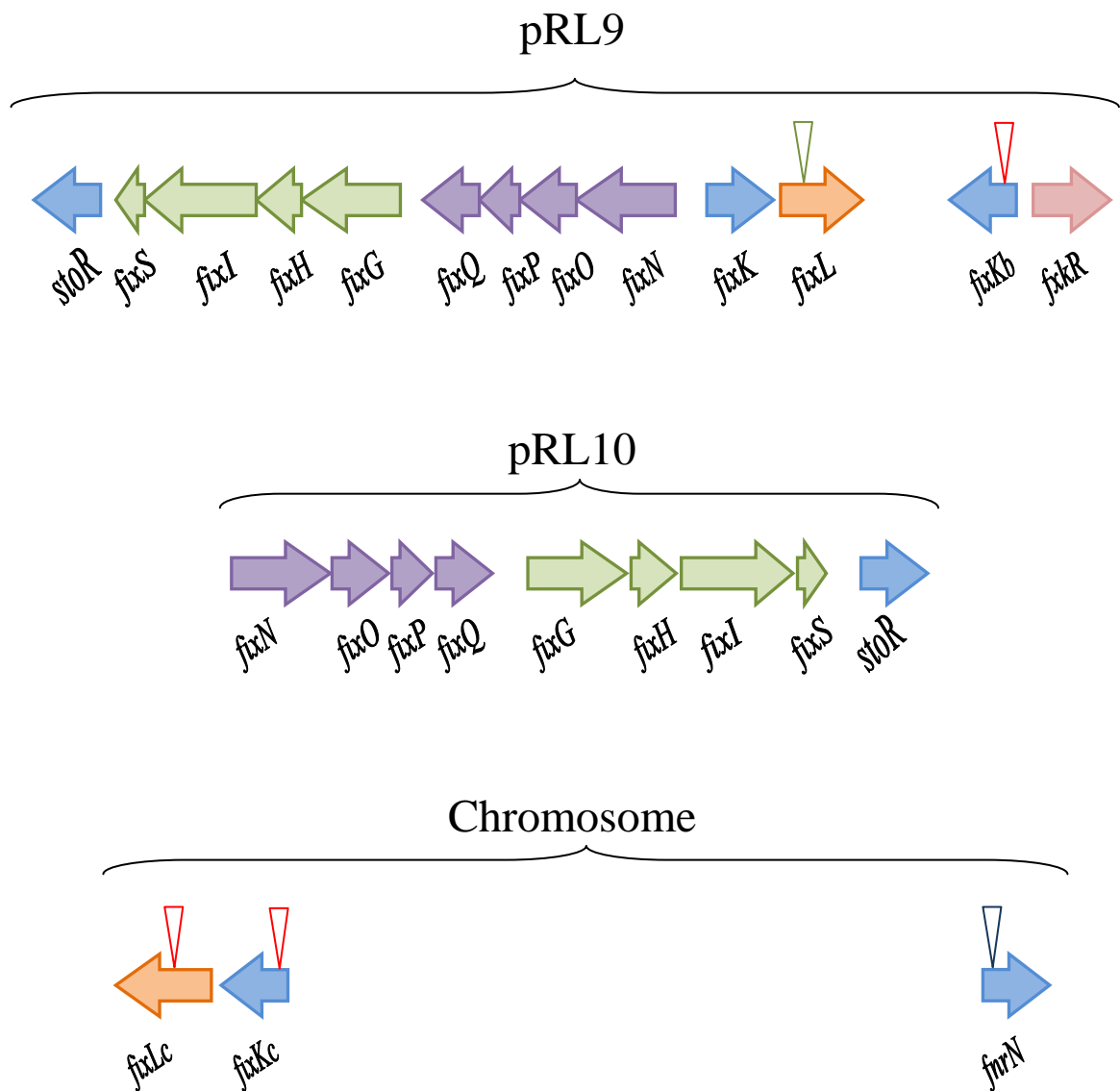
Fig 6.5 Maps showing the location of *fix* genes located on pRL9, pRL10 and the chromosome. Purple arrows represent genes encoding the cytochrome *cbb₃* terminal oxidase, green arrows represent genes encoding the assembly system for the terminal oxidase, blue arrows represent genes encoding regulators belonging to the CRP/FNR family, orange arrows represent genes encoding FixL and pink arrow represents the gene encoding for FxkR. Red, green or blue triangles indicate genes that have been mutated by pK19mob integration, ΩSpc or ΩTc mutagenesis (respectively).

```
CLUSTAL 2.1 multiple sequence alignment


FixL      MPHRLVSPRTVSSHELDAMVHVLDGADILIHRFDGTITHWSIGCENMYGW 50
FixLc     -----MVEHATSETDLDRIVRMFDGANLIVHGFDGVIQRWTSGCEQLYGW 45
               :  ::.*. :** :*:::***:::* ***.* :*: ***::***


FixL      AREEAIGEKVHELLATQFPEPVENIRDQLKSRGSWQGETTHRHKSGHDIH 100
FixLc     SASEAVGNVVHDLLDTQFPAGVEELRTEVRDKGFWTGQVGHRRKDGVRLA 95
           : .**:*: **:** **** **::* :::.:* * *:. **:*.*   :


FixL      VASRYVLVNLPDGDLAVIETNSDVSALKRSQEVVKSREAHLSSILDTVPD 150
FixLc     IVTRWTVLELGDPDTLIIQSNNDVTLMQQVGDELRERQAHLQSILATVPD 145
          :..:*:.:::* * *   :*::*.**: :::   : ::.*:***.*** ****


FixL      AMVVIDDKGVVLSFSKAAEKLFGMSSEQICGRNVSNLMPNPYRDAHDGYI 200
FixLc     AMIVIDDKGCIASFSTAAEKLFGYSADEAIGQNVSMLMPSPDREAHDGYL 195
          **:****** : ***.******* *:::   *:*** ***.* *:*****:


FixL      DHYLDTGEKRIIGYGRVVTGQRADGSQFPMELHVGEATANGERIFTGFVR 250
FixLc     DSYIRTGRRRIIGYGRVVVGLRKHGTTFPMELSVGEAVAGGKRTFTGFVR 245
          * *: **.:**********.* * .*: ***** ****.*.*:* ******


FixL      DLTSRYKIEEDLRQSQKMEAVGQLTGGIAHDFNNLLTVISGNLEMIEDKL 300
FixLc     DLTSRHRIEAELRQSQKMEAVGQLTGGLAHDFNNLLAVIIGNLEMLEARL 295
          *****::** :*****************:********:** *****:* :*


FixL      PPGNLREILGEAQAAAADGAVLTAQLLAFGRRQPLNPKRADLGQLVSGFS 350
FixLc     AEPGQLSLLREAQSAADDGARLTSQLLAFGRRQALAPTVLDVGALLGEFS 345
          .  .  .:* ***:** *** **:********.* *.   *:* *:. **


FixL      DLLRRTLGEDIRLSTVIDGSGLNVLVDSSQLQNAILNIALNARDAMPKGG 400
FixLc     DLVQRTLGDSVELRTIIPGRRLSAMADKAQLQSALLNLSINARDAMPAGG 395
          **::****:::.* *:* *  *...:.*.:***.*:**:::******* **


FixL      SLTTTISRVHLDADYAKMYPELRSGNFVLVTMDTGSGMTEEVKKHAIEP 450
FixLc     RLTIEISGVEIDADYVGMYPAIRPGRYVLISVTDTGTGMTSEVMERAFEP 445
           **   ** *.:****. *** :*.*.:**::****:***.** ::*:**


FixL      FFTTKEVGSGTGLGLSMVYGFVKQSGGHLQLYSEVGRGTAVRIYLPAING 500
FixLc     FFTTKPTGSGTGLGLSMVYGFAKQSAGHLQLYSEPGEGTTVRLFLPRADG 495
          ***** .*************** .***.******** *.**:**::** :*


FixL      VKPQEPAPDHGSDDNQLPQGDEVVLVVEDDARVRRVAVARLASMGYKVRE 550
FixLc     GR--DSHPDEQQVKDAPSPGTETILVVEDDARVRRVTISRLQTLGYSVIE 543
           :  :. **. . .:  . * *.:*************:::** ::**.* *


FixL      AENGHRALDLLKENPDVALLFTDIVMPGGMTGDELAKEVRILRPDIAVLF 600
FixLc     ATNGIDALKELEAGHDVALLFSDVAMPG-MNGDELARKVRERWPRVKILL 592
          * **   **. *: . ******:*:.*** *.*****::**   * : :*:


FixL      TSGYSEPGLAGNDTVPGAQWLRKPYTAKELALRVRELLDAK------ 641
FixLc     TSGFSEPHAAEKEIEAGAGWLKKPYTASEMSTRLRLLLDARHGSDSA 639
          ***:***   * ::  .** **:*****.*:: *:* ****:
```

Fig 6.6 Multiple amino acid sequence alignment of FixL and FixLc. ClustalW2 was used for the alignment (Larkin et al., 2007). (*) indicates conserved residues, (:) indicates strongly similar properties and (.) weakly similar properties.

6.2.2 Symbiotic requirement of *fixL*, *fixL*c and *fnrN*

To determine the requirement of the FixL-homologues, a single *fixL* mutant and a double *fixL fixL*c mutant were constructed. To construct *fixL*ΩSpc, primers pr1270 and pr1271 were used to amplify a 1 kb region containing *fixL*. The PCR product was subcloned into pJET1.2/blunt resulting in pLMB581. A SmaI fragment containing the ΩSpc cassette was cloned into pLMB581 at a unique StuI site blunted using the Klenow fragment. The *fixL*ΩSpc construct was then cloned into XbaI/XhoI-digested pJQ200SK as an *Xba*I/*Xho*I fragment, forming the plasmid pLMB590. Plasmid pLMB590 was conjugated into Rlv3841 to make LMB495 (*fixL*ΩSpc). A *fixL fixL*c double mutant was constructed by conjugating pLMB441 into LMB495 to make LMB496 (*fixL*ΩSpc *fixL*c:pK19mob).

P. sativum was inoculated with LMB403 (*fixL*c:pK19mob), LMB495 (*fixL*ΩSpc) or LMB496 (*fixL*ΩSpc *fixL*c:pK19mob). For all inoculations, rates of acetylene reductions were similar to Rlv3841 (Fig 6.7). This shows that in contrast to *S. meliloti*, *A. caulinodans* and *B. japonicum*, FixL-mediated regulation is not essential for N_2 fixation in *R. leguminosarum*.

Following this result, a single mutation was made in *fnrN* to confirm that FnrN-requirement is the same in Rlv3841 as it is in *R. leguminosarum* bv. viciae VF39 (Patschkowski et al., 1996). The double mutant *fnrN fixL*, double mutant *fnrN fixL*c and triple mutant *fnrN fixL fixL*c were also constructed in order to determine the symbiotic requirement of the three O_2-responsvie regulators.

To construct *fnrN*ΩTc, a 2.5 kb region containing *fnrN* was amplified from Rlv3841 using primers pr1381 and pr1382; the PCR product was then digested with *Xba*I/*Xho*I and cloned into *Xba*I/*Xho*I linearized pJQ200SK to make pLMB732. An *Eco*RI fragment containing ΩTc was cloned into pLMB732 at a unique *Mfe*I restriction site, resulting in pLMB733. The plasmid pLMB733 was conjugated into Rlv3841 to make LMB648 (*fnrN*ΩTc). Double mutants LMB730 (*fixL*c:pK19mob *fnrN*ΩTc) and LMB731 (*fixL*ΩSpc *fnrN*ΩTc) were constructed by conjugating

pLMB733 into LMB403 (*fixL*c:pK19mob) and LMB495 (*fixL*ΩSpc). Triple mutant LMB673 (*fixL*c:pK19mob *fixL*ΩSpc *fnrN*ΩTc) was constructed by transducing *fnrN*ΩTc from LMB648 (*fnrN*ΩTc) into LMB496 (*fixL*ΩSpc *fixL*c:pK19mob).
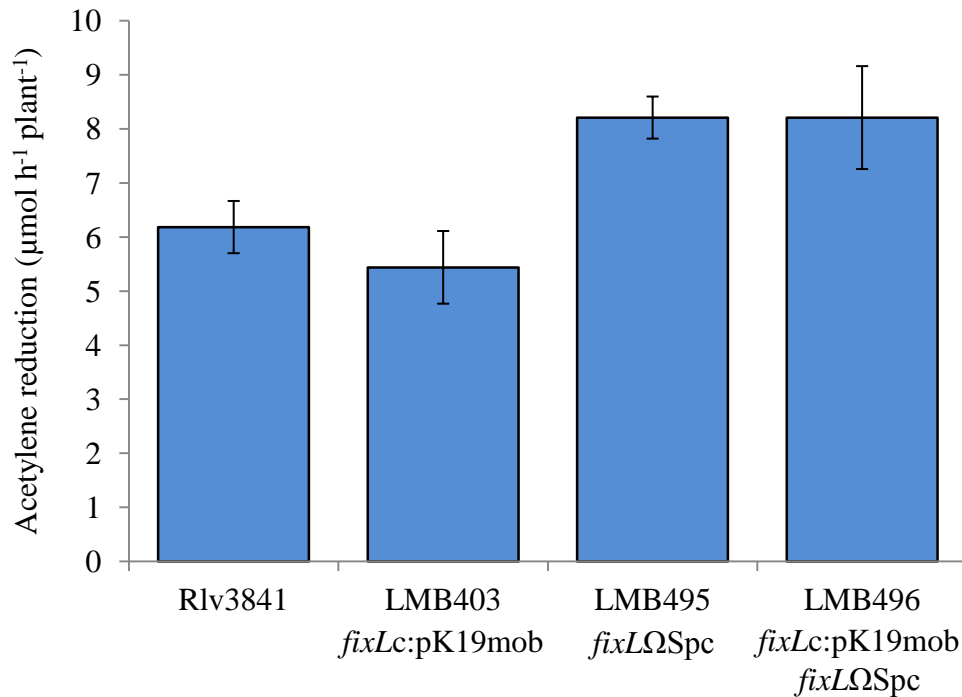
Fig 6.7 Rates of acetylene reduction for *P. sativum* inoculated with Rlv3841, LMB403 (*fixL*c:pK19mob), LMB495 (*fixL*ΩSpc) or LMB496 (*fixL*c:pK19mob *fixL*ΩSpc). Averaged from five plant ± SEM.

P. sativum was inoculated with the single, double or triple mutants. In agreement with *R. leguminosarum* bv. viciae VF39, disruption of *fnrN* in Rlv3841 (LMB648) caused a severe decrease (~90%) in acetylene reduction (Fig 6.8A); double mutants LMB730 (*fixL*c:pK19mob *fnrN*ΩTc) and LMB731 (*fixL*ΩSpc *fnrN*ΩTc) showed similar decreases (~85-90%) in acetylene reduction (Fig 6.8B). However, no acetylene reduction could be detected for the triple mutant LMB673 (*fixL*c:pK19mob *fixL*ΩSpc *fnrN*ΩTc) (Fig 6.8A).
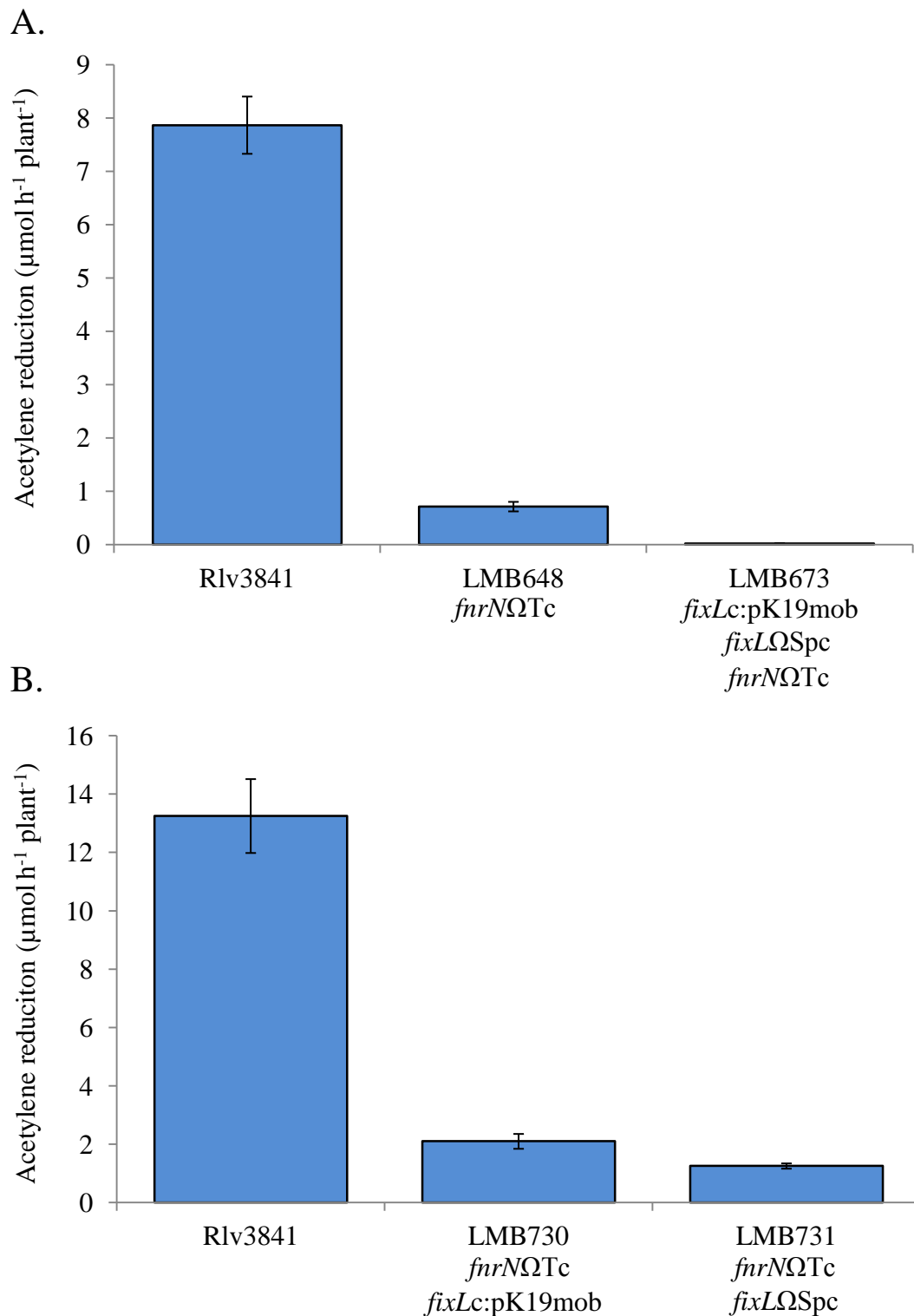
Fig 6.8 Rates of acetylene reduction for *P. sativum* inoculated with Rlv3841, (A) LMB648 (*fnrN*ΩTc), LMB673 (*fixL*c:pK19mob *fixL*ΩSpc *fnrN*ΩTc) (B) LMB730 (*fixL*c:pK19mob *fnrN*ΩTc) and LMB731 (*fixL*ΩSpc *fnrN*ΩTc). Averaged from five plants ± SEM.

6.3 Discussion

It is likely that two pathways govern the expression of the *fixNOPQ* operons in *R. leguminosarum*. One pathway requires FnrN and disruption of *fnrN* causes a severe reduction in N_2 fixation (Fig 6.8A). The second pathway requires FixL or a functional FixL-homolgue (Fig 6.6) annotated here as FixLc. In the absence of the FnrN-governed pathway, the FixL-homologues are essential for N_2 fixation (Fig 6.8A).

It is not known how FixL induces the *fixNOPQ* operons in *R. leguminosarum* (Schluter et al., 1997; Boesten and Priefer, 2004) and it is not known whether FixLc can also regulate *fixNOPQ*, although the symbiotic phenotypes of the double and triple mutants suggest it can (Figs 6.8A and 6.8B). The obvious model would have the FixL-homologues activating FxkR, which would then active the expression of *fixK* and FixK would then activate expression of *fixNOPQ* (Fig 6.4). This model would explain why in *R. leguminosarum* bv. viciae VF39 a *fixK fnrN* double mutant is Fix⁻ (Patschkowski et al., 1996), as both regulatory pathways would be negated. However, it is not known whether induction of *fixK* is dependent upon the FixL-homologues and furthermore, it was reported that FixK is dispensable for activation of both *fixNOPQ* operons in *R. leguminosarum* bv. viciae VF39 (Schluter et al., 1997). However, the non-requirement of FixK for *fixNOPQ*-activation may just suggest that FnrN is the major regulator of the *fixNOPQ* (consistent with the rates of acetylene reduction) and therefore, FixK might only cause noticeable changes in *fixNOPQ* expression in the absence of FnrN. Alternatively, it is also possible that the FixL-homologues activate *fixNOPQ* expression independently of FixK and that FixK and FnrN regulate additional genes that are essential to N_2 fixation.

It is clear that the regulons of all the regulators involved in switching on N_2 fixation in *R. leguminosarum* require better definition. This would be no small challenge due to the presence of six CRP/FNR-type regulators, two FixL-homologues and a novel FxkR-regulator. There is also likely to be a high-level of cross-talk between the regulators in accordance with what has been shown in *R. etli* (Granados-Baeza et al.,

2007) and *B. japonicum* (Mesa et al., 2008). Furthermore, regulons of FixLJ and FixK-type regulators have been shown to consist of a great number of genes (Bobik et al., 2006; Mesa et al., 2008).

The complexity of the networks that govern the expression of *fixNOPQ* and other genes required for N_2 fixation (see Terpolilli *et al*., 2012 for a review) implies that the regulation of N_2 fixation is tightly controlled. The multiple O_2-sensing regulators encoded by *R. leguminosarum* may have different affinities for O_2, resulting in a finely-tuned and sensitive response to changing levels of O_2. Furthermore, the multiple regulators downstream of the O_2-sensing regulators could allow the integration of multiple signals that impede or activate N_2 fixation e.g. ROS (Mesa et al., 2009) and pH (Table 6.1) (additional signals are reviewed in Terpolilli *et al*., 2012). However, O_2 is likely to be the major signal that governs the switch on of *fixNOPQ* and it has now been shown that three O_2-repsonsive regulators, FnrN, FixL and FixLc are required for N_2 fixation in Rlv3841.

Chapter 7: *Resistance to Organic Peroxide*

7.1 INTRODUCTION

Organic peroxides (ROOH) are highly toxic because of their tendency to form destructive organic peroxide radicals (RO·) (Akaike et al., 1992). They can be part of a plant's defence response so enzymes that detoxify organic peroxides have been studied in several plant pathogens (Mongkolsuk et al., 1998; Sukchawalit et al., 2001; Vattanaviboon et al., 2002; Klomsiri et al., 2005; Chuchue et al., 2007). Belonging to the OsmC/Ohr family, OsmC (osmotically inducible protein) provides resistance to both H_2O_2 and organic peroxides, whereas Ohr (organic hydroperoxide resistance protein) only provides resistance to organic peroxides (Atichartpongkul et al., 2001; Conter et al., 2001; Lesniak et al., 2003). AhpC belongs to the peroxiredoxin family and provides resistance to H_2O_2, peroxynitrite and organic peroxide (as discussed in 1.4.2) (Poole et al., 2011).

Disruption of *ohr* in *S. meliloti* caused hypersensitivity to organic peroxides t-butyl hydroperoxide (tBOOH) and cumene hydroperoxide (CuOOH) (Fontenelle et al., 2011). Expression of *ohr* is induced in response to organic peroxides and repressed by a MarR-type repressor (OhrR) under non-stressed conditions. In nodules, *ohr-lacZ* was highly expressed in the N_2 fixation zone, correlating with the presence of Ohr in a previous proteomics study (Djordjevic, 2004). Ohr however, is not essential for symbiosis, as *M. sativa* inoculated with an *ohr* mutant had a similar number of nodules and dry weight to *M. sativa* inoculated with wild type. This could be the result of functional redundancy between Ohr and another organic peroxide-resistance protein e.g. putative AhpC (SMb20964) or putative OsmC (SMc01944) (Fontenelle et al., 2011). Indeed, expression of *osmC* (SMc01944) is induced by the presence of organic peroxides in *S. meliloti* (Barloy-Hubler et al., 2004).

Five genes in Rlv3841 encode putative OsmC/Ohr proteins, including RL2927 and RL1302 (Table 7.1). RL2927 and RL1302 are highly upregulated during bacteroid development (Table 7.1). Upstream of RL1302 is a gene encoding a MarR-type repressor (RL1301A). In close proximity to RL2927 is another gene encoding for a

MarR-type repressor and is 4-fold upregulated in developing bacteroids. The putative products of RL1301A and RL2924 share 54% and 49% amino acid identity (respectively) to OhrR in *S. meliloti* (Fontenelle et al., 2011). Rlv3841 also encodes a putative AhpC-type peroxiredoxin (Altschul et al., 1990; Young et al., 2006).

Gene	Family of Product	7 day bacteroid	21 day bacteroid	Pea rhizosphere
RL2927	OsmC/Ohr	5.6	0.8	0.7
RL2737	OsmC/Ohr	1.8	1.0	1.8
pRL90318	OsmC/Ohr	0.9	1.6	1.3
RL1302	OsmC/Ohr	9.3	0.4	0.4
RL4226	OsmC/Ohr	0.8	0.5	1.3
RL2003 (ahpC)	AhpC	1.2	0.9	1.3

Table 7.1 Expression of genes encoding putative OsmC/Ohr or AhpC proteins in Rlv3841 isolated from *P. sativum* nodules at 7 dpi, 21 dpi or isolated from the *P. sativum* rhizosphere. Values correspond to fold-induction relative to free-living cells grown in minimal medium. Highlighted cells are >3-fold upregulated. (Karunakaran et al., 2009; Ramachandran et al., 2011).

Single mutations in RL1302 and RL2927 (strains LMB372 and LMB377 respectively) did not cause any reductions in N_2 fixation relative to Rlv3841 (Table 3.5). As expected, a mutation in the putative MarR-repressor, encoded by RL2924, (strain LMB400) also caused no reduction in N_2 fixation (Table 3.5).

7.2 RESULTS

7.2.1 Alignment of OsmC/Ohr family members

OsmC and Ohr orthologs cluster into two related subfamilies both of which contain two highly conserved cysteine residues (Fig 7.1) (Atichartpongkul et al., 2001). Site-directed mutagenesis confirmed that these two cysteine residues are essential for the catalytic activity of Ohr in *P. aeruginosa* and are proposed to be directly involved in metabolism of peroxides (Lesniak et al., 2002). A VCPY motif around the second conserved cysteine is conserved in the Ohr but not in the OsmC subfamily (Atichartpongkul et al., 2001). The product of RL1302 contains the VCPY motif, implying that it belongs to the Ohr family (Fig 7.1). The function of VCPY is unknown but might place the conserved cysteine residue in a nucleophilic environment, allowing it to react with peroxide molecules (Atichartpongkul et al., 2001). Hereafter, RL1302 will be provisionally annotated as *ohr*.

```
CLUSTAL 2.1 multiple sequence alignment

RL1302      ----------------------------MPILYTTKASATGGRA-GRA 19
Atu0847     ----------------------------MPILYTTKASATGGRA-GNA 19
SMc00040    ----------------------------MPILYRTTASATGGRA-GQA 19
Xanth_ohr   ------------------------MASPEKVLYTAHATATGGRE-GRA 23
Pseud_ohr   ------------------------MQT-IKALYTATATATGGRD-GRA 22
RL2737      ------------------------MTKIDKVLYTGKTHTTGGRD-GAS 23
RL2927      ------------------------MT--EKLLFTGKTHISGGRD-GSA 21
pRL90318    MVKCEVSLTRRIAPRWVDDADRLEIPVSNTQRVIYTAITDTIGGRESGVA 50
RL4226      ----------------------------MQINRTASAHWTGGLKDGKG 20
                                             :   **    *  .


RL1302      VSENGVLDVT-LTVPKELGGDGATGTNPEQLFAAGYSACFLGALKFVAGQ 68
Atu0847     KSEDGVLDVT-LTVPKELGGDGARGTNPEQLFAAGYSACFLGALKAVAGK 68
SMc00040    KSKDGVLDVT-LTVPKELGGDGARGTNPEQLFAAGYSACFLGALKFVAGK 68
Xanth_ohr   VSSDKALDAK-LSTPRELGGAGGDGTNPEQLFAAGYAACFIGAMKAVAAQ 72
Pseud_ohr   VSSDGVLDVK-LSTPRELGGQGGAATNPEQLFAAGYSACFIGALKFVAGQ 71
RL2737      HSDDGQLDIK-LSPPGS----NRAGTNPEQLFAAGWSACFIGAIGIAAGK 68
RL2927      RSGDGTIDIK-LPQP------HPAAEN---LFGIAWSACYIGAMELAAAQ 61
pRL90318    RSSDGVLDIR-FSAPGS----PRIGTNPEQLLSAGWSASFASAIALAAFN 95
RL4226      LISTQSGALKDYPYGFASRFEGVAGTNPEELIGAAHAGCFTMALSLILGE 70
                      .            . *     *:. . :..:  *:      :


RL1302      QKVKIPEDTTVSAKVGIGPREDGG-GFGIEVALTVNIPGLDRETAEKLAA 117
Atu0847     HKVKIPEDTTVTATVGIGPREDGT-GFGIEVTLKVNIPGLEREKAEELVA 117
SMc00040    EKVKLAEDTTVTGTVGIGPRDDGT-GFFIDAALEISSPGVEKAVLEDLVQ 117
Xanth_ohr   DKLKLPGEVSIDSSVGIG-QIPG--GFGIVVELRIAVPGMDKAELQTLVD 119
Pseud_ohr   RKQTLPADASITGKVGIG-QIPG--GFGLEVELHINLPGLEREAAEALVA 118
RL2737      LKVKLPADAAVNAEVDLG-ATDG--DYFLQARLKVSLPGIEADLARALVD 115
RL2927      RKITLPDGPEVDAEITLN-ADNG--SFFLRARLNVSLPGIDRDVAQELIE 108
pRL90318    RNIAFAGEVSIHAEVEIE--IDPV-SYTLSVRLHVRLPGIERALAQLLTA 142
RL4226      AG-FTAEHMETSAKVTLESVEGGFAITAIHLSLSGRIPGADEATFTELAN 119
                 .        . : :          :   *    ** :        *


RL1302      AAHIVCPYSHAMRTS-TEVPVTVA- 140
Atu0847     AAHIVCPYSHAMRTS-TEVPVSVA- 140
SMc00040    KAHIVCPYSHATRGN-VDVKLTVA- 140
Xanth_ohr   KAHQVCPYSNATRGN-IDVTLTLA- 142
Pseud_ohr   AAHQVCPYSNATRGN-IDVRLNVSV 142
RL2737      EAHRTCPYSKATRGN-INVELSIA- 138
RL2927      AAHGICPYSKATHGN-IDVETTLV- 131
pRL90318    EARRLCPFSSTIGRG-LAVAVDLD- 165
RL4226      KAKAGCPVSKALASVPITLDVKVV- 143
                *:   ** * :       :  :
```
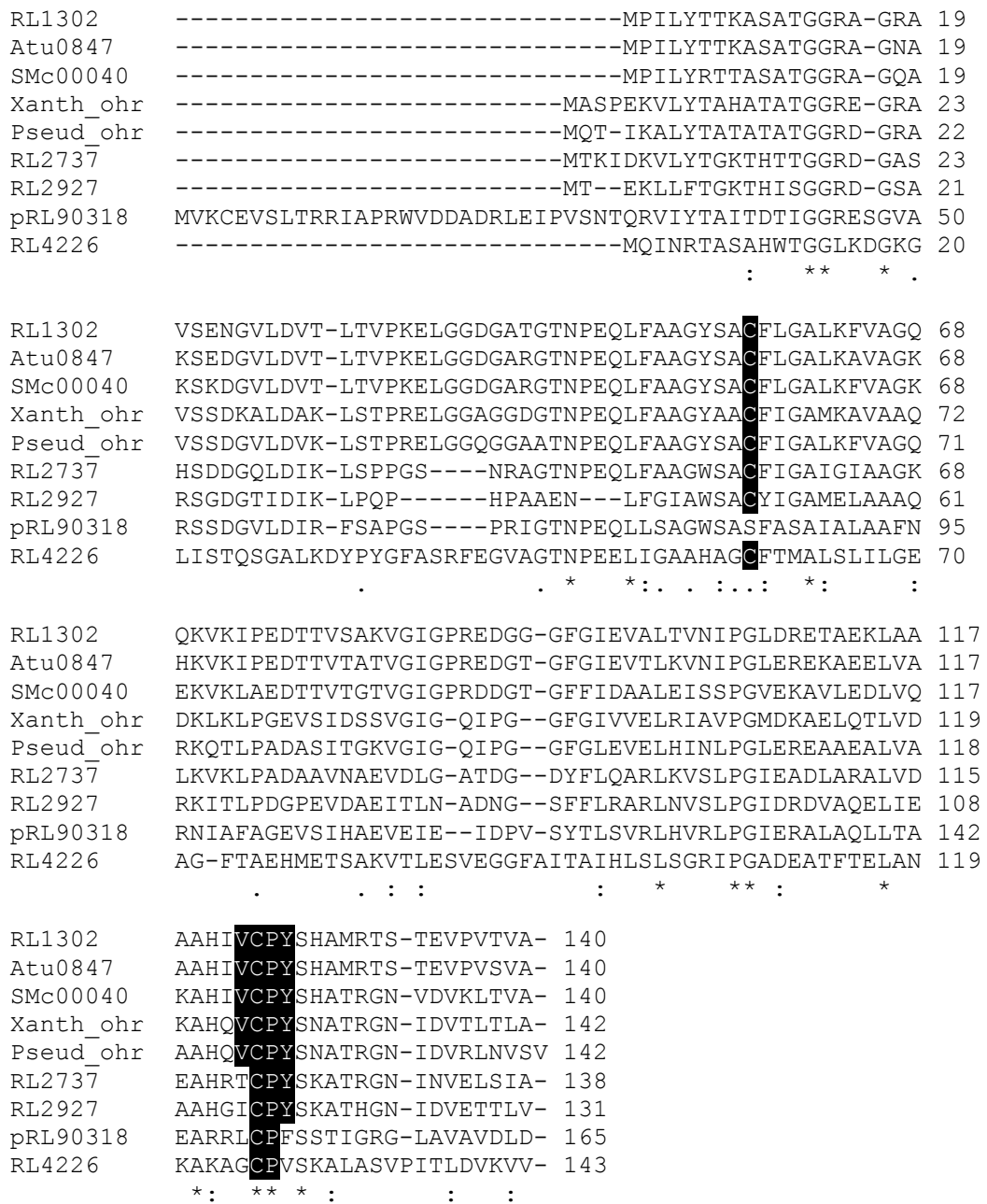
Fig. 7.1 Multiple amino acid sequence alignment of OsmC/Ohr family members. RL1302, RL2737, RL2927, pRL90318 and RL4226 from Rlv3841; Ohr (Atu0847) from *A. tumefaciens* (Chuchue et al., 2007), Ohr (SMc00040) from *S. meliloti* (Fontenelle et al., 2011), Ohr from *X. campestris* (Mongkolsuk et al., 1998) and Ohr from *P. aeruginosa* (Atichartpongkul et al., 2010). Black shading and white lettering highlight the conserved cysteine residues and the VCPY motif present in the Ohr subfamily (Atichartpongkul et al., 2001; Lesniak et al., 2002). ClustalW2 was used for the alignment (Larkin et al., 2007). (*) indicates conserved residues, (:) indicates strongly similar properties and (.) weakly similar properties.

7.2.2 Construction of double mutant

It was speculated that there is functional redundancy between the products of upregulated genes *ohr* and RL2927, explaining why no symbiotic phenotype was detected for LMB372 (*ohr*:pRU877) or LMB377 (RL2927:pRU877). A double mutant was constructed to test this.

To make the double mutant, a strain carrying the mutation *ohr*ΩSpc was constructed. Primers pr1385 and pr1386 were used to amplify a ~2.5 kb region containing *ohr*. The PCR product was subcloned into pJET1.2/blunt to make pLMB677. A *Sma*I fragment containing the ΩSpc cassette was cloned into pLMB677 at a unique *Bmg*BI site, resulting in pLMB688. The *Xba*I/*Xho*I fragment of pLMB677, containing *ohr*-ΩSpc, was cloned into *Xba*I/*Xho*I digested pJQ200SK, creating pLMB692. Plasmid pLMB692 was conjugated into Rlv3841 to make LMB603 (*ohr*ΩSpc). To construct the double mutant, RL2927:pRU877 was transduced from LMB377 into LMB603 (*ohr*ΩSpc) to make LMB620 (RL2927:pRU877 *ohr*ΩSpc)

7.2.3 Sensitivity to organic peroxides and H_2O_2

Disk assays (2.5.7) were used to determine the sensitivity of strains to CuOOH and H_2O_2. Disruption of *ohr* caused hypersensitivity to CuOOH, relative to Rlv3841 (Fig 7.2). Disruption of RL2927 however, had no effect, even in combination with *ohr*ΩSpc (Fig 7.2). None of the tested mutant strains showed hypersensitivity to H_2O_2 (Fig 7.3).
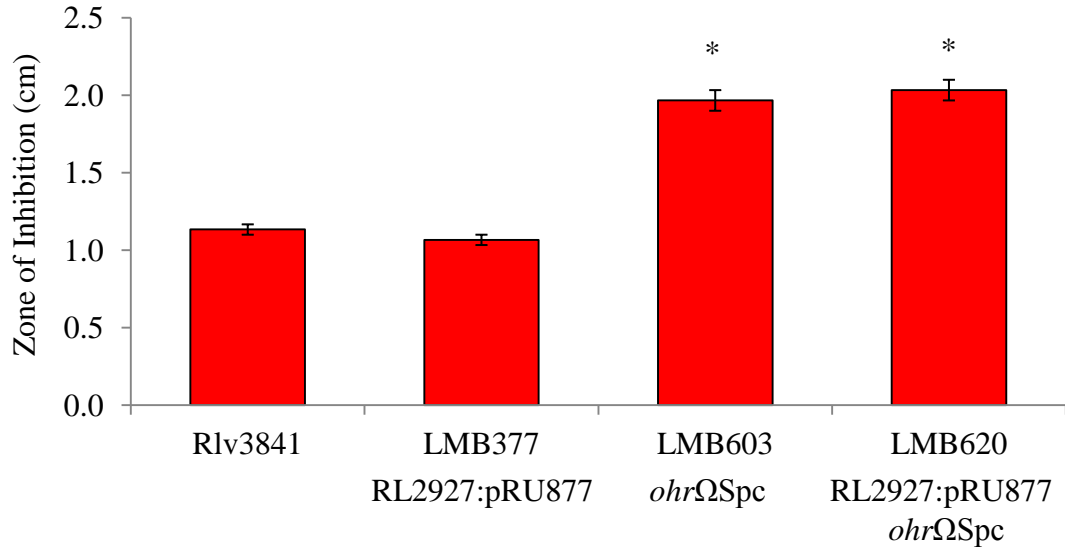
Fig 7.2 Disk assays testing resistance of Rlv3841, LMB377 (RL2927:pRU877), LMB603 (*ohr*ΩSpc) and LMB620 (RL2927:pRU877 *ohr*ΩSpc) to 0.1 M CuOOH. Averaged from three independent experiment ± SEM. * indicated a statistically significant (p ≤ 0.05) difference relative to Rlv3841.
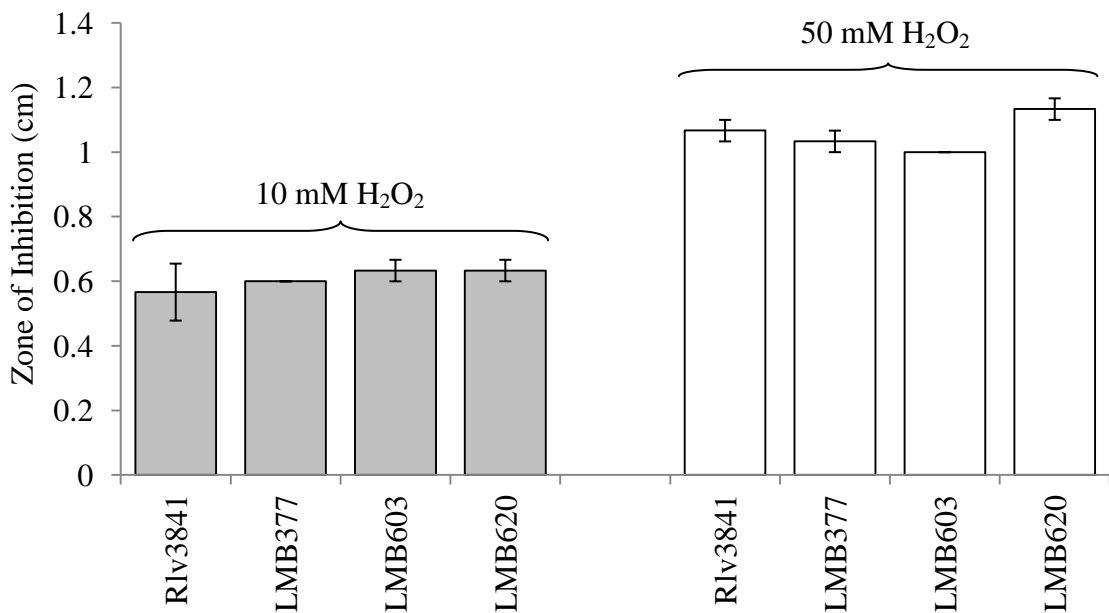

Fig 7.3 Disk assays testing resistance of Rlv3841, LMB377 (RL2927:pRU877), LMB603 (*ohr*ΩSpc) and LMB620 (RL2927:pRU877 *ohr*ΩSpc) to 10 mM (grey bars) and 50 mM (white bars) H_2O_2 . Averaged from three independent experiments ± SEM.

To confirm that the increased sensitivity of LMB603 (*ohr*ΩSpc) and LMB620 (RL2927:pRU877 *ohr*ΩSpc) to CuOOH was caused by the disruption of *ohr* and not the presence of the ΩSpc cassette, LMB372 (*ohr*:pRU877) was also tested for sensitivity to CuOOH. LMB372 (*ohr*:pRU877) was more sensitive to CuOOH compared to Rlv3841 (Fig 7.4) confirming that disruption of *ohr* is the cause of sensitivity. The requirement of RL2924 (encoding MarR-repressor upstream of RL2927) for organic peroxide resistance was also tested. As expected, LMB400 (RL2924:pK19mob) showed no increased sensitivity or resistance to CuOOH (Fig 7.4).
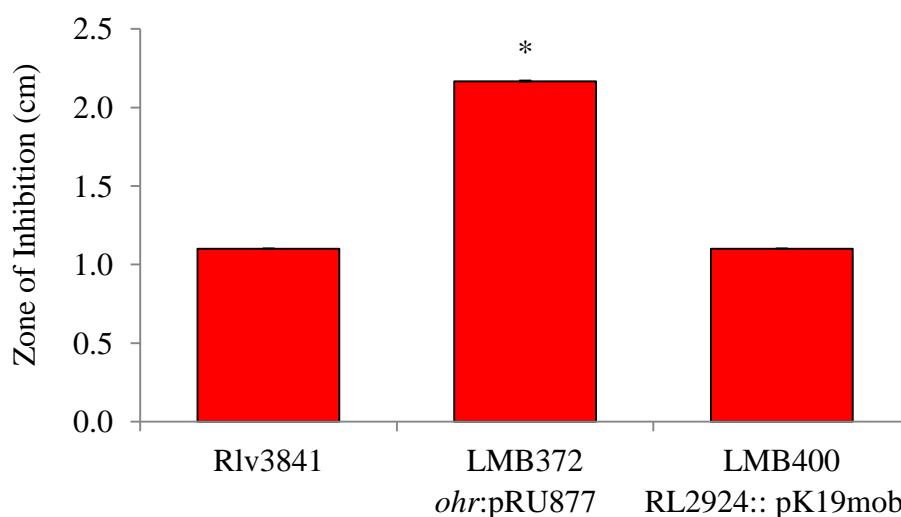

Fig 7.4 Disk assays testing resistance of Rlv3841, LMB372 (*ohr*:pRU877) and LMB400 (RL2924:pK19mob) to 0.1M CuOOH. Averaged from three independent experiments ± SEM. * indicated a statistically significant (p ≤ 0.05) difference relative to Rlv3841.

7.2.4 Symbiotic requirement of OsmC and Ohr

Rlv3841, LMB377 (RL2927:pRU877), LMB603 (*ohr*ΩSpc) or LMB620 (RL2927:pRU877 *ohr*ΩSpc) were used to inoculate *P. sativum*. All plants showed a Fix$^+$ phenotype and reduced acetylene at similar rates to Rlv3841 (Fig 7.5).
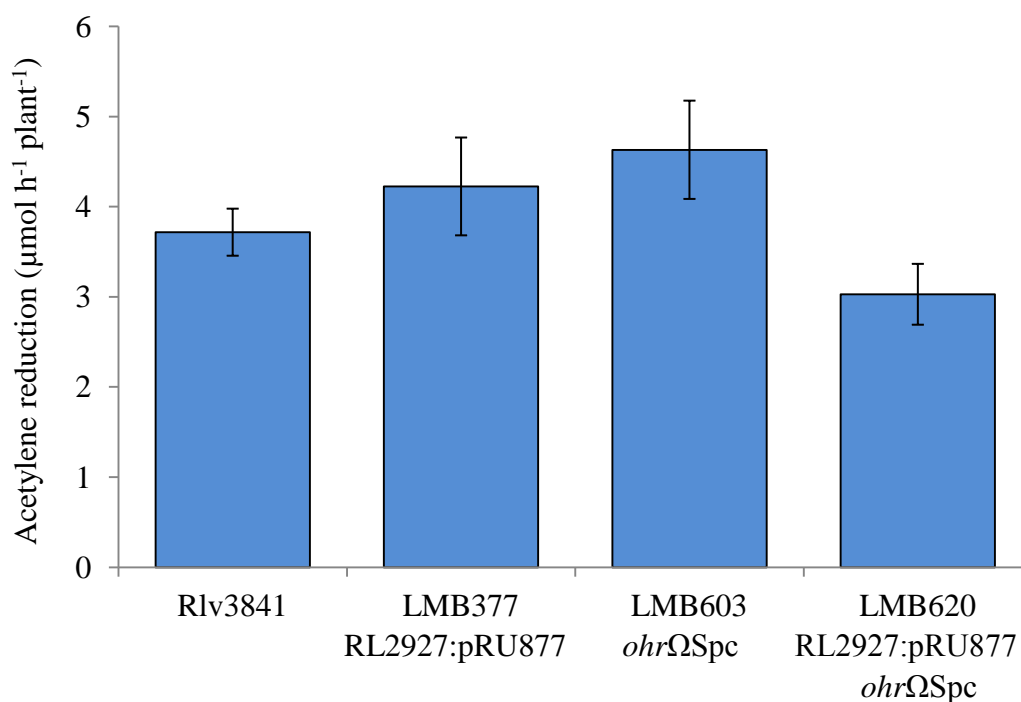

Fig 7.5 Rates of acetylene reduction for *P. sativum* inoculated with Rlv3841, LMB377 (RL2927:pRU877), LMB603 (*ohr*ΩSpc) or LMB620 (RL2927:pRU877 *ohr*ΩSpc). Averaged from five plants ± SEM.

7.3 DISCUSSION

The *ohr* (RL1302) gene encodes an organic peroxidase that confers resistance against organic peroxide but not H_2O_2 (Figs 7.2. and 7.3). RL2927 does not confer resistance to organic peroxide and subsequently, the double mutant LMB620 (RL2927:pRU877 *ohr*ΩSpc) was not more sensitive to organic peroxide relative to single mutant LMB603 (*ohr*ΩSpc) (Fig 7.2).

None of the mutations caused a significant symbiotic defect on *P.* sativum, therefore, either resistance to organic peroxides is not essential for bacteroid development or there is another organic peroxidise active during symbiosis. A strong candidate would be the product of RL2737 as it contains the two conserved cysteine resisdues, the VCPY motif (with the exception of a threonine residue in the place of valine) (Fig 7.1) and is 1.8-fold upregulated in developing bacteroids (Table 7.1). Alternatively, the putative AhpC encoded by RL2003 may also be active during symbiosis and confer resistance against organic peroxides.

It is not clear why Rlv3841 encodes multiple organic peroxidases. It is possible that they differ in their specificity for organic peroxides and therefore, each organic peroxidase may target a different subset of organic peroxides. For example, both Ohr from *P. aeruginosa* and OsmC from *E. coli* have a higher affinity for tBOOH and CuOOH over H_2O_2, however, the active site of OsmC is structurally different from Ohr. It has therefore been suggested that Ohr and OsmC may target structurally different peroxides (Lesniak et al., 2002, 2003). Further research could include identifying organic peroxides endogenous to both Rlv3841 and *P. sativum*, then determining whether the affinity for these endogenous peroxides differs between the putative organic peroxidases encoded by Rlv3841. Testing the requirement of organic peroxidases on other legumes compatible with Rlv3841 may also prove to be insightful e.g. *V. faba* and *V. hirsuta* may generate different types and amounts of organic peroxides.

It is clear that full resolution of this topic would require the construction of multiple mutants, possibly including a quadruple mutant. This was considered beyond the scope of this thesis.

Chapter 8: *AAA+ proteases encoded on pRL10 and pRL8*

8.1 INTRODUCTION

AAA+ proteases consist of one or two AAA+ (ATPases associated with diverse cellular activities) domains and a protease domain (a chamber where peptide degradation takes place) (Fig 8.1). The AAA+ domain(s) and the protease domain can either be contained within the same polypeptide (e.g. FtsH and Lon) or are comprised of separate polypeptides (HslUV, ClpXP, ClpAP and ClpCP) (Sauer and Baker, 2011). The AAA+ protein typically forms a hexameric ring that drives the unfolding of a protein targeted for destruction and then translocates it to the degradation chamber of the protease (Fig 8.1). This process is highly specific and involves recognition of certain amino acid motifs known as degrons by the AAA+ domain (Sauer and Baker, 2011).
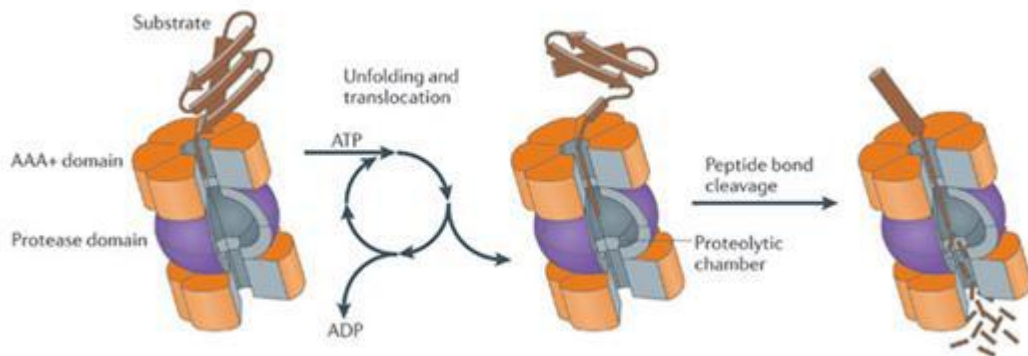

Fig 8.1 Arrangement and mechanism of AAA+ proteases. Reproduced from Gur *et al*., 2011.

AAA+ proteases have a number of different roles in the cell (Fig. 8.2), the most well-known being the degradation of damaged or misfolded proteins that might otherwise cause intracellular aggregates (Sauer and Baker, 2011). AAA+ proteases can also change a cell's transcriptome by targeting transcriptional regulators, an example of which, is the degradation of $FixK_2$ by ClpAP, a key regulator of N_2 fixation in *B. japonicum* (see Chapter six) (Jenal and Hengge-Aronis, 2003; Gur et al., 2011; Bonnet et al., 2013). AAA+ proteases have also been shown to target sigma factors and anti-sigma factors and so can determine the expression of entire regulons e.g. the heat shock regulon by degradation of σ^{32}, genes involved in envelope stress response by degradation of an anti-sigma factor that binds σ^{E} and genes involved in the general stress response by degradation of σ^{s} (Gur et al., 2011). AAA+ proteases are involved in controlling the life cycle of *Caulobacter crescentus* through degradation of cell cycle proteins, regulators and cellular machinery (Gur et al., 2011; Bhat et al., 2013). Proteases have also been proposed to target antimicrobial peptides after they have been imported into the cell (Shelton et al., 2011).
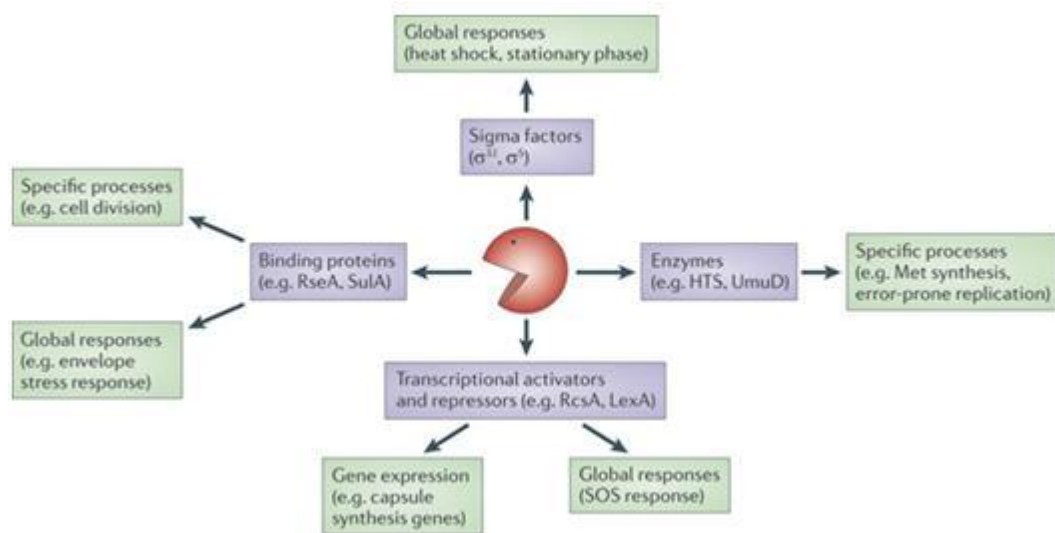

Fig 8.2 Diverse roles of AAA+ proteases. Reproduced from Gur *et al*., 2011.

Studies of AAA+ proteases in rhizobia are few in number. In *S. meliloti*, mutation of *lon*, encoding the Lon protease, caused ineffective symbiosis on *M. sativa* (Summers et al., 2000). Plants inoculated with this mutant weighed the same as an uninoculated control, were delayed in nodulation and initiated small nodules, from which, only a few bacteria could be recovered. The cause of this symbiotic phenotype has not been determined but it was observed that disruption of *lon* resulted in hyper-production of EPS and poor growth in minimal medium. Secondly, CtpA (carboxy-terminal protease) has been characterised in Rlv3841. Disruption of *ctpA* (RL4692) caused an increased sensitivity to detergents and susceptibility to desiccation on solid medium; the symbiotic requirement of CtpA was not reported (Gilbert et al., 2007).

Two putative AAA+ proteases in Rlv3841 are encoded by putative operons pRL80012-13 and pRL100036-35. The pRL80012-13 operon is 5-fold upregulated in developing bacteroids but pRL80012 was found to be non-essential for symbiosis (see Table 3.6). The putative pRL100036-35 operon is not upregulated in bacteroids but a mTn5 insertion at pRL100036 caused a defective symbiosis on *P. sativum* (Karunakaran et al., 2009). This data implies that both these putative AAA+ proteases are important to symbiosis and so they were investigated further, beginning with the characterisation of the symbiotic defect caused by the disruption of pRL100036 (Karunakaran et al., 2009).

8.2 RESULTS AND DISCUSSION

8.2.1 RU4067 (pRL100036::mTn5) forms bacteroids but is defective for N$_2$ fixation

P. sativum was inoculated with RU4067 (pRL100036::mTn5) to determine if any N$_2$ fixation can occur. Rates of acetylene reduction indicate that RU4067 (pRL100036::mTn5) could fix N$_2$ but at ~25% the rate of Rlv3841 (Fig 8.3). The nodules containing RU4067 (pRL100036::mTn5) had two different morphologies; some were white and elongated (Fig 8.4B) while others were small, white and spherical (Fig 8.4C). Generally however, plants inoculated with RU4067 (pRL100036::mTn5) had a higher number of nodules but a lower total nodule mass relative to plants inoculated with Rlv3841 (Figs 8.5A and 8.5B). Sections taken from these nodules revealed that RU4067 (pRL100036::mTn5) could infect plant cells (Fig 8.6) and that white-elongated nodules (Fig 8.6D) had more infected cells than the small-white-spherical nodules (Figs 8.6B and 8.6C).
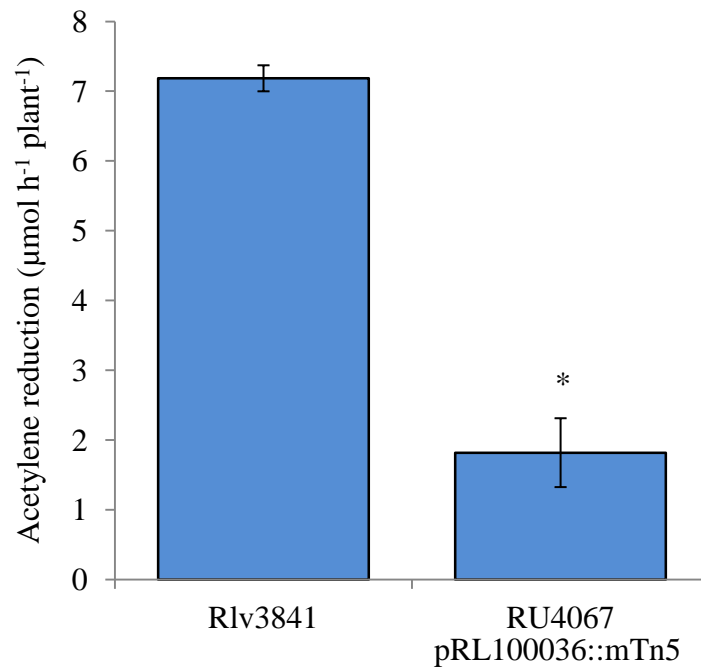
Fig 8.3 Rates of acetylene reduction for Rlv3841 and RU4067 (pRL100036::mTn5) on *P. sativum*. Averaged from five plants ± SEM. * indicates a statistically significant difference (p ≤ 0.05) relative to Rlv3841-inoculated plants.
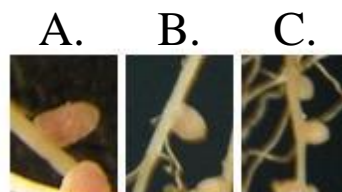

Fig 8.4 *P. sativum* nodules on plants inoculated with Rlv3841 (A) or RU4067 (pRL100036::mTn5) (B and C). Nodules formed on RU4067-inoculated plants were white and elongated (B) or white, small and spherical (C).
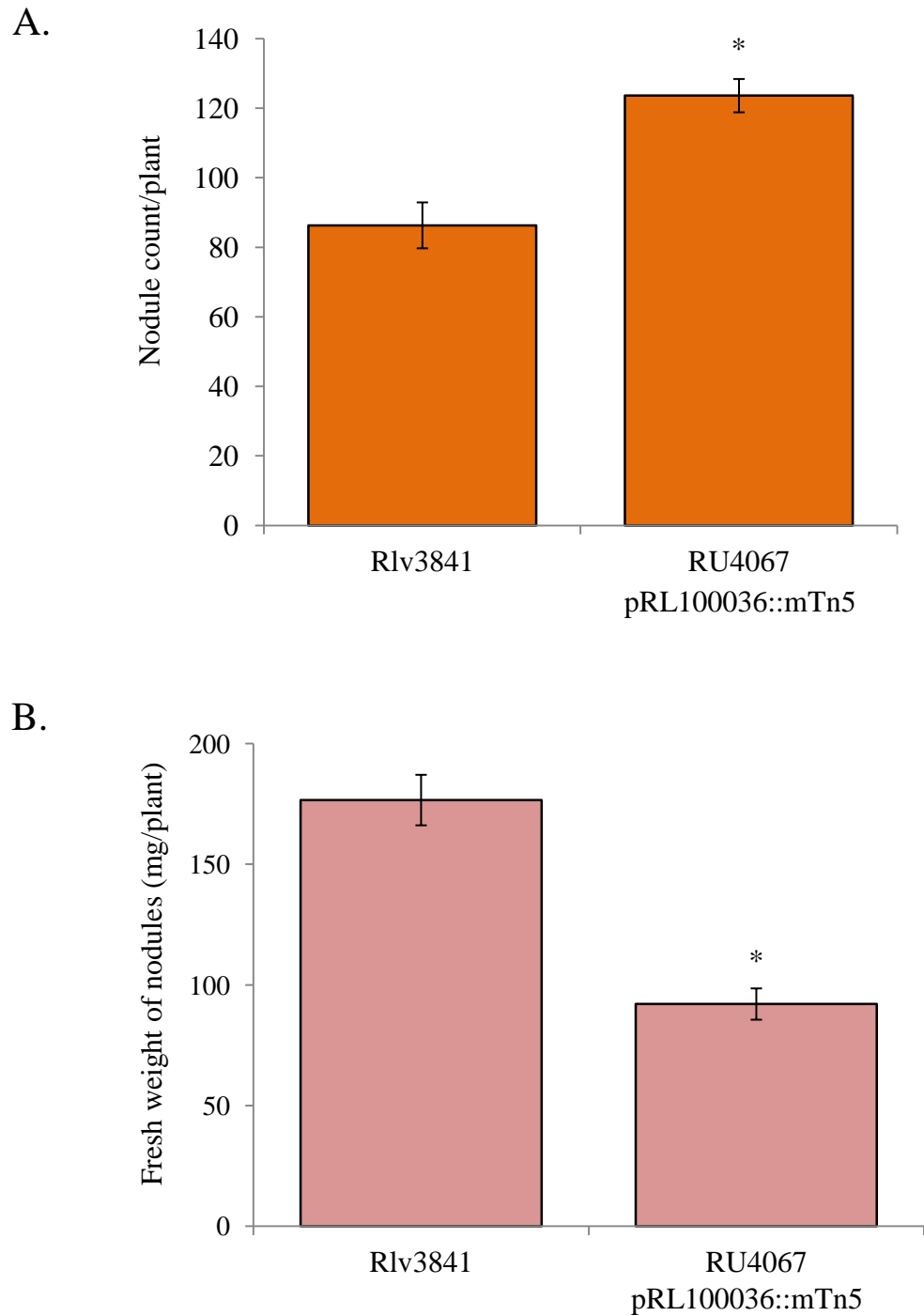
Fig 8.5 Nodule number (A) and fresh weight of nodules (B) on *P. sativum* inoculated with Rlv3841 or RU4067 (pRL100036::mTn5). Averaged from ten plants for Rlv3841 and five plants for RU4067 (pRL100036::mTn5) ± SEM. * indicates a statistically significant ($p \leq 0.05$) difference relative to Rlv3841-inoculated plants.

Fig 8.6 Sections of nodules taken from *P.sativum* inoculated with Rlv3841 (A) or RU4067 (pRL100036::mTn5) (B, C and D). Sections (B and C) show small spherical nodules and (D) shows a white, elongated nodule. Sections stained with toluidine blue. Visualised by light microscopy at magnification x 10.

Electron micrographs showed that RU4067 (pRL100036::mTn5) could form branch-shaped bacteroids (Fig 8.7B) and that a number of nodule cells contained increased numbers of starch granules, which are typical of an ineffective legume-rhizobia symbiosis (Figs 8.7C and 8.7D) (Udvardi and Poole, 2013).
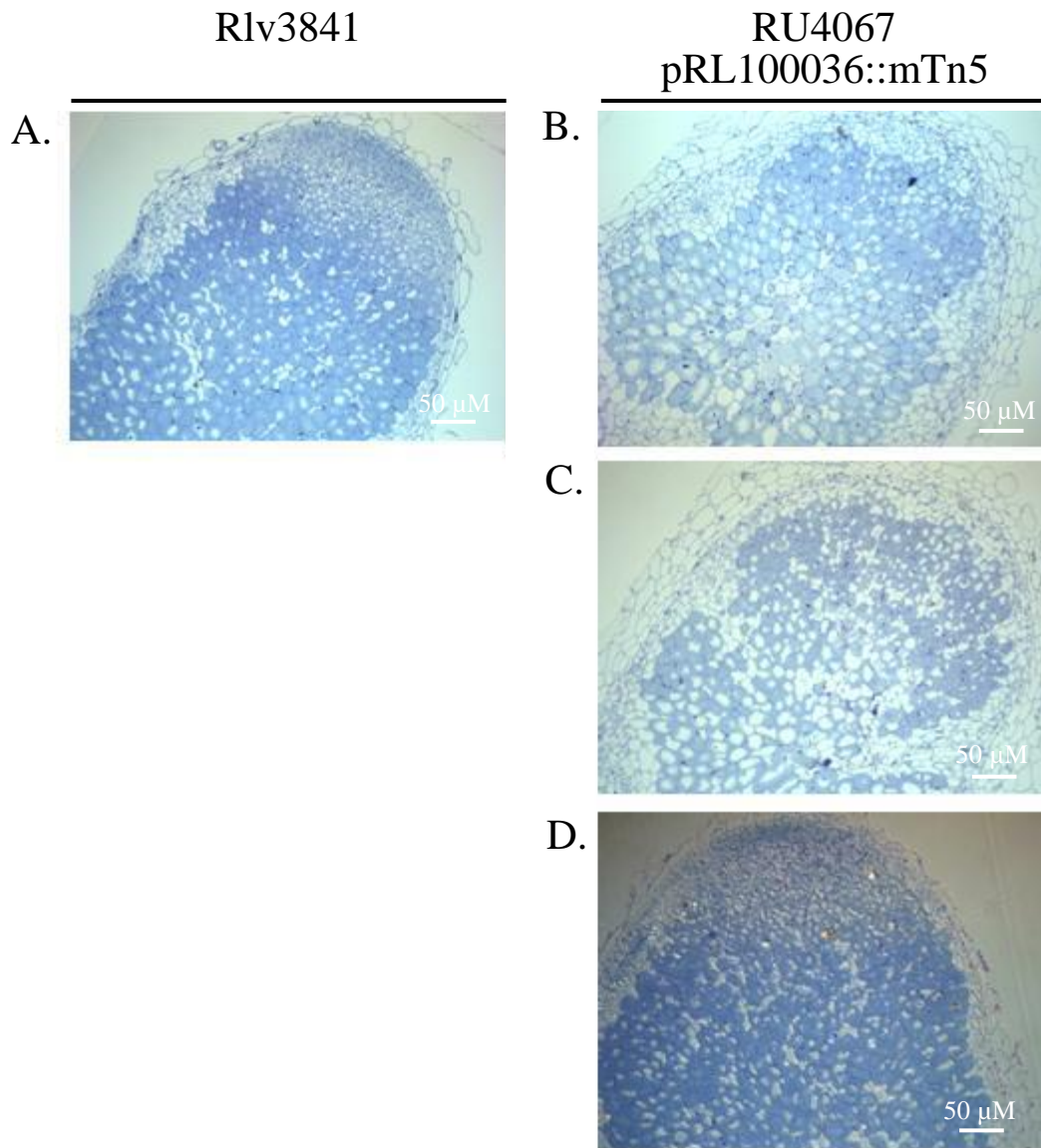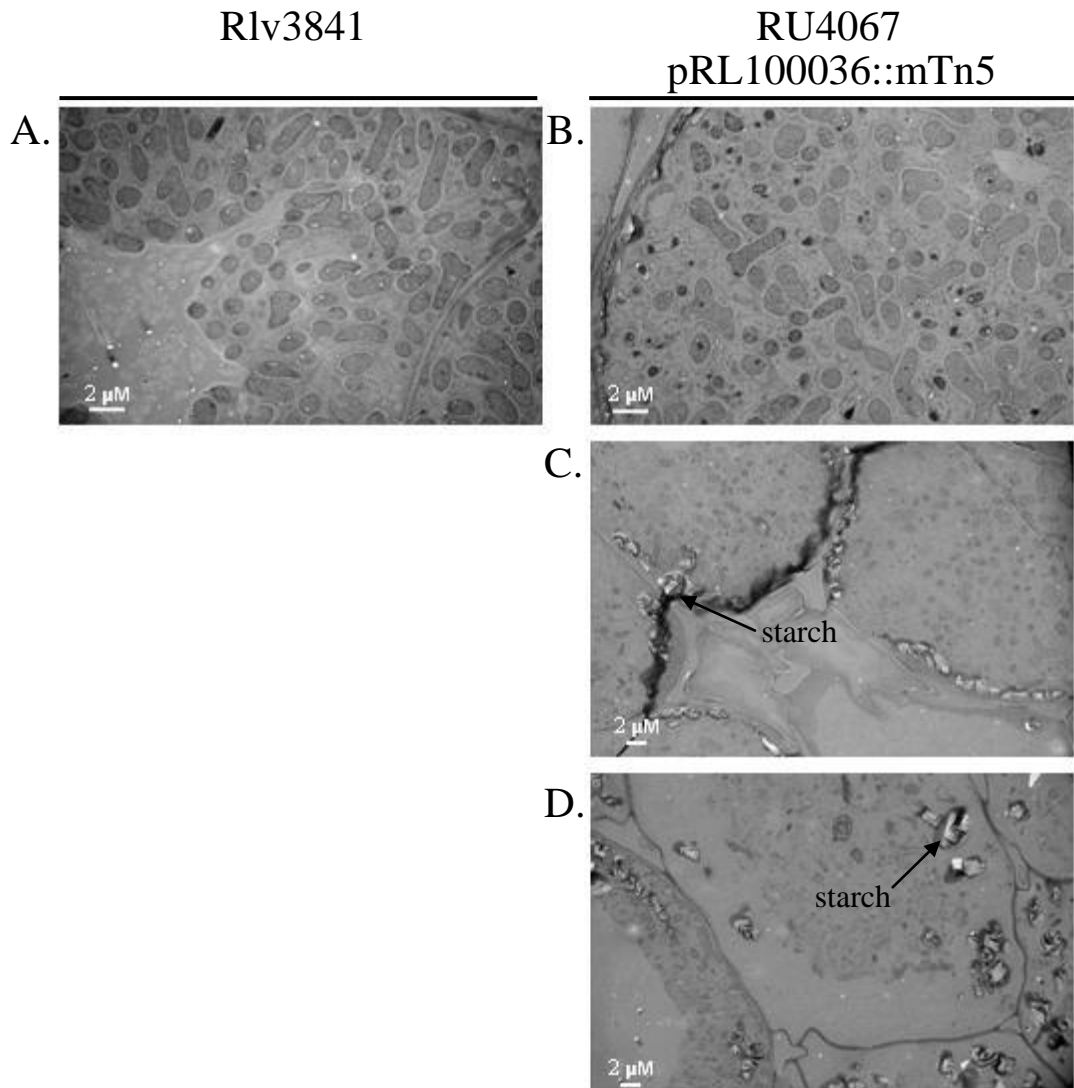
Fig 8.7 Ultrathin sections of nodules taken from *P.sativum* inoculated with Rlv3841 (A) or RU4067 (pRL100036::mTn5) (B, C and D). Visualised by TEM at magnification x 1500 (A and B) or x 800 (C and D).

To confirm that the pRL100036::mTn5 mutation caused the symbiotic defect and not a secondary mutation, a region containing pRL100036::mTn5 was transduced from RU4067 (pRL100036::mTn5) into Rlv3841, resulting in LMB449. LMB449 had severely reduced rates of acetylene reduction rates, suggesting that a secondary mutation was not the cause of the symbiotic defect (Fig 8.8).

Fig 8.8 Rates of acetylene reduction for Rlv3841 and LMB449 (pRL100036::mTn5) on *P. sativum*. Acetylene reduction for Rlv3841-inoculated was calculated from one plant and LMB449 (pRL100036::mTn5) was averaged from two plants ± SEM.

8.2.2 The putative AAA+ protease encoded by pRL100036-35 shows significant homology to a toxin-antitoxin system (IetAS) in *Agrobacterium tumefaciens*
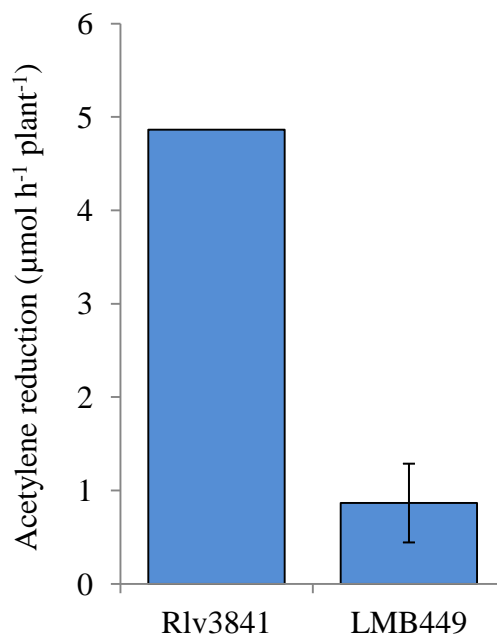
A search of the literature revealed that the putative AAA+ protease encoded by pRL100036-35 was homologous to IetA and IetS in *Agrobacterium tumefaciens* (59% and 50% amino acid identity, respectively) (Table 8.1) (Yamamoto et al., 2007; Yamamoto et al., 2009). IetA and IetS have been proposed to function as a toxin-antitoxin system that contributes to plasmid stability and incompatibility. It was speculated that the antitoxin (IetA) is able to neutralise the effects of its cognate toxin (IetS) by interacting with IetS or its target molecule (Yamamoto et al., 2009). This ensures plasmid stability because if the plasmid harbouring *ietAS* is lost from the host cell, the antitoxin is quickly degraded allowing the IetS toxin to initiate cell death or arrest cell growth (Fig 8.9) (Yamamoto et al., 2009; Yamaguchi et al., 2011). It is not known how IetS causes toxicity but synthesis of IetS in the absence

of IetA resulted in poor growth growth and reduced cell viability of *A. tumefacies* (Yamamoto et al., 2009).

Organism	Locus tag	AA identity (%)	Putative Product	No. of intervening nucleotides
Agrobacterium tumefaciens	Atu6082 (ietA)	100	AAA+	3
	Atu6083 (ietS)	100	Protease	
Xanthobacter autotrophicus	Xaut_4803	82	AAA+	0
	Xaut_4804	79	Protease	
Beijerinckia indica	Bind_2677	65	AAA+	15
	Bind_2676	51	Protease	
Rhizobium etli	RHE_PD00006	62	AAA+	−1
	RHE_PD00007	49	Protease	
Rhizobium leguminosarum	pRL100036 (*ietA*)	59	AAA+	15
	pRL100035 (*ietS*)	50	Protease	
Syntrophobacter fumaroxidans	Sfum_2857	54	AAA+	21
	Sfum_2858	43	Protease	
Magnetococcus **sp. strain MC-1**	Mmc1_1291	52	AAA+	20
	Mmc1_1292	40	Protease	
Thiobacillus denitrificans	Tbd_1692	52	AAA+	20
	Tbd_1693	41	Protease	
Anaeromyxobacter **sp. Fw109-5**	Anae109_4229	55	AAA+	90
	Anae109_4230	42	Protease	
Rhodococcus jostii	RHA1_ro11077	56	AAA+	17
	RHA1_ro11076	41	Protease	
Hahella chejuensis	HCH_03415	48	AAA+	17
	HCH_03413	39	Protease	

Table 8.1 Orthologues of IetAS from *A. tumefaciens*. Pink highlights Rlv3841. No. of intervening nucleotides corresponds to the number of nucleotides that separate the two open reading frames. AA= amino acid. Adapted from Yamamoto *et al.*, 2009.
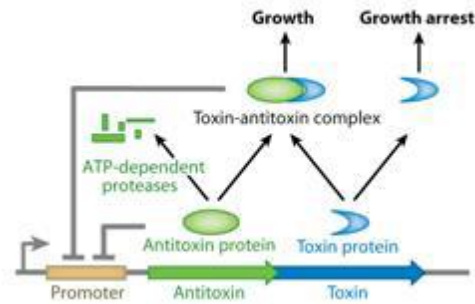
Fig 8.9 Model for the toxin-antitoxin system. The toxin and antitoxin are constitutively expressed; the toxin and its cognate antitoxin form a stable complex that attenuates the toxin's function. The antitoxin is less stable than the toxin or is targeted for proteolysis. Consequently, when the plasmid is lost, the antitoxin is quickly degraded, freeing toxins and enabling their toxic function. Reproduced from Yamaguchi *et al.*, 2011.

It is interesting that a putative toxin-antitoxin system should be located on pRL10 (the Sym plasmid) as this plasmid contains many of the genes essential to symbiosis, including the *nod* genes and the N$_2$ fixation genes (Young et al., 2006). Like *ietAS* in *A. tumefaciens*, pRL100036-35 is located near the *repABC* replicon, which is required for plasmid segregation and replication (Cevallos et al., 2008; Yamamoto et al., 2009; Mazur et al., 2011). Hereafter, owing to the homology the pRL100036-35-encoded putative AAA+ protease has with IetAS, pRL100036-35 is provisionally annotated as *ietAS*.
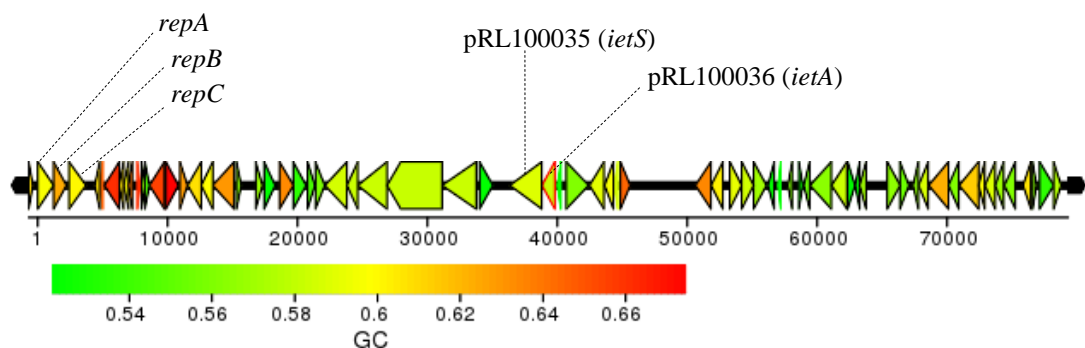

Fig 8.10 Map showing the location of *ietAS* (pRL100036-35) relative to *repABC* on pRL10 (Sym plasmid). Values correspond to length of region (base pairs).

185

8.2.3 RU4067 (*ietA*::mTn5) can be complemented by *ietA* alone and *ietAS* is not required for symbiosis

It is likely that *ietA* and *ietS* share the same operon as the open reading frames are only separated by 15 nt (Table 8.1). Therefore, the mTn5 insertion at *ietA* is likely to cause either a polar-mutation that would null expression or a non-polar mutation that would only reduce the expression of *ietS*. Non-polar mutations caused by the mTn5 construct present in RU4067 (*ietA*::mTn5) (Reeve et al., 1999; Karunakaran et al., 2009) have been reported in other studies, indeed the symbiotic defect caused by *sitA*::mTn5 in *S. meliloti* (see Chapter four) could be rescued by a plasmid containing *sitA* alone (as opposed the entire *sitABCD* operon) (Davies and Walker, 2007b). If expression of *ietS* is only reduced, the low levels of the IetS-toxin could be diluted out in free-living cells as a result of cellular division. In bacteroids however, which do not divide, a low level of *ietS* expression would eventually cause a high accumulation of the toxic IetS. Furthermore, bacteroids undergo extensive endoreduplication during symbiosis (having approximately 8-12 copies of the genome) (Mergaert et al., 2006; Prell et al., 2009), meaning that there might be multiple copies of *ietS* in bacteroids, resulting in higher levels of the toxin.

To test whether *ietA* alone could complement the symbiotic phenotype of RU4067 (*ietA*::mTn5), a plasmid containing *ietA* was constructed. Primers pr1237 and pr1238 were used to amplify *ietA* and the PCR product was cloned into pJET1.2/blunt, to make pLMB551. An *Xba*I/*Bam*HI fragment containing *ietA* was then cloned into *Xba*I/*Bam*HI digested pJP2, resulting in pLMB568. Plasmid pLMB568 was conjugated into RU4067 (*ietA*::mTn5) to create LMB472 (*ietA*::mTn5 pJP2*ietA*).

The plasmid pJP2*ietA* could complement RU4067 (*ietA*::mTn5) (Fig 8.11), supporting the hypothesis that if *ietS* is expressed in RU4067 (*ietA*::mTn5), IetA can suppress the toxicity of IetS and subsequently, rescue the symbiotic phenotype.

Alternatively, it could mean that the requirement of IetA is independent of IetS. Therefore, to determine whether *ietA* is essential or non-essential for symbiosis in the absence of *ietS*, a ~1.5 kb deletion was made in the putative *ietAS* operon (Fig

8.12). To make a deletion, primers pr1247 and pr1248 were used to amplify a 928 bp region containing the beginning 759 bp of *ietA* and primers pr1249 and pr1250 were used to amplify a 984 bp region containing 972 bp from the 3′ end of *ietS* (Fig 8.12). Both the PCR products were cloned into pJET1.2/blunt vectors, resulting in pLMB554 and pLMB555, respectively. An *Xho*I/*Bam*HI fragment from pLMB554 containing the 759 bp of *ietA* was cloned into *Xho*I/*Bam*HI digested pJQ200SK, to make pLMB566. A *Bam*HI/*Xba*I fragement from pLM555 containing 972 bp of *ietS* was then cloned into *Bam*HI/*Xba*I digested pLMB566, to make pLMB567. A *Bam*HI fragment containing ΩSpc cassette was cloned into *Bam*HI digested pLMB567, resulting in pLMB578. The plasmid pLMB578 was conjugated into Rlv3841 to make LMB482 (Δ*ietAS*ΩSpc). After inoculating *P. sativum* with LMB482 (Δ*ietAS*ΩSpc), it was revealed that the rate of acetylene reduction for the mutant was similar to Rlv3841, confirming that IetAS is not required for symbiosis.
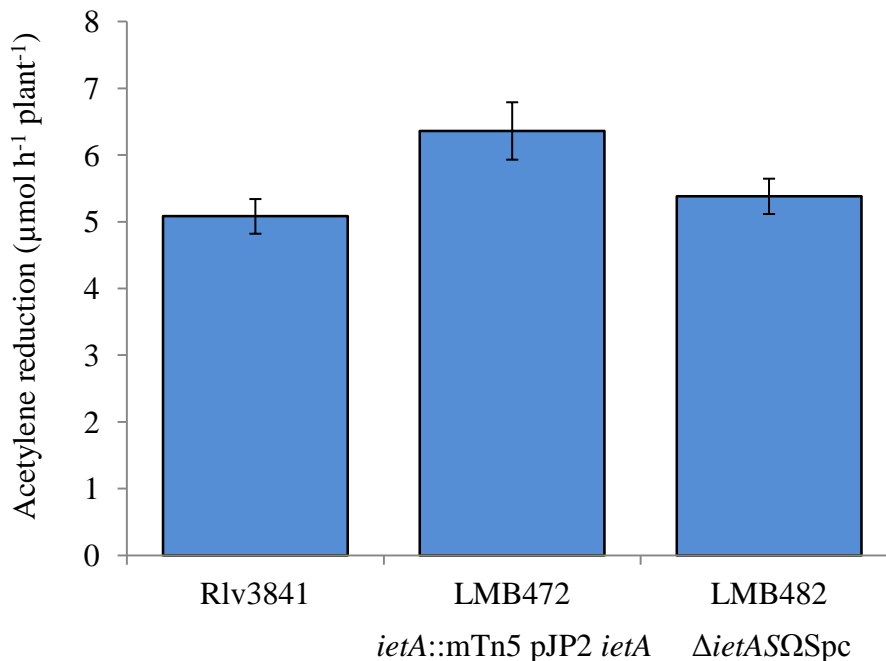
Fig 8.11 Rates of acetylene reduction for Rlv3841, LMB472 (*ietA*::mTn5 pJP2 *ietA*) and LMB482 (Δ*ietAS*ΩSpc) on *P. sativum*. Averaged from five plants ± SEM.
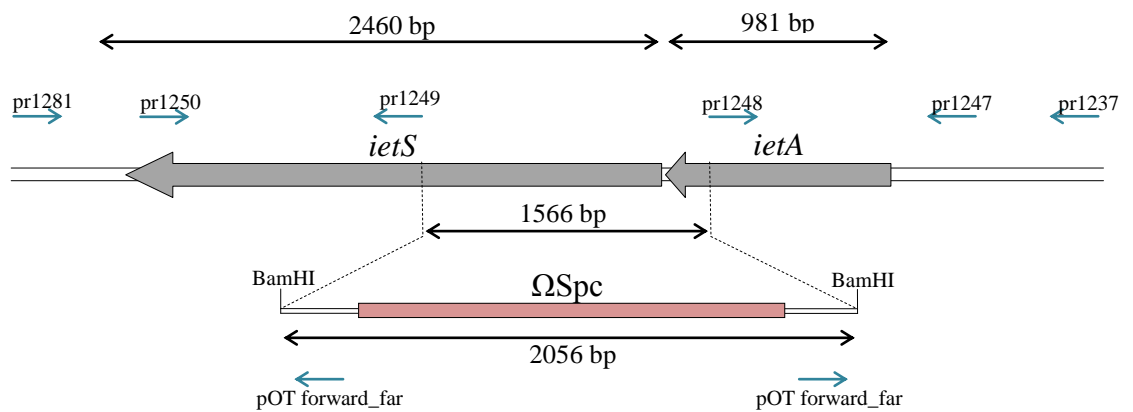
Fig 8.12 Deletion of a ~1.5 kb region from *ietAS*. The deletion and the presence of the ΩSpc cassette were confirmed by PCR with primers pOT forward_far with pr1237 and pOT forward_far with pr1281.

A strain carrying a single pK19mob integration in *ietS* was also constructed to confirm that IetS is not essential for symbiosis. Primers pr1189 and pr1190 were used to amplify the internal fragment of pRL100035 and the PCR product was cloned into pK19mob using the BD In-Fusion™ cloning kit (2.3.6) to create pLMB540. Plasmid pLMB540 was conjugated into Rlv3841 to make LMB457 (*ietS*:pK19mob). *P. sativum* was inoculated with LMB457 (*ietS*:pK19mob), grown for three weeks and Fig 8.13 shows that the rate of acetylene reduction for LMB457 (*ietS*:pK19mob) was equivalent to Rlv3841.
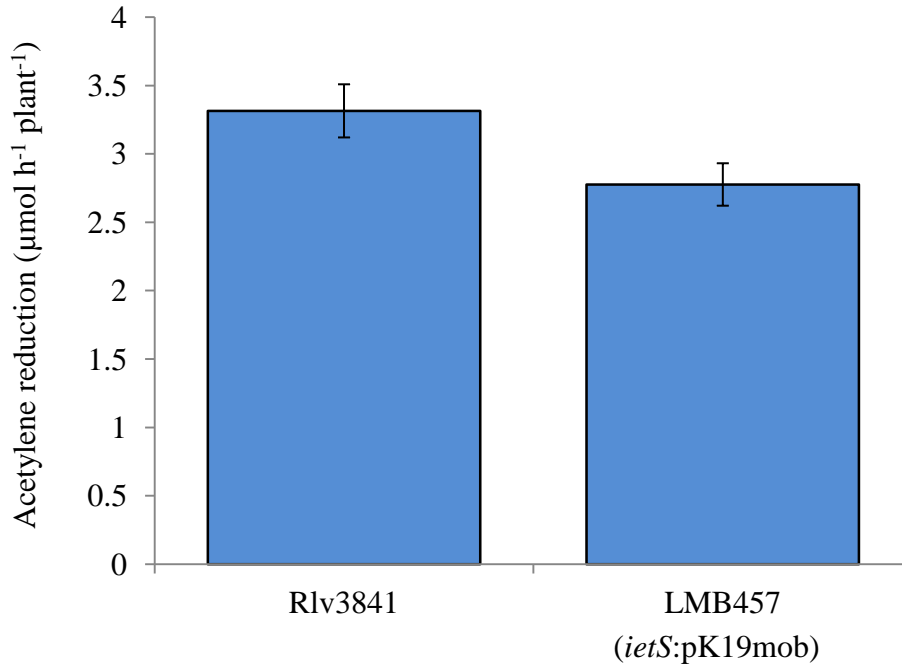
Fig 8.13 Rates of acetylene reduction for Rlv3841 and LMB457 (pRL100035:pK19mob) on *P. sativum*. Averaged from five plants ± SEM.

8.2.4 pRL80012-13 is located next to *repABC*

When considering the role of pRL80012-13 it was observed that the closest homologue to pRL80012 is *ietA* (32% amino acid identity) (Altschul et al., 1990; Young et al., 2006). Furthermore, like *ietAS*, pRL80012-13 is located near to the *repABC* operon (Fig 8.14) on the plasmid pRL8. Plasmid pRL8 contains a number of genes that are upregulated specifically in the pea rhizosphere (Ramachandran et al., 2011). To test if there is any redundancy between the two AAA+ proteins encoded by *ietA* and pRL80012, the double mutant LMB581 (pRL80012:pK19mob ΔietASΩSpc) was constructed by transducing ΔietASΩSpc into LMB365 (pRL80012:pK19mob). LMB581 (pRL80012:pK19mob ΔietASΩSpc) was inoculated onto *P. sativum* and harvested after three weeks. The plants inoculated with LMB581 (pRL80012:pK19mob ΔietASΩSpc) appeared healthy, had pink elongated nodules but unfortunately, due to a malfunction of the gas chromatograph on the day of harvest, rates of acetylene reduction could not be measured.
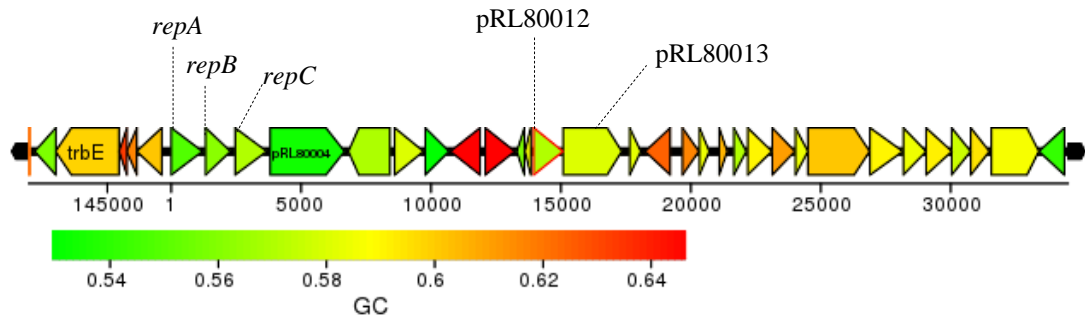
Fig 8.14 Map showing the location of pRL80012-13 relative to *repABC* on pRL8. Values correspond to length of DNA (base pairs).

A single mutation in pRL80013 was also made by pK19mob integration. Primers pr1192 and pr1193 were used to amplify the internal fragment of pRL80013. The PCR product was then cloned into pK19mob using the BD In-Fusion™ cloning kit (2.3.6) to create pLMB541. Plasmid pLMB541 was conjugated into Rlv3841 to make LMB458 (pRL80013:pK19mob. The double mutant LMB571 (pRL80013:pK19mob Δ*ietAS*ΩSpc) was also constructed by transducing Δ*ietAS*ΩSpc from LMB482 into LMB458 (pRL80013:pK19mob). Rates of acetylene reduction for LMB457 (pRL80013:pK19mob) and LMB571 (pRL80013:pK19mob Δ*ietAS*ΩSpc) were the same as Rlv3841, confirming that the two AAA+ proteases are not essential for symbiosis (Fig. 8.15).
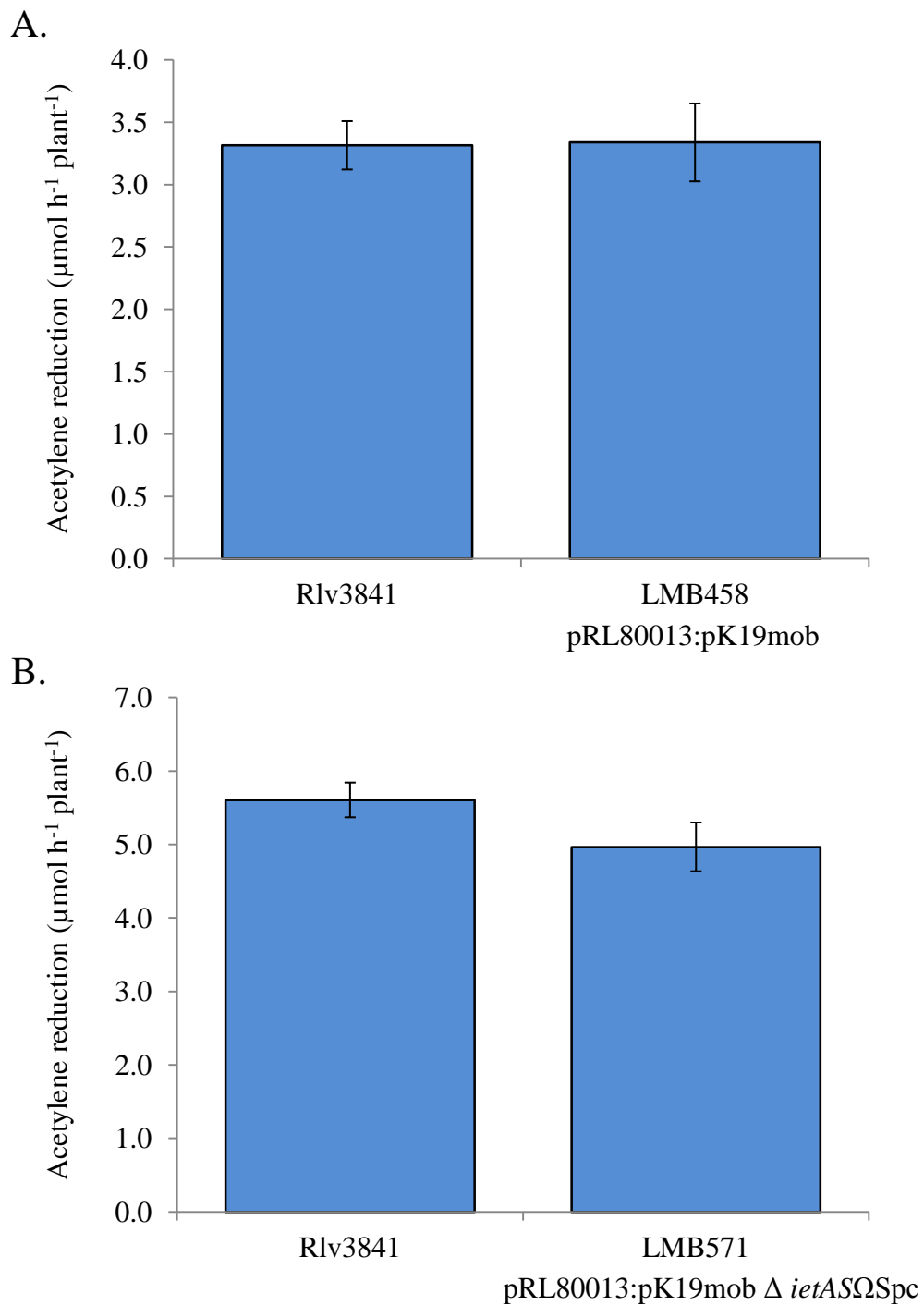
Fig 8.15 Rates of acetylene reduction for Rlv3841, LMB458 (pRL80013::pK19mob) (A) and LMB571 (pRL80013:pK19mob Δ*ietAS*ΩSpc) (B) on *P. sativum*. Averaged from five plants ± SEM.

8.2.5 Putative operons *ietAS* and pRL80012-13 confer resistance to 5% EtOH but not to tested antibiotics

Although low expression of *ietS* in the absence of *ietA* is likely to cause more toxicity to a non-dividing cell (i.e a bacteroid), it is possible that it would cause a level of toxicity in dividing cells (i.e. free-living cells) too. RU4067 (*ietA*::mTn5) did have a moderate growth phenotype in modified AMS glucose, reaching a lower maximal OD_{600} relative to Rlv3841 and having slower mean generation time of ~6 hrs (c.f. ~ 4 hrs for Rlv3841) (Fig 8.16A). However, LMB457 (*ietS*:pK19mob) shows an almost identical growth phenotype to RU4067 (*ietA*::mTn5) (Fig 8.16A) and furthermore, even though LMB482 (Δ*ietAS*ΩSpc) had a mean generation time of ~4 hrs, like RU4067 (*ietA*::mTn5) and LMB457 (*ietS*:pK19mob), it reached a lower maximal OD_{600} (Fig 8.16A). Therefore, the growth phenotype for RU4067 (*ietA*::mTn5) cannot be explained by low expression of *ietS* in the absence of IetA. LMB365 (pRL80012:pK19mob) and LMB458 (pRL80013:pK19mob) were also tested for growth and they too show a long mean generation time of ~6 hrs (Fig 8.16B). However, experiments measuring growth of all the AAA+ protease mutants have only been conducted once and therefore need to be repeated.

Other studies have shown AAA+ proteases to confer resistance to stresses such as EtOH, oxidative stress and heat stress (Gerth et al., 1998; Chatterjee et al., 2005; Xie et al., 2013). For this reason, cells were grown in AMS glucose with 5% EtOH (2.5.4) and Figs 8.16A and 8.16B suggest that mutants defective for either of the AAA+ proteases are hypersensitive to EtOH.
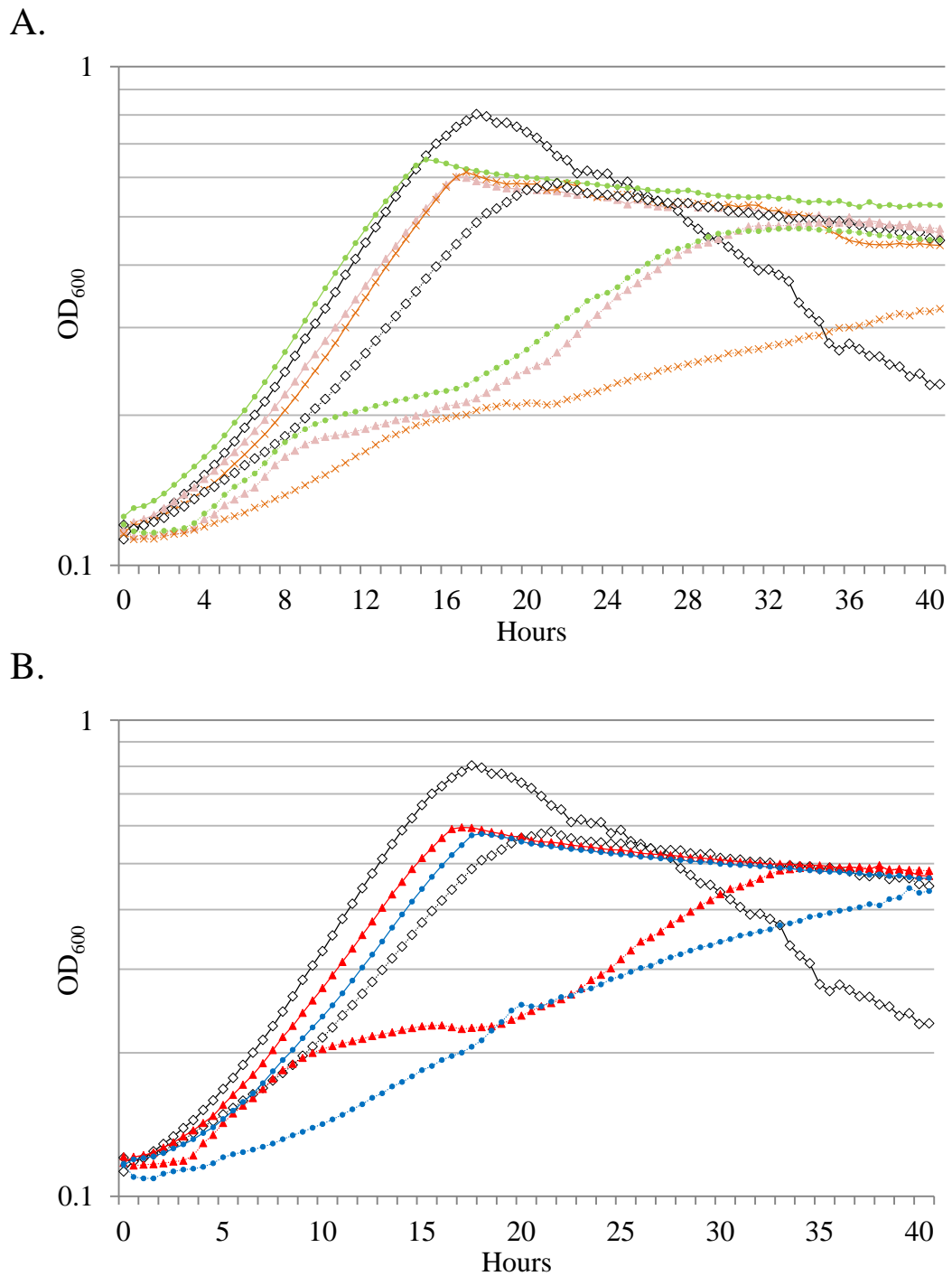
Fig 8.16 Growth of Rlv3841 and mutants in AMS glucose (solid line) and AMS glucose with 5% EtOH (broken line). Shown in (A) is Rlv3841 [white diamonds], RU4067 (*ietA*::mTn5) [pink triangles], LMB457 (*ietS*:pK19mob) [orange crosses) and LMB482 (Δ*ietAS*ΩSpc) [green circles]. Shown in (B) is Rlv3841 [white diamonds], LMB365 (pRL80012:pK19mob) [red triangles] and LMB458 (pRL80013:pK19mob) [blue circles]. Data from one experiment.

Mutations in genes encoding for AAA+ proteases have also been shown to cause sensitivity to various antibiotics (Rajagopal et al., 2002; Ulvatne et al., 2002; Yamaguchi et al., 2003; Gilbert et al., 2007; Hinz et al., 2011; Fernandez et al., 2012; McGillivray et al., 2012). Therefore, the sensitivity of Rlv3841, LMB482 (Δ*ietAS*ΩSpc), LMB365 (pRL80012:pK19mob) and LMB581 (pRL80012:pK19mob Δ*ietAS*ΩSpc) to gentamicin, polymyxin, chloramphenicol, piperacillin, ampicillin, tetracycline, rifampicin and bacitracin was also tested. RU4040 (*bacA*:pK19mob) (Karunakaran et al., 2009) was used a positive control as BacA had been shown to confer resistance to a number of antibiotics (Ichige and Walker, 1997; Ferguson et al., 2002; Karunakaran et al., 2009).

Disk assays (2.5.7) show that RU4040 (*bacA*:pK19mob) was hypersensitive to chloramphenicol, piperacillin, rifampicin, tetracycline and ampcillin. However, none of the AAA+ protease mutants were hypersensitive to any of the antibiotics at the tested concentrations.

Fig 8.17

Fig 8.17 *Cont'd*

Tetracycline (0.5 mg/ml)

Ampicillin (5 mg/ml)
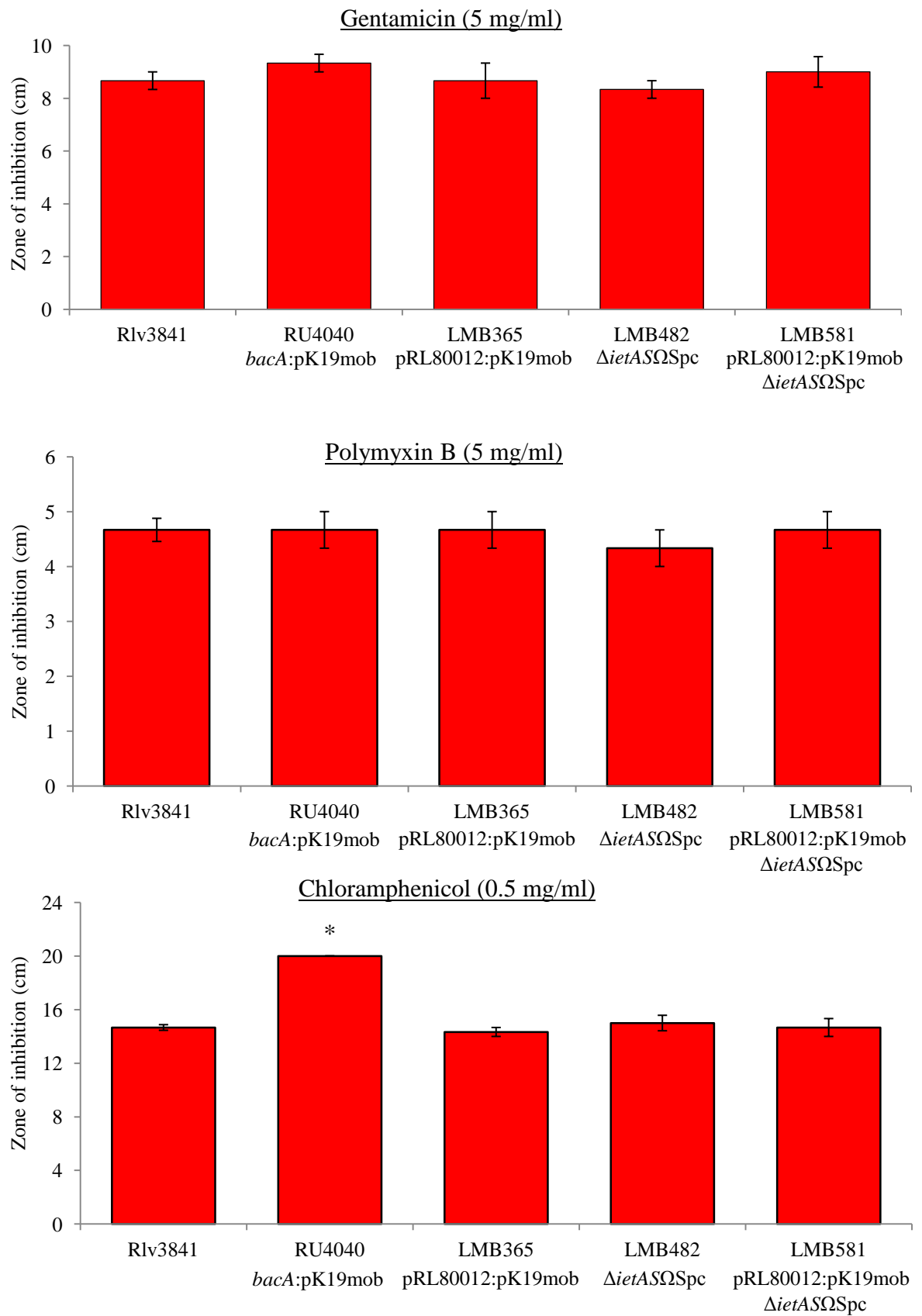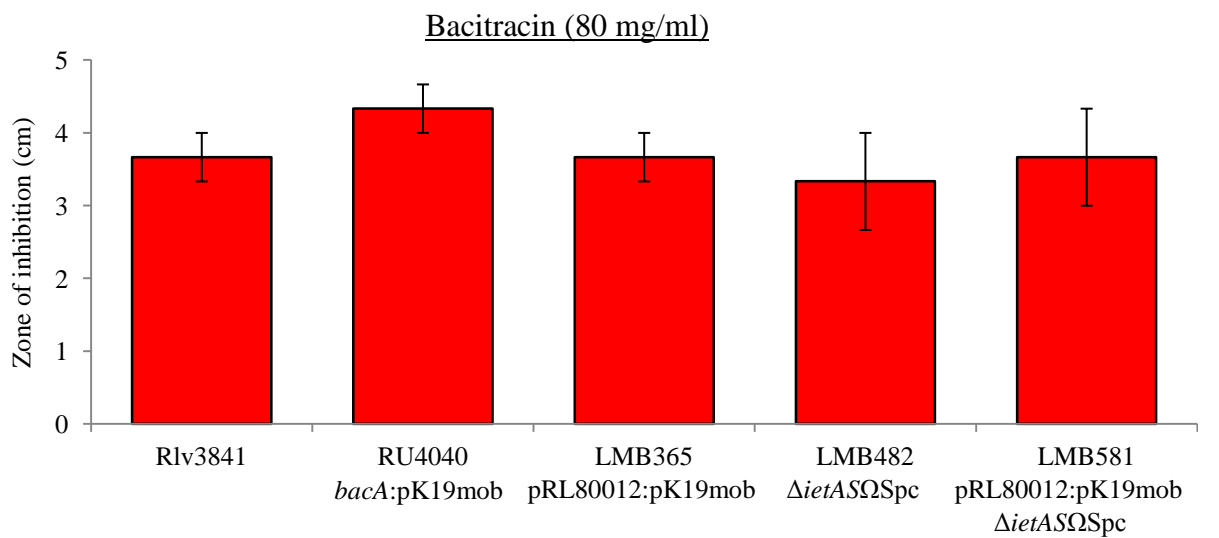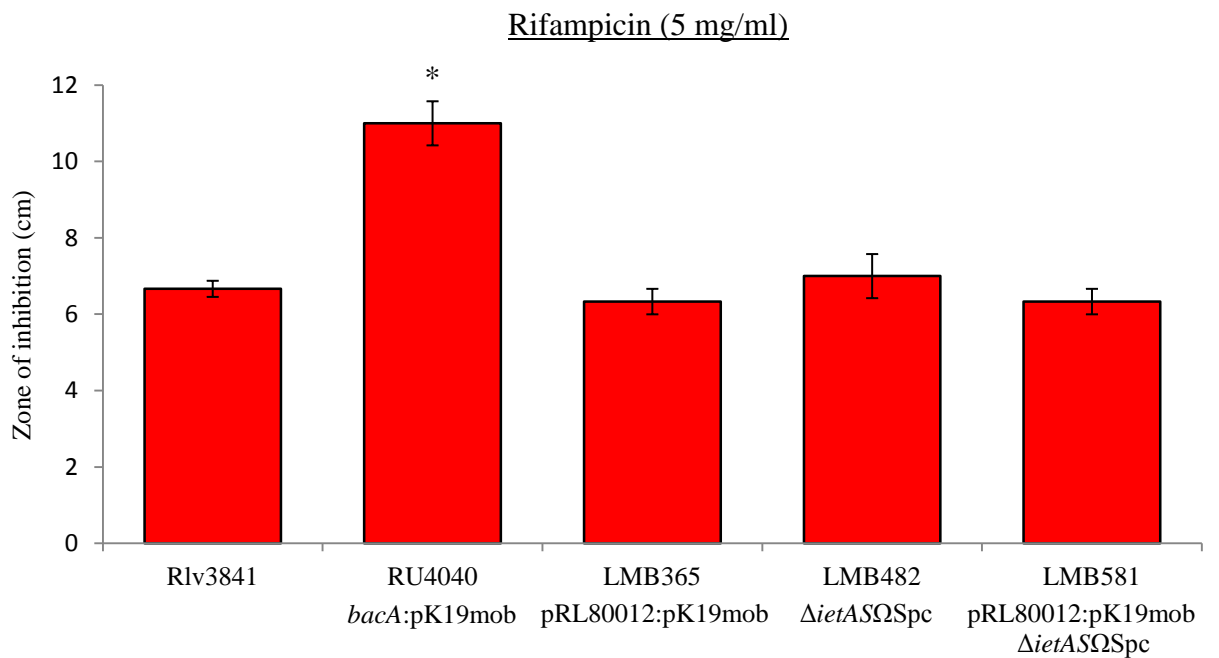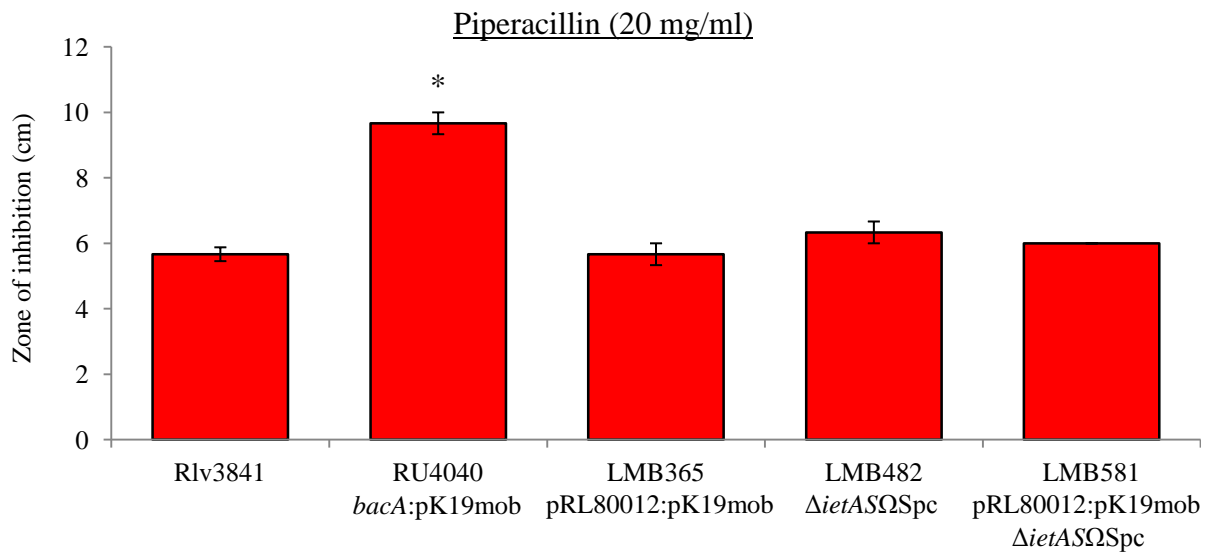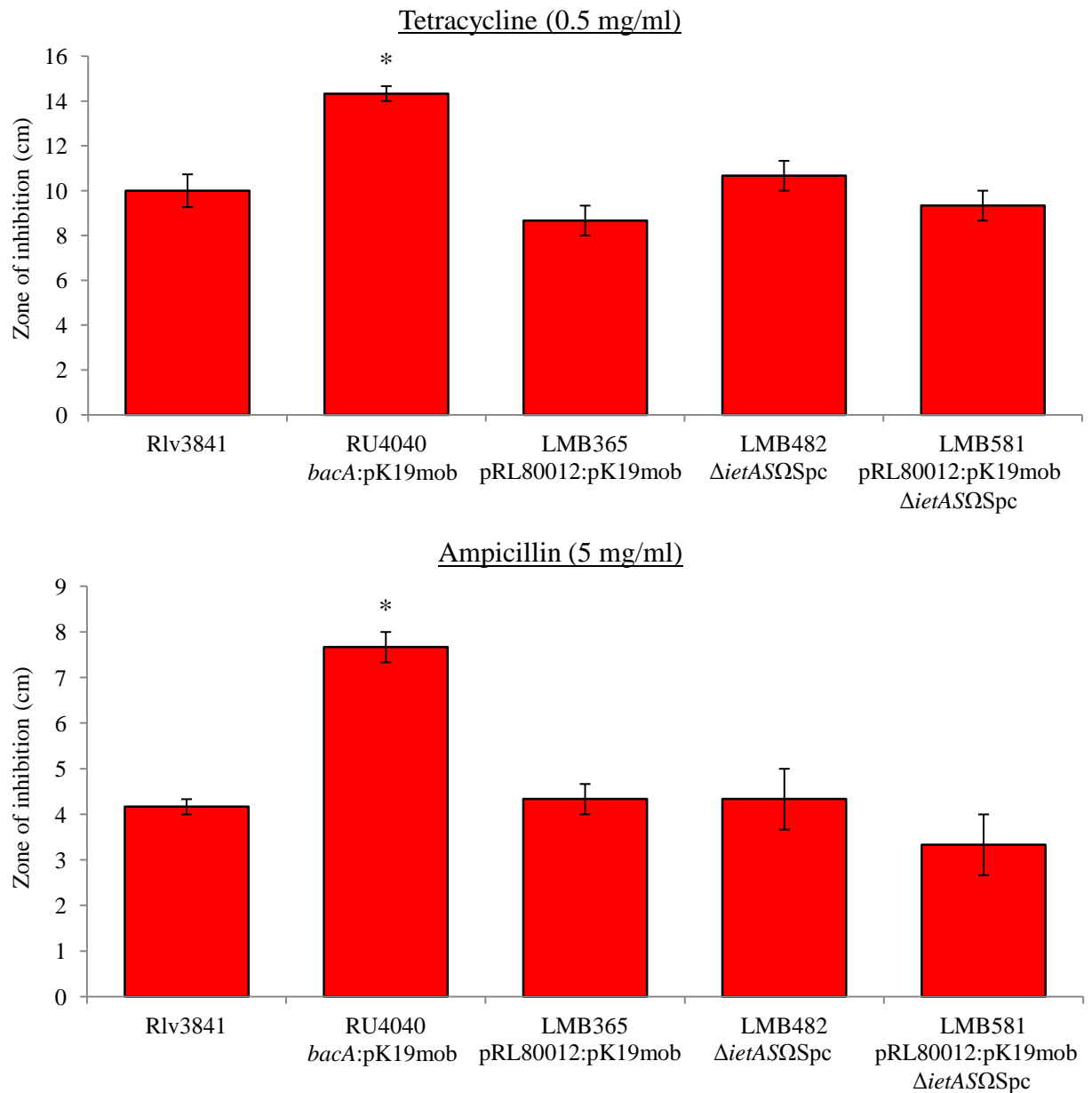
Fig 8.17 *Cont'd* Disc assays testing the sensitivity of Rlv3841, RU4040 (*bacA*:pK19mob), LMB365 (pRL80012:pK19mob), LMB482 (Δ*ietAS*ΩSpc) and LMB581 pRL80012:pK19mob Δ*ietAS*ΩSpc) to gentamicin (5 mg/ml), polymyxin B (5 mg/ml), chloramphenicol (0.5 mg/ml), piperacillin (20 mg/ml), rifampicin (5 mg/ml), bacitracin (80 mg/ml), tetracycline (0.5 mg/ml) and ampicillin (5 mg/ml). Averaged from three independent experiments ± SEM. * indicates a statistically significant (p ≤ 0.05) difference relative to Rlv3841.

197

8.3 CONCLUSION

The putative AAA+ protease encoded by *ietAS* (pRL100036-35) shows homology to a toxin-antitoxin system (Table 8.1) that is required for plasmid stability and incompatibility in *A. tumefaciens* (Yamamoto et al., 2007; Yamamoto et al., 2009). The putative AAA+ protease encoded by pRL80012-13, like *ietAS* in Rlv3841 and *A. tumefaciens*, is proximal to the *repABC* operon and the closest homologue for the AAA+ protein (pRL80012) is IetA; this suggests that pRL80012-13 may also encode a toxin-antitoxin system. However, further experimentation is required to determine if *ietAS* and pRL80012-13 confer plasmid stability and resistance against incompatible plasmids.

Although the presence of the IetS toxin may cause a symbiotic defect in the absence of IetA antitoxin (Figs 8.3-8.7), the IetAS system is not essential for symbiosis (Fig 8.11). Expression of *ietS* still needs to be demonstrated by qRT-PCR in RU4067 (*ietA*:mTn5) and the putative toxicity of IetS requires further investigation.

If the AAA+ proteases encoded by *ietAS* and pRL80012-13 are required for plasmid maintenance, they may also have a dual role in the stress response as disruption of either operon causes hypersensitivity to EtOH (Fig 8.16). A role in stress response could explain why pRL80012-13 is upregulated in developing bacteroids. One model that explains how AAA+ protease toxin-antitoxin systems could have dual roles in plasmid maintenance and stress response is: in the presence of IetA, IetAS targets misfolded of denatured proteins but in the absence of IetA, IetS may bind to an alternative AAA+ protein that would change its specificity to proteins with an essential cellular function.

Chapter 9: *Future perspectives*

9.1 SCREENING

The initial aim of this study was to investigate processes required for nodule-colonisation and bacteroid development. In Rlv3841, mutations were made in forty-two genes that were upregulated during bacteroid development. Even though five of the mutant strains were moderately reduced in their ability to initiate nodules and reduce acetylene on *P. sativum* (or *V. faba* in one case), it was evident that there was functional redundancy between certain genes. Instead of focusing on individual mutations that may cause moderate phenotypes or conducting further screening, e.g. ability of mutants to compete with Rlv3841 for nodule-colonisation, it was decided to investigate functional redundancy in order to further our understanding of critical processes during bacteroid development.

9.2 Mn^{2+} TRANSPORT

The most obvious example of functional redundancy was between the Mn^{2+} transporters SitABCD and MntH. The double mutant LMB466 (*sitA*:pK19mob *mntH*ΩSpc) was symbiotically-defective on *P. sativum*, whereas single mutations in *sitA* and *mntH* did not cause any obvious phenotypes (Fig 4.11). Transport assays, including experiments that test the ability of SitABCD and MntH to transport Fe^{2+} (in addition to Mn^{2+}) should be a prioritised because to this date, no bacterial Fe transporter is known to be essential for symbiosis. Further work is also needed to determine the stage at which bacteroid development of LMB466 (*sitA*:pK19mob *mntH*ΩSpc) is impeded. This is likely to involve quantifying infection threads, the use of cell-permeable fluorescent dyes e.g. SYTO 13 (stains nucleic acids) (Haynes et al., 2004) and visualisation of LMB466 (*sitA*:pK19mob *mntH*ΩSpc) carrying gfp/DsRed by confocal microscopy (Gage, 2002).

Mn^{2+} transporters are required by *R. leguminosarum* to develop into N_2-fixing bacteroids in indeterminate nodules formed on *P. sativum*, *V. faba* and *V. hirsuta*

(Figs 4.11, 4.18 and 4.22) but not in determinate nodules formed on *P. vulgaris* (Fig 4.24). Similarly, *S. meliloti* strains carrying mutations in *sitA* were reduced in their ability to fix N_2 in indeterminate nodules formed on *M. sativa* (Chao et al., 2004; Davies and Walker, 2007b) whereas MntH was not required by *B. japonicum* to form N_2-fixing bacteroids in determinate nodules formed on *G. max*, despite MntH being essential for growth in low concentrations of $MnCl_2$ (Hohle and O'Brian, 2009). Possible explanations for these differences include variability in the bioavailability of Mn^{2+}, varying levels of ROS or alternatively, the presence of NCR peptides in indeterminate nodules formed on galegoid legumes (e.g. *P. sativum*, *V. faba*, *V. hirsuta* and *M. sativa*) but absence in determinate nodules on phaseoloid legumes (e.g. *P. vulgaris*, *G.* max). This leaves a number of hypotheses that need to be tested.

The small quantity of Mn^{2+} in cells means that AAS should not be used to quantify Mn^{2+} and so alternative methodologies would have to be employed to determine if more Mn^{2+} is present in determinate relative to indeterminate nodules (discussed later). ROS could be visualised using Nitroblue tetrazolium (Santos et al., 2001), cerium chloride (Rubio et al., 2004) or ROS-sensitive fluorescent dyes (Cardenas et al., 2008) but determining whether there is a significant difference in the level of ROS in contact with bacteria infecting indeterminate nodules relative to determinate nodules would be difficult. Investigating the requirement of Mn^{2+} transporters in the presence of NCR peptides, may include testing whether a higher a concentration of Mn^{2+} is required to rescue growth of LMB466 (*sitA*:pK19mob *mntH*ΩSpc) when NCR peptides are added to the medium or alternatively, testing cell viability of Mn^{2+} starved cells in response to NCR peptides. In addition, the dye hydroxyphenyl fluorescein (HPF) (Setsukinai et al., 2003) could be used to test whether the presence of NCR peptides stimulates HO˙ generation in bacteria (Kohanski et al., 2007).

Mn^{2+} transport should be investigated in *M. loti*. Firstly, because the requirement of Mn^{2+} could be tested on another plant-host, *L. japonicus* (a robinioid legume that does not synthesis NCR peptides), and secondly, there are transgenic lines of *L. japonicus* available that can synthesise NCR035 peptide (Van de Velde et al., 2010). Thus, if a *M. loti* mutant lacking high-affinity Mn^{2+} transporters is Fix[+] on *L. japonicus* but Fix[-] on the NCR035-synthesising transgenic line, it would provide strong evidence for the NCR peptide-dependent requirement of Mn^{2+} transporters.

9.3 Mg^{2+} TRANSPORT

The discovery of a host-dependent requirement for Mn^{2+} transporters prompted characterisation of a putative Mg^{2+} channel, MgtE, known to be required for effective symbiosis on *P. sativum* (Karunakaran et al., 2009). MgtE was confirmed as a Mg^{2+} importer by its ability to complement an *E. coli* triple knock-out strain that could not grow on LB unless supplemented with a high concentration of $MgSO_4$ (Fig 5.2). Further characterisation of MgtE in free-living cells should include transport assays. Commercial availability of $^{28}Mg^{2+}$ is poor so kinetic studies will likely involve the use of cell-permeable fluorescent probes that can bind free Mg^{2+} ions e.g. Mag-fura (Life technologies) (London, 1991; Froschauer et al., 2004).

As with the *sitA*:pK19mob *mntH*ΩSpc double mutant defective for Mn^{2+} transport, the requirement of MgtE also depended upon the plant-host because RU4107 (*mgtE*::mTn5) was symbiotically defective on *P. sativum* and *V. hirsuta* (Figs 5.5 and 5.10) but not on *V. faba* (Fig 5.12). The quantification of Mg in the plant cytosol of *P. sativum* and *V. faba* nodules by AAS did not explain this difference in MgtE-requirement because *P. satium* nodules contained higher levels of Mg relative to *V. faba* nodules (Fig 5.15B). Analysis of nodule sections using synchrotron-based X-ray fluorescence (S-XRF) might prove to be more informative because this technique can spatially define the location of metals at a subcellular resolution (Rodriguez-Haas et al., 2013). For example, even though there is more total Mg in *P. sativum* nodules, S-XFR might reveal that there is more Mg allocated to the N_2 fixation zone in *V. faba* nodules. S-XFR might also determine if there is more Mn in *G. max* and *P. vulgaris* nodules relative to *P. sativum* etc., as is it can detect metals at submicromolar concentrations (Rodriguez-Haas et al., 2013).

Although the experiment needs to be repeated in an appropriately buffered-medium, the requirement of MgtE appeared to be dependent on pH (Fig 5.4) so the acidity of *P. sativum, V. hirsuta* and *V. faba* nodules should be investigated. This could be achieved by the use of cell-permeable fluorescent probes that can accurately measure pH i.e. DND-160 (Pierre et al., 2013). This might reveal that the symbiotic space

enclosing bacteroids in *P. sativum* and *V. hirsuta* nodules is more acidic relative to *V. faba* nodules.

It is possible that a plant-encoded Mg^{2+} transporter located on the symbiosome membrane, present in *V. faba* but not in *P. sativum* nodules, causes the difference in MgtE-requirement. If variation in the symbiotic-phenotype of RU4107 (*mgtE*::mTn5) existed between the parents of an available recombinant inbreed line (RIL) population of *P. sativum*, *V. hirsuta* or *V. faba*, the RILs could be used to map the relevant plant genes e.g. a plant gene that encodes an Mg^{2+} transporter.

It is also important to determine whether the requirement of MgtE on certain legumes is dependent on its ability to transport Mg^{2+} or on another property of MgtE e.g. possible redox function of the CBS domains (Yoo et al., 2011). Firstly, this will require making specific point mutations in *mgtE* that would render MgtE incapable of transporting Mg^{2+} (determined by complementation of the *E. coli* triple knock-out strain), as was done for *mgtE* in *P. aeruginosa* (Anderson et al., 2008). The ability of these MgtE-variants to complement the symbiotic defect of RU4107 (*mgtE*::mTn5) could then be tested. If MgtE-variants incapable of Mg^{2+} transport are able to complement the symbiotic defect of RU4107 (*mgtE*::mTn5) it would imply that the requirement of MgtE is independent of its ability to transport Mg^{2+}. Comparing the transcriptome of RU4107 (*mgtE*::mTn5) bacteroids with Rlv3841 bacteroids may also shed light on the role of MgtE e.g. are there upregulated-genes encoding other Mg^{2+} transporters or proteins involved in defence against ROS in the mutant bacteroids?

9.4 REGULATION OF *fix* GENES

The genes encoding for O_2-responsive regulators FnrN and FixL were upregulated during bacteroid development in addition to a gene encoding a FixL-homologue (FixLc). FnrN appears to be the major O_2-responsive regulator required for N_2 fixation but all three regulators need to be mutated to cause a Fix$^-$ phenotype (Fig 6.8).

Comparing the number of O_2-responsive regulators in Rlv3841 to *S. meliloti*, *A. caulinodans* and *B. japonicum* raises the question: why does *R. leguminosarum* have three O_2-responsive regulators? It is possible that, even though there is going to be some cross over between the regulatory pathways that they activate, some pathways may be unique to each regulator. Furthermore, the pathways activated by these regulators may not just regulate *fix* and *nif* genes, but might also regulate other processes required for bacteroid development in response to low O_2. Future work therefore should include chromatin immunoprecipitation experiments followed by sequencing (ChIP-seq) (Johnson et al., 2007; Mikkelsen et al., 2007; Furey, 2012) to first determine the regulon of FnrN but then to determine the regulons of the other five CRP/FNR-type regulators and FxkR. This sort of global analysis will shed light on the regulatory pathways required for a free-living cell to develop into a N_2 fixing bacteroid.

9.5 IetAS

A putative AAA+ protease, provisionally annotated as IetAS, was found to have homology to a plasmid-encoded toxin-antitoxin system in *A. tumefaciens* (Yamamoto et al., 2009). Insertion of a mTn5 at *ietA* (Karunakaran et al., 2009) severely reduced the rate of acetylene reduction on *P. sativum* (Fig 8.3). It is speculated that the *ietA*::mTn5 mutation is non-polar and therefore only reduces the expression of the toxin-encoding *ietS*. Consequently, the toxic IetS would accumulate in non-dividing bacteroids in the absence of its cognate antitoxin. Initially, further investigation should use qRT-PCR to confirm expression of *ietS* in RU4067 (*ietA*::mTn5). Secondly, yeast two-hybrid or bacterial two-hybrid could be used to determine whether IetA interacts with itself and IetS, as has been done with other AAA+ proteases (Lee et al., 2003; Lien et al., 2009).

Further work will determine whether the IetAS system confers maintenance of the Sym plasmid (pRL10), which could be achieved by following the protocols used by Yamamoto *et* al. (2009) to study the comparable toxin-antitoxin system in *A. tumefaciens*. The potential role of IetAS in response to stress (Fig 8.16) should also be investigated, initially by testing the sensitivity of the AAA+ protease mutants to

heat stress, oxidative stress, osmotic stress and NCR peptides. The same should be done for the second putative toxin-antitoxin encoded on pRL8 (pRL80012-13).

An in-depth analysis of the IetAS system will need to investigate how IetS causes toxicity. This might involve defining the substrates of IetAS. One method to identify substrates for AAA+ proteases involves engineering a proteolytically inactive protease to be used a 'trap' (Feng et al., 2013; Graham et al., 2013). IetS^{trap} proteins would retain but not degrade substrates translocated to its degradation chamber. Substrates captured by His-tagged IetS^{trap} would be co-purified and then identified by mass spectroscopy. This method should also confirm that IetS binds to IetA and possibly identify alternative AAA+ protein-binding partners.

9.6 CONCLUDING REMARKS

During bacteroid development, cellular functions of rhizobia change profoundly in response to oxidative stress, low O_2, antimicrobial secondary metabolites, low pH and antimicrobial peptides. The environment provided by a nodule can vary and consequently, a rhizobium's requirement of certain genes during bacteroid development will depend on the species of the host-legume. This has been illustrated in this thesis by the host-dependent requirement of Mn^{2+} transporters and a Mg^{2+} channel. In other rhizobia, reports of host-dependent requirements include an efflux system (Lindemann et al., 2010), phosphoenolpyruvate carboxykinase (Osteras et al., 1991), an uncharacterised ABC-type transport system (Koch et al., 2010), NAD^+-malic enzyme (Zhang et al., 2012), regulation of *nif* and *fix* genes (Miller et al., 2007) and BacA (Karunakaran et al., 2010). There is likely to be many more genes that have a host-dependent requirement yet to be discovered. So far, the study of host-dependent requirements has only identified obvious symbiotic defects e.g. poor nodulation and N_2 fixation. Further research into this area therefore, should also consider competition i.e. does the ability of a rhizobial strain to compete with other strains during nodule-colonisation also depend on the host. Investigating host-dependent requirements would lead to the development of better rhizobial inoculants that are both competitively and symbiotically effective on a wider range of legumes.

References

Abdel-Lateif, K., Bogusz, D., and Hocher, V. (2012) The role of flavonoids in the establishment of plant roots endosymbioses with arbuscular mycorrhiza fungi, rhizobia and Frankia bacteria. *Plant signaling & behavior* **7**: 636-641.

Adams, M.A., Udell, C.M., Pal, G.P., and Jia, Z.C. (2005) MraZ from *Escherichia coli*: cloning, purification, crystallization and preliminary X-ray analysis. *Acta Crystallographica Section F-Structural Biology and Crystallization Communications* **61**: 378-380.

Akaike, T., Sato, K., Ijiri, S., Miyamoto, Y., Kohno, M., Ando, M., and Maeda, H. (1992) Bactericidal activity of alkyl peroxyl radicals generated by heme-iron-catalyzed decomposition of organic peroxides. *Arch Biochem Biophys* **294**: 55-63.

Albus, U., Baier, R., Holst, O., Puhler, A., and Niehaus, K. (2001) Suppression of an elicitor-induced oxidative burst reaction in *Medicago sativa* cell cultures by *Sinorhizobium meliloti* lipopolysaccharides. *New Phytol* **151**: 597-606.

Altschul, S.F., Gish, W., Miller, W., Myers, E.W., and Lipman, D.J. (1990) Basic local alignment search tool. *J Mol Biol* **215**: 403-410.

Amtmann, A., and Blatt, M.R. (2009) Regulation of macronutrient transport. *New Phytol* **181**: 35-52.

Anderson, E.S., Paulley, J.T., Gaines, J.M., Valderas, M.W., Martin, D.W., Menscher, E. et al. (2009) The manganese transporter MntH is a critical virulence determinant for *Brucella abortus* 2308 in experimentally infected mice. *Infect Immun* **77**: 3466-3474.

Anderson, G.G., Moreau-Marquis, S., Stanton, B.A., and O'Toole, G.A. (2008) In vitro analysis of tobramycin-treated *Pseudomonas aeruginosa* biofilms on cystic fibrosis-derived airway epithelial cells. *Infect Immun* **76**: 1423-1433.

Anderson, G.G., Yahr, T.L., Lovewell, R.R., and O'Toole, G.A. (2010) The *Pseudomonas aeruginosa* magnesium transporter MgtE inhibits transcription of the type III secretion system. *Infect Immun* **78**: 1239-1249.

Andrews, S.C., Robinson, A.K., and Rodriguez-Quinones, F. (2003) Bacterial iron homeostasis. *FEMS Microbiol Rev* **27**: 215-237.

Andrews, S.C. (2011) Making DNA without iron - induction of a manganese-dependent ribonucleotide reductase in response to iron starvation. *Mol Microbiol* **80**: 286-289.

Anjem, A., Varghese, S., and Imlay, J.A. (2009) Manganese import is a key element of the OxyR response to hydrogen peroxide in *Escherichia coli*. *Mol Microbiol* **72**: 844-858.

Anjem, A., and Imlay, J.A. (2012) Mononuclear iron enzymes are primary targets of hydrogen peroxide stress. *J Biol Chem* **287**: 15544-15556.

Anthamatten, D., and Hennecke, H. (1991) The regulatory status of the fixL- and fixJ-like genes in *Bradyrhizobium japonicum* may be different from that in *Rhizobium meliloti*. *Mol Gen Genet* **225**: 38-48.

Appleby, C.A. (1984) Leghemoglobin and rhizobium respiraition. *Annu Rev of Plant Physiol and Plant Mol Bio* **35**: 443-478.

Archibald, F.S., and Fridovich, I. (1982) Investigations of the state of the manganese in Lactobacillus plantarum. *Arch Biochem Biophys* **215**: 589-596.

Atack, J.M., Harvey, P., Jones, M.A., and Kelly, D.J. (2008) The *Campylobacter jejuni* thiol peroxidases Tpx and Bcp both contribute to aerotolerance and peroxide-mediated stress resistance but have distinct substrate specificities. *J Bacteriol* **190**: 5279-5290.

Atichartpongkul, S., Loprasert, S., Vattanaviboon, P., Whangsuk, W., Helmann, J.D., and Mongkolsuk, S. (2001) Bacterial Ohr and OsmC paralogues define two protein families with distinct functions and patterns of expression. *Microbiology* **147**: 1775-1782.

Atichartpongkul, S., Fuangthong, M., Vattanaviboon, P., and Mongkolsuk, S. (2010) Analyses of the regulatory mechanism and physiological roles of *Pseudomonas aeruginosa* OhrR, a transcription regulator and a sensor of organic hydroperoxides. *J Bacteriol* **192**: 2093-2101.

Ayala-Castro, C., Saini, A., and Outten, F.W. (2008) Fe-S cluster assembly pathways in bacteria. *Microbiol Mol Biol Rev* **72**: 110-125.

Barloy-Hubler, F., Cheron, A., Hellegouarch, A., and Galibert, F. (2004) Smc01944, a secreted peroxidase induced by oxidative stresses in *Sinorhizobium meliloti* 1021. *Microbiology* **150**: 657-664.

Batut, J., Daveran-Mingot, M.L., David, M., Jacobs, J., Garnerone, A.M., and Kahn, D. (1989) fixK, a gene homologous with fnr and crp from *Escherichia coli*, regulates nitrogen fixation genes both positively and negatively in *Rhizobium meliloti*. *EMBO J* **8**: 1279-1286.

Batut, J., and Boistard, P. (1994) Oxygen control in Rhizobium. *Antonie Van Leeuwenhoek* **66**: 129-150.

Becker, L.A., Bang, I.S., Crouch, M.L., and Fang, F.C. (2005) Compensatory role of PspA, a member of the phage shock protein operon, in rpoE mutant *Salmonella enterica* serovar Typhimurium. *Mol Microbiol* **56**: 1004-1016.

Beinert, H., Holm, R.H., and Munck, E. (1997) Iron-sulfur clusters: nature's modular, multipurpose structures. *Science* **277**: 653-659.

Benson, H.P., Boncompagni, E., and Guerinot, M.L. (2005) An iron uptake operon required for proper nodule development in the *Bradyrhizobium japonicum*-soybean symbiosis. *Mol Plant Microbe Interact* **18**: 950-959.

Beringer, J.E. (1974) R factor transfer in *Rhizobium leguminosarum*. *J Gen Microbiol* **84**: 188-198.

Berlett, B.S., Chock, P.B., Yim, M.B., and Stadtman, E.R. (1990) Manganese(II) catalyzes the bicarbonate-dependent oxidation of amino acids by hydrogen peroxide and the amino acid-facilitated dismutation of hydrogen peroxide. *Proc Natl Acad Sci U S A* **87**: 389-393.

Bhat, N.H., Vass, R.H., Stoddard, P.R., Shin, D.K., and Chien, P. (2013) Identification of ClpP substrates in *Caulobacter crescentus* reveals a role for regulated proteolysis in bacterial development. *Mol Microbiol* **88**: 1083-1092.

Bidle, K.A., Kirkland, P.A., Nannen, J.L., and Maupin-Furlow, J.A. (2008) Proteomic analysis of *Haloferax volcanii* reveals salinity-mediated regulation of the stress response protein PspA. *Microbiology* **154**: 1436-1443.

Blair, J.M., and Piddock, L.J. (2009) Structure, function and inhibition of RND efflux pumps in Gram-negative bacteria: an update. *Curr Opin Microbiol* **12**: 512-519.

Blanc-Potard, A.B., and Groisman, E.A. (1997) The *Salmonella selC* locus contains a pathogenicity island mediating intramacrophage survival. *EMBO J* **16**: 5376-5385.

Bobik, C., Meilhoc, E., and Batut, J. (2006) FixJ: a major regulator of the oxygen limitation response and late symbiotic functions of *Sinorhizobium meliloti*. *J Bacteriol* **188**: 4890-4902.

Boesten, B., and Priefer, U.B. (2004) The C-terminal receiver domain of the *Rhizobium leguminosarum* bv. viciae FixL protein is required for free-living microaerobic induction of the *fnrN* promoter. *Microbiology* **150**: 3703-3713.

Bolintineanu, D., Hazrati, E., Davis, H.T., Lehrer, R.I., and Kaznessis, Y.N. (2010) Antimicrobial mechanism of pore-forming protegrin peptides: 100 pores to kill E. coli. *Peptides* **31**: 1-8.

Bonnet, M., Stegmann, M., Maglica, Z., Stiegeler, E., Weber-Ban, E., Hennecke, H., and Mesa, S. (2013) FixK(2), a key regulator in *Bradyrhizobium japonicum*, is a substrate for the protease ClpAP in vitro. *FEBS Lett* **587**: 88-93.

Brechenmacher, L., Lei, Z., Libault, M., Findley, S., Sugawara, M., Sadowsky, M.J. et al. (2010) Soybean Metabolites Regulated in Root Hairs in Response to the Symbiotic Bacterium *Bradyrhizobium japonicum*. *Plant Physiol* **153**: 1808-1822.

Brewin, N. (2004) Plant cell wall remodelling in the Rhizobium-legume symbiosis. *Crit Rev Plant Sci 23: 293–316.*

Brissette, J.L., Russel, M., Weiner, L., and Model, P. (1990) Phage shock protein, a stress protein of *Escherichia coli*. *Proc Natl Acad Sci U S A* **87**: 862-866.

Brito, B., Toffanin, A., Prieto, R.I., Imperial, J., Ruiz-Argueso, T., and Palacios, J.M. (2008) Host-dependent expression of *Rhizobium leguminosarum* bv. viciae hydrogenase is controlled at transcriptional and post-transcriptional levels in legume nodules. *Mol Plant Microbe Interact* **21**: 597-604.

Brogden, K.A. (2005) Antimicrobial peptides: pore formers or metabolic inhibitors in bacteria? *Nat Rev Microbiol* **3**: 238-250.

Broghammer, A., Krusell, L., Blaise, M., Sauer, J., Sullivan, J.T., Maolanon, N. et al. (2012) Legume receptors perceive the rhizobial lipochitin oligosaccharide signal molecules by direct binding. *Proc Natl Acad Sci U S A* **109**: 13859-13864.

Bsat, N., Chen, L., and Helmann, J.D. (1996) Mutation of the *Bacillus subtilis* alkyl hydroperoxide reductase (*ahpCF*) operon reveals compensatory interactions among hydrogen peroxide stress genes. *J Bacteriol* **178**: 6579-6586.

Buchanan-Wollaston, V. (1979) Gernalised Transduction in *Rhizobium leguminoarum*. *J General Microbiology* **112**: 135-142.

Capela, D., Filipe, C., Bobilk, C., Batut, J., and Bruand, C. (2006) *Sinorhizobium meliloti* differentiation during symbiosis with alfalfa: A transcriptomic dissection. *Mol Plant Microbe Interact* **19**: 363-372.

Cardenas, L., Martinez, A., Sanchez, F., and Quinto, C. (2008) Fast, transient and specific intracellular ROS changes in living root hair cells responding to Nod factors (NFs). *Plant J* **56**: 802-813.

Carrion, M., Gomez, M.J., Merchante-Schubert, R., Dongarra, S., and Ayala, J.A. (1999) *mraW*, an essential gene at the dcw cluster of *Escherichia coli* codes for a cytoplasmic protein with methyltransferase activity. *Biochimie* **81**: 879-888.

Caswell, C.C., Baumgartner, J.E., Martin, D.W., and Roop, R.M. (2012) Characterization of the organic hydroperoxide resistance system of *Brucella abortus* 2308. *J Bacteriol* **194**: 5065-5072.

Cevallos, M.A., Cervantes-Rivera, R., and Gutierrez-Rios, R.M. (2008) The *repABC* plasmid family. *Plasmid* **60**: 19-37.

Chao, T.C., Becker, A., Buhrmester, J., Puhler, A., and Weidner, S. (2004) The *Sinorhizobium meliloti* fur gene regulates, with dependence on Mn(II), transcription of the *sitABCD* operon, encoding a metal-type transporter. *J Bacteriol* **186**: 3609-3620.

Chao, T.C., Buhrmester, J., Hansmeier, N., Puhler, A., and Weidner, S. (2005) Role of the regulatory gene rirA in the transcriptional response of *Sinorhizobium meliloti* to iron limitation. *Appl Environ Microbiol* **71**: 5969-5982.

Chatterjee, I., Becker, P., Grundmeier, M., Bischoff, M., Somerville, G.A., Peters, G. et al. (2005) *Staphylococcus aureus* ClpC is required for stress resistance, aconitase activity, growth recovery, and death. *J Bacteriol* **187**: 4488-4496.

Chelikani, P., Fita, I., and Loewen, P.C. (2004) Diversity of structures and properties among catalases. *Cell Mol Life Sci* **61**: 192-208.

Chuchue, T., Tanboon, W., Prapagdee, B., Dubbs, J.M., Vattanaviboon, P., and Mongkolsuk, S. (2007) ohrR and ohr are the primary sensor/regulator and protective genes against organic hydroperoxide stress in *Agrobacterium tumefaciens*. *J Bacteriol* **189**: 4553-4553.

Clark, S.R., Oresnik, I.J., and Hynes, M.F. (2001) RpoN of *Rhizobium leguminosarum* bv. viciae strain VF39SM plays a central role in FnrN-dependent microaerobic regulation of genes involved in nitrogen fixation. *Mol Gen Genet* **264**: 623-633.

Colombo, M.V., Gutierrez, D., Palacios, J.M., Imperial, J., and Ruiz-Argueso, T. (2000) A novel autoregulation mechanism of fnrN expression in *Rhizobium leguminosarum* bv viciae. *Mol Microbiol* **36**: 477-486.

Colonna-Romano, S., Arnold, W., Schluter, A., Boistard, P., Puhler, A., and Priefer, U.B. (1990) An Fnr-like protein encoded in *Rhizobium leguminosarum* biovar viciae shows structural and functional homology to Rhizobium meliloti FixK. *Mol Gen Genet* **223**: 138-147.

Conte, S.S., and Walker, E.L. (2011) Transporters contributing to iron trafficking in plants. *Mol Plant* **4**: 464-476.

Conter, A., Gangneux, C., Suzanne, M., and Gutierrez, C. (2001) Survival of *Escherichia coli* during long-term starvation: effects of aeration, NaCl, and the rpoS and osmC gene products. *Res Microbiol* **152**: 17-26.

Cooper, J.E. (2007) Early interactions between legumes and rhizobia: disclosing complexity in a molecular dialogue. *J Appl Microbiol* **103**: 1355-1365.

Croft, K.P.C., Juttner, F., and Slusarenko, A.J. (1993) Volatile products of the liopoxygenase pathways evolved from *Phaseoli vulgaris* (L) Leaves inoculated with *Pseudomonas syringae* pv. phaseolicola. *Plant Physiol* **101**: 13-24.

Cromie, M.J., Shi, Y.X., Latifi, T., and Groisman, E.A. (2006) An RNA sensor for intracellular Mg^{2+}. *Cell* **125**: 71-84.

Crook, M.B., Lindsay, D.P., Biggs, M.B., Bentley, J.S., Price, J.C., Clement, S.C. et al. (2012) Rhizobial plasmids that cause impaired symbiotic nitrogen fixation and enhanced host invasion. *Mol Plant Microbe Interact* **25**: 1026-1033.

Cussiol, J.R., Alves, S.V., de Oliveira, M.A., and Netto, L.E. (2003) Organic hydroperoxide resistance gene encodes a thiol-dependent peroxidase. *J Biol Chem* **278**: 11570-11578.

Da Re, S., Schumacher, J., Rousseau, P., Fourment, J., Ebel, C., and Kahn, D. (1999) Phosphorylation-induced dimerization of the FixJ receiver domain. *Mol Microbiol* **34**: 504-511.

Dann, C.E., III, Wakeman, C.A., Sieling, C.L., Baker, S.C., Irnov, I., and Winkler, W.C. (2007) Structure and mechanism of a metal-sensing regulatory RNA. *Cell* **130**: 878-892.

D'Antuono, A.L., Ott, T., Krusell, L., Voroshilova, V., Ugalde, R.A., Udvardi, M., and Lepek, V.C. (2008) Defects in rhizobial cyclic glucan and lipopolysaccharide synthesis alter legume gene expression during nodule development. *Mol Plant Microbe Interact* **21**: 50-60.

David, M., Daveran, M.L., Batut, J., Dedieu, A., Domergue, O., Ghai, J. et al. (1988) Cascade regulation of nif gene expression in *Rhizobium meliloti*. *Cell* **54**: 671-683.

Davies, B.W., and Walker, G.C. (2007a) Identification of novel *Sinorhizobium meliloti* mutants compromised for oxidative stress protection and symbiosis. *J Bacteriol* **189**: 2110-2113.

Davies, B.W., and Walker, G.C. (2007b) Disruption of *sitA* compromises *Sinorhizobium meliloti* for manganese uptake required for protection against oxidative stress. *J Bacteriol* **189**: 2101-2109.

Delgado, M.J., Bedmar, E.J., and Downie, J.A. (1998) Genes involved in the formation and assembly of rhizobial cytochromes and their role in symbiotic nitrogen fixation. *Adv Microb Physiol* **40**: 191-231.

Delgado, M.J., Tresierra-Ayala, A., Talbi, C., and Bedmar, E.J. (2006) Functional characterization of the *Bradyrhizobium japonicum modA* and *modB* genes involved in molybdenum transport. *Microbiology* **152**: 199-207.

Denison, R.F. (2000) Legume sanctions and the evolution of symbiotic cooperation by rhizobia. *American Naturalist* **156**: 567-576.

Diaz-Mireles, E., Wexler, M., Sawers, G., Bellini, D., Todd, J.D., and Johnston, A.W. (2004) The Fur-like protein Mur of *Rhizobium leguminosarum* is a Mn(2+)-responsive transcriptional regulator. *Microbiology* **150**: 1447-1456.

Diaz-Mireles, E., Wexler, M., Todd, J.D., Bellini, D., Johnston, A.W.B., and Sawers, R.G. (2005) The manganese-responsive repressor Mur of *Rhizobium leguminosarum* is a member of the Fur-superfamily that recognizes an unusual operator sequence. *Microbiology* **151**: 4071-4078.

Ding, H., Yip, C.B., Geddes, B.A., Oresnik, I.J., and Hynes, M.F. (2012) Glycerol utilization by *Rhizobium leguminosarum* requires an ABC transporter and affects competition for nodulation. *Microbiology* **158**: 1369-1378.

Ditta, G., Stanfield, S., Corbin, D., and Helinski, D.R. (1980) Broad host range DNA cloning system for Gram-negative bacteria- construction of a gene bank of *Rhizobium meliloti. Proc Natl Acad Sci U S A* **77**: 7347-7351.

Dixon, R.A. (2001) Natural products and plant disease resistance. *Nature* **411**: 843-847.

Dixon, R., and Kahn, D. (2004) Genetic regulation of biological nitrogen fixation. *Nat Rev Micro* **2**: 621-631.

Djordjevic, M.A. (2004) *Sinorhizobium meliloti* metabolism in the root nodule: a proteomic perspective. *Proteomics* **4**: 1859-1872.

Dowling, D.N., and Broughton, W.J. (1986) Competition for nodulation of legumes. *Annu Rev Microbiol* **40**: 131-157.

Downie, J.A., Hombrecher, G., Ma, Q.S., Knight, C.D., Wells, B., and Johnston, A.W.B. (1983) Cloned nodulation genes of *Rhizobium leguminosarum* determine host range specificity. *Molecular & General Genetics* **190**: 359-365.

Downie, J.A. (2005) Legume haemoglobins: symbiotic nitrogen fixation needs bloody nodules. *Curr Biol* **15**: 196-198.

Driscoll, B.T., and Finan, T.M. (1993) NAD+-dependent malic enzyme of *Rhizobium meliloti* is required for symbiotic nitrogen fixation. *Mol Microbiol* **7**: 865-873.

Dufour, Y.S., Kiley, P.J., and Donohue, T.J. (2010) Reconstruction of the core and extended regulons of global transcription factors. *PLoS Genet* **6**: e1001027.

Dylan, T., Nagpal, P., Helinski, D.R., and Ditta, G.S. (1990) Symbiotic pseudorevertants of *Rhizobium meliloti* ndv mutants. *J Bacteriol* **172**: 1409-1417.

Eda, S., Mitsui, H., and Minamisawa, K. (2011) Involvement of the *smeAB* multidrug efflux pump in resistance to plant antimicrobials and contribution to nodulation competitiveness in *Sinorhizobium meliloti. Appl Environ Microbiol* **77**: 2855-2862.

Eyzaguir.J, Cornwell, E., Borie, G., and Ramirez, B. (1973) Two malic enzymes in *Pseudomonas aeruginosa. J Bacteriol* **116**: 215-221.

Ezraty, B., Vergnes, A., Banzhaf, M., Duverger, Y., Huguenot, A., Brochado, A.R., Su, S., Espinosa, L. and Loiseau, L. (2013) Fe-S Cluster Biosynthesis Controls Uptake of Aminoglycosides in a ROS-Less Death Pathway. *Science* **340**: 1583-87.

Faure, D., Vereecke, D., and Leveau, J.H.J. (2009) Molecular communication in the rhizosphere. *Plant and Soil* **321**: 279-303.

Fellay, R., Frey, J., and Krisch, H. (1987) Interposon mutagenesis of soil and water bacteria: a family of DNA fragments designed for in vitro insertional mutagenesis of Gram-negative bacteria. *Gene* **52**: 147-154.

Feng, J., Michalik, S., Varming, A.N., Andersen, J.H., Albrecht, D., Jelsbak, L. *et al.* (2013) Trapping and proteomic identification of cellular substrates of the ClpP protease in *Staphylococcus aureus*. *J Proteome Res* **12**: 547-558.

Ferguson, B.J., Indrasumunar, A., Hayashi, S., Lin, M.H., Lin, Y.H., Reid, D.E., and Gresshoff, P.M. (2010) Molecular analysis of legume nodule development and autoregulation. *J Integr Plant Biol* **52**: 61-76.

Ferguson, G.P., Roop, R.M. and Walker, G.C. (2002) Deficiency of a *Sinorhizobium meliloti* BacA mutant in alfalfa symbiosis correlates with alteration of the cell envelope. *J Bacteriol* **184**: 5625-5632.

Fernandez, L., Breidenstein, E.B., Song, D., and Hancock, R.E. (2012) Role of intracellular proteases in the antibiotic resistance, motility, and biofilm formation of *Pseudomonas aeruginosa*. *Antimicrob Agents Chemother* **56**: 1128-1132.

Finan, T.M., Hirsch, A.M., Leigh, J.A., Johansen, E., Kuldau, G.A., Deegan, S. et al. (1985) Symbiotic mutants of *Rhizobium meliloti* that uncouple plant from bacterial differentiation. *Cell* **40**: 869-877.

Finney, L.A., and O'Halloran, T.V. (2003) Transition metal speciation in the cell: insights from the chemistry of metal ion receptors. *Science* **300**: 931-936.

Fischer, H.M., Bruderer, T., and Hennecke, H. (1988) Essential and non-essential domains in the *Bradyrhizobium japonicum* NifA protein: identification of indispensable cysteine residues potentially involved in redox reactivity and/or metal binding. *Nucleic Acids Res* **16**: 2207-2224.

Fontenelle, C., Blanco, C., Arrieta, M., Dufour, V., and Trautwetter, A. (2011) Resistance to organic hydroperoxides requires ohr and ohrR genes in *Sinorhizobium meliloti*. *BMC Microbiology* **11**: 1471-2180.

Forrai, T., Vincze, E., Banfalvi, Z., Kiss, G.B., Randhawa, G.S., and Kondorosi, A. (1983) Localization of symbiotic mutations in *Rhizobium meliloti*. *J Bacteriol* **153**: 635-643.

Fowler, R.G., and Schaaper, R.M. (1997) The role of the *mutT* gene of *Escherichia coli* in maintaining replication fidelity. *FEMS Microbiol Rev* **21**: 43-54.

Frederix, M (2010) A novel mechanism of coupling quorum sensing systems in *Rhizobium leguminosarum* bv. viciae 3841. Thesis from the lab of Allan Downie.

Frederix, M., Edwards, A., McAnulla, C., and Downie, J.A. (2011) Co-ordination of quorum-sensing regulation in *Rhizobium leguminosarum* by induction of an anti-repressor. *Mol Microbiol* **81**: 994-1007.

Friesen, M.L., and Mathias, A. (2010) Mixed infections may promote diversification of mutualistic symbionts: why are there ineffective rhizobia? *J Evol Biol* **23**: 323-334.

Froschauer, E.M., Kolisek, M., Dieterich, F., Schweigel, M., and Schweyen, R.J. (2004) Fluorescence measurements of free [Mg2+] by use of mag-fura 2 in *Salmonella enterica*. *FEMS Microbiol Lett* **237**: 49-55.

Fuangthong, M., Atichartpongkul, S., Mongkolsuk, S., and Helmann, J.D. (2001) OhrR is a repressor of ohrA, a key organic hydroperoxide resistance determinant in *Bacillus subtilis*. *J Bacteriol* **183**: 4134-4141.

Furey, T.S. (2012) ChIP-seq and beyond: new and improved methodologies to detect and characterize protein-DNA interactions. *Nat Rev Genet* **13**: 840-852.

Gage, D.J., Bobo, T., and Long, S.R. (1996) Use of green fluorescent protein to visualize the early events of symbiosis between *Rhizobium meliloti* and alfalfa (*Medicago sativa*). *J Bacteriol* **178**: 7159-7166.

Gage, D.J. (2002) Analysis of infection thread development using Gfp- and DsRed-expressing *Sinorhizobium meliloti*. *J Bacteriol* **184**: 7042-7046.

Gage, D.J. (2004) Infection and invasion of roots by symbiotic, nitrogen-fixing rhizobia during nodulation of temperate legumes. *Microbiol Mol Biol Rev* **68**: 280-300.

Galibert, F., Finan, T.M., Long, S.R., Puhler, A., Abola, P., Ampe, F. et al. (2001) The composite genome of the legume symbiont *Sinorhizobium meliloti*. *Science* **293**: 668-672.

Gallon, J.R. (1992) Reconciling the incompatible N_2 fixation and O_2. *New Phytol* **122**: 571-609.

Galvez, A., Maqueda, M., Martinez-Bueno, M., and Valdivia, E. (1991) Permeation of bacterial cells, permeation of cytoplasmic and artificial membrane vesicles, and channel formation on lipid bilayers by peptide antibiotic AS-48. *J Bacteriol* **173**: 886-892.

Gapper, C., and Dolan, L. (2006) Control of plant development by reactive oxygen species. *Plant Physiol* **141**: 341-345.

Gebert, M., Meschenmoser, K., Svidova, S., Weghuber, J., Schweyen, R., Eifler, K. et al. (2009) A Root-Expressed Magnesium Transporter of the MRS2/MGT Gene Family in *Arabidopsis thaliana* Allows for Growth in Low-Mg^{2+} Environments. *Plant Cell* **21**: 4018-4030.

Gerth, U., Kruger, E., Derre, I., Msadek, T., and Hecker, M. (1998) Stress induction of the *Bacillus subtilis clpP* gene encoding a homologue of the proteolytic component of the Clp protease and the involvement of ClpP and ClpX in stress tolerance. *Mol Microbiol* **28**: 787-802.

Gibson, K.E., Kobayashi, H., and Walker, G.C. (2008) Molecular determinants of a symbiotic chronic infection. *Annu Rev of Genetics* **42**: 413-441.

Gilbert, K.B., Vanderlinde, E.M., and Yost, C.K. (2007) Mutagenesis of the carboxy terminal protease CtpA decreases desiccation tolerance in *Rhizobium leguminosarum*. *FEMS Microbiol Lett* **272**: 65-74.

Gilles-Gonzalez, M.A., Gonzalez, G., Perutz, M.F., Kiger, L., Marden, M.C., and Poyart, C. (1994) Heme-based sensors, exemplified by the kinase FixL, are a new class of heme protein with distinctive ligand binding and autoxidation. *Biochemistry* **33**: 8067-8073.

Girard, L., Brom, S., Davalos, A., Lopez, O., Soberon, M., and Romero, D. (2000) Differential regulation of fixN-reiterated genes in *Rhizobium etli* by a novel *fixL-fixK* cascade. *Mol Plant Microbe Interact* **13**: 1283-1292.

Giraud, E., Moulin, L., Vallenet, D., Barbe, V., Cytryn, E., Avarre, J.C. et al. (2007) Legumes symbioses: absence of Nod genes in photosynthetic bradyrhizobia. *Science* **316**: 1307-1312.

Glazebrook, J., Ichige, A., and Walker, G.C. (1993) A *Rhizobium meliloti* homolog of the *Escherichia coli* peptide-antibiotic transport protein SbmA is essential for bacteroid development. *Genes Dev* **7**: 1485-1497.

Gonzalez, V., Santamaria, R.I., Bustos, P., Hernandez-Gonzalez, I., Medrano-Soto, A., Moreno-Hagelsieb, G. *et al*. (2006) The partitioned *Rhizobium etli* genome: genetic and metabolic redundancy in seven interacting replicons. *Proc Natl Acad Sci U S A* **103**: 3834-3839.

Gonzalez-Pasayo, R., and Martinez-Romero, E. (2000) Multiresistance genes of *Rhizobium etli* CFN42. *Mol Plant Microbe Interact* **13**: 572-577.

Graham, J.W., Lei, M.G., and Lee, C.Y. (2013) Trapping and identification of cellular substrates of the *Staphylococcus aureus* ClpC chaperone. *J Bacteriol*.

Graham, T.L. (1991) Flavonoid and isoflavonoid distribution in developing soybean seedling tissues and in seed and root exudates. *Plant Physiol* **95**: 594-603.

Granados-Baeza, M.J., Gomez-Hernandez, N., Mora, Y., Delgado, M.J., Romero, D., and Girard, L. (2007) Novel reiterated Fnr-type proteins control the production of the symbiotic terminal oxidase *cbb3* in *Rhizobium etli* CFN42. *Mol Plant Microbe Interact* **20**: 1241-1249.

Green, J., Crack, J.C., Thomson, A.J., and LeBrun, N.E. (2009) Bacterial sensors of oxygen. *Curr Opin Microbiol* **12**: 145-151.

Groisman, E.A. (2001) The pleiotropic two-component regulatory system PhoP-PhoQ. *J Bacteriol* **183**: 1835-1842.

Guerinot, M.L., Meidl, E.J., and Plessner, O. (1990) Citrate as a siderophore in *Bradyrhizobium japonicum*. *J Bacteriol* **172**: 3298-3303.

Gur, E., Biran, D., and Ron, E.Z. (2011) Regulated proteolysis in Gram-negative bacteria--how and when? *Nat Rev Microbiol* **9**: 839-848.

Gutierrez, D., Hernando, Y., Palacios, J.M., Imperial, J., and Ruiz-Argueso, T. (1997) FnrN controls symbiotic nitrogen fixation and hydrogenase activities in *Rhizobium leguminosarum* biovar viciae UPM791. *J Bacteriol* **179**: 5264-5270.

Gutierrez, R.A. (2012) Systems biology for enhanced plant nitrogen nutrition. *Science* **336**: 1673-1675.

Haag, A.F., Baloban, M., Sani, M., Kerscher, B., Pierre, O., Farkas, A. et al. (2011) Protection of *Sinorhizobium* against host cysteine-rich antimicrobial peptides is critical for symbiosis. *PLoS Biol* **9**: e1001169.

Haag, A.F., Kerscher, B., Dall'Angelo, S., Sani, M., Longhi, R., Baloban, M. et al. (2012) Role of cysteine residues and disulfide bonds in the activity of a legume root nodule-specific, cysteine-rich peptide. *J Biol Chem* **287**: 10791-10798.

Haag, A.F., Arnold, M.F., Myka, K.K., Kerscher, B., Dall'Angelo, S., Zanda, M. et al. (2013) Molecular insights into bacteroid development during Rhizobium-legume symbiosis. *FEMS Microbiol Rev* **37**: 364-383.

Hakoyama, T., Niimi, K., Watanabe, H., Tabata, R., Matsubara, J., Sato, S. et al. (2009) Host plant genome overcomes the lack of a bacterial gene for symbiotic nitrogen fixation. *Nature* **462**: 514-517.

Hakoyama, T., Niimi, K., Yamamoto, T., Isobe, S., Sato, S., Nakamura, Y. et al. (2012) The integral membrane protein SEN1 is required for symbiotic nitrogen fixation in *Lotus japonicus* nodules. *Plant Cell Physiol* **53**: 225-236.

Hamza, I., Qi, Z., King, N.D., and O'Brian, M.R. (2000) Fur-independent regulation of iron metabolism by Irr in *Bradyrhizobium japonicum*. *Microbiology* **146**: 669-676.

Hanyu, M., Fujimoto, H., Tejima, K., and Saeki, K. (2009) Functional Differences of Two Distinct Catalases in *Mesorhizobium loti* MAFF303099 under Free-Living and Symbiotic Conditions. *J Bacteriol* **191**: 1463-1471.

Hardy, R.W.F., Burns, R.C., and Holsten, R.D. (1973) Applications of the acetylene ethylene assay for measurement of nitrogen fixation. *Soil Biology and Biochemistry* **5**: 47-81.

Hartwig, U.A., Maxwell, C.A., Joseph, C.M., and Phillips, D.A. (1990) Effects of alfalfa nod gene-inducing flavonoids on nodABC transcription in *Rhizobium meliloti* strains containing different *nodD* genes. *J Bacteriol* **172**: 2769-2773.

Hattori, M., Tanaka, Y., Fukai, S., Ishitani, R., and Nureki, O. (2007) Crystal structure of the MgtE Mg2+ transporter. *Nature* **448**: 1072-1075.

Hattori, M., Iwase, N., Furuya, N., Tanaka, Y., Tsukazaki, T., Ishitani, R. *et al*. (2009) Mg(2+)-dependent gating of bacterial MgtE channel underlies Mg(2+) homeostasis. *EMBO J* **28**: 3602-3612.

Hauser, F., Pessi, G., Friberg, M., Weber, C., Rusca, N., Lindemann, A. et al. (2007) Dissection of the *Bradyrhizobium japonicum* NifA+sigma54 regulon, and identification of a ferredoxin gene (fdxN) for symbiotic nitrogen fixation. *Mol Genet Genomics* **278**: 255-271.

Haynes, J.G., Czymmek, K.J., Carlson, C.A., Veereshlingam, H., Dickstein, R., and Sherrier, D.J. (2004) Rapid analysis of legume root nodule development using confocal microscopy. *New Phytol* **163**: 661-668.

Helmann, J.D. (2007) Measuring metals with RNA. *Mol Cell* **27**: 859-860.

Hicks, D.B., Wang, Z., Wei, Y., Kent, R., Guffanti, A.A., Banciu, H. *et al.* (2003) A tenth *atp* gene and the conserved *atpI* gene of a Bacillus *atp* operon have a role in Mg^{2+} uptake. *Proc Natl Acad Sci U S A* **100**: 10213-10218.

Higgins, C.F. (2007) Multiple molecular mechanisms for multidrug resistance transporters. *Nature* **446**: 749-757.

Hinz, A., Lee, S., Jacoby, K., and Manoil, C. (2011) Membrane Proteases and Aminoglycoside Antibiotic Resistance. *J Bacteriol* **193**: 4790-4797.

Hirano, M., Onishi, Y., Yanagida, T., and Ide, T. (2011) Role of the KcsA channel cytoplasmic domain in pH-dependent gating. *Biophys J* **101**: 2157-2162.

Hirsch, A.M. (1999) Role of lectins (and rhizobial exopolysaccharides) in legume nodulation. *Curr Opin Plant Biol* **2**: 320-326.

Hmiel, S.P., Snavely, M.D., Florer, J.B., Maguire, M.E., and Miller, C.G. (1989) Magnesium transport in *Salmonella typhimurium*- genetic characterisation and cloning of 3 magnesium transport loci. *J Bacteriol* **171**: 4742-4751.

Hohle, T.H., and O'Brian, M.R. (2009) The *mntH* gene encodes the major Mn^{2+} transporter in *Bradyrhizobium japonicum* and is regulated by manganese via the Fur protein. *Mol Microbiol* **72**: 399-409.

Hohle, T.H., and O'Brian, M.R. (2010) Transcriptional control of the *Bradyrhizobium japonicum* irr gene requires repression by fur and Antirepression by Irr. *J Biol Chem* **285**: 26074-26080.

Hohle, T.H., Franck, W.L., Stacey, G., and O'Brian, M.R. (2011) Bacterial outer membrane channel for divalent metal ion acquisition. *Proc Natl Acad Sci U S A* **108**: 15390-15395.

Hohle, T.H., and O'Brian, M.R. (2012) Manganese is required for oxidative metabolism in unstressed *Bradyrhizobium japonicum* cells. *Mol Microbiol* **84**: 766-777.

Hoover, T.R., Imperial, J., Ludden, P.W., and Shah, V.K. (1989) Homocitrate is a component of the iron molybdenum cofactor of nitrogenase. *Biochemistry* **28**: 2768-2771.

Hosie, A.H., Allaway, D., Galloway, C.S., Dunsby, H.A., and Poole, P.S. (2002) *Rhizobium leguminosarum* has a second general amino acid permease with unusually broad substrate specificity and high similarity to branched-chain amino acid transporters (Bra/LIV) of the ABC family. *J Bacteriol* **184**: 4071-4080.

Hotter, G.S., and Scott, D.B. (1991) Exopolysaccharide mutants of *Rhizobium loti* are fully effective on a determinate nodulating host but are ineffective on an indeterminate nodulating host. *J Bacteriol* **173**: 851-859.

Huala, E., and Ausubel, F.M. (1989) The central domain of *Rhizobium meliloti* NifA is sufficient to activate transcription form the *R. meliloti nifH* promoter. *J Bacteriol* **171**: 3354-3365.

Huala, E., Moon, A.L., and Ausubel, F.M. (1991) Aerobic inactivation of *Rhizobium meliloti* NifA in *Escherichia coli* is mediated by lon and two newly identified genes, *snoB* and *snoC*. *J Bacteriol* **173**: 382-390.

Ichige, A., and Walker, G.C. (1997) Genetic analysis of the *Rhizobium meliloti bacA* gene: functional interchangeability with the *Escherichia coli sbmA* gene and phenotypes of mutants. *J Bacteriol* **179**: 209-216.

Igamberdiev, A.U., and Kleczkowski, L.A. (2001) Implications of adenylate kinase-governed equilibrium of adenylates on contents of free magnesium in plant cells and compartments. *Biochem J* **360**: 225-231.

Igamberdiev, A.U., and Kleczkowski, L.A. (2011) Magnesium and cell energetics in plants under anoxia. *Biochem J* **437**: 373-379.

Ignoul, S., and Eggermont, J. (2005) CBS domains: structure, function, and pathology in human proteins. *Am J Physiol Cell Physiol* **289**: 1369-1378.

Imlay, J.A. (2013) The molecular mechanisms and physiological consequences of oxidative stress: lessons from a model bacterium. *Nat Rev Microbiol* **11**: 443-454.

Indrasumunar, A., Kereszt, A., Searle, I., Miyagi, M., Li, D., Nguyen, C.D. et al. (2010) Inactivation of duplicated nod factor receptor 5 (NFR5) genes in recessive loss-of-function non-nodulation mutants of allotetraploid soybean (*Glycine max* L. Merr.). *Plant Cell Physiol* **51**: 201-214.

Indrasumunar, A., Searle, I., Lin, M.H., Kereszt, A., Men, A., Carroll, B.J., and Gresshoff, P.M. (2011) Nodulation factor receptor kinase 1-alpha controls nodule organ number in soybean (Glycine max L. Merr). *Plant J* **65**: 39-50.

Ishitani, R., Sugita, Y., Dohmae, N., Furuya, N., Hattori, M., and Nureki, O. (2008) Mg^{2+}-sensing mechanism of Mg^{2+} transporter MgtE probed by molecular dynamics study. *Proc Natl Acad Sci U S A* **105**: 15393-15398.

Jalloul, A., Montillet, J.L., Assigbetse, K., Agnel, J.P., Delannoy, E., Triantaphylides, C. et al. (2002) Lipid peroxidation in cotton: *Xanthomonas* interactions and the role of lipoxygenases during the hypersensitive reaction. *Plant J* **32**: 1-12.

Jamet, A., Sigaud, S., Van de Sype, G., Puppo, A., and Herouart, D. (2003) Expression of the bacterial catalase genes during *Sinorhizobium meliloti-Medicago sativa* symbiosis and their crucial role during the infection process. *Mol Plant Microbe Interact* **16**: 217-225.

Jamet, A., Mandon, K., Puppo, A., and Herouart, D. (2007) H_2O_2 is required for optimal establishment of the *Medicago sativa/Sinorhizobium meliloti* symbiosis. *J Bacteriol* **189**: 8741-8745.

Jenal, U., and Hengge-Aronis, R. (2003) Regulation by proteolysis in bacterial cells. *Curr Opin Microbiol* **6**: 163-172.

Jervis, A.J., and Green, J. (2007) In vivo demonstration of FNR dimers in response to lower O(2) availability. *J Bacteriol* **189**: 2930-2932.

Johnson, D.S., Mortazavi, A., Myers, R.M., and Wold, B. (2007) Genome-wide mapping of in vivo protein-DNA interactions. *Science* **316**: 1497-1502.

Johnston, A.W., and Beringer, J.E. (1975) Identification of the rhizobium strains in pea root nodules using genetic markers. *J Gen Microbiol* **87**: 343-350.

Johnston, A.W., Todd, J.D., Curson, A.R., Lei, S., Nikolaidou-Katsaridou, N., Gelfand, M.S., and Rodionov, D.A. (2007) Living without Fur: the subtlety and complexity of iron-responsive gene regulation in the symbiotic bacterium Rhizobium and other alpha-proteobacteria. *Biometals* **20**: 501-511.

Joly, N., Engl, C., Jovanovic, G., Huvet, M., Toni, T., Sheng, X. et al. (2010) Managing membrane stress: the phage shock protein (Psp) response, from molecular mechanisms to physiology. *FEMS Microbiol Rev* **34**: 797-827.

Jones, K.M., Kobayashi, H., Davies, B.W., Taga, M.E., and Walker, G.C. (2007) How rhizobial symbionts invade plants: the *Sinorhizobium-Medicago* model. *Nat Rev Microbiol* **5**: 619-633.

Kahn, D., David, M., Domergue, O., Daveran, M.L., Ghai, J., Hirsch, P.R., and Batut, J. (1989) *Rhizobium meliloti fixGHI* sequence predicts involvement of a specific cation pump in symbiotic nitrogen fixation. *J Bacteriol* **171**: 929-939.

Kaiser, B.N., Moreau, S., Castelli, J., Thomson, R., Lambert, A., Bogliolo, S. et al. (2003) The soybean NRAMP homologue, GmDMT1, is a symbiotic divalent metal transporter capable of ferrous iron transport. *Plant J* **35**: 295-304.

Kaminski, P.A., and Elmerich, C. (1991) Involvement of *fixLJ* in the regulation of nitrogen fixation in *Azorhizobium caulinodans*. *Mol Microbiol* **5**: 665-673.

Kaminski, P.A., Mandon, K., Arigoni, F., Desnoues, N., and Elmerich, C. (1991) Regulation of nitrogen fixation in *Azorhizobium caulinodans*: identification of a *fixK*-like gene, a positive regulator of nifA. *Mol Microbiol* **5**: 1983-1991.

Kaneko, T., Nakamura, Y., Sato, S., Minamisawa, K., Uchiumi, T., Sasamoto, S. *et al.* (2002) Complete genomic sequence of nitrogen-fixing symbiotic bacterium *Bradyrhizobium japonicum* USDA110. *DNA Res* **9**: 189-197.

Karlinsey, J.E., Maguire, M.E., Becker, L.A., Crouch, M.L., and Fang, F.C. (2010) The phage shock protein PspA facilitates divalent metal transport and is required for virulence of *Salmonella enterica* sv. Typhimurium. *Mol Microbiol* **78**: 669-685.

Karunakaran, R., Ramachandran, V.K., Seaman, J.C., East, A.K., Mouhsine, B., Mauchline, T.H. et al. (2009) Transcriptomic Analysis of *Rhizobium leguminosarum* Biovar viciae in Symbiosis with Host Plants *Pisum sativum* and *Vicia cracca*. *J Bacteriol* **191**: 4002-4014.

Karunakaran, R., Haag, A.F., East, A.K., Ramachandran, V.K., Prell, J., James, E.K. et al. (2010) BacA is essential for bacteroid development in nodules of galegoid, but not phaseoloid, legumes. *J Bacteriol* **192**: 2920-2928.

Keen, N.T., Tamaki, S., Kobayashi, D., and Trollinger, D. (1988) Improved broad-host-range plasmids for DNA cloning in Gram-negative bacteria. *Gene* **70**: 191-197.

Kehres, D.G., Zaharik, M.L., Finlay, B.B., and Maguire, M.E. (2000) The NRAMP proteins of *Salmonella typhimurium* and *Escherichia coli* are selective manganese transporters involved in the response to reactive oxygen. *Mol Microbiol* **36**: 1085-1100.

Kehres, D.G., Janakiraman, A., Slauch, J.M., and Maguire, M.E. (2002a) SitABCD is the alkaline Mn(2+) transporter of Salmonella enterica serovar Typhimurium. *J Bacteriol* **184**: 3159-3166.

Kehres, D.G., Janakiraman, A., Slauch, J.M., and Maguire, M.E. (2002b) Regulation of *Salmonella enterica* serovar Typhimurium *mntH* transcription by H(2)O(2), Fe(2+), and Mn(2+). *J Bacteriol* **184**: 3151-3158.

Kehres, D.G., and Maguire, M.E. (2003) Emerging themes in manganese transport, biochemistry and pathogenesis in bacteria. *FEMS Microbiol Rev* **27**: 263-290.

Kersey, C.M., Agyemang, P.A., and Dumenyo, C.K. (2012) CorA, the magnesium/nickel/cobalt transporter, affects virulence and extracellular enzyme production in the soft rot pathogen *Pectobacterium carotovorum*. *Mol Plant Pathol* **13**: 58-71.

Klomsiri, C., Panmanee, W., Dharmsthiti, S., Vattanaviboon, P., and Mongkolsuk, S. (2005) Novel roles of ohrR-ohr in *Xanthomonas* sensing, metabolism, and physiological adaptive response to lipid hydroperoxide. *J Bacteriol* **187**: 3277-3281.

Kobayashi, H., Yamamoto, M., and Aono, R. (1998) Appearance of a stress-response protein, phage-shock protein A, in *Escherichia coli* exposed to hydrophobic organic solvents. *Microbiology* **144**: 353-359.

Kobayashi, R., Suzuki, T., and Yoshida, M. (2007) *Escherichia coli* phage-shock protein A (PspA) binds to membrane phospholipids and repairs proton leakage of the damaged membranes. *Mol Microbiol* **66**: 100-109.

Koch, M., Delmotte, N., Rehrauer, H., Vorholt, J.A., Pessi, G., and Hennecke, H. (2010) Rhizobial adaptation to hosts, a new facet in the legume root-nodule symbiosis. *Mol Plant Microbe Interact* **23**: 784-790.

Kohanski, M.A., Dwyer, D.J., Hayete, B., Lawrence, C.A., and Collins, J.J. (2007) A common mechanism of cellular death induced by bactericidal antibiotics. *Cell* **130**: 797-810.

Kondorosi, E., Mergaert, P., and Kereszt, A. (2013) A paradigm for endosymbiotic life: cell differentiation of Rhizobium bacteria provoked by host plant factors. *Annu Rev Microbiol* **67**: 611-628.

Kouchi, H., and Yoneyama, T. (1984) Dynamics of carbon photosynthetically assimilated in nodulated soya bean-plants under state-state conditions. *Annals of Botany* **53**: 883-896.

Krehenbrink, M (2006) Protein secretion in *Rhizobium leguminosarum* biovar viciae. Thesis from the lab of Allan Downie

Krehenbrink, M., Edwards, A., and Downie, J.A. (2011) The superoxide dismutase SodA is targeted to the periplasm in a SecA-dependent manner by a novel mechanism. *Mol Microbiol* **82**: 164-179.

Krusell, L., Krause, K., Ott, T., Desbrosses, G., Kramer, U., Sato, S. et al. (2005) The sulfate transporter SST1 is crucial for symbiotic nitrogen fixation in *Lotus japonicus* root nodules. *Plant Cell* **17**: 1625-1636.

Kuzma, M.M., Hunt, S., and Layzell, D.B. (1993) Role of Oxygen in the Limitation and Inhibition of Nitrogenase Activity and Respiration Rate in Individual Soybean Nodules. *Plant Physiol* **101**: 161-169.

Lamb, J.W., Hombrecher, G., and Johnston, A.W.B. (1982) Plasmid-determined nodulation and nitrogen fixation abilities in *Rhizobium phaseoli*. *Molecular & General Genetics* **186**: 449-452.

Larkin, M.A., Blackshields, G., Brown, N.P., Chenna, R., McGettigan, P.A., McWilliam, H. et al. (2007) Clustal W and clustal X version 2.0. *Bioinformatics* **23**: 2947-2948.

Lee, K.B., De Backer, P., Aono, T., Liu, C.T., Suzuki, S., Suzuki, T. et al. (2008) The genome of the versatile nitrogen fixer *Azorhizobium caulinodans* ORS571. *BMC Genomics* **9**: 271.

Lee, Y.Y., Chang, C.F., Kuo, C.L., Chen, M.C., Yu, C.H., Lin, P.I., and Wu, W.F. (2003) Subunit oligomerization and substrate recognition of the *Escherichia coli* ClpYQ (HslUV) protease implicated by in vivo protein-protein interactions in the yeast two-hybrid system. *J Bacteriol* **185**: 2393-2401.

Leigh, J.A., Signer, E.R., and Walker, G.C. (1985) Exopolysaccharide-deficient mutants of *Rhizobium meliloti* that form ineffective nodules. *Proc Natl Acad Sci U S A* **82**: 6231-6235.

Lesniak, J., Barton, W.A., and Nikolov, D.B. (2002) Structural and functional characterization of the *Pseudomonas* hydroperoxide resistance protein Ohr. *EMBO J* **21**: 6649-6659.

Lesniak, J., Barton, W.A., and Nikolov, D.B. (2003) Structural and functional features of the *Escherichia coli* hydroperoxide resistance protein OsmC. *Protein Sci* **12**: 2838-2843.

LeVier, K., and Walker, G.C. (2001) Genetic analysis of the *Sinorhizobium meliloti* BacA protein: Differential effects of mutations on phenotypes. *J Bacteriol* **183**: 6444-6453.

Lewis, K. (2000) Translocases: a bacterial tunnel for drugs and proteins. *Curr Biol* **10**: R678-681.

Li, C., Tao, J., Mao, D., and He, C. (2011) A novel manganese efflux system, YebN, is required for virulence by *Xanthomonas oryzae* pv. oryzae. *PLoS One* **6**: e21983.

Li, L., Stoeckert, C.J., Jr., and Roos, D.S. (2003) OrthoMCL: identification of ortholog groups for eukaryotic genomes. *Genome Res* **13**: 2178-2189.

Li, L.G., Tutone, A.F., Drummond, R.S.M., Gardner, R.C., and Luan, S. (2001) A novel family of magnesium transport genes in Arabidopsis. *Plant Cell* **13**: 2761-2775.

Li, R., Knox, M.R., Edwards, A., Hogg, B., Ellis, T.H.N., Wei, G., and Downie, J.A. (2011) Natural Variation in Host-Specific Nodulation of Pea Is Associated with a Haplotype of the SYM37 LysM-Type Receptor-Like Kinase. *Mol Plant Microbe Interact* **24**: 1396-1403.

Lien, H.Y., Shy, R.S., Peng, S.S., Wu, Y.L., Weng, Y.T., Chen, H.H. et al. (2009) Characterization of the *Escherichia coli* ClpY (HslU) substrate recognition site in the ClpYQ (HslUV) protease using the yeast two-hybrid system. *J Bacteriol* **191**: 4218-4231.

Lill, R. (2009) Function and biogenesis of iron-sulphur proteins. *Nature* **460**: 831-838.

Lim, B., Sim, S.-H., Sim, M., Kim, K., Jeon, C.O., Lee, Y. et al. (2012) RNase III Controls the Degradation of *corA* mRNA in *Escherichia coli*. *J Bacteriol* **194**: 2214-2220.

Limpens, E., Moling, S., Hooiveld, G., Pereira, P.A., Bisseling, T., Becker, J.D., and Kuster, H. (2013) cell- and tissue-specific transcriptome analyses of *Medicago truncatula* root nodules. *PLoS One* **8**: e64377.

Lindemann, A., Koch, M., Pessi, G., Muller, A.J., Balsiger, S., Hennecke, H., and Fischer, H.M. (2010) Host-specific symbiotic requirement of BdeAB, a RegR-controlled RND-type efflux system in *Bradyrhizobium japonicum*. *FEMS Microbiol Lett* **312**: 184-191.

Llewellyn, A.C., Jones, C.L., Napier, B.A., Bina, J.E., and Weiss, D.S. (2011) Macrophage Replication Screen Identifies a Novel *Francisella* Hydroperoxide Resistance Protein Involved in Virulence. *Plos One* **6**.

Lodwig, E.M., Hosie, A.H., Bourdes, A., Findlay, K., Allaway, D., Karunakaran, R. et al. (2003) Amino-acid cycling drives nitrogen fixation in the legume-Rhizobium symbiosis. *Nature* **422**: 722-726.

Lodwig, E., and Poole, P. (2003) Metabolism of Rhizobium Bacteroids. *Critical Reviews in Plant Sciences* **22**: 37-78.

Lodwig, E., Kumar, S., Allaway, D., Bourdes, A., Prell, J., Priefer, U., and Poole, P. (2004) Regulation of L-alanine dehydrogenase in *Rhizobium leguminosarum* bv. viciae and its role in pea nodules. *J Bacteriol* **186**: 842-849.

Lohar, D.P., Haridas, S., Gantt, J.S., and VandenBosch, K.A. (2007) A transient decrease in reactive oxygen species in roots leads to root hair deformation in the legume-rhizobia symbiosis. *New Phytol* **173**: 39-49.

Lois, A.F., Ditta, G.S., and Helinski, D.R. (1993) The oxygen sensor FixL of *Rhizobium meliloti* is a membrane protein containing four possible transmembrane segments. *J Bacteriol* **175**: 1103-1109.

London, R.E. (1991) Methods for measurement of intracellular magnesium- NMR and fluorescence. *Annu Rev of Physiology* **53**: 241-258.

Lopez, O., Morera, C., Miranda-Rios, J., Girard, L., Romero, D., and Soberon, M. (2001) Regulation of gene expression in response to oxygen in *Rhizobium etli*: role of FnrN in *fixNOQP* expression and in symbiotic nitrogen fixation. *J Bacteriol* **183**: 6999-7006.

Lu W, Du J, Wacker T, Gerbig-Smentek E, Andrade SL, et al. (2011) pH-dependent gating in a FocA formate channel. Science **332**: 352-354.

Maathuis, F.J.M. (2009) Physiological functions of mineral macronutrients. *Curr Opin Plant Bio* **12**: 250-258.

MacLean, A.A., MacPherson, G., Aneja, P., and Finan, T.M. (2006) Characterization of the beta-ketoadipate pathway in *Sinorhizobium meliloti*. *Appl and Environ Microbiol* **72**: 5403-5413.

Madsen, E.B., Madsen, L.H., Radutoiu, S., Olbryt, M., Rakwalska, M., Szczyglowski, K. et al. (2003) A receptor kinase gene of the LysM type is involved in legume perception of rhizobial signals. *Nature* **425**: 637-640.

Maftah, A., Renault, D., Vignoles, C., Hechard, Y., Bressollier, P., Ratinaud, M.H. et al. (1993) Membrane permeabilization of *Listeria monocytogenes* and mitochondria by the bacteriocin mesentericin Y105. *J Bacteriol* **175**: 3232-3235.

Maguire, M.E. (2006) Magnesium transporters: properties, regulation and structure. *Front Biosci* **11**: 3149-3163.

Mahmood, N.A., Biemans-Oldehinkel, E., and Poolman, B. (2009) Engineering of ion sensing by the cystathionine beta-synthase module of the ABC transporter OpuA. *J Biol Chem* **284**: 14368-14376.

Makui, H., Roig, E., Cole, S.T., Helmann, J.D., Gros, P., and Cellier, M.F. (2000) Identification of the *Escherichia coli* K-12 Nramp orthologue (MntH) as a selective divalent metal ion transporter. *Mol Microbiol* **35**: 1065-1078.

Mandon, K., Kaminski, P.A., Mougel, C., Desnoues, N., Dreyfus, B., and Elmerich, C. (1993) Role of the *fixGHI* region of *Azorhizobium caulinodans* in free-living and symbiotic nitrogen fixation. *FEMS Microbiol Lett* **114**: 185-189.

Mandon, K., Kaminski, P.A., and Elmerich, C. (1994) Functional analysis of the *fixNOPQ* region of *Azorhizobium caulinodans*. *J Bacteriol* **176**: 2560-2568.

Marchler-Bauer, A., Anderson, J.B., Chitsaz, F., Derbyshire, M.K., DeWeese-Scott, C., Fong, J.H. et al. (2009) CDD: specific functional annotation with the Conserved Domain Database. *Nucleic Acids Res* **37**: 205-210.

Marchler-Bauer, A., Lu, S., Anderson, J.B., Chitsaz, F., Derbyshire, M.K., DeWeese-Scott, C. et al. (2011) CDD: a Conserved Domain Database for the functional annotation of proteins. *Nucleic Acids Res* **39**: 225-229.

Marlow, V.L., Haag, A.F., Kobayashi, H., Fletcher, V., Scocchi, M., Walker, G.C., and Ferguson, G.P. (2009) Essential role for the BacA protein in the uptake of a truncated eukaryotic peptide in *Sinorhizobium meliloti*. *J Bacteriol* **191**: 1519-1527.

Martin, J.E., and Imlay, J.A. (2011) The alternative aerobic ribonucleotide reductase of *Escherichia coli*, NrdEF, is a manganese-dependent enzyme that enables cell replication during periods of iron starvation. *Mol Microbiol* **80**: 319-334.

Martinez-Abarca, F., Herrera-Cervera, J.A., Bueno, P., Sanjuan, J., Bisseling, T., and Olivares, J. (1998) Involvement of salicylic acid in the establishment of the *Rhizobium meliloti* - Alfalfa symbiosis. *Mol Plant Microbe Interact* **11**: 153-155.

Maruya, J., and Saeki, K. (2010) The *bacA* gene homolog, mlr7400, in *Mesorhizobium loti* MAFF303099 is dispensable for symbiosis with *Lotus japonicus* but partially capable of supporting the symbiotic function of bacA in *Sinorhizobium meliloti*. *Plant Cell Physiol* **51**: 1443-1452.

Masson-Boivin, C., Giraud, E., Perret, X., and Batut, J. (2009) Establishing nitrogen-fixing symbiosis with legumes: how many rhizobium recipes? *Trends in Microbiology* **17**: 458-466.

Matsuzaki, K., Sugishita, K., Harada, M., Fujii, N., and Miyajima, K. (1997) Interactions of an antimicrobial peptide, magainin 2, with outer and inner membranes of Gram-negative bacteria. *Biochim Biophys Acta* **1327**: 119-130.

Mauchline, T.H., Fowler, J.E., East, A.K., Sartor, A.L., Zaheer, R., Hosie, A.H. *et al.* (2006) Mapping the *Sinorhizobium meliloti* 1021 solute-binding protein-dependent transportome. *Proc Natl Acad Sci U S A* **103**: 17933-17938.

Mazur, A., Majewska, B., Stasiak, G., Wielbo, J., and Skorupska, A. (2011) repABC-based replication systems of *Rhizobium leguminosarum* bv. trifolii TA1 plasmids: incompatibility and evolutionary analyses. *Plasmid* **66**: 53-66.

McEwan, A.G. (2009) New insights into the protective effect of manganese against oxidative stress. *Mol Microbiol* **72**: 812-814.

McGillivray, S.M., Tran, D.N., Ramadoss, N.S., Alumasa, J.N., Okumura, C.Y., Sakoulas, G. *et al*. (2012) Pharmacological inhibition of the ClpXP protease increases bacterial susceptibility to host cathelicidin antimicrobial peptides and cell envelope-active antibiotics. *Antimicrob Agents Chemother* **56**: 1854-1861.

Mergaert, P., Nikovics, K., Kelemen, Z., Maunoury, N., Vaubert, D., Kondorosi, A., and Kondorosi, E. (2003) A novel family in *Medicago truncatula* consisting of more than 300 nodule-specific genes coding for small, secreted polypeptides with conserved cysteine motifs. *Plant Physiol* **132**: 161-173.

Mergaert, P., Uchiumi, T., Alunni, B., Evanno, G., Cheron, A., Catrice, O. et al. (2006) Eukaryotic control on bacterial cell cycle and differentiation in the Rhizobium-legume symbiosis. *Proc Natl Acad Sci U S A* **103**: 5230-5235.

Merino, S., Gavin, R., Altarriba, M., Izquierdo, L., Maguire, M.E., and Tomas, J.M. (2001) The MgtE Mg^{2+} transport protein is involved in *Aeromonas hydrophila* adherence. *FEMS Microbiol Lett* **198**: 189-195.

Mesa, S., Hauser, F., Friberg, M., Malaguti, E., Fischer, H.M., and Hennecke, H. (2008) Comprehensive assessment of the regulons controlled by the FixLJ-FixK2-FixK1 cascade in *Bradyrhizobium japonicum*. *J Bacteriol* **190**: 6568-6579.

Mesa, S., Reutimann, L., Fischer, H.M., and Hennecke, H. (2009) Posttranslational control of transcription factor FixK2, a key regulator for the *Bradyrhizobium japonicum*-soybean symbiosis. *Proc Natl Acad Sci U S A* **106**: 21860-21865.

Mikkelsen, T.S., Ku, M., Jaffe, D.B., Issac, B., Lieberman, E., Giannoukos, G. *et al.* (2007) Genome-wide maps of chromatin state in pluripotent and lineage-committed cells. *Nature* **448**: 553-560.

Miller, R.W., and Sirois, J.C. (1983) Calcium and magnesium effects on symbiotic nitrogen fixation in the alfalfa (*Medicago sativa*)-*Rhizbobium meliloti* system. *Physiologia Plantarum* **58**: 464-470.

Miller, S.H., Elliot, R.M., Sullivan, J.T., and Ronson, C.W. (2007) Host-specific regulation of symbiotic nitrogen fixation in *Rhizobium leguminosarum* biovar trifolii. *Microbiology* **153**: 3184-3195.

Monahan-Giovanelli, H., Pinedo, C.A., and Gage, D.J. (2006) Architecture of infection thread networks in developing root nodules induced by the symbiotic bacterium *Sinorhizobium meliloti* on *Medicago truncatula*. *Plant Physiol* **140**: 661-670.

Moncrief, M.B., and Maguire, M.E. (1999) Magnesium transport in prokaryotes. *J Biol Inorg Chem* **4**: 523-527.

Mongkolsuk, S., Praituan, W., Loprasert, S., Fuangthong, M., and Chamnongpol, S. (1998) Identification and characterization of a new organic hydroperoxide resistance (*ohr*) gene with a novel pattern of oxidative stress regulation from *Xanthomonas campestris* pv. phaseoli. *J Bacteriol* **180**: 2636-2643.

Mongkolsuk, S., Whangsuk, W., Vattanaviboon, P., Loprasert, S., and Fuangthong, M. (2000) A *Xanthomonas* alkyl hydroperoxide reductase subunit C (*ahpC*) mutant showed an altered peroxide stress response and complex regulation of the compensatory response of peroxide detoxification enzymes. *J Bacteriol* **182**: 6845-6849.

Montiel, J., Nava, N., Cardenas, L., Sanchez-Lopez, R., Arthikala, M.K., Santana, O. et al. (2012) A *Phaseolus vulgaris* NADPH Oxidase Gene is Required for Root Infection by Rhizobia. *Plant and Cell Physiology* **53**: 1751-1767.

Moomaw, A.S., and Maguire, M.E. (2008) The unique nature of Mg^{2+} channels. *Physiology (Bethesda)* **23**: 275-285.

Moore, L.J., and Kiley, P.J. (2001) Characterization of the dimerization domain in the FNR transcription factor. *J Biol Chem* **276**: 45744-45750.

Moore, L.J., Mettert, E.L., and Kiley, P.J. (2006) Regulation of FNR dimerization by subunit charge repulsion. *J Biol Chem* **281**: 33268-33275.

Moreau, S., Thomson, R.M., Kaiser, B.N., Trevaskis, B., Guerinot, M.L., Udvardi, M.K. et al. (2002) GmZIP1 encodes a symbiosis-specific zinc transporter in soybean. *J Biol Chem* **277**: 4738-4746.

Morett, E., Fischer, H.M., and Hennecke, H. (1991) Influence of oxygen on DNA binding, positive control, and stability of the *Bradyrhizobium japonicum* NifA regulatory protein. *J Bacteriol* **173**: 3478-3487.

Moris, M., Dombrecht, B., Xi, C., Vanderleyden, J., and Michiels, J. (2004) Regulatory role of *Rhizobium etli* CNPAF512 *fnrN* during symbiosis. *Appl Environ Microbiol* **70**: 1287-1296.

Mulley, G., Lopez-Gomez, M., Zhang, Y., Terpolilli, J., Prell, J., Finan, T., and Poole, P. (2010) Pyruvate Is Synthesized by Two Pathways in Pea Bacteroids with Different Efficiencies for Nitrogen Fixation. *J Bacteriol* **192**: 4944-4953.

Murray, J.D. (2011) Invasion by invitation: rhizobial infection in legumes. *Mol Plant Microbe Interact* **24**: 631-639.

Mutch, L.A., and Young, J.P. (2004) Diversity and specificity of *Rhizobium leguminosarum* biovar viciae on wild and cultivated legumes. *Mol Ecol* **13**: 2435-2444.

Nanda, A.K., Andrio, E., Marino, D., Pauly, N., and Dunand, C. (2010) Reactive Oxygen Species during Plant-microorganism Early Interactions. *J of Integrative Plant Biology* **52**: 195-204.

Nellen-Anthamatten, D., Rossi, P., Preisig, O., Kullik, I., Babst, M., Fischer, H.M., and Hennecke, H. (1998) *Bradyrhizobium japonicum* FixK2, a crucial distributor in the FixLJ-dependent regulatory cascade for control of genes inducible by low oxygen levels. *J Bacteriol* **180**: 5251-5255.

Niemietz, C.M., and Tyerman, S.D. (2000) Channel-mediated permeation of ammonia gas through the peribacteroid membrane of soybean nodules. *FEBS Lett* **465**: 110-114.

O'Connor, K., Fletcher, S.A., and Csonka, L.N. (2009) Increased expression of Mg(2+) transport proteins enhances the survival of *Salmonella enterica* at high temperature. *Proc Natl Acad Sci U S A* **106**: 17522-17527.

Okereke, A., and Montville, T.J. (1992) Nisin dissipates the proton motive force of the obligate anaerobe Clostridium sporogenes PA 3679. *Appl Environ Microbiol* **58**: 2463-2467.

Oldroyd, G.E.D., and Downie, J.M. (2008) Coordinating nodule morphogenesis with rhizobial infection in legumes. *Annu Rev of Plant Biology* **59**: 519-546.

Oldroyd, G.E., Murray, J.D., Poole, P.S., and Downie, J.A. (2011) The rules of engagement in the legume-rhizobial symbiosis. *Annu Rev Genet* **45**: 119-144.

Oono, R., Denison, R.F., and Kiers, E.T. (2009) Controlling the reproductive fate of rhizobia: how universal are legume sanctions? *New Phytol* **183**: 967-979.

Osteras, M., Finan, T.M., and Stanley, J. (1991) Site-directed mutagenesis and DNA sequence of *pckA* of *Rhizobium* NGR234, encoding phosphoenolpyruvate carboxykinase: gluconeogenesis and host-dependent symbiotic phenotype. *Mol Gen Genet* **230**: 257-269.

Ott, T., van Dongen, J.T., Gunther, C., Krusell, L., Desbrosses, G., Vigeolas, H. et al. (2005) Symbiotic leghemoglobins are crucial for nitrogen fixation in legume root nodules but not for general plant growth and development. *Current Biology* **15**: 531-535.

Panek, H.R., and O'Brian, M.R. (2004) KatG is the primary detoxifier of hydrogen peroxide produced by aerobic metabolism in *Bradyrhizobium japonicum*. *J Bacteriol* **186**: 7874-7880.

Papp, K.M., and Maguire, M.E. (2004) The CorA Mg2+ transporter does not transport Fe^{2+}. *J Bacteriol* **186**: 7653-7658.

Papp-Wallace, K.M., and Maguire, M.E. (2006) Manganese transport and the role of manganese in virulence. *Annu Rev Microbiol* **60**: 187-209.

Papp-Wallace, K.M., and Maguire, M.E. (2008) Regulation of CorA Mg^{2+} channel function affects the virulence of *Salmonella enterica* serovar Typhimurium. *J Bacteriol* **190**: 6509-6516.

Papp-Wallace, K.M., Nartea, M., Kehres, D.G., Porwollik, S., McClelland, M., Libby, S.J. et al. (2008) The CorA Mg^{2+} channel is required for the virulence of *Salmonella enterica* serovar typhimurium. *J Bacteriol* **190**: 6517-6523.

Parniske, M., Schmidt, P.E., Kosch, K., and Muller, P. (1994) Plant defence response of host plants with determinate nodule are induced by EPS-defective *exoB* mutants of *Bradyrhizobium japonicum*. *Mol Plant Microbe Interact* **7**: 631-638.

Patschkowski, T., Schluter, A., and Priefer, U.B. (1996) *Rhizobium leguminosarum* bv. viciae contains a second *fnr/fixK*-like gene and an unusual *fixL* homologue. *Mol Microbiol* **21**: 267-280.

Patton-Vogt, J. (2007) Transport and metabolism of glycerophosphodiesters produced through phospholipid deacylation. *Biochim Biophys Acta* **1771**: 337-342.

Patzer, S.I., and Hantke, K. (2001) Dual repression by Fe^{2+}-Fur and Mn^{2+}-MntR of the *mntH* gene, encoding an NRAMP-like Mn2+ transporter in *Escherichia coli*. *J Bacteriol* **183**: 4806-4813.

Pauly, N., Pucciariello, C., Mandon, K., Innocenti, G., Jamet, A., Baudouin, E. et al. (2006) Reactive oxygen and nitrogen species and glutathione: key players in the legume-Rhizobium symbiosis. *J Exp Bot* **57**: 1769-1776.

Peck, M.C., Fisher, R.F., and Long, S.R. (2006) Diverse flavonoids stimulate NodD1 binding to nod gene promoters in *Sinorhizobium meliloti*. *J Bacteriol* **188**: 5417-5427.

Peleg-Grossman, S., Volpin, H., and Levine, A. (2007) Root hair curling and Rhizobium infection in *Medicago truncatula* are mediated by phosphatidylinositide-regulated endocytosis and reactive oxygen species. *J Exp Bot* **58**: 1637-1649.

Perret, X., Staehelin, C., and Broughton, W.J. (2000) Molecular basis of symbiotic promiscuity. *Microbiol Mol Biol Rev* **64**: 180-201.

Perry, R.D., Craig, S.K., Abney, J., Bobrov, A.G., Kirillina, O., Mier, I., Jr. et al. (2012) Manganese transporters Yfe and MntH are Fur-regulated and important for the virulence of *Yersinia pestis*. *Microbiology* **158**: 804-815.

Pfeiffer, J., Guhl, J., Waidner, B., Kist, M., and Bereswill, S. (2002) Magnesium uptake by CorA is essential for viability of the gastric pathogen *Helicobacter pylori*. *Infect Immun* **70**: 3930-3934.

Pierre, O., Engler, G., Hopkins, J., Brau, F., Boncompagni, E., and Herouart, D. (2013) Peribacteroid space acidification: a marker of mature bacteroid functioning in *Medicago truncatula* nodules. *Plant Cell Environ.* doi: 10.1111/pce.12116

Platero, R.A., Jaureguy, M., Battistoni, F.J., and Fabiano, E.R. (2003) Mutations in sit B and sit D genes affect manganese-growth requirements in *Sinorhizobium meliloti*. *FEMS Microbiol Lett* **218**: 65-70.

Platero, R., de Lorenzo, V., Garat, B., and Fabiano, E. (2007) *Sinorhizobium meliloti* fur-like (Mur) protein binds a fur box-like sequence present in the mntA promoter in a manganese-responsive manner. *Appl Environ Microbiol* **73**: 4832-4838.

Poole, L.B. (2005) Bacterial defenses against oxidants: mechanistic features of cysteine-based peroxidases and their flavoprotein reductases. *Arch Biochem Biophys* **433**: 240-254.

Poole, L.B., Hall, A., and Nelson, K.J. (2011) Overview of peroxiredoxins in oxidant defense and redox regulation. *Curr Protoc Toxicol* **7**:1-20.

Poole, P.S., Schofield, N.A., Reid, C.J., Drew, E.M., and Walshaw, D.L. (1994) Identification of chromosomal genes located downstream of *dctD* that affect the requirement for calcium and the lipopolysaccharide layer of *Rhizobium leguminosarum*. *Microbiology* **140:** 2797-2809.

Preisig, O., Anthamatten, D., and Hennecke, H. (1993) Genes for a microaerobically induced oxidase complex in *Bradyrhizobium japonicum* are essential for a nitrogen-fixing endosymbiosis. *Proc Natl Acad Sci U S A* **90**: 3309-3313.

Preisig, O., Zufferey, R., and Hennecke, H. (1996) The *Bradyrhizobium japonicum fixGHIS* genes are required for the formation of the high-affinity cbb3-type cytochrome oxidase. *Arch Microbiol* **165**: 297-305.

Prell, J., Boesten, B., Poole, P., and Priefer, U.B. (2002) The *Rhizobium leguminosarum* bv. viciae VF39 gamma-aminobutyrate (GABA) aminotransferase gene (*gabT*) is induced by GABA and highly expressed in bacteroids. *Microbiology* **148**: 615-623.

Prell, J., White, J.P., Bourdes, A., Bunnewell, S., Bongaerts, R.J., and Poole, P.S. (2009) Legumes regulate Rhizobium bacteroid development and persistence by the supply of branched-chain amino acids. *Proc Natl Acad Sci U S A* **106**: 12477-12482.

Prell, J., Bourdes, A., Kumar, S., Lodwig, E., Hosie, A., Kinghorn, S. et al. (2010) Role of symbiotic auxotrophy in the Rhizobium-legume symbioses. *PLoS One* **5**: e13933.

Puri, S., Hohle, T.H., and O'Brian, M.R. (2010) Control of bacterial iron homeostasis by manganese. *Proc Natl Acad Sci U S A* **107**: 10691-10695.

Quandt, J., and Hynes, M.F. (1993) Versatile suicide vectors which allow direct selection for gene replacement in gram-negative bacteria. *Gene* **127**: 15-21.

Ragumani, S., Sauder, J.M., Burley, S.K., and Swaminathan, S. (2010) Structural studies on cytosolic domain of magnesium transporter MgtE from *Enterococcus faecalis. Proteins-Structure Function and Bioinformatics* **78**: 487-491.

Rajagopal, S., Sudarsan, N., and Nickerson, K.W. (2002) Sodium dodecyl sulfate hypersensitivity of *clpP* and *clpB* mutants of *Escherichia coli. Appl Environ Microbiol* **68**: 4117-4121.

Ramachandran, V.K., East, A.K., Karunakaran, R., Downie, J.A., and Poole, P.S. (2011) Adaptation of Rhizobium leguminosarum to pea, alfalfa and sugar beet rhizospheres investigated by comparative transcriptomics. *Genome Biology* **12**. R106

Ramu, S.K., Peng, H.M., and Cook, D.R. (2002) Nod factor induction of reactive oxygen species production is correlated with expression of the early nodulin gene rip1 in *Medicago truncatula. Mol Plant Microbe Interact* **15**: 522-528.

Recourt, K., van Brussel, A.A., Driessen, A.J., and Lugtenberg, B.J. (1989) Accumulation of a nod gene inducer, the flavonoid naringenin, in the cytoplasmic membrane of *Rhizobium leguminosarum* biovar viciae is caused by the pH-dependent hydrophobicity of naringenin. *J Bacteriol* **171**: 4370-4377.

Reeve, W., O'Hara, G., Chain, P., Ardley, J., Braeu, L., Nandesena, K. et al. (2010) Complete genome sequence of *Rhizobium leguminosarum* bv trifolii strain WSM2304, an effective microsymbiont of the South American clover Trifolium polymorphum. *Standards in Genomic Sciences* **2**: 66-76.

Reeve, W.G., Tiwari, R.P., Worsley, P.S., Dilworth, M.J., Glenn, A.R., and Howieson, J.G. (1999) Constructs for insertional mutagenesis, transcriptional signal localization and gene regulation studies in root nodule and other bacteria. *Microbiology* **145**: 1307-1316.

Reid, D.E., Ferguson, B.J., Hayashi, S., Lin, Y.H., and Gresshoff, P.M. (2011) Molecular mechanisms controlling legume autoregulation of nodulation. *Ann Bot* **108**: 789-795.

Ren, Q., Chen, K., and Paulsen, I.T. (2007) TransportDB: a comprehensive database resource for cytoplasmic membrane transport systems and outer membrane channels. *Nucleic Acids Research* **35**: D274-D279.

Renalier, M.H., Batut, J., Ghai, J., Terzaghi, B., Gherardi, M., David, M. et al. (1987) A new symbiotic cluster on the pSym megaplasmid of *Rhizobium meliloti* 2011 carries a functional *fix* gene repeat and a nod locus. *J Bacteriol* **169**: 2231-2238.

Rocha, E.R., and Smith, C.J. (1999) Role of the alkyl hydroperoxide reductase (*ahpCF*) gene in oxidative stress defense of the obligate anaerobe *Bacteroides fragilis*. *J Bacteriol* **181**: 5701-5710.

Roche, P., Maillet, F., Plazanet, C., Debelle, F., Ferro, M., Truchet, G. et al. (1996) The common *nodABC* genes of *Rhizobium meliloti* are host-range determinants. *Proc Natl Acad Sci U S A* **93**: 15305-15310.

Rodgers, K.R. (1999) Heme-based sensors in biological systems. *Curr Opin Chem Biol* **3**: 158-167.

Rodionov, D.A., Gelfand, M.S., Todd, J.D., Curson, A.R., and Johnston, A.W. (2006) Computational reconstruction of iron- and manganese-responsive transcriptional networks in alpha-proteobacteria. *PLoS Comput Biol* **2**: e163.

Rodriguez-Haas, B., Finney, L., Vogt, S., Gonzalez-Melendi, P., Imperial, J., and Gonzalez-Guerrero, M. (2013) Iron distribution through the developmental stages of *Medicago truncatula* nodules. *Metallomics* **5**: 1247-1253

Rosch, J.W., Gao, G., Ridout, G., Wang, Y.D., and Tuomanen, E.I. (2009) Role of the manganese efflux system mntE for signalling and pathogenesis in *Streptococcus pneumoniae*. *Mol Microbiol* **72**: 12-25.

Rubio, L.M., and Ludden, P.W. (2008) Biosynthesis of the iron-molybdenum cofactor of nitrogenase. *Annu Rev Microbiol* **62**: 93-111.

Rubio, M.C., James, E.K., Clemente, M.R., Bucciarelli, B., Fedorova, M., Vance, C.P., and Becana, M. (2004) Localization of superoxide dismutases and hydrogen peroxide in legume root nodules. *Mol Plant Microbe Interact* **17**: 1294-1305.

Runyen-Janecky, L., Dazenski, E., Hawkins, S., and Warner, L. (2006) Role and regulation of the *Shigella flexneri* Sit and MntH systems. *Infect Immun* **74**: 4666-4672.

Sabri, M., Leveille, S., and Dozois, C.M. (2006) A SitABCD homologue from an avian pathogenic *Escherichia coli* strain mediates transport of iron and manganese and resistance to hydrogen peroxide. *Microbiology* **152**: 745-758.

Sabri, M., Caza, M., Proulx, J., Lymberopoulos, M.H., Bree, A., Moulin-Schouleur, M. et al. (2008) Contribution of the SitABCD, MntH, and FeoB metal transporters to the virulence of avian pathogenic *Escherichia coli* O78 strain chi7122. *Infect Immun* **76**: 601-611.

Saikolappan, S., Sasindran, S.J., Yu, H.D., Baseman, J.B., and Dhandayuthapani, S. (2009) The *Mycoplasma genitalium* MG_454 Gene Product Resists Killing by Organic Hydroperoxides. *J Bacteriol* **191**: 6675-6682.

Salazar, E., Diaz-Mejia, J.J., Moreno-Hagelsieb, G., Martinez-Batallar, G., Mora, Y., Mora, J., and Encarnacion, S. Characterization of the NifA-RpoN Regulon in *Rhizobium etli* in Free Life and in Symbiosis with *Phaseolus vulgaris*. *Appl and Environ Microbiol* **76**: 4510-4520.

Santos, R., Bocquet, S., Puppo, A., and Touati, D. (1999) Characterization of an atypical superoxide dismutase from *Sinorhizobium meliloti*. *J Bacteriol* **181**: 4509-4516.

Santos, R., Herouart, D., Puppo, A., and Touati, D. (2000) Critical protective role of bacterial superoxide dismutase in Rhizobium-legume symbiosis. *Mol Microbiol* **38**: 750-759.

Santos, R., Herouart, D., Sigaud, S., Touati, D., and Puppo, A. (2001) Oxidative burst in alfalfa-*Sinorhizobium meliloti* symbiotic interaction. *Mol Plant Microbe Interact* **14**: 86-89.

Santos-Beneit, F., Rodriguez-Garcia, A., Apel, A.K., and Martin, J.F. (2009) Phosphate and carbon source regulation of two PhoP-dependent glycerophosphodiester phosphodiesterase genes of *Streptomyces coelicolor*. *Microbiology* **155**: 1800-1811.

Sauer, R.T., and Baker, T.A. (2011) AAA+ proteases: ATP-fueled machines of protein destruction. *Annu Rev Biochem* **80**: 587-612.

Schafer, A., Tauch, A., Jager, W., Kalinowski, J., Thierbach, G., and Puhler, A. (1994) Small mobilizable multi-purpose cloning vectors derived from the *Escherichia coli* plasmids pK18 and pK19: selection of defined deletions in the chromosome of Corynebacterium glutamicum. *Gene* **145**: 69-73.

Schalk, I.J., Yue, W.W., and Buchanan, S.K. (2004) Recognition of iron-free siderophores by TonB-dependent iron transporters. *Mol Microbiol* **54**: 14-22.

Scheidle, H., Gross, A., and Niehaus, K. (2005) The Lipid A substructure of the *Sinorhizobium meliloti* lipopolysaccharides is sufficient to suppress the oxidative burst in host plants. *New Phytol* **165**: 559-565.

Schluter, A., Patschkowski, T., Quandt, J., Selinger, L.B., Weidner, S., Kramer, M. et al. (1997) Functional and regulatory analysis of the two copies of the *fixNOQP* operon of *Rhizobium leguminosarum* strain VF39. *Mol Plant Microbe Interact* **10**: 605-616.

Schmeisser, C., Liesegang, H., Krysciak, D., Bakkou, N., Le Quere, A., Wollherr, A. et al. (2009) *Rhizobium* sp. strain NGR234 possesses a remarkable number of secretion systems. *Appl Environ Microbiol* **75**: 4035-4045.

Schock, I., Gregan, J., Steinhauser, S., Schweyen, R., Brennicke, A., and Knoop, V. (2000) A member of a novel Arabidopsis thaliana gene family of candidate Mg^{2+} ion transporters complements a yeast mitochondrial group II intron-splicing mutant. *J* **24**: 489-501.

Seaver, L.C., and Imlay, J.A. (2001) Alkyl hydroperoxide reductase is the primary scavenger of endogenous hydrogen peroxide in *Escherichia coli*. *J Bacteriol* **183**: 7173-7181.

Seefeldt, L.C., Hoffman, B.M., and Dean, D.R. (2009) Mechanism of Mo-dependent nitrogenase. *Annu Rev Biochem* **78**: 701-722.

Setsukinai, K., Urano, Y., Kakinuma, K., Majima, H.J., and Nagano, T. (2003) Development of novel fluorescence probes that can reliably detect reactive oxygen species and distinguish specific species. *J Biol Chem* **278**: 3170-3175.

Shaw, S.L., and Long, S.R. (2003) Nod factor inhibition of reactive oxygen efflux in a host legume. *Plant Physiol* **132**: 2196-2204.

Shelton, C.L., Raffel, F.K., Beatty, W.L., Johnson, S.M., and Mason, K.M. (2011) Sap transporter mediated import and subsequent degradation of antimicrobial peptides in Haemophilus. *PLoS Pathog* **7**: e1002360.

Sigaud, S., Becquet, V., Frendo, P., Puppo, A., and Herouart, D. (1999) Differential regulation of two divergent *Sinorhizobium meliloti* genes for HPII-like catalases during free-living growth and protective role of both catalases during symbiosis. *J Bacteriol* **181**: 2634-2639.

Simsek, S., Ojanen-Reuhs, T., Stephens, S.B., and Reuhs, B.L. (2007) Strain-ecotype specificity in *Sinorhizobium meliloti-Medicago truncatula* symbiosis is correlated to succinoglycan oligosaccharide structure. *J Bacteriol* **189**: 7733-7740.

Small, S.K., Puri, S., Sangwan, I., and O'Brian, M.R. (2009) Positive control of ferric siderophore receptor gene expression by the Irr protein in *Bradyrhizobium japonicum*. *J Bacteriol* **191**: 1361-1368.

Smith, R.L., Thompson, L.J., and Maguire, M.E. (1995) Cloning and characterization of MgtE, a putative new class of Mg^{2+} transporter from *Bacillus firmus* OF4. *J Bacteriol* **177**: 1233-1238.

Smith, R.L., and Maguire, M.E. (1995) Distribution of the CorA Mg^{2+} transport system in Gram-negative bacteria. *J Bacteriol* **177**: 1638-1640.

Smith, R.L., and Maguire, M.E. (1998) Microbial magnesium transport: unusual transporters searching for identity. *Mol Microbiol* **28**: 217-226.

Snavely, M.D., Florer, J.B., Miller, C.G., and Maguire, M.E. (1989) Magnesium transport in *Salmonella typhimurium* ^{28}Mg^{2+} transport by the CorA, MgtA and MgtB systems. *J Bacteriol* **171**: 4761-4766.

Soto, M.J., Dominguez-Ferreras, A., Perez-Mendoza, D., Sanjuan, J., and Olivares, J. (2009) Mutualism versus pathogenesis: the give-and-take in plant-bacteria interactions. *Cell Microbiol* **11**: 381-388.

Soupene, E., Foussard, M., Boistard, P., Truchet, G., and Batut, J. (1995) Oxygen as a key development regulator of *Rhizobium meliloti* N$_2$ fixation gene-expression within the alfalfa root nodule. *Proc Natl Acad Sci U SA* **92**: 3759-3763.

Stacey, G., McAlvin, C.B., Kim, S.Y., Olivares, J., and Soto, M.J. (2006) Effects of endogenous salicylic acid on nodulation in the model legumes *Lotus japonicus* and *Medicago truncatula*. *Plant Physiol* **141**: 1473-1481.

Streeter, J.G. (1995) Recent developments in carbon transport and metabolism in symbiotic systems. *Symbiosis* **19**: 175-196.

Sukchawalit, R., Loprasert, S., Atichartpongkul, S., and Mongkolsuk, S. (2001) Complex regulation of the organic hydroperoxide resistance gene (*ohr*) from *Xanthomonas* involves OhrR, a novel organic peroxide-inducible negative regulator, and posttranscriptional modifications. *J Bacteriol* **183**: 4405-4412.

Sullivan, J.T., Brown, S.D., and Ronson, C.W. (2013) The NifA-RpoN regulon of *Mesorhizobium loti* strain R7A and its symbiotic activation by a novel LacI/GalR-family regulator. *PLoS One* **8**: e53762.

Summers, M.L., Botero, L.M., Busse, S.C., and McDermott, T.R. (2000) The *Sinorhizobium meliloti* Lon protease is involved in regulating exopolysaccharide synthesis and is required for nodulation of alfalfa. *J Bacteriol* **182**: 2551-2558.

Sun, H., Xu, G., Zhan, H., Chen, H., Sun, Z., Tian, B., and Hua, Y. (2010) Identification and evaluation of the role of the manganese efflux protein in *Deinococcus radiodurans*. *BMC Microbiol* **10**: 319.

Sutton, V.R., Mettert, E.L., Beinert, H., and Kiley, P.J. (2004) Kinetic analysis of the oxidative conversion of the 4Fe-4S (2+) cluster of FNR to a 2Fe-2S (2+) cluster. *J Bacteriol* **186**: 8018-8025.

Takahashi, Y., and Tokumoto, U. (2002) A third bacterial system for the assembly of iron-sulfur clusters with homologs in archaea and plastids. *J Biol Chem* **277**: 28380-28383.

Takanashi, K., Yokosho, K., Saeki, K., Sugiyama, A., Sato, S., Tabata, S. et al. (2013) LjMATE1: a citrate transporter responsible for iron supply to the nodule infection zone of *Lotus japonicus*. *Plant Cell Physiol* **54**: 585-594.

Taylor, B.L., and Zhulin, I.B. (1999) PAS domains: internal sensors of oxygen, redox potential, and light. *Microbiol Mol Biol Rev* **63**: 479-506.

Terpolilli, J.J., Hood, G.A., and Poole, P.S. (2012) What determines the efficiency of N(2)-fixing Rhizobium-legume symbioses? *Adv Microb Physiol* **60**: 325-389.

Thony-Meyer, L. (1997) Biogenesis of respiratory cytochromes in bacteria. *Microbiol Mol Biol Rev* **61**: 337-376.

Todd, J.D., Sawers, G., Rodionov, D.A., and Johnston, A.W.B. (2006) The *Rhizobium leguminosarum* regulator IrrA affects the transcription of a wide range of genes in response to Fe availability. *Molecular Genetics and Genomics* **275**: 564-577.

Tokumoto, U., Kitamura, S., Fukuyama, K., and Takahashi, Y. (2004) Interchangeability and distinct properties of bacterial Fe-S cluster assembly systems: functional replacement of the *isc* and *suf* operons in *Escherichia coli* with the *nifSU*-like operon from *Helicobacter pylori*. *J Biochem* **136**: 199-209.

Trainer, M.A., and Charles, T.C. (2006) The role of PHB metabolism in the symbiosis of rhizobia with legumes. *Appl Microbiol Biotechnol* **71**: 377-386.

Trinick, M.J., Dilworth, M.J., and Grounds, M. (1976) Factors affecting reduction of acetylene by root nodules of Lupinus species. *New Phytol* **77**: 359-370.

Triplett, E.W., and Sadowsky, M.J. (1992) Genetics of competition for nodulation of legumes. *Annu Rev Microbiol* **46**: 399-428.

Tuckerman, J.R., Gonzalez, G., and Gilles-Gonzalez, M.A. (2001) Complexation precedes phosphorylation for two-component regulatory system FixL/FixJ of *Sinorhizobium meliloti*. *J Mol Biol* **308**: 449-455.

Tyerman, S.D., Whitehead, L.F., and Day, D.A. (1995) A channel-like transport for the NH_4^+ on the symbiotic interface of the N_2-fixing plants. *Nature* **378**: 629-632.

Udvardi, M., and Poole, P.S. (2013) Transport and Metabolism in Legume-Rhizobia Symbioses. *Annu Rev Plant Biol*.

Ulvatne, H., Haukland, H.H., Samuelsen, O., Kramer, M., and Vorland, L.H. (2002) Proteases in *Escherichia coli* and *Staphylococcus aureus* confer reduced susceptibility to lactoferricin B. *J of Antimicrobial Chemotherapy* **50**: 461-467.

Van de Velde, W., Zehirov, G., Szatmari, A., Debreczeny, M., Ishihara, H., Kevei, Z. et al. (2010) Plant Peptides Govern Terminal Differentiation of Bacteria in Symbiosis. *Science* **327**: 1122-1126.

van Spronsen, P.C., Tak, T., Rood, A.M., van Brussel, A.A., Kijne, J.W., and Boot, K.J. (2003) Salicylic acid inhibits indeterminate-type nodulation but not determinate-type nodulation. *Mol Plant Microbe Interact* **16**: 83-91.

van Workum, W.A.T., van Slageren, S., van Brussel, A.A.N., and Kijne, J.W. (1998) Role of exopolysaccharides of *Rhizobium leguminosarum* bv. viciae as host plant-specific molecules required for infection thread formation during nodulation of *Vicia sativa*. *Mol Plant Microbe Interact* **11**: 1233-1241.

Vargas Mdel, C., Encarnacion, S., Davalos, A., Reyes-Perez, A., Mora, Y., Garcia-de los Santos, A. et al. (2003) Only one catalase, *katG*, is detectable in *Rhizobium etli*, and is encoded along with the regulator OxyR on a plasmid replicon. *Microbiology* **149**: 1165-1176.

Vasse, J., Billy, F., and Truchet, G. (1993) Abortion of infection during the *Rhizobium meliloti*—alfalfa symbiotic interaction is accompanied by a hypersensitive reaction. *The Plant J* **4**: 555-566.

Vattanaviboon, P., Whangsuk, W., Panmanee, W., Klomsiri, C., Dharmsthiti, S., and Mongkolsuk, S. (2002) Evaluation of the roles that alkyl hydroperoxide reductase and Ohr play in organic peroxide-induced gene expression and protection against organic peroxides in *Xanthomonas campestris*. *Biochem and Biophys Res Comm* **299**: 177-182.

Viguier, C., Cuiv, P.O., Clarke, P., and O'Connell, M. (2005) RirA is the iron response regulator of the rhizobactin 1021 biosynthesis and transport genes in *Sinorhizobium meliloti* 2011. *FEMS Microbiol Lett* **246**: 235-242.

Virts, E.L., Stanfield, S.W., Helinski, D.R., and Ditta, G.S. (1988) Common regulatory elements control symbiotic and microaerobic induction of *nifA* in *Rhizobium meliloti*. *Proc Natl Acad Sci U S A* **85**: 3062-3065.

Vrancken, K., Van Mellaert, L., and Anne, J. (2008) Characterization of the *Streptomyces lividans* PspA response. *J Bacteriol* **190**: 3475-3481.

Wang, D., Griffitts, J., Starker, C., Fedorova, E., Limpens, E., Ivanov, S. et al. (2010) A nodule-specific protein secretory pathway required for nitrogen-fixing symbiosis. *Science* **327**: 1126-1129.

Wang, D., Yang, S., Tang, F., and Zhu, H. (2012) Symbiosis specificity in the legume: rhizobial mutualism. *Cell Microbiol* **14**: 334-342.

Waters, L.S., Sandoval, M., and Storz, G. (2011) The Escherichia coli MntR miniregulon includes genes encoding a small protein and an efflux pump required for manganese homeostasis. *J Bacteriol* **193**: 5887-5897.

Wehmeier, S., Arnold, M.F., Marlow, V.L., Aouida, M., Myka, K.K., Fletcher, V. et al. (2010) Internalization of a thiazole-modified peptide in *Sinorhizobium meliloti* occurs by BacA-dependent and -independent mechanisms. *Microbiology* **156**: 2702-2713.

Weiner, L., and Model, P. (1994) Role of an *Escherichia coli* stress-response operon in stationary-phase survival. *Proc Natl Acad Sci U S A* **91**: 2191-2195.

Wexler, M., Yeoman, K.H., Stevens, J.B., De Luca, N.G., Sawers, G., and Johnston, A.W.B. (2001) The *Rhizobium leguminosarum tonB* gene is required for the uptake of siderophore and haem as sources of iron. *Mol Microbiol* **41** 801-16.

White, J., Prell, J., James, E.K., and Poole, P. (2007) Nutrient sharing between symbionts. *Plant Physiol* **144**: 604-614.

Wolfram, T.J., LeVeque, R.M., Kastenmayer, R.J., and Mulks, M.H. (2009) Ohr, an in vivo-induced gene in *Actinobacillus pleuropneumoniae*, is located on a genomic island and requires glutathione-S-transferase for activity. *FEMS Immun and Med Microbiol* **57**: 59-68.

Xie, F., Murray, J.D., Kim, J., Heckmann, A.B., Edwards, A., Oldroyd, G.E., and Downie, J.A. (2012) Legume pectate lyase required for root infection by rhizobia. *Proc Natl Acad Sci U S A* **109**: 633-638.

Xie, F., Zhang, Y., Li, G., Zhou, L., Liu, S., and Wang, C. (2013) The ClpP protease is required for the stress tolerance and biofilm formation in *Actinobacillus pleuropneumoniae*. *PLoS One* **8**: e53600.

Xu, G., Fan, X., and Miller, A.J. (2012) Plant nitrogen assimilation and use efficiency. *Annu Rev Plant Biol* **63**: 153-182.

Xu, X.M., and Moller, S.G. (2008) Iron-sulfur cluster biogenesis systems and their crosstalk. *Chembiochem* **9**: 2355-2362.

Xu, Y., Ambudkar, I., Yamagishi, H., Swaim, W., Walsh, T.J., and O'Connell, B.C. (1999) Histatin 3-mediated killing of *Candida albicans*: effect of extracellular salt concentration on binding and internalization. *Antimicrob Agents Chemother* **43**: 2256-2262.

Yamaguchi, Y., Tomoyasu, T., Takaya, A., Morioka, M., and Yamamoto, T. (2003) Effects of disruption of heat shock genes on susceptibility of *Escherichia coli* to fluoroquinolones. *BMC Microbiol* **3**: 16.

Yamaguchi, Y., Park, J.H., and Inouye, M. (2011) Toxin-antitoxin systems in bacteria and archaea. *Annu Rev Genet* **45**: 61-79.

Yamamoto, S., Uraji, M., Tanaka, K., Moriguchi, K., and Suzuki, K. (2007) Identification of pTi-SAKURA DNA region conferring enhancement of plasmid incompatibility and stability. *Genes Genet Syst* **82**: 197-206.

Yamamoto, S., Kiyokawa, K., Tanaka, K., Moriguchi, K., and Suzuki, K. (2009) Novel toxin-antitoxin system composed of serine protease and AAA-ATPase homologues determines the high level of stability and incompatibility of the tumor-inducing plasmid pTiC58. *J Bacteriol* **191**: 4656-4666.

Yang, J., Sangwan, I., Lindemann, A., Hauser, F., Hennecke, H., Fischer, H.M., and O'Brian, M.R. (2006) *Bradyrhizobium japonicum* senses iron through the status of haem to regulate iron homeostasis and metabolism. *Mol Microbiol* **60**: 427-437.

Yoo, K.S., Ok, S.H., Jeong, B., Jung, K.W., Cui, M.H., Hyoung, S., Lee, M., Song, H.K. and Shin, JS (2011) Single cystathionine β-synthase domain-containing proteins modulate development by regulating the thioredoxin system in *Arabidopsis*. *Plant Cell* **23**: 3577-94.

Young, J.P., Crossman, L.C., Johnston, A.W., Thomson, N.R., Ghazoui, Z.F., Hull, K.H. et al. (2006) The genome of *Rhizobium leguminosarum* has recognizable core and accessory components. *Genome Biol* **7**: R34.

Young, N.D., Debelle, F., Oldroyd, G.E., Geurts, R., Cannon, S.B., Udvardi, M.K. et al. (2011) The Medicago genome provides insight into the evolution of rhizobial symbioses. *Nature* **480**: 520-524.

Yurgel, S.N., and Kahn, M.L. (2004) Dicarboxylate transport by rhizobia. *FEMS Microbiol Rev* **28**: 489-501.

Zaharik, M.L., Cullen, V.L., Fung, A.M., Libby, S.J., Choy, S.L.K., Coburn, B. et al. (2004) The *Salmonella enterica* serovar typhimurium divalent cation transport systems MntH and SitABCD are essential for virulence in an Nramp1(G169) murine typhoid model. *Infect Immun* **72**: 5522-5525.

Zamorano-Sanchez, D., Reyes-Gonzalez, A., Gomez-Hernandez, N., Rivera, P., Georgellis, D., and Girard, L. (2012) FxkR provides the missing link in the *fixL-fixK* signal transduction cascade in *Rhizobium etli* CFN42. *Mol Plant Microbe Interact* **25**: 1506-1517.

Zhang, Y., Aono, T., Poole, P., and Finan, T.M. (2012) NAD(P)(+)-Malic Enzyme Mutants of *Sinorhizobium* sp Strain NGR234, but not *Azorhizobium caulinodans* ORS571, Maintain Symbiotic N_2 Fixation Capabilities. *Appl and Environ Microbiol* **78**: 2803-2812.

Zhao, G., Kong, W., Weatherspoon-Griffin, N., Clark-Curtiss, J., and Shi, Y. (2011) Mg^{2+} facilitates leader peptide translation to induce riboswitch-mediated transcription termination. *EMBO J* **30**: 1485-1496.

Zhukov, V., Radutoiu, S., Madsen, L.H., Rychagova, T., Ovchinnikova, E., Borisov, A. et al. (2008) The pea Sym37 receptor kinase gene controls infection-thread initiation and nodule development. *Mol Plant Microbe Interact* **21**: 1600-1608.

Zuanazzi, J.A.S., Clergeot, P.H., Quirion, J.C., Husson, H.P., Kondorosi, A., and Ratet, P. (1998) Production of *Sinorhizobium meliloti* nod gene activator and repressor flavonoids from *Medicago sativa* roots. *Mol Plant Microbe Interact* **11**: 784-794.

Zuber, P. (2009) Management of oxidative stress in *Bacillus*. *Annu Rev Microbiol* **63**: 575-597.